Magma Ocean, Water, and the Early Atmosphere of Venus

Arnaud Salvador, Guillaume Avice, Doris Breuer, Cédric Gillmann, Helmut Lammer, Emmanuel Marcq, Sean N Raymond, Haruka Sakuraba, Manuel Scherf, M J Way

Space Science Reviews (2023) 219:51
https://doi.org/10.1007/s11214-023-00995-7

Magma Ocean, Water, and the Early Atmosphere of Venus

Arnaud Salvador[1,2,3] · Guillaume Avice[4] · Doris Breuer[5] · Cédric Gillmann[6] · Helmut Lammer[7] · Emmanuel Marcq[8] · Sean N. Raymond[9] · Haruka Sakuraba[10] · Manuel Scherf[7,11,12] · M.J. Way[13,14]

Received: 22 February 2023 / Accepted: 10 August 2023

Abstract
The current state and surface conditions of the Earth and its twin planet Venus are drastically different. Whether these differences are directly inherited from the earliest stages of planetary evolution, when the interior was molten, or arose later during the long-term evolution is still unclear. Yet, it is clear that water, its abundance, state, and distribution between the different planetary reservoirs, which are intimately related to the solidification and outgassing of the early magma ocean, are key components regarding past and present-day habitability, planetary evolution, and the different pathways leading to various surface conditions.

In this chapter we start by reviewing the outcomes of the accretion sequence, with particular emphasis on the sources and timing of water delivery in light of available constraints, and the initial thermal state of Venus at the end of the main accretion. Then, we detail the processes at play during the early thermo-chemical evolution of molten terrestrial planets, and how they can affect the abundance and distribution of water within the different planetary reservoirs. Namely, we focus on the magma ocean cooling, solidification, and concurrent formation of the outgassed atmosphere. Accounting for the possible range of parameters for early Venus and based on the mechanisms and feedbacks described, we provide an overview of the likely evolutionary pathways leading to diverse surface conditions, from a temperate to a hellish early Venus. The implications of the resulting surface conditions and habitability are discussed in the context of the subsequent long-term interior and atmospheric evolution. Future research directions and observations are proposed to constrain the different scenarios in order to reconcile Venus' early evolution with its current state, while deciphering which path it followed.

Keywords Venus · Interior evolution · Atmosphere · Degassing

1 Introduction

Water is not only an essential element for the chemical and biological processes responsible for the emergence and development of life and living organisms (e.g., Westall and Brack 2018; Hoehler et al. 2018). Its abundance and distribution within and between the different

Venus: Evolution Through Time
Edited by Colin F. Wilson, Doris Breuer, Cédric Gillmann, Suzanne E. Smrekar, Tilman Spohn and Thomas Widemann

Extended author information available on the last page of the article

reservoirs of a rocky planet, from the deep interior to the exosphere, is also of fundamental importance in controlling their properties and thus the physical and chemical processes at play within and between these reservoirs, making it a crucial factor in setting the conditions suitable for the development of life and for the overall planetary evolution (e.g., Kasting and Catling 2003; Hirschmann 2006; Karato 2015; Foley and Driscoll 2016; Korenaga et al. 2017; Ohtani 2020). Understanding the mechanisms shaping the water budget within the planets and how they evolve through time is thus required to build a consistent picture of planetary evolution and characterize the potential habitability of terrestrial planets (classically defined as the ability of a planet to sustain liquid water at its surface; e.g., Kasting et al. 1993b).

From that perspective, the early stages of planetary evolution appear to be of first importance. Indeed, during this relatively short but intense period of time, the combination of different heat sources, in particular the energy delivered by successive collisions of planetary building-blocks during planetary accretion and growth, is believed to substantially melt the planetary body (e.g., Safronov 1978; Kaula 1979; Tonks and Melosh 1993; Nakajima et al. 2021), resulting in the creation of a so-called "magma ocean" ("MO"): a possibly global, from mantle-thick to near-surface shell of magma of low, water-like viscosity (hence "ocean"; e.g., Warren 1985). During this magma ocean stage, because of the molten surface, the absence of a thick, long-lasting boundary layer between the planetary interior and the atmosphere allows for free and extremely efficient thermal and chemical exchanges between these reservoirs.

The modern concept of magma ocean originally took root in the study of the mineralogy of the Moon's surface from the lunar samples brought back to Earth in the seventies. The formation of the bright anorthositic crust, making up the ancient lunar highlands covering most of the surface (e.g., Ji et al. 2022), was proposed to result from the flotation of light Ca- and Al-rich anorthite minerals (plagioclase feldspar) over a crystallizing, denser molten silicate layer, hence requiring the upper part of the lunar mantle to be initially molten (e.g., Smith et al. 1970; Wood et al. 1970; Warren 1985; Binder 1986). Early and extensive melting of the surface and subsurface was confirmed by trace element analysis and experimental petrology (Schnetzler and Philpotts 1971; Taylor 1986). The origin of the lunar magma ocean was then tied to the formation process of the Moon itself and in particular to the energetics of collisional accretion (e.g., Wetherill 1976; Taylor 1986; Matsui and Abe 1986c; Hartmann 1986; Cameron 1986), where conversion of kinetic energy into heat from impacts could increase the temperature up to the melting point of silicates and potentially melt the surface and the interior of the impacted body to an extent depending primarily on the impactor size and resulting heat burial.

Reciprocally, the Earth was thought to be significantly heated and molten as a result of the Moon-forming event(s) and more generally out of the accretion sequence (Safronov 1978; Kaula 1979; Wetherill 1985), thought to be of increasing violence with time, with the increasing size of impactors. By considering each plausible combination of heating mechanisms involved in melting the Moon, Hostetler and Drake (1980) extended the analysis on the early thermal state of the Earth and other terrestrial planets and suggested that early global melting (and differentiation) was also likely for all terrestrial planets (e.g., Drake 2000). The hypothesis of a single moon-forming giant impact gained popularity and became the overarching paradigm for lunar origin (e.g., Hartmann and Davis 1975; Cameron and Ward 1976; Benz et al. 1986; Boss 1986; Taylor 1986; Newsom and Ross Taylor 1989; Drake 2000; Canup and Asphaug 2001). The reciprocal idea that the Earth experienced a planetary-scale global magma ocean, possibly melting the entire mantle molten (Wetherill 1985), as a result of such collision (or from violent accretion) gained interest (Melosh 1990;

Tonks and Melosh 1993). The existence of a molten stage on rocky planets was also independently confirmed by early melting in planetesimals triggered by radiogenic heating from the decay of radioactive elements (e.g., Urey 1955; Fish et al. 1960; Lee et al. 1976). It is now generally accepted that all terrestrial planets, including Venus, experience at least a transient magma ocean stage early in history but the number of occurrences, timing, timescale and depth of the molten layer may significantly vary from one planet to another (see Elkins-Tanton 2012; Schaefer and Elkins-Tanton 2018, for reviews).

In this phase, some of the major processes shaping the conditions at the surface and in the interior of the planet take place, and set the initial conditions for the later long-term state and evolution of the planet (e.g., Schaefer and Elkins-Tanton 2018). The volatile and "atmophile" (i.e., air-loving) species dissolved within the molten mantle are outgassed and build-up the atmosphere, the rapid segregation of heavy metallic iron (and associated "siderophile", i.e., metal-loving, elements) and lighter silicate (and "lithophile", i.e., stone-loving, elements) favored by the low viscosity of the melt is responsible for the chemical differentiation of the planet. The distribution of water between the different reservoirs, the amount reaching the surface as well as the early climate and associated liquid water sustainability at the surface are direct outcomes of the magma ocean solidification. The resulting internal structure and elemental distribution thus set the starting point for the onset of mantle convection and for the long-term evolution of the planet. These early stages of planetary evolution are thus of fundamental importance in controlling the potential past and present-day habitability of a planet and in understanding the pathways to the present-day surface conditions.

For a planet to be habitable, two *sine qua non* conditions must be achieved. First, water needs to reach and be abundant enough at the surface of the planet, and second, the surface conditions (pressure and temperature) must allow for the water to condense. These two conditions are often addressed separately, while implicitly assuming that the other condition is satisfied. One positive condition does not imply the other, yet they are intricately linked. As mentioned above, these two requirements strongly rely on the outcomes of the magma ocean phase. On the other hand, maintaining a temperate and stable climate with sustainable water oceans long enough for life to emerge then relies on additional processes such as atmospheric escape and geochemical cycles, which affect the planetary environment over longer timescales, throughout the entire evolution of the planet, including when the internal heat is no longer climatologically significant.

Given the fact that planetary surface conditions are essentially controlled by atmospheric and climate dynamics, habitable zone and habitability-related studies have been historically conducted from an atmospheric point-of-view, using atmospheric models as main tools to assess the surface temperature and pressure and infer the presence of liquid water at the planetary surface (e.g., Kasting et al. 1993b; Selsis et al. 2007; Kopparapu et al. 2013; Ramirez 2018). Despite being highly influential, the early evolution stages have been neglected in habitable zone studies, thus possibly missing important pieces of the puzzle. Only recently has the importance of interior–atmosphere feedback on habitability been recognized (e.g., Zahnle et al. 2007; Noack et al. 2014; Foley and Driscoll 2016; Ramirez et al. 2018; Dehant et al. 2019).

The case of Venus is still puzzling and these neglected components might hold the key. Given their vicinity in the inner Solar System, the Earth and Venus likely experienced many similarities during their formation, including analogous accretion sequences, chemical elements endowments and volatile delivery. Their nearly identical sizes and bulk densities suggesting similar bulk compositions (e.g., Smrekar et al. 2018) are also indicative of a common past. Yet, Earth's present-day liquid water- and life-sustaining temperate climate

differs strikingly from the mostly dry and hellish Venusian surface conditions. Whether these differences are directly inherited from the tumultuous magma ocean stage or appeared later in history remains unclear. Studying the planetary evolution and in particular this common molten past, at the earliest ages of the Solar System, may be one of the keys to resolving this paradox and unveil the evolutionary pathway(s) leading to a habitable and inhabited planet. This is the object of the present chapter, with particular emphasis on the role and feedback of and between water and interior-atmosphere interaction when the planet was molten. Throughout the chapter, we will then address the following key questions:

- What are the initial conditions and water content of the molten interior of Venus? (Sect. 2)
- What processes affect the thermal evolution of the magma ocean and the concurrent atmospheric formation? (Sect. 3)
- How is water distributed between the solidifying mantle, the molten interior, and the atmosphere during magma ocean evolution? (Sect. 3)
- What are the outcomes of the magma ocean phase and the corresponding implications for the habitability and long-term evolution of the planet? (Sect. 4)
- When and how did the Earth and Venus surface conditions diverge? (Sect. 4)
- What are the next steps to achieve towards a better understanding of early Venusian evolution? (Sect. 5)

To do so, the chapter is organized as follows: Sect. 2 describes the initial conditions of the molten stage evolution, by focusing on its initial thermo-chemical state resulting from the accretion sequence, and on the initial amount of water accreted as a function of the different sources and processes of volatiles delivery. Section 3 focuses on the processes at play during magma ocean thermal evolution and concurrent formation of the atmosphere, including the feedback between the interior and the atmospheric reservoirs. Section 4 examines the possible outcomes of the magma ocean cooling sequence and how the different evolutionary paths could influence the subsequent surface conditions and long-term evolution of the planet. Finally, Sect. 5 discusses how further research directions combined with future observations and measurements could provide clues to decipher the early evolution of Venus and choose between the different scenarios to eventually reconstruct a consistent picture of the history of the planet.

2 Water Delivery and Initial Conditions for the Molten Mantle Evolution: What do We Start with?

Near the end of planetary accretion, the planet's water inventory and thermal state play the two key roles in its subsequent evolution. Yet, even for Earth, these parameters are highly unconstrained. In this section, we provide an overview of the processes that could be responsible for water delivery on early Venus. We estimate the amount of water delivered, and describe the early energy sources that control the initial heat budget of the planet. In Sect. 2.1 we discuss the possibility for Venus to produce water from the nebular gas gravitationally captured within the protoplanetary disk. We then describe the outcomes of the accretion sequence as a function of the different planetary formation scenarios in Sect. 2.2. While the sources, timing, and amount of water delivered to Earth are still debated, in Sect. 2.2.1 we discuss how the different planetary formation scenarios and their implications for water delivery apply to Venus. We also describe the different heat sources at play and the corresponding thermal state of the mantle resulting from the accretion sequence (Sect. 2.2.2). We then examine scenarios of water delivery, budget, and fate in light of available constraints from isotopic ratios in Sect. 2.3.

2.1 Proto-Venus and H_2/He Envelope: Did Early Venus Produce Water from the Protoplanetary Nebula?

If proto-Venus accreted a sufficient mass within the protoplanetary disk lifetime, the growing planet could have captured an H_2-dominated primordial atmosphere by accreting nebular gas from the circumstellar disk, which could have then been quickly lost by Extreme UltraViolet-driven (EUV) hydrodynamic escape after the disk dissipated (e.g., Hayashi et al. 1979; Stökl et al. 2016; Sharp 2017). If this was the case, the efficient hydrodynamic hydrogen flow dragged heavier elements such as noble gas isotopes with it, leading to modifications of their initial isotope ratios (Pepin 1991).

Recently, Lammer et al. (2020b) applied a hydrodynamic upper atmosphere and a Smooth Particle Hydrodynamics (SPH) impact model for the loss calculations of captured H_2-dominated envelopes. This was done for various protoplanetary masses and a wide range of possible EUV-activity evolution tracks of the young Sun and initial atmospheric compositions based on mixtures of captured nebula gas, outgassed and delivered materials. As shown in Fig. 1, these authors could reproduce the present Venus atmospheric $^{36}Ar/^{38}Ar$, $^{20}Ne/^{22}Ne$ isotope ratios if proto-Venus accreted a mass of ∼0.84–1.0 M_{Venus} (∼0.68–0.81 $M_{\oplus}$) during the disk lifetime of ∼3–4.5 Myr (Bollard et al. 2017; Wang et al. 2017) after the origin of the Sun.

Lammer et al. (2020b) also showed that proto-Venus could have captured primordial H_2-dominated envelopes with hydrogen surface partial pressures between ∼40–1000 bar (Fig. 1). The blanketing effect of such dense and opaque atmospheres would be responsible

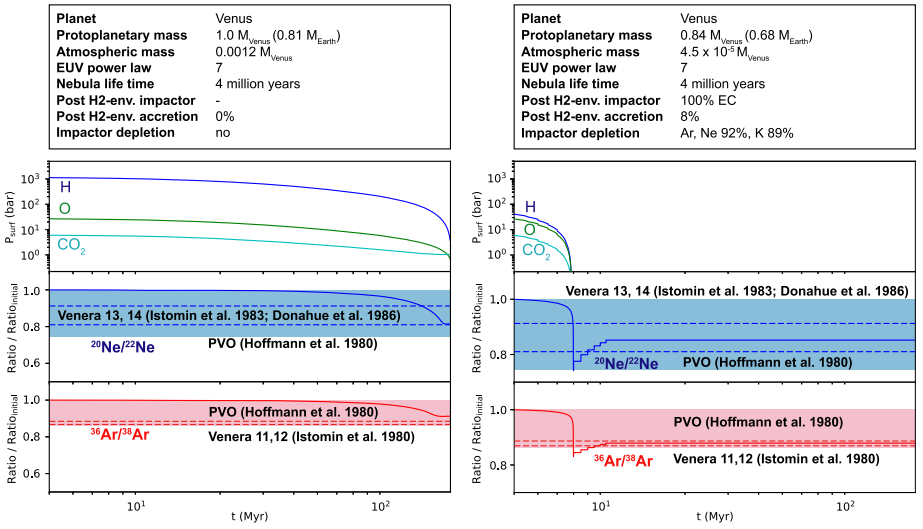

Fig. 1 a) Successful reproduction attempt of the Pioneer Venus, Venera 11 and 12 $^{36}Ar/^{38}Ar$, and Venera 13 and 14 $^{20}Ne/^{22}Ne$ noble gas isotope ratios within the measured error bars if Venus accreted its final mass during the disk lifetime. In such a case the planet would have lost, a hydrogen-dominated primordial atmosphere with ∼1000 bar partial pressure after ≥ 200 Myr if the young Sun was a weakly to moderately active young G-star. b) Successful reproduction attempt of the Venera 11 and 12 $^{36}Ar/^{38}Ar$, and Venera 13 and 14 $^{20}Ne/^{22}Ne$ noble gas ratios within the measured error bars for a proto-Venus with ∼0.84 M_{Venus} (∼0.68 $M_{\oplus}$). We use a 100% EC-like building block composition that accreted about 17% of the planet mass after a primordial atmosphere with a hydrogen partial pressure of ∼40 bar was lost until ∼7 Myr after the origin of the Sun and ∼3 Myr after the disk evaporated (after Lammer et al. 2020b)

for extensive mantle melting (e.g., Hayashi et al. 1979; Olson and Sharp 2019). Then, if proto-Venus grew partly within the gas disk (Ikoma and Genda 2006; Ikoma et al. 2018), the primordial atmospheric H_2 can be oxidized by interactions between the gas and the underlying molten surface. This requires surface temperatures above the melting point of silicate ($\sim$1400 K), thereby producing water that originates from the protoplanetary nebula. Hydrogen and water would thus be ingassed into the molten interior while some other fraction of hydrogen would possibly be sequestered into the core (e.g., Sharp 2017; Wu et al. 2018; Olson and Sharp 2018, 2019; Young et al. 2023). How much water can be produced from the nebula depends both on the mass of the surrounding H_2-envelope and on the oxidation state of the magma ocean, characterized by the available iron oxides (e.g., wüstite and magnetite) and fayalite (Fe_2SiO_4) in the magma ocean (Ikoma and Genda 2006). Logically, the amount of water produced from primordial H_2 increases with the increasing chemical potential of oxygen (i.e., oxygen fugacity; see Sect. 3.2.5), as more oxygen atoms available combine with hydrogen atoms to produce more water. Indeed, according to Ikoma and Genda (2006), at 1500 K the mass ratio of produced H_2O to the primordial atmospheric H_2, M_{H_2O}/M_{H_2}, increases from approximately 0.49 to 0.88, and to 24.02 for increasingly oxidizing environments, corresponding to the buffer assemblages of quartz-iron-fayalite (QIF):

$$\underset{\text{iron}}{2\,\text{Fe}} + \underset{\text{quartz}}{\text{SiO}_2} + \text{O}_2 \rightleftarrows \underset{\text{fayalite}}{\text{Fe}_2\text{SiO}_4}, \tag{R1}$$

iron-wüstite (IW):

$$\underset{\text{iron}}{2\,x\,\text{Fe}} + \text{O}_2 \rightleftarrows \underset{\text{wüstite}}{2\,\text{Fe}_x\text{O}}, \tag{R2}$$

and wüstite-magnetite (WM):

$$\underset{\text{wüstite}}{6/(4x-3)\,\text{Fe}_x\text{O}} + \text{O}_2 \rightleftarrows \underset{\text{magnetite}}{2x/(4x-3)\,\text{Fe}_3\text{O}_4} \tag{R3}$$

respectively (e.g., Frost 1991). Note that the side of the reaction that has greater entropy,[1] that is the side with oxygen, is stable at higher temperature than the other side (e.g., Fig. 1 in Frost 1991). Ikoma and Genda (2006) used values of $x = 0.947$ for IW and $x = 0.974$ for WM taken from Robie et al. (1978).

Note that the oxidation state of the magma ocean, and therefore water production efficiency, relates to the timing and location of metal–silicate separation. If metallic iron has not yet segregated from the magma ocean and coexists with the molten silicate, as believed for the earliest evolution steps, the magma ocean is thought to be reducing. It would be at the QIF or IW redox buffer rather than at the WM buffer, thus producing less water than if the metallic iron has already segregated into the core (see Sect. 3.2.5 for definitions of mineral redox buffers and discussion regarding the magma ocean oxidation state). However, the picture might be more complicated, making the influence of the magma ocean oxidation state on the process of hydrogen ingassing and water production less straightforward. For instance, the ingassing hydrogen may cause Fe reduction, followed by iron removal to the core. In this case, Sharp (2017) suggested that far larger amounts of H_2 could be incorporated into the melt, which could in turn enhance water production even with abundant metallic iron in a reducing environment.

[1] By convention reactions are written with the high entropy side on the right. Here we kept it on the left, so that the oxidation reads from left to right.

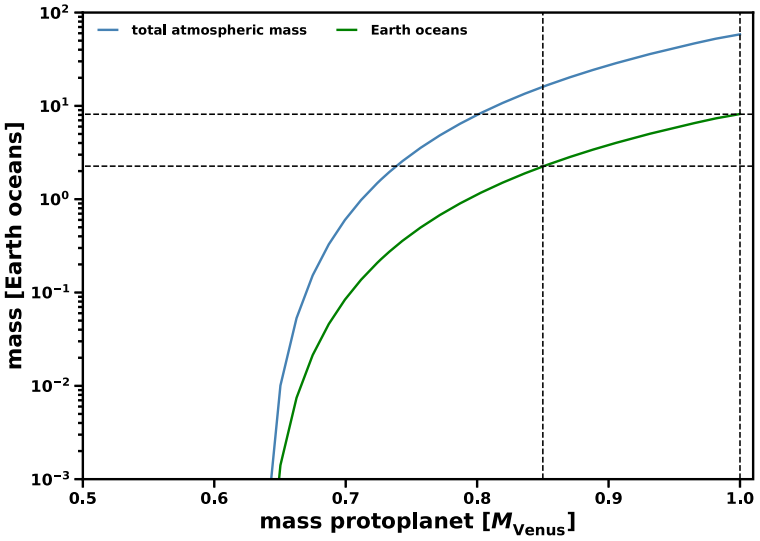

Fig. 2 The amount of Earth oceans (green line) that may be produced by a captured H_2-dominated primordial atmosphere (blue line) due to gas–melt interactions between the atmosphere and a magma ocean according to Ikoma and Genda (2006). The vertical and horizontal dashed-lines correspond to the possible proto-Venus mass and corresponding primordial atmospheric mass ranges where Venus' present-day Ar and Ne isotope ratios can be reproduced within the error bars

If one applies the same assumption as Ikoma and Genda (2006) for the hydrogen envelopes as simulated by Lammer et al. (2020b), shown in Fig. 1, and assumes that such oxygen buffers (i.e., QIF, IW, and WM) are available, a proto-Venus with a mass of ∼0.84 $M_{\rm Venus}$ could produce a water reservoir on early Venus from the captured H_2-envelope of at least ∼2 Earth oceans, as shown in Fig. 2. In case proto-Venus accreted its final mass during the disk lifetime, then a nebular-based H_2O amount of at least ∼8 Earth oceans could have been produced (see Fig. 2). The probability of terrestrial planet formation within the nebular gas is still debated. This is because the dissipation mechanisms remain uncertain. Yet, the capture of other nebular gases such as Ne followed by their incorporation into molten planetary interiors has further been inferred from mantle isotopic ratios (Williams and Mukhopadhyay 2019). It supports the idea that terrestrial planets may partly form before the nebular gas dissipated. One should note that molten silicate–metallic core separation may not be complete by the time the nebular gas fully vanishes, suggesting a rather reducing magma ocean and associated relatively low water production (e.g., at the water production rates imposed by the QIF or IW buffers).

In comparison, Lammer et al. (2020a) found that Earth's present-day atmospheric $^{36}Ar/^{38}Ar$, $^{20}Ne/^{22}Ne$, and $^{36}Ar/^{22}Ne$ isotope ratios could only be reproduced if the protoplanet grew a mass of $\leq 0.6\ M_{\oplus}$ within the solar nebula. It implies that, contrary to Venus, only ∼2% of the current value of Earth's seawater could have been produced from the protoplanetary nebula. This low value for the Earth lies within the error bars of the D/H seawater-carbonaceous chondrite "match" of $150\pm10\ \times10^{-6}$ (Robert et al. 2000; Pahlevan et al. 2019), and is in agreement with measurements of the D/H ratios in glassy melt inclusions in two deep mantle basaltic rock samples (Hallis et al. 2015). This suggests that only a small fraction of Earth's water was derived from nebular accretion (e.g., Wu et al. 2018). Nevertheless, Young et al. (2023) recently emphasized that primordial H_2 atmospheres re-

main an influential and promising mechanism to explain fundamental chemical features of terrestrial planets, such as Earth's water content, core density, and oxidation state.

If proto-Venus grew partly within the gas disk and produced nebula-based water, its initial D/H ratio of $21\pm5 \times 10^{-6}$ could then resemble that of nebular gas which is $\sim$7 times lower than Earth's seawater (Geiss and Gloeckler 1998; Robert et al. 2000) and CCs (e.g., Marty 2012) measured D/H ratios. If this was the case, then Venus' present-day D/H ratio of $160\pm20 \times 10^{-4}$ (Donahue et al. 1982) would be $\sim$762 times higher than initially instead of $\sim$106 times, if the planets initial H_2O inventory were CC-based as on Earth. In such a case atmospheric escape must have fractionated D/H much more significantly than expected in previous studies (Donahue 1999).

Note that many stars are surrounded by gaseous and dusty debris disks. Compared to the protoplanetary disks surrounding young newly formed stars, those long-lasting (possibly for hundreds of millions of years; Wyatt 2008; Matrà et al. 2017) debris disks can be found and remain after planets have already formed. They result from the collisions and destruction of asteroids, comets, planetesimals, and dwarf planets (rather than being of primordial origin as the younger protoplanetary disks; e.g., Dent et al. 2014; Hughes et al. 2018; Matrà et al. 2019). Rather than being dominated by hydrogen and helium, the gas of those disks is mainly composed of CO, carbon, and oxygen (e.g., Cataldi et al. 2014; Kral et al. 2017). Terrestrial planets could form massive atmospheres from the capture of the gas contained in those debris disks (Kral et al. 2020). Yet, the amount of water produced and incorporated into the planet from such accreted atmospheres has not been assessed. It may be limited compared to protoplanetary disks due to the absence of hydrogen in their carbon and oxygen rich compositions (e.g., Cataldi et al. 2014; Kral et al. 2017).

2.2 Outcomes of Planetary Formation Scenarios

2.2.1 Water Delivery

Understanding the growth of the rocky planets is essential because it sets their volatile inventories. Yet our picture of the growth of the rocky planets remains incomplete. This comes in large part from a lack of hard constraints during the era of accretion. The initial conditions for Solar System formation are likely represented in the circumstellar disks that are directly observed around nearby young stars, for instance with the ALMA telescope (e.g., ALMAPartnership et al. 2015; Andrews et al. 2018). The population of known exoplanets represent thousands of outcomes of planet formation (e.g., Winn and Fabrycky 2015). At intermediate size- and time scales between young circumstellar disks and mature planetary systems, empirical constraints are hard to find.

The current paradigm of Solar System formation involves a series of different stages of growth (for a review, see Raymond and Morbidelli 2022). First, micron-sized dust grains collide and coagulate until they reach one of several growth barriers at roughly mm-sizes (Blum and Wurm 2008; Zsom et al. 2010). These large dust grains are commonly called "pebbles", and have sufficient inertia that their orbits are mainly Keplerian (see Johansen and Lambrechts 2017). However, the gas orbits slightly slower than the Keplerian speed because of partial pressure support. Pebbles therefore feel a headwind from the gas, which causes them to lose orbital energy and spiral inward – or rather, along the local pressure gradient – on short timescales (Weidenschilling 1977; Haghighipour and Boss 2003). Pebbles generally drift inward, but can become concentrated in regions in pressure bumps within the gas disk (Birnstiel et al. 2012). When pebbles are sufficiently concentrated in any given region, they can be further concentrated by the streaming instability and directly clump into

10–100 km-scale planetesimals (Youdin and Goodman 2005; Johansen et al. 2009, 2014). These are generally considered the "building blocks" of the planets. While the classical model assumes that planetesimals formed uniformly across the disk (e.g., Raymond et al. 2014), new models propose that planetesimals form in different regions at different times, often at (moving) condensation fronts (Armitage et al. 2016; Drążkowska and Alibert 2017; Drążkowska and Dullemond 2018; Morbidelli et al. 2022; Izidoro et al. 2022). Planetesimals continue to grow by both collisions between planetesimals and by accreting pebbles that continue to drift within the disk (Johansen and Lambrechts 2017; Ormel 2017). The giant planet cores are thought to have rapidly accreted by accreting pebbles (Lambrechts and Johansen 2014; Levison et al. 2015). In contrast, the terrestrial planets are generally thought to have mainly grown by planetesimal accretion (Raymond et al. 2009; Chambers 2016; Izidoro et al. 2021b), although a new class of models proposes that pebble accretion may have played a role (Johansen et al. 2021). Next, planetesimals grow into terrestrial planet embryos and giant planet cores. In the terrestrial planet-forming region, planetary embryos were perhaps a Mars-mass ($\sim$10% of an Earth-mass; Morbidelli et al. 2012), whereas the giant planets' cores are thought to have been $\sim$10–20 $M_{\oplus}$. The final assembly of the terrestrial planets is thought to have involved giant impacts between planetary embryos as well as a sweep-up of leftover planetesimals (for reviews, see Morbidelli et al. 2012; Raymond et al. 2014; Jacobson and Walsh 2015; Raymond and Morbidelli 2022).

Because it is smaller and faster orbiting, Venus is significantly more likely to have experienced more "hit-and-run" (bouncing; e.g., Asphaug et al. 2006; Reufer et al. 2012) collisions than Earth (Emsenhuber et al. 2021). In addition, Emsenhuber et al. (2021) showed that Venus is expected to eventually accrete most of its runners while Earth loses about half, with many of those ending up at Venus. Generally, Venus serves as a sink of runners emerging from farther out collisions and is more likely to have accreted a massive outer Solar System body. This means that despite their proximity, the collisional histories of the two planets were not identical.

The first quantitative model for terrestrial planet formation, developed from the 1970s to the 2000s, is commonly referred to as the "classical model", and was built upon the work of several pioneers in the field, notably that of George Wetherill (key papers include Safronov 1972; Greenberg et al. 1978; Wetherill 1978, 1985, 1990). Yet, the classical model – which assumes that a smooth disk of planetesimals existed between the present-day orbits of Venus and Jupiter upon dissipation of the Sun's gaseous disk – systematically fails to reproduce the planets' orbital architecture, forming Mars analogs that are as massive as Earth (Wetherill 1991; Raymond et al. 2009; Lammer et al. 2020a). In recent years, three planetesimal accretion-based solutions have been proposed to this "small Mars" problem and are illustrated in Fig. 3 (for details, see Raymond et al. 2020). The Low-mass asteroid belt model proposes that Venus and Earth grew within a narrow ring/annulus of planetesimals, but few planetesimals ever formed in the primordial asteroid belt. Mars was stranded outside this ring and its growth was stunted (Hansen 2009; Drążkowska et al. 2016; Raymond and Izidoro 2017b; Izidoro et al. 2022). The Grand Tack model starts from the same extended planetesimal disk assumed in the classical model, but Mars' feeding zone was strongly depleted by Jupiter's gas-driven orbital migration, which first drove the gas giant inward to 1.5–2 AU, then back outward past 5 AU (Walsh et al. 2011; Jacobson and Morbidelli 2014; Raymond and Morbidelli 2014; Brasser et al. 2016). The third model is based on the giant planets' instability, which has been invoked by many studies to explain the giant planets' orbits and populations of small Solar System bodies (for a review, see Nesvorný 2018). While it was originally invoked as a late instability (Gomes et al. 2005), re-analysis of the dynamics and constraints suggest that it instead took place within 100 million years

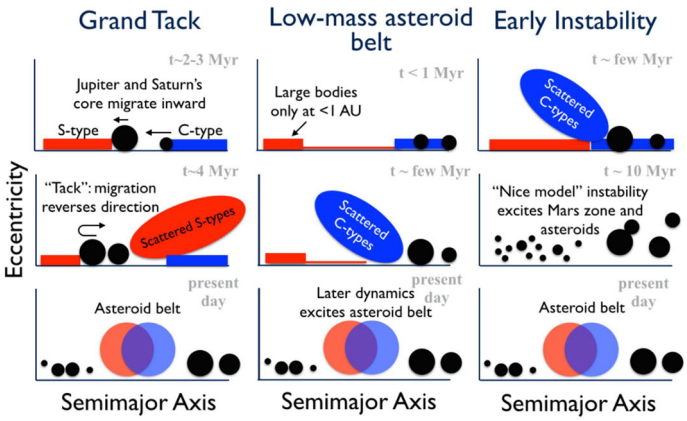

Fig. 3 Cartoon depiction of three global models of terrestrial planet formation that can match the inner Solar System (adapted from Raymond et al. 2020)

of the start of planet formation (Zellner 2017; Nesvorný et al. 2018; Morbidelli et al. 2018; Mojzsis et al. 2019), and perhaps during the dispersal of the gas disk itself (Liu et al. 2022b). An early instability naturally depletes the planetesimal disk exterior to Earth's present-day orbit and can match the terrestrial planets and asteroid belt (Clement et al. 2018, 2019,b, 2021). Finally, two recent models have proposed that pebble accretion and gas-driven migration may have been the dominant processes in terrestrial planet formation (Johansen et al. 2021; Brož et al. 2021), with just a single late giant impact to explain the formation of the Moon (Ćuk and Stewart 2012; Canup 2012).

Recent measurements have uncovered a dichotomy in the isotopic signatures of meteorites (Warren 2011; Kleine and Walker 2017; Kruijer et al. 2020). These signatures are apparent in a number of different elements with different chemical characteristics. This has led to a change in paradigm regarding the source material that built the planets: rather than a smooth gradient of chemical characteristics across a broad planetesimal disk, it is thought that two distinct reservoirs of planetesimals formed concurrently during the gas disk lifetime in different regions within the Solar System (e.g., Budde et al. 2016). In fact, recent analysis of samples of the asteroid Ryugu, returned from JAXA's Hayabusa2 mission, indicates that the meteorite isotopes actually represent a "trichotomy," with three distinct clusters such that there may have been three distinct planetesimal reservoirs in the Sun's planet-forming disk (Hopp et al. 2022). Exactly how the different reservoirs were kept apart is debated: the flux of inward-drifting pebbles may have been cut off by Jupiter's growing core (Kruijer et al. 2017) or by a pressure bump in the disk (Brasser and Mojzsis 2020; Izidoro et al. 2021a) or by something else (Lichtenberg et al. 2021b; Liu et al. 2022). The two main types of meteorites are called non-carbonaceous and carbonaceous. The parent bodies of non-carbonaceous meteorites are thought to have originated in the inner Solar System, whereas carbonaceous meteorites likely originated beyond Jupiter's orbit. The present-day orbital distributions of the different types of meteorites overlap in the asteroid belt (DeMeo and Carry 2014), but they almost certainly formed far apart (Raymond and Izidoro 2017b; Raymond and Nesvorný 2022).

Meteorite isotopes constrain the origin of Earth's water, and although we do not have comparison samples from Venus, we can use dynamical arguments to extrapolate to Venus. It has long been known that bulk Earth's D/H and $^{15/14}$N ratios are well-matched by carbonaceous chondrite meteorites (Marty and Yokochi 2006; Marty 2012). For the past 20

years it has been generally accepted that most of Earth's water was delivered from a carbonaceous source (Morbidelli et al. 2000; Meech and Raymond 2020). To match the isotopic signatures of a range of meteorites, Earth must have accreted almost entirely from non-carbonaceous (Enstatite chondrite-like) bodies indigenous to the inner Solar System, but with a ∼5% contribution from carbonaceous material, assumed to have originated beyond the orbit of Jupiter (Burkhardt et al. 2021). This small "pollution" of carbonaceous chondrite-like planetesimals represents the source of Earth's water in this context. However, recent measurements of Enstatite chondrites revealed that these objects contain far more water than previously thought, and with D/H and $^{15/14}$N ratios consistent with inner Earth (Piani et al. 2020). Measurements and analysis of zinc isotopes in different types of meteorites can concurrently match the isotope ratios of hydrogen, nitrogen and zinc if roughly two-thirds of Earth's volatiles were sourced locally and one-third was delivered from a carbonaceous source (Steller et al. 2022; Savage et al. 2022). Future isotopic measurements of other volatiles will certainly refine this analysis and give stronger constraints on the relative fraction of Earth's water that was sourced locally vs. delivered.

The question remains: what was the source of the carbonaceous component of Earth's water? In the classical model, Earth's feeding zone was broad enough that it extended past 2.5 AU, where it is assumed that water-rich planetesimals and planetary embryos originated (Morbidelli et al. 2000; Raymond et al. 2006). This mechanism delivered a modestly-smaller amount of water to Venus than Earth, simply because the tails of feeding zones of closer-in planets are less extended (Raymond et al. 2004). However, the initial conditions of the classical model are suspect, as it assumes that carbonaceous and non-carbonaceous planetesimals formed as close neighbors, which would predict a gradient in isotopic compositions rather than the observed dichotomy. Indeed, the present-day orbits of water-rich asteroids cannot represent the correct initial conditions for Solar System formation. Rather, carbonaceous asteroids were likely implanted from beyond Jupiter's orbit during the gas giants' growth (Raymond and Izidoro 2017) or migration (Walsh et al. 2011; Raymond and Izidoro 2017). During this implantation, a large population of scattered carbonaceous planetesimals would also have crossed the orbits of the terrestrial planets (Walsh et al. 2011; O'Brien et al. 2014; Raymond and Izidoro 2017; O'Brien et al. 2018). Given their source beyond Jupiter, scattered planetesimals would more efficiently deliver water to rocky planets at larger orbital radii. Earth (or its building blocks) would have accreted modestly more scattered planetesimals than Venus.

In the pebble accretion framework, water can be delivered by water-rich pebbles but only to planets orbiting beyond the snow line (Sato et al. 2016; Ida et al. 2019). As the disk cools in time, the snow line moves inward, and most models find a snow line interior to 1 AU during the late phases of the disk (Lecar et al. 2006; Kennedy and Kenyon 2008; Martin and Livio 2012; Bitsch et al. 2015). If the flux of carbonaceous pebbles was not blocked at this time, then Earth could have accreted water from drifting pebbles (as in the models of Johansen et al. 2021; Brož et al. 2021). Earth and Venus (or their building blocks) would have accreted similar amounts of water unless the snow line happened to lie in between the planets' orbits, in which case Earth could have accreted much wetter than Venus. While this is a narrow range of orbital radii, that range falls within the potential values for the snow line's position for reasonable disk parameters (Martin and Livio 2012; Bitsch et al. 2015). However, the relative contribution of carbonaceous material could not have been more than ∼5% according to meteorite isotopic studies that include a number of different elements (Burkhardt et al. 2021). This makes it difficult to reconcile the pebble accretion scenario with the terrestrial planets' growth and water delivery.

We can make an educated guess as to Venus' initial water content. Let us first assume that two-thirds of Earth's water was indeed sourced locally, as suggested by recent zinc isotopic

analyses (Savage et al. 2022; Steller et al. 2022), and that the rest was delivered by scattered carbonaceous planetesimals (Walsh et al. 2011; Raymond and Izidoro 2017b). Given their near-identical feeding zones (Izidoro et al. 2022), Venus would presumably have the same concentration of locally-sourced water as Earth. However, water delivery from scattered planetesimals has a radial gradient in efficiency such that Venus was likely delivered somewhat less water from carbonaceous sources than Earth (O'Brien et al. 2014; Raymond and Izidoro 2017b), implying an overall amount of water delivery within a factor of a few between the two planets, with Earth being modestly more water-rich. While there is still some variation in water contents in different Enstatite chondrites (Piani et al. 2020), it is hard to imagine that Venus could have formed completely dry.

The relative amount of incorporated water within Earth and Venus sensitively depends on the delivery mechanism, as well as their relative growth rates and the behavior of the underlying gaseous disk. Models for the source of Earth and Venus' water are clearly heavily influenced by isotopic measurements of different types of meteorites. We expect that new measurements that include a wider range of elements – in particular, more and more volatile elements and elements with different chemical properties – will guide our future thinking.

2.2.2 Energy Delivery, Heat Sources, and Mantle Initial Thermal State

In addition to water and other volatiles, the accretion process delivers a substantial amount of energy to the growing planets through impacts. Whether due to the accumulation of accretional energy after successive impacts (e.g., Safronov 1978; Tonks and Melosh 1993) or resulting from the thermal blanketing effect of a proto-atmosphere (e.g., Hayashi et al. 1979; Abe and Matsui 1985), the early stages of planetary evolution have long been thought to be punctuated by one or several events of surface and mantle melting (see Elkins-Tanton 2012, for a review). Yet, the extent and timing of this molten phase remains unclear. We review below the early heating mechanisms at play during planetary formation and discuss how they may affect the initial thermal state of the Venusian mantle.

Accretional Heating Several processes likely contribute significantly to increasing the protoplanet temperature and thus favor melting. During the accretion phase, planetary growth by impacts is thought to provide a large amount of kinetic energy. This is dissipated in the form of heat upon impact and responsible for local to global melting of the surface, extending throughout the mantle (Safronov 1978). The size/mass of colliding bodies, the impact velocity, angle, and frequency are key parameters controlling the time- and spatial-extent of melting (e.g., Nakajima et al. 2021).

During the so-called runaway accretion phase (e.g., Kokubo and Ida 1996; Kortenkamp et al. 2001), frequent successive/continuous collisions and associated heat accumulation are thought to provide an important heat source leading possibly to global-scale melting events. At the end of the accretion phase, planetary system formation models (e.g., N-body simulations) predict that the size of impactors increases so that collisions, although less frequent and well separated in time, become more and more energetic (e.g., Kokubo and Ida 1998, 2000; Chambers 2010; Morbidelli et al. 2012). Several tens of Mars-sized protoplanets are thought to form from planetesimal accretion, thus leading to several giant impacts between these protoplanets in the late accretion stages (e.g., Quintana et al. 2016). This ultimately implies melting episodes of greater extent (Kaula 1979; Tonks and Melosh 1993; Nakajima and Stevenson 2015), but likely more isolated in time. Giant impacts, followed by isostatic readjustement are even expected to entirely melt the mantle (Canup 2008; Nakajima and Stevenson 2015). However, in these late accretion stages, it has been suggested that the

energy of the giant impacts could be quickly (∼1 Myr) radiated to space because of their low frequency (Zahnle et al. 2007). Other studies suggest that the accretional heat generation rate does not significantly change with time, i.e., planetary heating is almost constant with/insensitive to planetary growth time, as longer time implies higher relative velocities, larger planetesimals and thus deeper heat burial (Kaula 1979). Furthermore, a remnant or outgassing steam atmosphere could sustain a runaway greenhouse state (e.g., Hamano et al. 2013) and significantly slow down the cooling of the protoplanet, and thus possibly maintaining a molten surface and mantle between successive giant collisions.

On early Earth, the hypothesis of a moon-forming single giant impact is often referred to as being responsible for the last global-scale mantle melting event (Canup 2004; Nakajima and Stevenson 2015). On Venus, the apparent absence of a moon and associated late giant impact may challenge the occurrence of such a deep and global magma ocean. Yet, it should be noted that the standard model of a single giant moon-forming impact is still debated for the Earth (e.g., Asphaug 2014). Alternative scenarios, involving smaller multiple impacts have been proposed and may better explain the compositional similarity of the Earth and Moon (Rufu et al. 2017). Regardless, the absence of a giant moon-forming impact cannot completely discard the likelihood of a fully or large-scale molten mantle stage, neither on Earth nor on Venus. The frequency of impacts and thus the accretion time scale must be considered. The collisional histories of the two planets may not have been identical, with Venus experiencing more hit-and-run collisions (that could explain its lack of satellite; Emsenhuber et al. 2021). Yet, giant impacts and associated tremendous energy delivery remain ubiquitous in inner Solar System planetary accretion (Quintana et al. 2016), thus suggesting that magma oceans were common events in the early evolution of terrestrial planets (e.g., Elkins-Tanton 2012; Schaefer and Elkins-Tanton 2018).

However, the absence of a Venusian moon certainly rules out the possibility of substantial tidal heating (solid-body tidal dissipation from the Sun alone could still slow Venus' rotation rate and induce tidal heating; Way and Del Genio 2020). This additional heat source affects solid materials more than the melt and thus is likely concentrated at the bottom of the crystallizing mantle (Zahnle et al. 2007). As mentioned previously, bulk similarities between the Earth and Venus, in terms of sizes and densities, suggest that the two planets have similar bulk compositions (e.g., Smrekar et al. 2018). Combined with their vicinity in the Solar System, and although no moon orbits Venus, it seems reasonable to think that they are composed of similar materials. As discussed above they likely accreted in a relatively similar way with associated accretional heating and therefore analogous thermal histories including substantial interior melting.

Radiogenic Heating The presence of radioactive elements, generating heat with decay, is also thought to be a significant *internal* heat source of rocky planets, thus contributing to melting of the planetary interior (e.g., Elkins-Tanton 2012; Solomatov 2015). Active on a timescale of about one million years and thus affecting the earliest evolutionary stages (within the first few million years after CAI formation[2]), radioactive decay of short-lived radionuclides, such as now extinct ^{26}Al and ^{60}Fe isotopes (half-lives of 0.717 Myr and 2.61 Myr, respectively), contributed to the heating and differentiation of early forming and growing bodies: planetary embryos, planetesimals, and proto-planets, starting before the end of the accretion phase (Urey 1955; Merk et al. 2002; Yoshino et al. 2003; Elkins-Tanton et al. 2011; Šrámek et al. 2012; Fu et al. 2017; Bhatia 2021). ^{26}Al decay dominates the heat budget while the decay of other radionuclides such as ^{10}Be, ^{53}Mn, ^{146}Sm, ^{182}Hf, or ^{244}Pu have

[2] **C**alcium-**A**luminum-rich **I**nclusions are believed to be the earliest formed materials in the Solar System and thus define its formation age, ∼4.568 billion years ago (Bouvier et al. 2007; Burkhardt et al. 2008).

a minor contribution (Lee et al. 1976; Chaussidon and Gounelle 2007; Elkins-Tanton 2012; Fu et al. 2017; Lugaro et al. 2018). To a lesser extent but on longer timescales and still active today (e.g., Schubert et al. 2001; Jaupart et al. 2015), long-lived radioactive elements ^{238}U, ^{235}U, ^{40}K, and ^{232}Th (half-lives ranging between 0.7 and 15 Gyr) were more abundant early in the Solar System and also took part in the early heat budget (Urey 1955; Lebrun et al. 2013; Nikolaou et al. 2019).

The amount of radiogenic heat produced relates directly to the abundance of the radioactive elements. As mentioned above the proximity of Earth and Venus combined with their similar bulk compositions (e.g., Smrekar et al. 2018), also suggest that they have accreted roughly similar materials with similar endowments of radioactive elements. Both planets have thus likely experienced similar amounts of radiogenic heating and resulting extent of interior melting.

Thermal Blanketing Effect of a Primordial Atmosphere Whether the energy sources primarily heat up the surface and extend downward through the mantle (accretional heating) or primarily affect the interior (radiogenic heating), as soon as the planet is heated, the excess energy must escape to reach thermal equilibrium with the relatively cold surroundings. Then, whole planet cooling involves heat being radiated to space. This is particularly important when the surface is molten.

Without an atmosphere, the planet radiates directly into interplanetary space as a black body with the temperature of the planet's surface, making radiation of energy very efficient (dashed purple line, Fig. 4). In such a case, the cooling stops when the planet reaches thermal equilibrium, i.e., when the surface temperature reaches the equilibrium temperature of the planet (that is the temperature at which the power supplied by the star is equal to the power emitted by the planet).

In the presence of an atmosphere, radiative dissipation of energy from the surface is buffered by the thermal blanketing effect of the surrounding atmosphere and heat is retained. This can maintain the surface temperature above the rock melting point. Several works have reviewed the different stages of the evolution, corresponding to different types of early/primordial atmosphere (i.e., not outgassed from the interior during the solidification process) and related forming-mechanisms.

In the earliest disk-embedded stages of planetary evolution (if the proto-planet accreted enough mass within the disk lifetime), the gravitational capture of gas from the surrounding solar nebula (see Sect. 2.1) and the blanketing effect of the accreted opaque atmosphere is itself thought to keep the surface temperature of the proto-planet above the silicate melting point (e.g., Hayashi et al. 1979; Ikoma and Genda 2006; Olson and Sharp 2019). Ikoma and Genda (2006) have shown that starting from 0.5 Earth masses, proto-planets surrounded by such nebula-captured atmospheres are expected to have a molten surface. If the surface is already molten because of the previously discussed energy sources, such an atmosphere would undoubtedly favor a long-lasting molten layer. Depending on the thermal opacity of the primordial atmosphere and on the prior thermal state of the interior, the molten shell is thought to extend more or less deeply into the mantle. The interior could thus be maintained in a partially or fully molten state throughout the protoplanetary disk lifetime, until dissipation of the solar nebula and the primordial atmosphere.

In the eighties, Abe & Matsui pioneering magma ocean-related studies addressed the evolution of an impact-generated steam atmosphere and its implications for the early thermal history of the Earth (Matsui and Abe 1984; Abe and Matsui 1985; Matsui and Abe 1986a,b; Abe and Matsui 1988). Such atmospheres result from the devolatilization of incoming planetesimals upon impact, thus releasing volatile species, such as H_2O (due to shock dehydration; e.g., Benlow and Meadows 1977; Boslough et al. 1980; Lange and Ahrens 1982) and

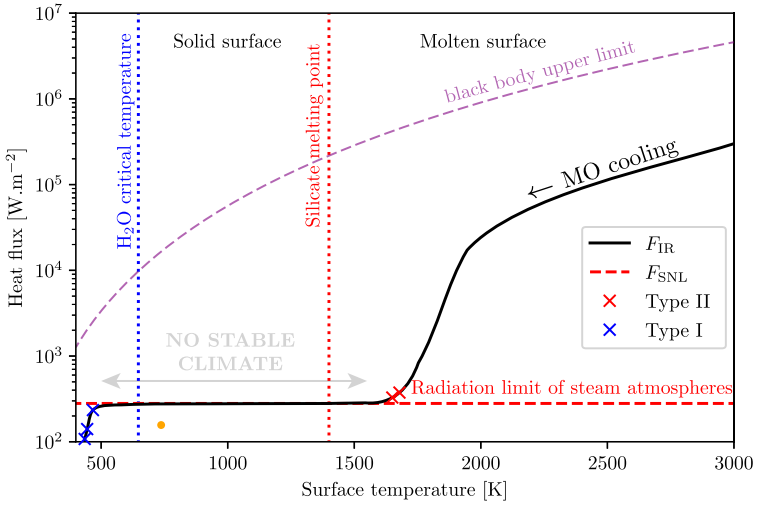

Fig. 4 Outgoing thermal flux emitted at the top of the atmosphere (F_{IR}, black line) as a function of surface temperature for a steam (H_2O-dominated) atmosphere (see Fig. 13 for CO_2-dominated atmospheres). Global radiative equilibrium and associated climate stability are reached on either sides of the radiation limit of steam atmospheres: the asymptotic Simpson–Nakajima limit ($F_{SNL} \approx 280$ W.m^{-2}, dashed red line), when the thermal emissions balance the absorbed insolation ($F_{IR} \approx F_{abs}$). This radiation limit is responsible for a runaway greenhouse. At the ERCS (i.e., when the heat flux from the interior of the planet becomes negligible compared to the net absorbed stellar flux; see Sect. 3.3), climate stability can be reached either with temperate surface conditions and a water ocean (Type I planets, e.g., blue crosses), for planets whose net absorbed flux is below the radiation limit ($F_{abs} < F_{SNL}$), or with a molten surface (Type II planets, e.g., red crosses), for planets whose absorbed flux exceeds the radiation limit ($F_{abs} > F_{SNL}$). Crosses indicate the surface conditions reached at the ERCS for early Venus (i.e., at Venus' orbital distance around the young Sun) and considering different Bond albedo values ($\alpha = [0.2, 0.3, 0.5, 0.7, 0.77]$ from right to left). These crosses correspond to the ones shown in the lower part of Fig. 12. Depending on its Bond albedo at the end of the rapid cooling stage, early Venus can either be habitable or not. Reciprocally, these surface conditions would be reached on a planet absorbing (and emitting) the corresponding amount of solar radiation, i.e., located at various orbital distances, while considering a constant Bond albedo. The orange dot denotes present-day Venus

CO_2, directly *into* the atmosphere. Alongside other early studies (Zahnle et al. 1988; Kasting 1988), they showed that once such an impact-generated atmosphere is formed, its thermal blanketing effect is responsible for heating the surface of the accreting Earth up to its melting point (∼1400 K), thus forming a magma ocean. This may also apply to Venus. Matsui and Abe (1986b) emphasized that the distance from the star and the heat flux equilibria at the end of the magma ocean stage might explain the current differences between the Earth and Venus, thus demonstrating the importance of the early evolution of terrestrial planets in setting their potential habitability. These results were revisited almost 30 years later in the light of a more sophisticated molten interior–atmosphere coupled model (Hamano et al. 2013, see Sects. 3 and 4). Note that a hybrid-type proto-atmosphere, made of a mixture of both solar nebula and impact degassing products is also thought to be thermally opaque enough to produce a deep magma ocean, and hence sustain an already existing one (Abe et al. 2000; Saito and Kuramoto 2017).

The increase of atmospheric water vapor concentration, or the increase of heat to be radiated through a steam atmosphere after an energy delivery (such as after an impact), results in high surface temperatures triggered by the runaway greenhouse effect of steam dominated atmospheres (e.g., Simpson 1927; Kasting 1988; Nakajima et al. 1992). This runaway be-

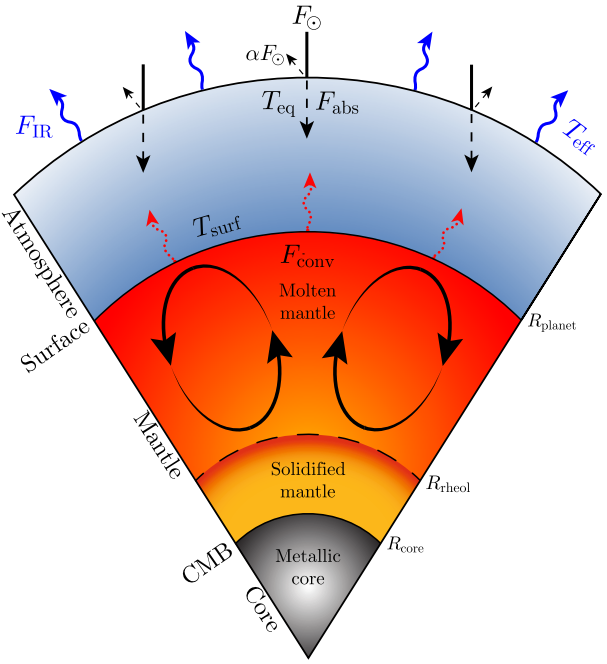

Fig. 5 Schematic cross section of a planet in the magma ocean stage surrounded by an atmosphere and associated heat fluxes. The vigorous convection of the molten mantle provides a substantial heat flux at the surface of the planet, $F_{\rm conv}$ (dotted red arrows). A fraction α, the Bond albedo, of the total solar radiation received by the planet $F_\odot$ (plain lines at the top of the atmosphere) is reflected back into space. The remaining flux is absorbed by the atmosphere ($F_{\rm abs}$, dashed black arrows entering the atmosphere). These two incoming heat fluxes balance the outgoing infrared/thermal flux radiated at the top of the atmosphere, $F_{\rm IR}$ (blue arrows), that ultimately control the cooling of the whole planet

havior is due to the existence of a nearly-asymptotic radiation limit in the thermal (infrared) radiation a planet can emit as a function of its temperature (Fig. 4). This asymptotic radiation limit is often referred to as the Simpson–Nakajima limit (see Goldblatt and Watson 2012, for a review), whose corresponding flux value is $F_{\rm SNL} \approx 280$ W.m^{-2}. In planetary atmospheres, steady-state global radiative balance, and thus climate stability, is achieved by the equilibrium between the net, absorbed incoming stellar radiation, $F_{\rm abs}$, and the outgoing thermal radiation ($F_{\rm IR}$) emitted by the atmosphere (also referred to as the outgoing longwave radiation, OLR) (Fig. 5), as a response to the heating of the surface and atmosphere resulting from their absorption of the stellar flux (sunlight). The net, absorbed incoming stellar radiation is:

$$F_{\rm abs} = (1 - \alpha) \times F_\odot \quad , \tag{1}$$

where α is the fraction of the total incident solar radiation scattered back out into space in all directions and integrated spatially over the whole globe (spherically) and spectrally over all wavelengths, i.e., the global bolometric or Bond albedo (e.g., Hanel et al. 2003). $F_\odot$ is the total incident stellar flux received at the top of the atmosphere (TOA) of a planet orbiting the host star at a distance D (in AU) and averaged over the planetary surface area:

$$F_\odot = \frac{1}{4} \frac{\mathcal{S}_\odot^{\rm N}}{D^2} \quad . \tag{2}$$

$\mathcal{S}_\odot^{\rm N} = 1361$ W.m^{-2} is the total solar irradiance, i.e., the spectrally integrated, mean total electromagnetic energy received from the Sun at a distance of 1 AU per unit area (Kopp and Lean 2011; Prša et al. 2016). The factor 1/4 comes from the ratio of the planet's cross-sectional area to its surface area: the planet intercepts the incident solar beam as a disk but radiates as a sphere over its entire surface (e.g., Pierrehumbert 2010). Thus, if there is a heat

supply, through an increase of the absorbed stellar flux or after an impact, the planet warms and consequently emits more thermal radiation to space to maintain energy balance. In the steam atmosphere case, most of this emission occurs through the water vapor infrared atmospheric "window," between ∼8–13 μm. It thus matches the Wien peak in surface thermal emission at 10 μm; the spectral region essentially transparent (with relatively little absorption) to infrared radiation. However, when the heat flux reaches the critical radiation limit, or when atmospheric water vapor becomes too abundant as a result of oceans evaporation or following impact-degassing, the moist atmosphere becomes optically too thick for heat to be radiated. The outgoing thermal flux can no longer increase and lose heat despite an increasing temperature, i.e., surface warming no longer leads to more thermal emission. This inevitably leads to an increase in the surface temperature $T_{\rm surf}$, hence a runaway greenhouse. This remains until the planet is warm enough to radiate heat in the 4 μm water vapor window, when $T_{\rm surf}$ reaches about 1600 K (which is above the surface melting point), thus restoring radiative balance and climate stability (e.g., Goldblatt and Watson 2012; Goldblatt et al. 2013, see Fig. 4, Sects. 3 and 4 for more details and implications for habitability). This explains the abrupt transition between these extreme stable climatic states on either side of the radiation limit (Fig. 4): temperate or relatively cold surface conditions on one side ($F_{\rm IR} < F_{\rm SNL}$), and a molten surface on the other side ($F_{\rm IR} > F_{\rm SNL}$). Conversely, a molten surface state can only transition to a temperate climate by two means. Through removing water vapor from the atmosphere by photo-dissociation and hydrogen escape, thus decreasing atmospheric opacity. Alternatively it is possible via a decrease of the thermal radiation: if the additional heat supply stops and the absorbed stellar flux remains below the radiation limit for instance.

However, it is important to note that the runaway greenhouse effect and associated abrupt climate transition occurs only for H_2O-dominated atmospheres, as their main component is both a condensable and thermal absorber species. Its triggering radiation threshold value may be sensitive to the atmospheric relative humidity and planetary mass (e.g., Ishiwatari et al. 2002; Goldblatt 2015). For other atmospheric compositions, the radiation limit, if relevant, is not that steep and radiative balance and thus stable climates can be reached for intermediate conditions where the surface is not molten (e.g., Type III planets in Salvador et al. 2017, see Fig. 13 and Sect. 4 for a detailed discussion). In the presence of such "moderately-blanketing" primordial atmospheres, the atmosphere may not melt the surface by itself, but would still buffer the dissipation of heat resulting from other processes, thus contributing to maintaining a molten surface.

Overall, the blanketing effect of a proto-atmosphere, regardless if it is nebula-captured, impact-degassed, or a mixture of both, can melt the planetary surface. Consequently, if the surface is already molten, it will buffer radiative dissipation and maintain the surface temperature above the melting point. If not, it will enhance the thermal effect of any heating mechanism, significantly increasing the likelihood and subsistence of a magma ocean. Yet, it is important to note that any pre-existing primordial atmosphere is subject to depletion, either through the disk dissipation for nebula-captured atmospheres, or through impact erosion. In the case of a nebula-captured atmosphere, the timescale of disk dissipation and following atmospheric escape must be compared to the energy delivery timescale (accretion + radioactive decay timescales) to evaluate the thermal contribution of the atmosphere in maintaining the molten surface.

For an impact-generated atmosphere, if the atmospheric mass added by impact degassing overcomes or balances atmospheric losses due to impact erosion, the atmosphere keeps being replenished after successive collisions or keeps a roughly constant mass and its thermal

blanketing effect is maintained over time. In such a scenario, the atmosphere helps to maintain the molten surface between successive impacts and the heat generated keeps accumulating. This likely keeps the planet molten during the entire accretion sequence. Conversely, if the atmosphere loses mass after each collision, its blanketing power would decrease according to the accretion time scale and resulting erosion rate until it becomes too thin to retain heat. Then, heat would more efficiently dissipate and the atmosphere would not be responsible for melting the surface or keeping it molten during the entire accretion sequence. If the heating rate due to the other mechanisms is lower than the dissipation rate, the planet would only experience transient and local magma oceans/ponds. Depending on the dissipation timescale of the proto-solar nebula relative to Venus' accretion timescale, and in case a protoatmosphere survives atmospheric erosion by late impacts, the blanketing effect provides an additional heat source to extend and enhance the existing ones.

Based on element partitioning analysis, Sakuraba et al. (2019) suggested that the survival of the primordial atmosphere through the late accretion may partially account for the present-day atmosphere of Venus. This implies that such an early and long-lasting atmosphere maintained a strong greenhouse effect during the accretion of Venus. Thus it would significantly retain any heat produced – strongly supporting the idea that Venus' evolution started with a molten surface and an extensively molten mantle.

Metal–Silicate Differentiation and Core Formation The early thermal state and melting extent of the mantle is tightly linked to metal–silicate segregation and metal downwards migration that relate to core formation. Due to the strong fractionation of lithophile (silicate-loving) Hf from siderophile (metal-loving) W during core formation, the ^{182}Hf–^{182}W system (^{182}Hf decays to ^{182}W with a half life of 8.9 Ma, which can be used to date processes in the first ~60 Myr) is particularly well suited to trace and date metal–silicate differentiation (Lee and Halliday 1995; Harper and Jacobsen 1996; Lee and Halliday 1997; Horan et al. 1998; Quitté et al. 2000; Jacobsen 2005; Rubie et al. 2015b).

Early work on ^{182}Hf–^{182}W chronometry of meteorites indicate that an idealized, instant core formation in the terrestrial planets must have been completed during the first ~30 Myr of the Solar System history (Kleine et al. 2002; Yin et al. 2002). Yet, this simplistic instantaneous core formation model only provides a lower time constraint and does not apply for larger, Earth-sized bodies, where core formation did not occur as a single event but rather as a combination of discrete delivery of metallic components to the deep interior (e.g., Kleine et al. 2009; Deguen et al. 2014; Rubie et al. 2015b; Nimmo and Kleine 2015).

Accounting for the different mechanisms of core formation in more realistic scenarios leads to estimates ranging between 30 to 200 Myr (e.g., Chambers 2001) at the very most (see Rubie et al. 2015b; Nimmo and Kleine 2015, for extensive reviews). Similarly, the more radiogenic W isotopic composition of the silicate Earth compared to that of chondritic meteorites demonstrates that Earth has differentiated into a mantle and core within the lifetime of ^{182}Hf (~30–50 Myr; e.g., Jacobsen 2005). Rapid terrestrial planet formation and early metal–silicate separation are also consistent with rapid planetesimals formation and differentiation informed from ^{53}Mn–^{53}Cr (Lugmair and Shukolyukov 1998) and ^{26}Al–^{26}Mg (Srinivasan et al. 2000) systematics (Nyquist et al. 2001; Wadhwa et al. 2006; Nyquist et al. 2009), and observations of other planetary systems (Briceño et al. 2001; Bodenheimer and Lin 2002).

Core formation is a complex, multi-stage phenomenon most likely resulting from the combination of different processes operating over different timescales such as percolation of liquid metal through a compacting solid silicate matrix, iron droplets sinking through a magma ocean, negative diapirism generated by Rayleigh-Taylor instability, or hydraulic

fracturing (e.g., Ricard et al. 2009; Deguen et al. 2014; Rubie et al. 2015b; Landeau et al. 2016; Wacheul and Le Bars 2018; Clesi et al. 2020; Landeau et al. 2021). Because the relative contribution and timing of each process is still unclear, large uncertainties remain. In any case, mechanisms of core formation depend on the thermal state of the planetary body and require some extent of partial melting (e.g., Rubie et al. 2015b). Given its suggested relatively short timescale, core formation is also generally thought to require a mechanism for efficiently segregating metal (Stevenson 1990; Yoshino et al. 2003). The low viscosity of the melt and high temperatures facilitate material deformation needed for mass redistribution (e.g., Šrámek et al. 2010, 2012; Nimmo and Kleine 2015). Therefore, large extent of mantle melting is thought to facilitate metal–silicate segregation and metal migration. Thus, a great extent of mantle melting is believed to favor rapid core formation suggested by geochemical evidence. This view is also supported by the mantellic abundance of moderately siderophile elements (MSEs; e.g., Fe, Ni, Co, W, and Mo) that may be explained by a final metal–silicate equilibration at very high P and T, i.e., at the base of a deep magma ocean (e.g., Li and Agee 1996; Righter and Drake 1997, 1999; Rubie et al. 2003, 2015b). Note however that alternative mechanisms, such as percolation of iron-rich melt through solid silicate, have been proven to result in rapid core formation without necessarily involving a substantial amount of mantle melting (Ghanbarzadeh et al. 2017; Berg et al. 2018). The respective contribution and timing of the different mechanisms involved in core formation need to be further considered to draw a realistic picture of this complex, multi-stage phenomenon, accounting for both geochemical and geophysical constraints (e.g., Badro et al. 2015).

Other terrestrial isotopic data analysis suggest that the mantle experienced early and global/major chemical differentiation (^{146}Sm–^{142}Nd system; Caro et al. 2003, Boyet et al. 2003, Boyet and Carlson 2005), and that the growth of continental crust began early (^{176}Lu–^{176}Hf and ^{147}Sm–^{143}Nd; e.g., Bennett et al. 1993, Amelin et al. 1999, Bizzarro et al. 2003, Harrison et al. 2005), within 30 Myr and in the first 200 Myr of evolution, respectively, which both might require a global, deep magma ocean (Harrison 2009; Caro 2011; Solomatov 2015). Yet, one should note that these results could reflect multiple possible scenarios given the uncertainties affecting the isotopic measurements themselves, their representativeness and the various fractionation processes. One promising way to overcome individual limitations of each isotopic system and to provide tight constraints on the timescale of accretion and early differentiation is to build scenarios that satisfy several different isotopic systems simultaneously and that are consistent with the results of dynamical models (e.g., Halliday 2004; Wood and Halliday 2005; Nimmo and Kleine 2015).

Overall, geochemical constraints may indicate that core formation and large-scale mantle differentiation occurred at similar timescales. These are likewise comparable to the accretion timescales constrained by planetary formation models. If planetary accretion, core formation, and mantle differentiation occurred concurrently and on short timescales, the rapidity of the processes themselves would be indicative of a significant degree of mantle melting. The amount of energy involved would induce large-scale melting, thus likely suggesting the existence of a global and deep magma ocean (Solomatov 2015).

Core formation is not only linked to the degree of mantle melting through the ease of metal–silicate segregation and iron migration but has also important energetic implications for the mantle thermal state (e.g., Jaupart et al. 2015; Solomatov 2015). Indeed, the release of gravitational energy from the gravitational differentiation between metallic and silicate materials during core formation, is dissipated by viscous heating in both the iron and silicate phases. This supplies an additional and substantial source of heat supporting a whole molten silicate layer scenario (e.g., Solomon 1979; Sasaki and Nakazawa 1986; Ricard et al. 2009; Monteux et al. 2009; Šrámek et al. 2010; Samuel et al. 2010; Rubie et al. 2015b; Landeau et al. 2016). The energy released by rapid core formation, itself favored by extensive

mantle melting, could be responsible for heating the entire Earth to ∼1700 K (Tozer 1965; Flasar and Birch 1973). Additional release of gravitational energy due to the redistribution of chemical and thermal heterogeneities in the mantle and segregation of leftover iron (density heterogeneities) following core formation is also thought to increase the temperature by several hundred degrees (Tonks and Melosh 1992; Solomatov 2015).

Numerical simulations of giant impacts emphasize that during collisions of large differentiated bodies the iron core of the impactor is the most heated material (Canup 2004). After its presumably rapid segregation into the impacted protoplanetary core, a substantial fraction of the associated gravitational potential energy might be retained within the segregated iron, resulting in an early superheated core (Stevenson 2001; Solomatov 2015). The heat transferred to the mantle may induce additional mantle melting or sustain its molten state and extend the magma ocean lifetime (Ke and Solomatov 2006, 2009).

Similarly and over longer timescales, once the core is formed, the release of heat from the core at the core–mantle boundary (CMB) constitutes an additional heat source. While little is known about early magma ocean–core interactions, they certainly affect each other's evolution. Indeed, the core constitutes an evolving boundary condition of the mantle and contributes to the heat budget of the interior. It thus certainly affects the cooling timescale and crystallization pattern of the magma ocean. In turn, the lower mantle conditions resulting from the magma ocean evolution may buffer the heat loss from the core and provide additional heat. This could thus affect the thermal state and dynamics of the core and influence the resulting dynamo and potential magnetic field strength with time (e.g., Stevenson 2001; Ke and Solomatov 2009). However, in the absence of evidence of a present or past magnetic field on Venus, that could inform the thermal and dynamical state of its core, the core–mantle interactions and their effects on the thermal history of the planet remain highly unconstrained. For the early Earth, estimates of the initial CMB temperature are above the mantle melting temperature and thus indicate extensive lower mantle melting at that time, therefore implying a deep magma ocean (e.g., Andrault et al. 2016, see Fiquet 2018 for a review). Relics of this early magma ocean retained at the CMB may exist today as a hypothetical deep molten zone on top of the Earth's core that might explain the current zones/patches of extremely low seismic velocities (ultra-low velocity zones, ULVZs) shown by seismology. On Venus, the supposedly less efficient cooling of the interior relative to Earth due to the absence of plate tectonics might favor the existence of a thick basal magma ocean today (O'Rourke 2020), inherited from the primordial heat accumulated. Testing this hypothesis might provide constraints on Venus early state and accretion vigor.

Young Sun Stars are expected to be significantly more active during their early evolution, and as a result, stellar evolution models predict that both the X-ray–EUV emissions and the magnetic field strength of the Sun were larger in the past (e.g., Bahcall et al. 2001; Ribas et al. 2005; Tu et al. 2015; Johnstone et al. 2021). On top of affecting planets' atmospheric properties and habitability (e.g., Gallet et al. 2017), the energetic environment in which forming planets and planetesimals are embedded can be responsible for significantly heating and possibly melting their interiors. In particular, the strong magnetic field and enhanced solar wind of young stars generates electromagnetic induction heating that could substantially melt planetary mantles and result in the formation of magma oceans (Sonett et al. 1968; Herbert et al. 1977; Kislyakova et al. 2017; Kislyakova and Noack 2020; Noack et al. 2021). While this energy source was likely effective during the early stages of planetary formation and certainly affected proto-Venus, its contribution remains unconstrained. Finally, despite a relatively weaker contribution compared to the other aforementioned mechanisms, the enhanced high energy X-ray and EUV emissions of the young Sun (e.g., Ribas et al.

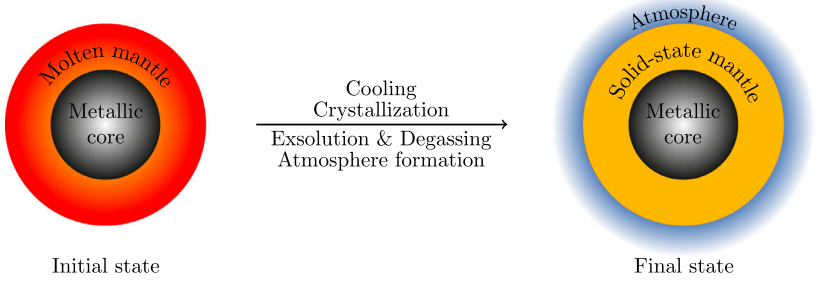

Fig. 6 Sketches of the hypothetical initial and final states usually considered in magma ocean–atmosphere thermal evolution numerical studies. Initially, as the aftermath of a hypothetical last giant impact, the silicate mantle is assumed to be fully molten, meaning that the magma ocean extends throughout the entire mantle. Any primary, captured atmosphere (if one existed at all) has been lost. All volatile species are then assumed to be initially dissolved within the molten mantle. Heavier, core-forming elements, such as metallic iron, are thought to have already fully segregated to the core, meaning that the metallic core is already formed. During the cooling and crystallization of the magma ocean, volatile species initially dissolved within the melt are exsolved and outgassed, thus progressively building-up the atmosphere. One should distinguish the end of the molten stage, that is when the mantle has fully solidified, from the end of the rapid cooling stage (ERCS; see Sect. 3.3). The latter is reached when the heat flux from the interior of the planet becomes negligible compared to the net absorbed stellar flux ($F_{\rm abs}$) that thereafter balances the thermal emissions at the top of the atmosphere, $F_{\rm IR}$ (i.e., the planet has reached global radiative equilibrium), and controls the surface conditions. Depending on the net absorbed flux, the planet can achieved global radiative balance with a fully or partially solidified mantle at the ERCS. Once the ERCS is reached, the evolution is no longer controlled by the molten mantle (if still molten) but rather by the balance between the absorbed stellar flux and the thermal emissions

2005; Johnstone et al. 2021) may also induce additional heating of the planetary surface and atmosphere, and should then be accounted for in the thermal budget.

Initial Thermal State To conclude, the respective contribution and timing of each individual heating source to the warming and melting of the terrestrial planets' mantle remain unclear. Their combination and temporal overlap imply that generated temperatures were high enough to melt a large part – if not all – of the silicate mantle. Furthermore, the different heat sources involved are likely common and inherent to the early history of rocky planets. Thus, it seems reasonable to assume that, like Earth, Venus experienced at least one global magma ocean phase extending throughout the entire mantle during its early evolution.

For the sake of simplicity, thermal evolution studies of the early magma ocean phase generally model the cooling of a hypothetical last episode of mantle global-scale melting. By cooling down and crystallizing, the molten, liquid-state mantle evolves toward a solid-state mantle, which represents the starting point for the long-term evolution of the planet (Fig. 6; see Sects. 3 and 4). Note that depending on the absorbed stellar flux, global radiative equilibrium can be reached with a molten or solidified surface (see Sect. 3.3). For the Earth, such a global melting event often refers to the result of the late, giant moon-forming impact scenario. Yet, as discussed above, it seems reasonable to follow the same approach to address the early evolution of Venus (and other Earth-sized rocky planets) even in the absence of a Venusian moon. It should be noted that subsequent events such as late giant impacts may substantially affect, at least locally, the heat budget, interior stratification, and volatile distribution of the solidifying planet (e.g., Gabriel and Cambioni 2023). The classically described early thermal evolution sequence remains a simple and theoretical view.

As mentioned above, isotopic signatures can provide more specific constraints on the timescales and energetic of the accretion phase and early evolution and thus on the resulting

early thermal state of rocky planets. Such future measurements on Venus would provide helpful constraints to decipher its evolutionary pathway and understand why it ended up being so different from Earth (see Sect. 5 and Widemann et al. 2023, in this collection).

2.3 Constraints from Isotopes

The very high D/H ratio of hydrogen in the Venus atmosphere (157 times higher than terrestrial water; Von Zahn et al. 1983) has often been interpreted as evidence that Venus underwent intense episodes of hydrogen escape (Donahue et al. 1982). These escape episodes would be responsible for the low abundance of water on Venus and would have influenced the entire geological evolution of the planet (Baines et al. 2013). However, fractionation of D from H isotopes during atmospheric escape of hydrogen depends on the regime and parameters of atmospheric escape (Hunten et al. 1987). Some escape regimes of hydrogen create only a limited isotopic fraction of the remaining hydrogen (Zahnle et al. 1990). Thus the D/H ratio gives only partial information and it remains unclear how much water really escaped from Venus. One could imagine a scenario in which considerable amounts of water escaped but that the isotopic fractionation was relatively inefficient. Conversely, the planet could have accreted almost dry and lost only a small amount of water but with a regime of escape leading to intense isotopic fractionation.

The initial D/H ratio of water is an important unknown in models of hydrogen escape from Venus. This ratio was probably lower than it is today but by how much remains unclear. It cannot be excluded that Venus' water was initially sourced by comets which can show elevated D/H ratios (e.g., 3 times the terrestrial value for water emitted from comet 67P/Churyumov–Gerasimenko; Altwegg et al. 2015). Interestingly, there is a high abundance of neon in the atmosphere of Venus and its isotopic composition seems intermediate between solar and meteoritic components (see Avice et al. 2022, this collection). Comets are likely to be devoid or highly depleted in neon (whose $T_{\text{condensation}} \approx 20$ K). The presence of neon in its atmosphere likely indicates that comets cannot be the sole contributors to volatile elements on Venus. Cometary water could have been brought to Venus and added to an original solar- or chondritic-derived atmosphere, or primordial neon could have been degassed from the mantle through time. The value of the Ar/Ne elemental ratio of Venus' atmosphere seems high compared to what would be expected from a pure mixture between solar and chondritic neon. While the large error bars on the Ar/Ne ratio does not allow one to draw any firm conclusions, a high Ar/Ne would be compatible with a cometary contribution to the Venus atmosphere. Such cometary contribution has been identified for Earth, based on the isotopic composition of primordial Earth's atmospheric xenon (Pepin 1991; Marty et al. 2017; Avice et al. 2017). However, the D/H ratio of Earth's water is close to a chondritic value, meaning that comets probably contributed less than 1 percent of Earth's total water budget (Fig. 7; Marty et al. 2016, Bekaert et al. 2020). Yet, this estimate is only valid if data collected for 67P/C–G are representative of cometary diversity. The possibility of an asteroid–comet continuum makes definitive statements difficult given the few available measurements and their uncertainties (Gounelle 2011). Furthermore, D/H ratio interpretations remain problematic given the number, uncertainties, and complexity of the processes affecting them (Stephant et al. 2016, 2018; Piani et al. 2020; Stephant et al. 2020).

It must be noted that elements such as noble gases can also escape from planetary atmospheres during episodes of hydrogen escape and that such escape would lead to elemental and isotopic fractionation of these elements (Hunten et al. 1987; Zahnle et al. 2019). Future data on the elemental and isotopic composition of noble gases collected in the atmosphere of Venus, for example during the recently selected DAVINCI (NASA) mission (Garvin et al.

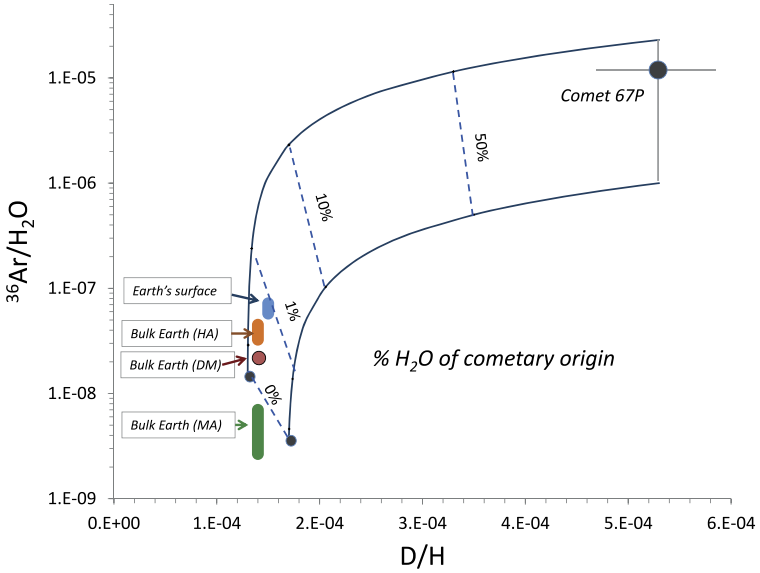

Fig. 7 $^{36}Ar/H_2O$ versus D/H mixing diagram between cometary (represented by 67P/C–G) and chondritic end-members. The mixing curves depend on the elemental and isotopic composition of the end-members. Comets have high Ar/H_2O ratios implying that more than 90% of Ar could of cometary origin while only about 1% of Earth's water would have been brought by comets (without altering the initial chondritic-like D/H ratio). HA, DM and MA are the bulk Earth estimates from Halliday (2013), Dauphas and Morbidelli (2014) and Marty (2012), respectively. Figure modified after Marty et al. (2016, see also refs. therein)

2020, 2022), will certainly help to put constraints on models attempting to track the joint history of water and noble gases on Venus and to compare the case of Venus with other terrestrial planets (Avice and Marty 2020).

3 Magma Ocean Evolution and the Formation of the Secondary Atmosphere

3.1 Magma Ocean Cooling and Solidification

There is no strict definition of what is referred to as "magma ocean". The term "magma" refers to a multiphase mixture of liquid (melts), solid (crystals), and gas (bubbles) composing a molten rock (e.g., Lesher and Spera 2015) and "ocean" was used to reflect the low, water-like viscosity of the mixture and the fact that the system is virtually 100% liquid (e.g., Warren 1985; Solomatov 2015). The magma ocean must then behave rheologically as a liquid, with a crystal fraction small enough that crystals are suspended within the melt without being interconnected. In addition, previous definitions include a criterion regarding the extent of melt, such that the magma must encompass a substantial fraction (more than 10%) of the body (Taylor and Norman 1992).

This general definition can be confusing as it may encompass a large variety of cases. These include drastically different scenarios such as a periodically molten planet as a result of tidal heating in an eccentric orbit, and a planet *ad-aeternum* molten owing to its proximity to the star. A fundamental distinction can be made compared to the early transient

molten stage. The latter is likely inherent to the early evolution of rocky planets. This is in contrast to the long-lasting, steady-state molten stage experienced by planets in close-in orbits around their star; sometimes referred to as "lava worlds". Here we focus on the former, which is likely experienced by most terrestrial planets due to the combination of the heat sources detailed in Sect. 2.2.2. Compared to the steady-state, sustained molten stage of lava worlds, early transient magma oceans are not in thermal equilibrium with their colder stellar environment. They are cooling down, losing excess heat to reach equilibrium. As a fluid-like material, the magma ocean can efficiently transport and lose heat by advecting matter. Its dynamics and cooling are thus controlled by thermal convection. More precisely, as the molten mantle loses its internal heat while being cooled from above, it corresponds to the classical problem of Rayleigh-Bénard convection.

In such a case, the Navier–Stokes equations are used to describe the motion and evolution of the fluid. Using appropriate characteristic scales, two key dimensionless parameters regarding the fluid convective dynamics arise from the non-dimensional form of the momentum conservation equation (itself originating from Newton's second law): the Rayleigh number, Ra, and the Prandtl number, Pr. The thermal Rayleigh number,

$$Ra = \frac{\theta g \Delta T L^3}{\kappa \nu} \quad , \tag{3}$$

compares the thermal buoyancy force that drives convection to the advection-resisting effects of thermal and momentum diffusion (viscous dissipation). The motion-driving parameters are the thermal expansion coefficient, θ, gravity, g, the superadiabatic temperature difference ΔT across the convective layer of thickness L (here being the magma ocean thickness). The parameters buffering advection are the thermal diffusivity, κ, and the kinematic viscosity, $\nu = \eta/\rho$, where η is the dynamic viscosity, and ρ is the fluid density. The Rayleigh number is thus a measure of the convective vigor. It is estimated to be up to $Ra = 10^{31}$ for a typical magma ocean encompassing an Earth-sized mantle (e.g., Solomatov 2000). It decreases with magma ocean crystallization (the present-day Earth's mantle is estimated to be between 10^6 and 10^8; e.g., Ricard 2015). The Prandtl number is

$$Pr = \frac{\nu}{\kappa} \quad , \tag{4}$$

and expresses the ratio of momentum to heat diffusion. For the present-day solid-state mantle of Solar System terrestrial planets $Pr \gg 1$ ($Pr > 10^{23}$ on Earth where mantle convection is essentially a buoyancy-driven Stokes flow; e.g., Schubert et al. 2001, Ricard 2015), which implies that fluid motions stop as soon as the heat source disappears because of negligible inertial effects compared to viscous effects. Conversely, inertia cannot be neglected in the frame of vigorously convective, low viscosity magma oceans. In that case $Pr \approx 1$ for a global Earth-sized mantle magma ocean and progressively increases with solidification. These two parameters characterize the convective dynamics.

The heat loss is a function of the convective vigor so that the dimensionless heat flux, i.e., the Nusselt number, Nu, which is the ratio of convective to conductive heat transfer ($Nu = 1$ when heat is dissipated by conduction only, and exceeds unity as soon as convection starts), is representative of the heat flux (F_{conv}) leaving the magma ocean through the top boundary of the convective layer (i.e., the surface). F_{conv} scales as a power-law of the Rayleigh number (e.g., Jaupart et al. 2015):

$$Nu = \frac{F_{\text{conv}} L}{k \Delta T} = a_{Nu} Ra^{\gamma_{Nu}} \quad , \tag{5}$$

where the scaling law pre-factor a_{Nu} and exponent γ_{Nu} values depend on the convective regime and patterns (e.g., Malkus 1954; Grossmann and Lohse 2000; Chillà and Schumacher 2012; Stevens et al. 2013, 2018). For extremely vigorous and turbulent convection relevant to magma ocean parameters, the convective heat flux is usually parameterized using $a_{Nu} = 0.089$ and $\gamma_{Nu} = 1/3$ (e.g., Siggia 1994, Solomatov 2015; regime IV_u in Grossmann and Lohse 2000). This implies that the heat loss is governed solely by local instabilities of the upper thermal boundary layer and is independent of the magma ocean thickness (e.g., Lebrun et al. 2013; Salvador et al. 2017; Nikolaou et al. 2019).

Given its low viscosity and the large temperature difference between the base of the MO and the surface, the convection is highly vigorous. The temperature across the molten layer is nearly adiabatic and isentropic (e.g., Abe 1997; Solomatov 2015). For a one-phase system, such as for the completely molten or completely solid and homogeneous layer, it can be expressed as:

$$\frac{\mathrm{d}T}{\mathrm{d}P} = \frac{\alpha T}{\rho c_p} \quad , \tag{6}$$

where P is the pressure and c_p is the isobaric specific heat. In two-phase systems, i.e., where the melt and crystals co-exist, the equation for the adiabat is modified to account for the effects of phase changes (e.g., Abe 1997; Solomatov and Stevenson 1993; Solomatov 2015). The secular cooling of the magma ocean is then often computed by integrating the equation of conservation of energy over the evolving magma ocean thickness (e.g., Abe 1997; Lebrun et al. 2013; Jaupart et al. 2015).

Starting from a magma ocean extending throughout the entire mantle, the depth at which crystallization starts is the depth at which the adiabat first intersects the liquidus (above which temperature the material is completely liquid). Where it starts and how it proceeds with cooling thus firstly depends on the respective slopes of the melting curves (in particular that of the liquidus) and the adiabat (Fig. 8e). While the liquidus is well constrained over the first 1000 km of Earth's mantle, it remains uncertain at lower depth (e.g., Andrault et al. 2017; Fiquet 2018; Andrault 2019, for reviews). If the $P - T$ slope of the adiabatic temperature of the magma ocean is flatter than the liquidus (such as for a chondritic composition; Andrault et al. 2011), crystallization would start at the base of the mantle and proceeds from the bottom upward, as generally assumed in magma ocean studies (Fig. 8a–c, e and f). But this may vary if the liquidus profile presents a strong curvature at mid-lower mantle depths (such as for a fertile peridotite; Fiquet et al. 2010; Thomas et al. 2012), resulting in a crystallization starting at mid-mantle depths, where a growing shell of solid mantle material would form. Such a scenario would induce the formation of a persistent molten layer at the base of the mantle, a so-called "basal magma ocean" (Labrosse et al. 2007), and an early thermochemical separation between the upper and lower parts of the molten mantle. Whether the differences between these two crystallization scenarios arise from the different compositions considered or from experimental uncertainties remains unclear.

The depth at which crystallization starts is insufficient information to describe the subsequent solidification pattern of the magma ocean. Of equal importance is the relative buoyancy and thus the density difference between crystals and melts, which controls the way solid–liquid segregation proceeds (e.g., Boukaré and Ricard 2017; Caracas et al. 2019; see Andrault et al. 2017; Asimow 2018, for detailed reviews). At low pressures, forming crystals are typically assumed to be denser than the surrounding melt and thus sink to the bottom. Yet, the larger compressibility of liquids compared to that of crystals may induce the latter to be buoyant with respect to silicate melts in the lower mantle (Nomura et al. 2011;

Andrault et al. 2012; Thomas et al. 2012). Changes of Fe melt–crystal partition coefficient may also result in denser (and sinking) Fe-rich melts than co-existing crystals (e.g., Tateno et al. 2014; Andrault et al. 2017). This scenario contrasts with the classical view of crystals settling, compaction, and melt ejection in a crystallizing magma ocean (Solomatov 2007; Boukaré et al. 2015), and could also produce an early, isolated basal magma ocean above the CMB. Accounting for the effect of convective dynamics on the settling behavior of crystals (resulting from the competition between crystals settling and entrainment within the convective flow; e.g., Maas and Hansen 2015, 2019; Patočka et al. 2020, 2022) as a function of their evolving properties such as their shape, size, density, and distribution may also significantly affect the solidification and differentiation pattern (e.g., Solomatov 2015). The location of initial crystallization as well as the subsequent solidification pattern have critical implications regarding both the chemical and thermal stratification of the mantle, and may significantly affect the distribution of volatile species within the planetary interior and their outgassing. Despite being an open question whose influence is still poorly constrained, it might profoundly affect the early and long-term evolution of terrestrial planets.

As a result of cooling and crystallization, the melt fraction of the magma, ϕ_{melt}, decreases. Conversely its crystal fraction, $\phi_{\text{crystal}} = 1 - \phi_{\text{melt}}$, increases. It depends on the temperature at which crystals start to form, i.e., the liquidus T_{liq}, and on the temperature below which the material is completely solid, i.e., the solidus T_{sol}. In a linear and simplified form it can be written (Abe 1997):

$$\phi_{\text{melt}} = \frac{T - T_{\text{sol}}}{T_{\text{liq}} - T_{\text{sol}}} \quad . \tag{7}$$

Because the temperature, T, is a function of depth and time, ϕ_{melt} varies accordingly and globally decreases with magma ocean cooling from $\phi_{\text{melt}} = 1$ ($T \geqslant T_{\text{liq}}$), when no crystals are present ($\phi_{\text{crystal}} = 0$), to $\phi_{\text{melt}} = 0$ ($T \leqslant T_{\text{sol}}$), when the magma is fully crystallized ($\phi_{\text{crystal}} = 1$).

The viscosity of the magma and associated rheological behavior greatly varies as a function of the temperature/crystal content and controls virtually all dynamic processes in the magma ocean. For instance, it strongly affects the convective vigor, the associated heat redistribution, and thus, the amount of heat the mantle can release. Throughout the magma ocean lifetime, viscosity changes over several orders of magnitude (Fig. 8d). Where and when the magma temperature is above liquidus, the dynamic viscosity of the silicate melt can be as low as the viscosity of water at ambient conditions ($\eta \approx 10^{-3}$ Pa.s; e.g., Urbain et al. 1982, Solomatov 2007, Kono 2018). A rheological transition associated with an abrupt viscosity increase occurs when the crystal fraction becomes large enough such that the connectivity of the crystals hampers efficient, liquid-like motion (e.g., Lejeune and Richet 1995; Abe 1993b, 1997). The mantle depth at which the rheological transition occurs is called the rheological front and separates the upper, low viscosity, vigorously convective, melt-dominated-motion mantle from the lower, rheologically solid-like mantle. The critical melt fraction at which this transition occurs is classically taken to be $\phi_{\text{melt,c}} \approx 0.4$ (Marsh 1981; Abe 1993b), but other mechanisms, such as diffusion creep and melt contiguity (Faul and Jackson 2007; Takei and Holtzman 2009a), may keep the viscosity low and fluid-like even at significantly lower melt fractions (from $\phi_{\text{melt,c}} \approx 0.019$ for 15 μm grain size and down to $\phi_{\text{melt,c}} \approx 10^{-4}$ for typical mantle grain size of 3 mm; Takei and Holtzman 2009b). Assuming that the solidification of the magma ocean proceeds from the bottom upward, with crystals efficiently segregating from the melt and accumulating downward, two layers of very distinct rheological behaviors exist from either side of the rheological front (Fig. 8b).

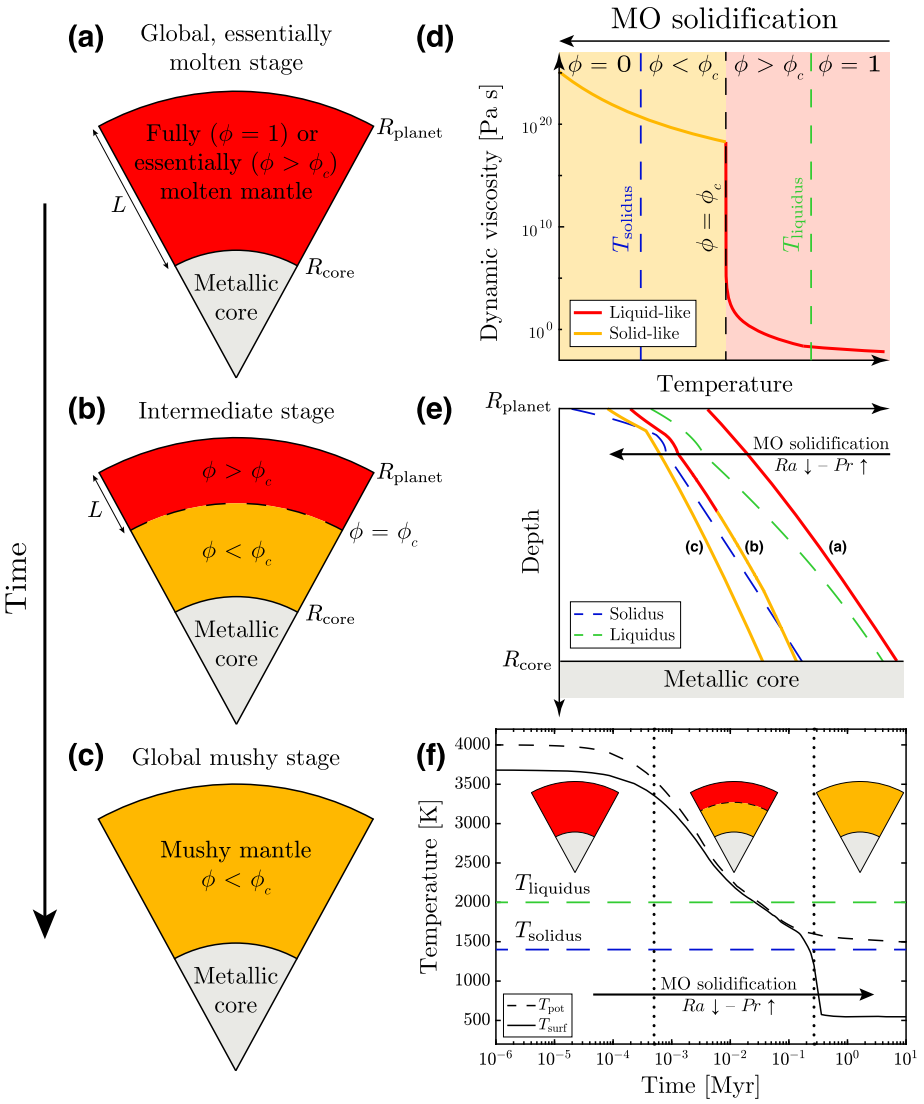

Fig. 8 (a–c) Magma ocean schematic evolution sequence from (a) a fully ($\phi = 1$)/essentially ($\phi_c < \phi < 1$) molten stage of global extent ($L = R_{\rm planet} - R_{\rm core}$), to (b) an intermediate stage where an essentially molten upper unit coexists with a lower mushy unit, to (c) a globally mushy stage where the liquid fraction is below the critical value of the rheological transition everywhere. (d) Viscosity and (e) temperature profile of the silicate mantle as a function of its evolving temperature/melt fraction. (f) Typical thermal evolution of an Earth-like magma ocean overlaid with an outgassing H_2O–CO_2–N_2 atmosphere (modified from Salvador et al. 2017)

Here we consider that the magma ocean is rheologically liquid-like, either fully ($\phi_{\rm melt} = 1$) or essentially molten, with a melt fraction above $\phi_{\rm melt,c}$ ($\phi_{\rm melt,c} < \phi_{\rm melt} \leqslant 1$), while the "mushy" layer below ($0 \leqslant \phi_{\rm melt} \leqslant \phi_{\rm melt,c}$) convects less vigorously and behaves rheologically more like the present-day solidified terrestrial mantle, with a melt fraction-dependent viscosity. Starting from a fully molten mantle, the magma ocean thus extends from the sur-

face to the rheological front (Figs. 5 and 8a and b) and with time, it shrinks until the rheological front reaches the surface (Fig. 8c). From then on, the mantle dynamics and mixing is much less vigorous and the associated convective flux is much lower: the end of the transient magma ocean stage is reached.

Note that global thermal equilibrium can be reached independently of the magma ocean end: the former does not necessarily imply that the magma ocean phase is over. Indeed, global thermal equilibrium and climate stability depend on the radiative balance between the net absorbed insolation (F_{abs}) and the outgoing radiation (F_{IR}), and can thus be achieved at surface temperatures higher than the surface melting point. This can be the case for close-in planets that can keep their planetary surface molten indefinitely (e.g., lava worlds). For early Venus, depending on the atmospheric composition and on the absorbed solar flux resulting in part from the cloud–albedo feedback, climate stability may have been achieved with a molten or solidified surface (see Sects. 3.3 and 4, and Fig. 12).

3.2 Water/Volatiles Partitioning and Outgassing

At a given magma ocean crystallization stage, water and other volatile species are distributed between the different planetary reservoirs, from the deep interior to the atmosphere. These volatile species are chemical compounds with a low boiling point that thus vaporize readily and partition preferentially into a fluid or gas phase (e.g., Chap. 7 in White 2013). We first describe how this distribution proceeds at a given crystallization stage and then how it evolves with magma ocean cooling and solidification.

3.2.1 Melt–Crystal Volatile Partitioning

Within the molten mantle, the partitioning of a species between the co-existing melt (silicate liquid) and solid phase (crystals) is determined through partition coefficients that dictate how much of a given volatile species dissolved in the melt can be incorporated into a given mineral phase at given thermodynamic conditions. This is sometimes referred to as the storage capacity (e.g., Hirschmann et al. 2005). "Water" is not incorporated as an integral part of the crystal structure. It occurs mostly in the form of hydroxyl groups (–OH) in hydrous minerals, or as hydrogen atoms decorating point defects of nominally anhydrous minerals, the so-called NAMs, and bonded to structural oxygen, but rarely as molecular water. For extensive reviews regarding hydrogen/"water" in the solid mantle, refer to Hirschmann et al. (2005), Hirschmann (2006), Keppler and Bolfan-Casanova (2006), Demouchy and Bolfan-Casanova (2016), Peslier et al. (2017). Most coupled magma ocean–atmosphere thermal evolution studies consider a single solid–melt partition coefficient (ψ_{vol}) throughout the entire mantle (Hamano et al. 2013, 2015; Schaefer et al. 2016; Bower et al. 2019; Barth et al. 2021), usually taken as the partition coefficient of perovskite ($\psi_{\mathrm{H_2O}} = 10^{-4}$ for water; except in Schaefer et al. (2016) and Barth et al. (2021), where $\psi_{\mathrm{H_2O}} = 10^{-2}$ is close from the partition coefficient of lherzolite). Or they consider the partition coefficient of lherzolite for the upper mantle ($\psi_{\mathrm{H_2O}} = 1.1 \times 10^{-2}$), and of perovskite for the lower mantle ($\psi_{\mathrm{H_2O}} = 10^{-4}$; after Bolfan-Casanova et al. 2003), thus accounting for differences due to pressure and associated stable mineral phases (Elkins-Tanton 2008; Lebrun et al. 2013; Salvador et al. 2017; Nikolaou et al. 2019).

In addition to water partitioning between silicate melts and cumulates (i.e., crystals accumulated by gravitational settling in a magma), another process responsible for the incorporation of water into solidifying silicates is the interstitial trapping of water-enriched melt (Elkins-Tanton 2008; Hamano et al. 2013, 2015; Ikoma et al. 2018). Some models assume that 1% of the melt mass is incorporated into cumulates through interstitial trapping

throughout solidification (Elkins-Tanton 2008; Hamano et al. 2013, 2015). Yet, as discussed in Hamano et al. (2013), estimates for magma ocean solidification remain highly unconstrained. They are based on the degree of melting at which melt separation starts for abyssal peridotites (Johnson and Dick 1992) and likely overestimates the mass fraction of interstitially trapped melt. Furthermore, interstitial trapping would only store significant amounts of water into cumulates in the presence of water-rich melts. The latter correspond to evolved magmas found at late solidification stages where water exsolution and outgassing are highly efficient (e.g., Elkins-Tanton and Grove 2011; Lebrun et al. 2013; Salvador et al. 2017; Nikolaou et al. 2019; Bower et al. 2019) and thought to be the water-draining dominant processes. Yet, it has been recently suggested that this interstitial trapping and melt retention process might be highly effective at the magma ocean freezing front (i.e., at the rheological transition) and may retain a substantial fraction of volatile-rich melt at the end of magma ocean evolution (Hier-Majumder and Hirschmann 2017; Miyazaki and Korenaga 2021, 2022). Volatile species that are highly soluble in the melt, such as water, would be very sensitive to this process and largely incorporated into the primordial solidified mantle. As this relates to volatile partitioning during the entire magma ocean evolution and crystallization sequence rather than being specific to a given crystallization stage, we discuss it in more detail in Sect. 3.2.4.

If one does not take into account volatile trapping in the porous melt phase, the incorporation of volatile species into the solidifying mantle is negligible compared to its partitioning into the melt during the magma ocean crystallization. Volatile trapping in the solidified mantle might thus be ignored to first order when addressing magma ocean and atmospheric thermal evolution (Lichtenberg et al. 2021). Yet this very process is of major importance when the magma ocean is eventually fully solidified, and when addressing the long term evolution of the planet and the dynamics of the solidified mantle.

Water has a strong effect on solid-state mantle creep strength (Hirth and Kohlstedt 1995; Mei and Kohlstedt 2000; Hirth and Kohlstedt 2004; Demouchy and Bolfan-Casanova 2016), melting relations (Hirth and Kohlstedt 1996; Asimow and Langmuir 2003), shear zones development (e.g., Skemer et al. 2013), viscosity and density (e.g., Lange 1994), and phase transitions (Wood 1995). Its partition between the melt and the solidifying mantle during the crystallization of the magma ocean will be of fundamental importance for the style and strength of convective flow during the following stages of planetary evolution (e.g., Schaefer and Elkins-Tanton 2018). Namely, the distribution of water within the planet has been proposed to resolve the distinct tectonic behaviors between the Earth's wet mantle and that supposedly dry of Venus (Mackwell et al. 1998; Richards et al. 2001). This water could be directly inherited from the magma ocean stage in the case of a gravitationally stable stratified crystallization sequence, or acquired later after mantle global overturn (e.g., Tikoo and Elkins-Tanton 2017). Furthermore, by decreasing the solidus temperature and thus facilitating melting at greater depth and greater extent (because water lowers the Gibbs free energy of the melt), water abundance in the solid mantle is a crucial parameter for Earth's mantle melting and volcanism. Particularly at subduction zones, mid-ocean ridges and for intraplate hotspot volcanism (e.g., Hirschmann 2006; Litasov and Ohtani 2007; Ni et al. 2016). The resulting interior melting and volcanism can in turn affect the atmospheric composition, climate, volatile cycling, and consequently, the surface conditions and habitability on rocky planets (e.g., Foley and Driscoll 2016; Dehant et al. 2019).

3.2.2 Melt–Gas Volatile Partitioning

Compared to crystals (i.e., magma's solid phase), the melt (i.e., magma's liquid phase) can contain a large amount of volatile species, including water, that are dissolved within the

latter. Water is sometimes said to be more soluble in the melt than in the crystals/solid phase. This even though, technically, water is rather incorporated in the solid phase than dissolved within it. Thus, compared to the crystallizing solid mantle, the molten mantle has a larger volatile storage capacity. Unsurprisingly, the thicker the magma ocean, the more water can be dissolved into it.

Yet, while water is highly soluble in the silicate melt, the molten mantle still has a limited maximum storage capacity for dissolved water. This is also referred to as the so-called water solubility (see Moore 2008; Baker and Alletti 2012, for reviews). The solubility of volatile species in melts has been constrained both experimentally (e.g., Holloway and Blank 1994) and theoretically (e.g., Ottonello et al. 2018). It depends primarily on the volatile species considered, on the melt composition, and pressure, but also changes according to temperature, and volatile species mixture (H_2O only or $H_2O + CO_2$ for instance; see Papale 1997, 1999, Papale et al. 2006).

It is important to note that rather than giving the actual water content, solubility studies constrain the storage capacity of the mantle. This is the maximum amount of water that may be stored, which is the mantle saturation limit (e.g., Keppler and Bolfan-Casanova 2006). It does not give any constraint on its saturation state, i.e., if it is actually volatile-saturated or not. It means that the solubility of a given volatile species into the melt does not provide any information regarding the amount of this very species delivered to the planet. It is rather a bulk property of the molten mantle, so that one should always distinguish the actual water content of the magma ocean, inherited from the planetary formation, from its intrinsic storage capacity.

For a given melt composition and mass fraction of water, the higher the pressure, the larger amount of a volatile species can be maintained dissolved within the melt (Fig. 9). In the deep molten mantle, i.e., at high pressure, the silicate melt can retain more than 10 wt% of water and carbon dioxide in solution (e.g., Papale 1997). Thus, the decrease of ambient overburden pressure experienced by a fluid parcel rising up through convective motions will be responsible for a decrease of the melt storage capacity (Fig. 9), similarly to magma ascent in volcanic systems (e.g., Chap. 5 in Parfitt and Wilson 2008; Sparks et al. 1994; Gonnermann 2015; Wallace et al. 2015). This overburden pressure is the lithostatic load, that is the pressure at a given depth below the surface due to the weight of the overlying layers of silicate material. When the water-dissolved maximum storage capacity is reached, the molten mantle is water-saturated, meaning that all supplementary water exceeding the saturation limit cannot remain dissolved within the liquid phase and is thus exsolved out of the melt to form gas bubbles (i.e., decompression-induced degassing; Figs. 9 and 10; e.g., Edmonds and Woods 2018). Due to their low density compared to the ambient liquid, gas bubbles naturally tend to rise up through the fluid towards the surface, unless they are entrained downwards by the convective currents. Mantle degassing and atmosphere formation and replenishment then occur when gas bubbles reach and burst at the surface of the magma ocean, thus transferring volatile species from the gas phase of the magma to the atmosphere.

In volcanic systems, ascent of gas bubbles is a complex process. Whether they are able to reach and burst at the surface involves the interplay between diffusion, bubbles coalescence, growth, and re-entrainment, which are influenced by several parameters such as magma viscosity and melt–bubble relative density, themselves controlled by the amount of dissolved/exsolved volatiles (e.g., Berlo et al. 2011). Thus far this has been poorly investigated in the context of magma ocean outgassing. For volcanic eruptions, it is believed that rapid growth and ascent of gas bubbles is favored by the high temperatures and low viscosity of the magma, which allows gas to easily segregate from the melt in the form of small bubbles that can themselves easily merge leading to larger bubbles with a faster ascending

speed (Sparks 1978; Sparks et al. 1994; Lesher and Spera 2015). The dynamics of a magma ocean may significantly differs from that of a volcanic erupting system. Yet, it is generally assumed that as soon as bubbles are formed, they also rapidly reach the surface without being re-entrained downwards by convective current, albeit vigorous, thus assuming optimistic efficient outgassing.

Instead of outgassing after bubbles formation and ascent to the surface, water can also be released to the atmosphere by molecular diffusion through the upper thermal boundary layer (e.g., Hamano et al. 2013, 2015; Massol et al. 2016; Ikoma et al. 2018). This degassing process dominates if bubbles are too small to rise up and reach the surface before being transported back downwards by vigorous convective flow. Such a diffusion-limited volatile flux provides a minimum estimate for the degassing rate. Using an experimentally-derived molecular diffusion coefficient for basaltic melts (Zhang et al. 2007), Hamano et al. (2013) found that even with a modest degree of supersaturation, this mechanism can still be responsible for the formation of a massive steam atmosphere, by keeping its water content in solution equilibrium with that of the silicate melt.

3.2.3 The Core as an Additional Reservoir of Hydrogen/Water

The metallic core may also be an additional reservoir of water (in the form of hydrogen) ($M^{\text{core}}_{\text{H}_2\text{O}}$ in Eq. (8)), potentially storing several oceans' mass equivalents (e.g., Genda 2016; Peslier et al. 2017). The core density deficit and sound velocity excess (compared to those of pure iron) inferred from seismology (e.g., Birch 1952; Poirier 1994) suggest that the inner core contains a few percents of light elements (see Hirose et al. 2021, for a recent review). Similarly, the density of Earth's outer core is estimated to be 5–10 wt% lower than that of pure iron. Approximately 10 wt% light alloys in the core have been suggested (e.g., Birch 1952; Hirose et al. 2013). Furthermore, some outer core temperature estimates, about 400 K lower than previously thought, would also support a similar fraction of elements lighter than iron to maintain its liquid state (Nomura et al. 2014).

During the differentiation, core-forming metal transports hydrogen and other volatile species from the magma ocean to the core (e.g., Rubie et al. 2015b; Dasgupta and Grewal 2019). Iron-loving elements are prone to be incorporated with metal droplets suspended in the magma ocean, and then partitioned into the core. A large amount of H may be partitioned into the metallic iron at high pressure and be incorporated to the core this way (e.g., Kuramoto and Matsui 1996; Okuchi 1997; Abe et al. 2000; Shibazaki et al. 2009; Li et al. 2020). Umemoto and Hirose (2015) found that $\sim$1 wt% of H in the outer core (equivalent to the hydrogen content of $\sim$130 oceans of water) can reproduce its lower density and faster bulk compressional sound velocity. More conservative estimates suggest an equivalent of 0.2 to up to 90 Earth oceans mass if H is the only volatile in the core (see Peslier et al. 2017, and references therein). The partitioning process is controlled by the chemical equilibration between metal liquids and silicate melt. The partitioning coefficients depend on the $P-T$ conditions at which silicate melt–metal equilibration and core sequestration occur, and on the redox state of the magma ocean (e.g., Li and Agee 1996; Okuchi 1997; Badro et al. 2015).

H has been proposed as a strong candidate because of its abundance in the Solar System and in planetary interiors and its high incompatibility in Fe liquid metal (Okuchi 1997; Abe et al. 2000; Iizuka-Oku et al. 2017). Recent ab initio molecular dynamics calculations have suggested that at the $P-T$ conditions of both magma ocean and the current Earth's CMB, H_2 and H_2O are both more compatible in the core than in silicate melts (Yuan and Steinle-Neumann 2020; Li et al. 2020). This implies that the Earth's core can potentially

act as a large reservoir of water. This is also supported by recent experimentally determined partitioning of hydrogen between liquid Fe and molten silicate under high pressures and temperatures relevant to the conditions of core-forming metal segregation from silicate (Tagawa et al. 2021).

However, other recent experimental results contradict H strong siderophile behavior (Clesi et al. 2018; Malavergne et al. 2019), favoring alternative light elements such as O, S, C, or Si (e.g., Helffrich and Kaneshima 2004; Badro et al. 2015; Shahar et al. 2016). The long-standing question of hydrogen in the Earth's core still remains an unresolved topic. Determining if this discussion applies to Venus would first require estimates of its core structure and density, that may be assessed through future ionospheric and/or ground-based seismology and would certainly improve our understanding of current and early interior processes. As a first approximation it seems reasonable to think that such process may also apply to Venus. This relies on Earth and Venus having similar bulk density and composition, and if one considers that they experienced roughly similar accretion sequences due to their vicinity (which might be challenged; see Emsenhuber et al. 2021), Although little is know about Venus' interior today, future exploration missions, such as NASA's VERITAS (Smrekar et al. 2022) and ESA's EnVision are promising to provide some constraints on its physical properties (see Widemann et al. 2023, this collection).

3.2.4 Evolution During Magma Ocean Solidification

Distribution Between the Different Reservoirs As the magma ocean crystallizes, each volatile species is distributed between the different and evolving reservoirs of the magma ocean–atmosphere system: the solid mantle, the remaining melt (molten mantle), and the atmosphere. As discussed above, some amount of volatile species may also be incorporated into the core during the segregation of metallic iron to the core if metal–silicate separation is not completed. This distribution can be described by the mass conservation equation. For water, it is (following Lebrun et al. 2013; Schaefer et al. 2016; Salvador et al. 2017):

$$M_{\mathrm{H_2O}}^{\mathrm{MO},t=0} = M_{\mathrm{H_2O}}^{\mathrm{melt}} + M_{\mathrm{H_2O}}^{\mathrm{solid}} + M_{\mathrm{H_2O}}^{\mathrm{atm}} + M_{\mathrm{H_2O}}^{\mathrm{core}} \ , \tag{8}$$

where the initial and total mass of water of the system, dissolved within the molten mantle at $t = 0$, $M_{\mathrm{H_2O}}^{\mathrm{MO},t=0}$, is distributed between the molten part of the mantle, the solidifying mantle, and the atmosphere, whose water masses are $M_{\mathrm{H_2O}}^{\mathrm{melt}}$, $M_{\mathrm{H_2O}}^{\mathrm{solid}}$, and $M_{\mathrm{H_2O}}^{\mathrm{atm}}$, respectively. The mass of water transferred to the core, $M_{\mathrm{H_2O}}^{\mathrm{core}}$, is often neglected as it is generally assumed that metallic iron has fully segregated into the core by the time of the last hypothetical global magma ocean, and that chemical exchanges between the mantle and the core are then limited. Before metallic iron has fully segregated to the core, a substantial amount of hydrogen may be incorporated into the core that could thus possibly contain a significant amount of water initially accreted by the planet (Sect. 3.2.3). Here, $t = 0$ represents the starting point of the cooling of the last and global magma ocean stage following a giant impact, whose timing is uncertain (e.g., Elkins-Tanton 2012), and implicitly relies on the accretion timeline.

The magma ocean initial water content is usually expressed as a mass fraction of water, $X_{\mathrm{H_2O}}^{\mathrm{MO},t=0}$, relative to the initial magma ocean mass, $M_{\mathrm{MO},t=0}$:

$$M_{\mathrm{H_2O}}^{\mathrm{MO},t=0} = X_{\mathrm{H_2O}}^{\mathrm{MO},t=0} \times M_{\mathrm{MO},t=0} \ . \tag{9}$$

This initial water content delivered to the planet is highly unconstrained. For Earth, it is estimated to be 18^{+81}_{-15} times the equivalent mass of the oceans (Peslier et al. 2017), and implicitly

relies on assumptions regarding the accretion sequence (see Sect. 2). This includes, but is not limited to the timing and dynamics of planetary formation, both affecting the sources and the processes of water delivery (e.g., Morbidelli et al. 2012; Marty 2012; O'Brien et al. 2018). It is generally assumed that any pre-existing atmosphere has been blown away due to the energetics of the giant impact such that water and other volatile species are initially dissolved within the molten interior. Yet, atmospheric erosion may not be as efficient (e.g., Genda and Abe 2003; Pham et al. 2011; Schlichting et al. 2015) and a fraction of accreted volatiles may be released directly into the atmosphere upon impact (e.g., Lange and Ahrens 1982; Matsui and Abe 1986b). $M_{\mathrm{H_2O}}^{\mathrm{melt}}$ is the mass of water dissolved within the molten part of the mantle and staying in the residual liquid as solidification proceeds. It is a mass fraction of the rheologically liquid-like magma ocean, $X_{\mathrm{H_2O}}^{\mathrm{melt}}$, of mass M_{melt}, and is given by:

$$M_{\mathrm{H_2O}}^{\mathrm{melt}} = X_{\mathrm{H_2O}}^{\mathrm{melt}} \times M_{\mathrm{melt}} \ . \tag{10}$$

The mass of water stored within the solidifying mantle depends both on the melt–crystals partition coefficient, $\psi_{\mathrm{H_2O}}$, and on the mass fraction of water incorporated through interstitial melt trapping, $X_{\mathrm{H_2O}}^{\mathrm{inter}}$, following:

$$M_{\mathrm{H_2O}}^{\mathrm{solid}} = \psi_{\mathrm{H_2O}} X_{\mathrm{H_2O}}^{\mathrm{melt}} M_{\mathrm{solid}} + X_{\mathrm{H_2O}}^{\mathrm{inter}} M_{\mathrm{melt}} \iota \ , \tag{11}$$

where ι is the mass fraction of melt incorporated into the solid mantle through interstitial trapping. It is relative to the melt mass, M_{melt}, taken as $\iota = 1\%$ of M_{melt} in Elkins-Tanton 2008, Hamano et al. 2013, 2015. Note that most coupled magma ocean–atmosphere studies do not consider any incorporation of water through interstitial trapping of water-enriched melt (i.e., $\iota = 0$), so that the corresponding last term in the right-hand side of Eq. (11) is neglected.

The partition coefficient is either computed as a mantle-averaged value and taken as such (e.g., Hamano et al. 2013, 2015; Schaefer et al. 2016; Bower et al. 2019; Barth et al. 2021), or written as (Lebrun et al. 2013; Salvador et al. 2017):

$$\psi_{\mathrm{H_2O}} = \frac{M_{\mathrm{perov}}^{\mathrm{solid}} \psi_{\mathrm{H_2O}}^{\mathrm{melt-perov}} + M_{\mathrm{lherz}}^{\mathrm{solid}} \psi_{\mathrm{H_2O}}^{\mathrm{melt-lherz}}}{M_{\mathrm{perov}}^{\mathrm{solid}} + M_{\mathrm{lherz}}^{\mathrm{solid}}} \ , \tag{12}$$

when considering distinct and specific melt–solid partition coefficients for the lower and upper mantle mineral phases, such as perovskite and lherzolite (e.g., Elkins-Tanton 2008; Lebrun et al. 2013; Salvador et al. 2017; Nikolaou et al. 2019). In such a case, $M_{\mathrm{perov}}^{\mathrm{solid}}$ and $M_{\mathrm{lherz}}^{\mathrm{solid}}$ stand for the evolving masses of the perovskite and lherzolite mineral phases, and $\psi_{\mathrm{H_2O}}^{\mathrm{melt-perov}}$ and $\psi_{\mathrm{H_2O}}^{\mathrm{melt-lherz}}$ their melt–solid partition coefficients. Because of its dependence on the mass of crystallized phases, $\psi_{\mathrm{H_2O}}$ changes with solidification.

Finally, the mass of outgassed atmospheric water ($M_{\mathrm{H_2O}}^{\mathrm{atm}}$) when considering a pure steam atmosphere is given as (e.g., Elkins-Tanton 2008; Schaefer et al. 2016):

$$M_{\mathrm{H_2O}}^{\mathrm{atm}} = 4\pi R_{\mathrm{p}}^2 \frac{P_{\mathrm{H_2O}}^{\mathrm{atm}}}{g} \ , \tag{13}$$

where R_{p} is the planetary radius, $P_{\mathrm{H_2O}}^{\mathrm{atm}}$ is the atmospheric partial pressure of water (at the planetary surface), and g is the gravity. Importantly, one should note that when considering multi-species atmospheres, the molar mass needs to be considered to relate the partial pressure of each volatile species to its atmospheric mass (e.g., Pierrehumbert 2010; Bower et al.

2019):

$$M_{\mathrm{vol}}^{\mathrm{atm}} = 4\pi R_{\mathrm{p}}^2 \left(\frac{\mu_{\mathrm{vol}}}{\bar{\mu}} \right) \frac{P_{\mathrm{vol}}}{g} \quad , \tag{14}$$

where $M_{\mathrm{vol}}^{\mathrm{atm}}$ is the mass of the volatile species vol in the atmosphere, μ_{vol} is its molar mass, P_{vol} its atmospheric partial pressure at the planetary surface, and $\bar{\mu}$ is the mean molar mass of the atmosphere. As discussed above, the atmospheric partial pressure of a volatile species at the surface comes from its outgassing from the interior. Its efficiency depends mainly on its abundance and solubility within the melt, as well as on the convective style and crystallization sequence of the molten mantle.

Because water is an incompatible element, it partitions preferentially into the remaining silicate melt relative to the silicate solid when the magma crystallizes. Therefore, as magma ocean crystallization proceeds, the residual and thinning melt layer becomes more and more enriched in water. Its mass fraction of dissolved water (relative to the magma ocean mass), $X_{\mathrm{H_2O}}^{\mathrm{melt}} = M_{\mathrm{H_2O}}/M_{\mathrm{MO}}$, increases with time (e.g., Elkins-Tanton 2008; Massol et al. 2016; Ikoma et al. 2018). The magma ocean mass, M_{MO}, decreases with mantle solidification while the mass of dissolved water $M_{\mathrm{H_2O}}$ remains similar due its preferential partitioning into the melt (unless a significant amount of water goes into the solid phase). This facilitates the water saturation of the melt with magma ocean solidification (Fig. 9). Yet, a parcel of magma still needs to reach shallow depths and pressures low enough for saturation and exsolution to occur (Figs. 9 and 10).

Given its low, liquid-like viscosity (∼0.1 Pa.s) and associated vigorous convection, magma ocean large convective velocities (v_{conv}, on the order of 0.5 m.s^{-1}; see Solomatov 2000, 2015; Elkins-Tanton 2008) are expected to rapidly carry volatile-bearing melt close to the surface (black arrows in Fig. 10). There exsolution can occur at the exsolution depth, d_{exsol}; blue dashed line in Fig. 10. The complete circulation of a deep magma ocean would be achieved in about 1 to 3 weeks (Elkins-Tanton 2008). Compared to the solidification timescale, this is fast enough for the entire magma ocean volume to reach the exsolution depth and outgas its volatiles before the solidification front substantially rises-up. Its velocity is v_{sol}; see yellow arrow in Fig. 10. Furthermore, this 1–3 weeks timescale being smaller than computational time-steps, magma ocean–atmosphere models generally assume that at each time-step, all the magma ocean volume has "seen" the surface, reached volatile saturation, and has thus virtually instantaneously outgassed all its volatiles in excess of saturation at each modeling time-step (Zahnle et al. 1988; Elkins-Tanton 2008; Hamano et al. 2013; Lebrun et al. 2013; Hamano et al. 2015; Schaefer et al. 2016; Salvador et al. 2017; Nikolaou et al. 2019; Bower et al. 2019; Lichtenberg et al. 2021; Barth et al. 2021; Krissansen-Totton et al. 2021). Based on this optimistic and efficient outgassing assumption, these models simulate volatile degassing by considering the pressure equilibrium of the gas phase between the magma and the atmosphere (i.e., on either side of the planetary surface). All volatiles in excess of saturation are thus directly transferred to the atmosphere. Solubility laws are then used to relate the atmospheric partial pressure of each volatile, $P_{\mathrm{vol}}^{\mathrm{atm}}$, to its abundance in the melt, $X_{\mathrm{vol}}^{\mathrm{melt}}$, according to (e.g., Elkins-Tanton 2008; Lebrun et al. 2013; Massol et al. 2016):

$$P_{\mathrm{vol}}^{\mathrm{atm}} = \left(\frac{X_{\mathrm{vol}}^{\mathrm{melt}}}{\zeta_{\mathrm{vol}}} \right)^{\beta_{\mathrm{vol}}} \quad , \tag{15}$$

where ζ_{vol} and β_{vol} are volatile-specific solubility constants taken from experimental data (such as Pan et al. 1991; Papale 1997). In magma ocean–atmosphere models, the atmospheric pressures are generally computed out of the volatile species abundances in the melt based on their solubility.

Typical Outgassing Sequence Under this assumption and outgassing treatment, typical coupled magma ocean–atmosphere models describe the formation of an H_2O–CO_2 atmosphere through magma ocean degassing as follows[3] (e.g., Elkins-Tanton 2008; Lebrun et al. 2013; Salvador et al. 2017; Nikolaou et al. 2019; Bower et al. 2019). Given the low solubility of CO_2 in silicate melts, it exsolves from magma at much greater depths beneath the surface than H_2O and outgasses early. Most of the carbon dioxide is outgassed to the atmosphere in the very first time-steps, resulting in high CO_2 atmospheric partial pressures, P_{CO_2}, at the earliest evolutionary stages.

Water being much more soluble in the melt, its outgassing occurs later on (starting after $\sim 10^4$ years of cooling), as it requires a more advanced crystallization stage for its concentration in the melt to be high enough to reach saturation. Once it starts, H_2O outgassing and resulting atmosphere build-up reflects the progressive replacement of melt mantle volume with solid mantle volume that has a smaller volatile storage capacity (e.g., Lebrun et al. 2013; Massol et al. 2016; Nikolaou et al. 2019). As an example, Fig. 11 shows the progressive partitioning of water between the different reservoirs during a typical magma ocean outgassing sequence (derived from Salvador et al. 2017 simulations). Interestingly, because the exsolution of a given volatile species depends on its concentration within the melt, lower initial abundances of water within the magma ocean may result in larger relative amounts of water stored in the planet's interior after the magma ocean ends (Nikolaou et al. 2019).

Compared to the H_2O–CO_2 atmospheres typically considered, Lichtenberg et al. (2021) has comprehensively studied how alternative atmospheric components may individually affect the radiative transfer of the atmosphere and the cooling of the magma ocean. How the combination of these individual components in more complex and realistic multi-species atmospheres would affect the heat transfer and magma ocean cooling rate has recently been investigated in a model framework considering variable oxidation states of the magma ocean (e.g., Katyal et al. 2020; Bower et al. 2022; Gaillard et al. 2022a; Maurice et al. 2023, see Sect. 3.2.5 for a detailed discussion).

Solubility Laws The implicit and model-dependent choice of solubility law has strong implications regarding magma ocean outgassing efficiency. That is because it ultimately dictates the outgassing rate, timescale, and the volatile amounts that can be dissolved in/exsolved out of the melt. Yet, this is poorly emphasized in the literature. Solubility laws obtained for basaltic systems are generally used (e.g., Elkins-Tanton 2008; Lebrun et al. 2013; Massol et al. 2016) as they are more appropriate for magma oceans since basalts, i.e., relatively low silica content melts, are high temperature and low viscosity melts (e.g., Sparks et al. 1994; Lesher and Spera 2015). Yet, they also have high gas diffusivity and tend to have more modest volatile contents than more viscous, silicic melts such as rhyolitic (as considered in Lichtenberg et al. 2021) or dacitic melts. In the case of water, at a given depth, a silicate liquid of basaltic composition can contain less dissolved water than one of rhyolitic composition (Fig. 9). Reciprocally, for a given water content, basaltic melts become saturated and exsolve H_2O at greater depths, i.e., at larger confining pressures, compared to rhyolitic melts. This facilitates exsolution and outgassing in basalt compared to rhyolite as the magma reaches saturation deeper and does not have to travel to shallower depths, that are closer to the surface (Fig. 9).

[3] Recall that coupled magma ocean–atmosphere models that consider the outgassing from the molten interior (in contrast to impact-generated atmosphere) generally assume that any prior atmosphere has dissipated after a giant impact responsible for melting the entire mantle, so that no pre-existing atmosphere is considered at the beginning of the simulations.

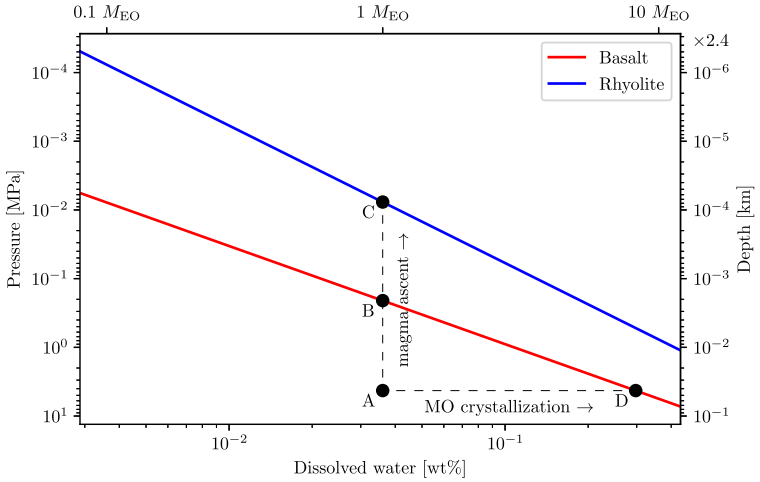

Fig. 9 Water solubility in basalt (red) and rhyolite (blue) as a function of the pressure acting on the magma (i.e., confining pressure) and corresponding depth beneath the surface. The top axis indicates the amount of water dissolved within a fully molten Earth-sized mantle corresponding to the mass fractions of dissolved water of the bottom axis. For a given water content, the saturation curve gives the location of the exsolution depth, d_{exsol}, at which gas bubbles start to form (Fig. 10, blue dashed line). At a given cooling stage, a parcel of magma ascending from a depth corresponding to point A undergoes decompression and would become saturated in H_2O at point B if it were a basalt and would start exsolving the excess of water, if any. If it were a rhyolite, it would not become saturated until it had ascended to the lower pressure marked by point C. Reciprocally, the saturation curve indicates the maximum amount of water that can be dissolved within the melt at a given pressure. As solidification proceeds, water partitions readily into the silicate melt, whose volume decreases owing to crystallization, such that evolving magma ocean liquids become more and more enriched in water. With magma ocean crystallization, a melt starting at a mass fraction of dissolved water corresponding to point A would see its water concentration increase and would become saturated in H_2O at point D. Once saturation is reached, the melt's mass fraction of dissolved water would evolve along the saturation curve. Solubility laws taken from Parfitt and Wilson (2008) and Carroll and Holloway (1994)

However, it should be noted that additional complexities may arise. For instance, the viscosity of mafic and ultramafic melts (such as basalt and komatiite, respectively) is comparatively much less affected by the dissolved water content than that of polymerized, low temperatures rhyolitic or dacitic melts (e.g., Fig. 5.5 in Lesher and Spera 2015, and references therein). In turn, viscosity influences magma motion and transport and may affect the amount of melt reaching the exsolution depth.

Furthermore, even for a given silicate melt composition, several solubility laws are available and their differences will affect outgassing efficiency as described before. These differences become more and more important when decreasing the mass fraction of dissolved water and are thus larger for low water contents and increase with planetary size for a given absolute water content (see Appendix A in Salvador and Samuel 2023, for a detailed discussion). Predictions regarding magma ocean outgassing, both in terms of degassing timescale and amount of outgassed volatiles, are thus ultimately influenced by the generally implicit and model-dependent choice of solubility law. In turn, the solubility law choice will alter the cooling rate of the magma ocean through the amount of radiative energy that can be dissipated to space, which is dictated by the outgassed atmospheric composition.

In addition, while the solubility of each volatile species is often treated separately when several volatile species are present in the magma ocean (for instance, H_2O and CO_2), solubility functions are actually more complex in such a case. This is in fact virtually always

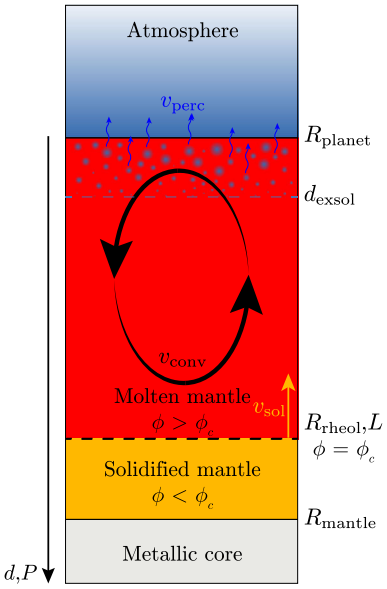

Fig. 10 Schematic of the magma ocean degassing process and associated velocities. $v_{\rm sol}$ is the upward solidification velocity associated with the uprising rheological front where $\phi = \phi_c$ (assuming that solidification proceeds from bottom-up). $v_{\rm conv}$ is the liquid-like convection velocity and $v_{\rm perc}$ is the percolation velocity of the gas bubbles rising up to the surface. $d_{\rm exsol}$ is the exsolution depth above which oversaturated volatiles are exsolved out of the melt and start forming gas bubbles. In a rapidly convecting magma ocean, volatile-bearing melt is assumed to reach the exsolution depth much faster than solidification proceeds and loses its volatiles in excess of saturation on that occasion. The outgassing is thus often assumed to be efficient. Adapted from Salvador and Samuel (2023)

the case: the gas phase is never just pure H_2O or CO_2. Then, chemical interactions between the volatiles themselves and the magma affect the solubility (e.g., Papale 1997; Papale et al. 2006; Massol et al. 2016; Edmonds and Woods 2018). For instance, as soon as the least soluble volatile starts to exsolve and form gas bubbles, some small amounts of most of the other species present will also diffuse into those bubbles (e.g., Parfitt and Wilson 2008). Such migration of the molecules of volatiles into the gas bubbles will increase the concentration gradient in the surrounding liquid, which will enhance the diffusion of more molecules toward the growing bubble. The non-ideal mixing behavior of the volatile species in the vapor phase is also responsible for the curvature of the saturation curves (see Papale et al. 2006; Moore 2008; Berlo et al. 2011, for detailed discussions).

Limits of the Efficient Degassing Assumption Stemming from the vigorous convection of the magma ocean, the efficient degassing scenario, relying on one a priori robust – yet debatable – assumption is mainly considered. Yet, despite high convective velocities, several mechanisms may buffer the outgassing efficiency of the magma ocean (see Table 1 for a summary). Alternatively, minimal to no degassing scenarios may be considered (e.g., Ikoma et al. 2018), where a substantial fraction of volatiles is retained in the melt on longer timescales and possibly ends up being trapped in the solidified mantle.

Although vigorous convection is prone to efficient and rapid magma ocean mixing, the fluid motions at relevant magma ocean dynamics can be organized according to large-scale circulations (e.g., Krishnamurti and Howard 1981; Castaing et al. 1989; Siggia 1994). This

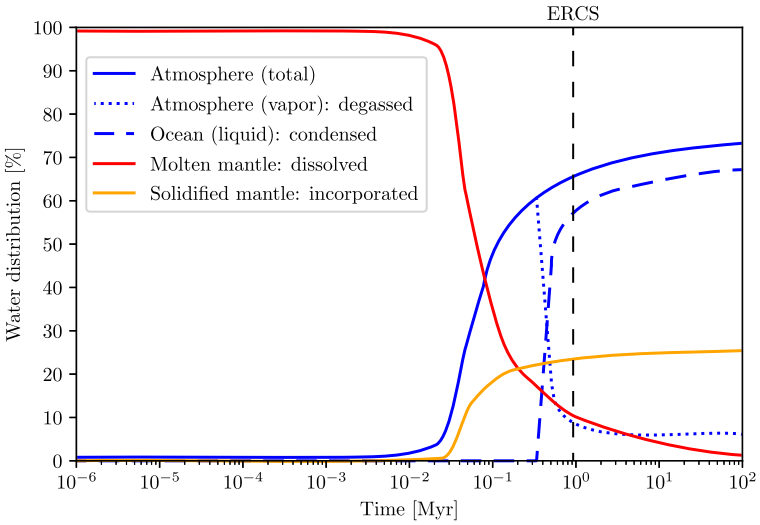

Fig. 11 Evolution of the distribution of water between the molten (red) and solidified (orange) mantle, the atmosphere (plain blue line for the total amount of water outgassed, including both vapor and liquid phase) and the ocean (dashed blue) during magma ocean solidification of an Earth-sized planet, while assuming efficient outgassing. The vertical dashed line indicates the time at which the End of the Rapid Cooling Stage is reached, i.e., when the planet has lost its excess of internal heat and reached global radiative balance with the net absorbed solar flux. Derived from Salvador et al. (2017) simulations

may isolate a significant part of the magma ocean from the surface in the center of large-scale convection rolls (e.g., Fig. 1 in Banzhaf 2003), thereby limiting the amount of silicate melt reaching low pressures at which volatiles are exsolved, and thus, tamping down magma outgassing. Using numerical fluid dynamics experiments, a recent study investigated how the detailed convective patterns may influence the time-dependent ability of the convecting fluid to reach shallow depths at which volatile exsolution and degassing proceeds (Salvador and Samuel 2023). They showed that vigorous convection and associated mixing does not ensure magma ocean chemical homogeneity. Rather, vortex-like small-scale features entrained in large-scale convective currents might generate local chemical heterogeneities. Then, despite high convective velocities and effective mixing, additional convective cycles and longer timescales would be required to erase those small-scale heterogeneities and to bring the volatile-rich melt blobs close to the surface where exsolution and degassing can occur. In some cases, these timescales may be comparable to or even larger than the magma ocean time spent in a given dynamic regime. Accumulated over the whole magma ocean lifetime, the amount of outgassed water may substantially decrease. There may be cases resulting in no outgassing of water initially dissolved deeper than the exsolution depth.

The crystallization sequence of the magma ocean may also significantly affect volatile distribution and outgassing efficiency. If the crystallization of the magma ocean starts from mid-mantle depths (Fiquet et al. 2010), rather than proceeding from bottom-up as it is commonly assumed in coupled magma ocean–atmosphere models, two distinct and separate molten layers may exist on either side of the crystallization front (e.g., Labrosse et al. 2007). While the upper molten layer would remain in contact with the surface where exsolution and outgassing may proceed as described above, the lower, deep basal magma ocean may keep its volatile species dissolved thanks to the large pressures at depth. The two molten layers would have diverging compositions, with the upper one being progressively depleted in

volatiles and dehydrated through outgassing, while the primordial lower one would become more and more volatile-rich with crystallization due to volatiles' melt affinity. Depending on the volume of this lower molten layer, dictated by the depth at which crystallization would start, a substantial amount of volatile species might remain isolated from the surface and thus unable to be outgassed.

In a similar fashion, melt–crystals relative density and resulting segregation (e.g., Boukaré and Ricard 2017; Caracas et al. 2019) may prevent possibly volatile-rich melt to reach the surface. If the melt becomes more dense than coexisting minerals at pressures near the base of the mantle (Mosenfelder et al. 2007; Asimow 2018), denser melts and their dissolved volatiles would be entrained downwards. Solidification would then proceed downward from a septum, and the dissolved volatiles would be trapped in the deep interior rather than rising-up throughout the melt and being released in the atmosphere (Elkins-Tanton 2011). Finally, even within a given reservoir of magma, the mode of crystallization, and more specifically melt–crystals segregation is believed to affect the amount of exsolved volatiles. In particular, the fraction of exsolved volatiles from a given magma is enhanced if the evolved liquids and exsolved volatiles are efficiently segregated from their crystalline products (e.g., Edmonds and Woods 2018).

If the magma ocean crystallization results in a gravitationally stable mantle stratification (e.g., Solomatov 2015), volatile species that have not been outgassed may remain in the solidified mantle and mantle chemical heterogeneities may persist until the present-day. On the other hand, if the crystallization leads to an unstable cumulate density stratification, the solidified mantle may overturn to a stable configuration (e.g., Elkins-Tanton et al. 2003). Mantle overturn may induce late episodes of outgassing through the melting of remnant volatile-rich mantle reservoirs, thus possibly releasing to the atmosphere volatile species that have not been outgassed during magma ocean solidification.

The planetary rotation rate may also affect the chemical structure of the crystallizing magma ocean and favor the development of chemical heterogeneities (Maas and Hansen 2015, 2019). In particular, for moderate and high rotation rates, the resulting crystallization pattern may induce an inhomogeneous magma ocean solidification with changes in depth and latitude. Major chemical segregation in distinct reservoirs might isolate a substantial magma ocean fraction from efficiently and rapidly reaching shallow depths where volatile exsolution occurs. Similarly to a basal magma ocean, these molten layers would likely retain their dissolved volatiles and outgassing may not be as efficient as commonly modeled. Yet, if the rotation rate of Venus during magma ocean crystallization was similar to its present-day value, this process would most likely not induce significant latitudinal crystal dynamics variations and would thus be negligible.

Another mechanism, that may significantly alter magma ocean outgassing efficiency and contradicts the classical efficient degassing assumption, is the efficient retention of interstitial, volatile-rich melt at the freezing front of a rapidly crystallizing magma ocean (Hier-Majumder and Hirschmann 2017; Miyazaki and Korenaga 2021, 2022). It stems from the fact that, if crystal–melt separation, matrix compaction, and melt upwards percolation are not efficient, a substantial fraction of melt and dissolved volatiles could be trapped within the crystallizing magma ocean.

The crystallizing melt is a solid-dominated, yet porous matrix with interstitial melt. McKenzie (2011) emphasized that depending on the competition between compaction within the freezing front and the rate of freezing, a substantial volume of the melt could be trapped during melt crystallization in a magma chamber, given no horizontal variations. Compaction within the freezing front expels out trapped melt, while rapid crystallization of the front freezes the melt in place and thus inhibits expulsion. Using a two-phase flow (of

melt and matrix) model, Hier-Majumder and Hirschmann (2017) showed that for magma ocean crystallization characteristic timescales, compaction within the moving freezing front is inefficient. Hence melt keeps being trapped at the rheological front while solidification proceeds. Then, if melt percolates upward through the solidified mantle insufficiently fast, Rayleigh-Taylor instabilities would continuously transport the newly formed solid matrix downwards (Miyazaki and Korenaga 2021, 2022), thus entraining the trapped melt and its dissolved volatiles at depth. Volatiles would thus also be trapped within the solidifying mantle and then sequestered in the deep mantle, rather than enriching the remaining melt. Volatile trapping would be enhanced by the fact that their solubility is greater at depth, where magma ocean crystallization is often thought to start, thus trapping melts with high volatile storage capacity and potential high water content. This way, up to 77% H_2O and 12% CO_2 of the total accretion-delivered volatile content could have been trapped in the mantle during magma ocean crystallization (Hier-Majumder and Hirschmann 2017). Yet, the low volatile storage capacity of solid mantle mineral phases (e.g., Bolfan-Casanova et al. 2003; Shcheka et al. 2006) do not support such large amounts of remnants water and carbon. To reconcile their results with such a low volatile storage capacity, Hier-Majumder and Hirschmann (2017) suggest different storage sites for the magma ocean crystallization leftover volatiles. Mantle carbon would be stored in solid carbonates and carbonate-rich melts in the upper mantle, and in diamond and metal carbides in the mid and lower mantle. Volatile-rich accessory minerals and water-enriched melt remaining along grain boundaries or as hydrous fluids or melts would act as storage sites of mantle water. They argue that such a buffered magma ocean outgassing reconciles the fact that the Earth's deep interior contains significant reservoirs of volatiles despite their incompatible nature. This process would be more effective in the case of equilibrium crystallization, where crystals and liquid remain in equilibrium (i.e., in contact) throughout crystallization. As opposed to fractional crystallization where melt–crystal separation is efficient. Assuming that 1% of the melt mass is interstitially trapped, lower estimates of the initial amount of water retained in the solid mantle range from 3% (Hamano et al. 2013) to 13% (Elkins-Tanton 2008; Hier-Majumder and Hirschmann 2017).

Note that in several cases, the amount of remnant water in the solidified mantle would mainly depend on the crystal–melt partition coefficients and on its solubility in the melt. This would include cases of high compaction and resulting efficient expulsion of melt from the porous matrix, or cases of slow magma ocean solidification relative to the compaction rate. It would also apply to cases of efficient crystal–melt separation at the rheological front. The latter owing to effective fractional crystallization or even tearing off and re-entrainment of the newly formed solid matrix within the molten mantle by vigorous convection currents and subsequent settle down of individual crystals.

Miyazaki and Korenaga (2021, 2022) have studied how such hampered magma ocean degassing and subsequent solidified mantle evolution and degassing patterns might affect the formation of early water oceans on rocky planets. Hamano et al. (2013) suggested that the rapidly-outgassed, steam atmosphere of Venus had prevented its climate from being temperate owing to the strong thermal blanketing effect. Miyazaki and Korenaga (2021) have suggested that, even for inefficient water degassing during the magma ocean phase, Venus may have continued to lack oceans throughout its history whereas Earth was able to form water oceans since the solidification of the mantle surface (Miyazaki and Korenaga 2022). In particular, if no ocean were formed upon solidification of the surface on early Venus, comparable rates of subsequent solid-state mantle degassing and water loss (through hydrogen escape) would not supply enough water to allow for later ocean formation.

Overall, any process that significantly reduces the amount of melt reaching the low pressures at which volatile exsolution (i.e., melt–gas partitioning) occurs during magma ocean

Table 1 Mechanisms possibly stifling magma ocean outgassing by isolating volatile-rich melt from the surface and contrasting with the classical efficient outgassing scenario

Mechanism	Reference(s)
Magma ocean crystallization starting at mid-mantle depth	Labrosse et al. (2007), Fiquet et al. (2010)
Planetary rotation and asymmetric crystal settling	Maas and Hansen (2015, 2019)
Melt–crystal density-driven segregation	Boukaré and Ricard (2017), Caracas et al. (2019)
Interstitial melt retention at magma ocean freezing front	Hier-Majumder and Hirschmann (2017), Miyazaki and Korenaga (2021)
Magma ocean convective dynamics	Salvador and Samuel (2023)

crystallization would alter outgassing efficiency and contrast with the classical view (Table 1). Then, if the melt exsolves volatiles, gas bubbles further need to reach the surface. If not, this would also stifle magma ocean outgassing. The global contribution of these combined mechanisms is still poorly constrained but the amount of volatile species remaining in the solidified mantle during the magma ocean solidification may have strong implications regarding the early and long-term evolution of the planet and should be accounted for in the future generation of models.

3.2.5 Influence of the Mantle Redox State

Generalities Molten mantle chemistry plays an important role in magma ocean outgassing. This is less by affecting its efficiency and the *amount* of outgassed species, such as the physical mechanisms mentioned above, than by controlling the *type* of outgassed species (see Table 2 for a summary of the different early outgassed atmospheres and underlying assumptions/constraints). In particular, the oxidation (redox) state of the mantle is critical. It has been interpreted in different ways but can be fundamentally defined by its availability of electrons and the resulting oxidation/valence state of its constituent elements (e.g., McCammon 2005a,b).

Oxidation–reduction reactions are chemical reactions generally[4] involving a transfer of electrons between two species. One is an electron donor (a chemical reductant or reducing agent, which readily gives up electrons) that becomes oxidized and the other an electron acceptor (a chemical oxidant or oxidizing agent, which possesses a strong affinity for electrons) that becomes reduced (e.g., Chap. 3 in White 2013; Kasting 2014). Oxidation thus refers to the loss of one or more electrons and the increase in the oxidation state/number. Reduction[5] is the gain of one or more electrons.

To maintain conservation of electrons (i.e., electrical neutrality), the oxidation of one compound necessarily implies the reduction of another, as electrons are transferred from one species to another. While originally used to refer to the reaction of a compound with oxygen (oxygen being the most common electron acceptor), hence oxidation, the term oxidation has

[4]While the transfer of electrons will always cause a change in oxidation state, there are many reactions that are classified as redox reactions even though no electron transfer occurs, such as those involving covalent bonds.

[5]The term reduction originates from the loss in weight upon heating a metallic ore, such as a metal oxide, to extract the metal: the ore was then "reduced" to the metal. Its meaning has then been generalized to any processes involving a gain of electrons.

been generalized to any electron-transfer reactions, without necessarily involving oxygen, after realizing that electron loss was the core of a substance being oxidized.

Yet, as it is the most common electron acceptor, the abundance of oxygen usually controls the oxidation state of a system, which is the case for the mantle, but this need not be the case. The oxidation state of the mantle is controlled by its chemical potential of oxygen, commonly referred to as the "oxygen fugacity", f_{O_2}. It is the equivalent of the partial pressure of oxygen in a particular environment corrected for the non-ideal character of the gas. It describes the formal abundance of O_2 gas in units of atmospheres (although often not representing an actual gas phase). Given its strong oxidizing power, a high oxygen fugacity/abundance corresponds to an oxidized environment while a low oxygen fugacity is associated with abundant reduced species in a reduced environment.

While most major elements constituting the mantle have only one stable oxidation state (e.g., Si, Al, Mg, O, Ca, Na, Ti), others, like Fe and several minor elements (e.g., C, S, Ni, Co, V) exhibit several stable oxidation states. Their geochemical behavior is thus affected by oxidation–reduction processes and reciprocally, their distribution, behavior, and abundance affect the oxidation state of their mantellic environment (e.g., Wood et al. 1990; Mallmann and O'Neill 2009). Because of their abundance, iron- and carbon-bearing solid species play an important role in controlling the oxygen fugacity.

Oxidation States of Iron and Redox Buffers From its most reduced to most oxidized state, iron most commonly occurs as metallic iron (oxidation state 0, noted Fe^0, Fe(O), or simply Fe), ferrous (divalent) iron (oxidation state of +2, meaning that it lost 2 electrons in the oxidation process; noted Fe^{2+} or Fe(II)), and ferric (trivalent) iron (oxidation state of +3 after the loss of 3 electrons; noted Fe^{3+} or Fe(III)). Iron is, by mass, the most abundant element on Earth (followed by oxygen). It is the most abundant element with a variable oxidation state. Iron's relative abundance in different oxidation states is also indicative of that of the mantle.

Furthermore, some specific iron-bearing (but not only) mineral assemblages, are in chemical equilibrium at a certain oxygen fugacity. For these two reasons, such mineral assemblages, called *redox buffers* (e.g., Reactions (R1), (R2), and (R3)), are used as references to constrain the oxygen fugacity of the mantle, hence its oxidation state (e.g., Frost 1991; Hirschmann 2021). For instance, in a given set of physicochemical conditions, at a given temperature, the oxidation of fayalite (F, which contains two ferrous ions Fe^{2+}) to magnetite (M, which contains one Fe^{2+} and two Fe^{3+}) and quartz (Q) imposes or "buffers" a specific value of f_{O_2} at equilibrium when all three mineral species are present. The reaction is (e.g., Frost 1991):

$$\underset{\text{fayalite}}{3\ Fe_2SiO_4} + O_2 \rightleftarrows \underset{\text{magnetite}}{2\ Fe_3O_4} + \underset{\text{quartz}}{3\ SiO_2}. \tag{R4}$$

This particular quartz-fayalite-magnetite (QFM) redox buffer is representative of relatively oxidized conditions that are typical of modern Earth's volcanic degassing and presumably of Earth's upper mantle. It is important to understand that the oxygen fugacity is fixed at a given value in a given oxygen fugacity–pressure–temperature space (e.g., Wood et al. 1990). This is simply by the equilibrium coexistence of fayalite, magnetite, and quartz. The oxygen fugacity does not depend on the proportion of these minerals. This is why it is appropriately called a buffer. This can be illustrated by considering a magma containing some amount of fayalite, magnetite, quartz, and oxygen. If the oxygen fugacity is increased by adding oxygen to the system, equilibrium in Reaction (R4) is driven to the right until the log of the oxygen fugacity returns to the given value (which is temperature and pressure dependent).

Only when all fayalite is converted to magnetite (and quartz) can the oxygen fugacity rise (e.g., Chap. 3 in White 2013). A decrease of oxygen fugacity would be buffered in exactly the opposite way until all magnetite and quartz were gone.

Another common buffer of oxygen fugacity is the iron-wüstite (IW) buffer (Reaction (R2)), which describes the coexistence of metallic (Fe) and ferrous (Fe^{2+}, which combines with O^{2-} to form FeO) iron and indicates a highly reducing environment. Here, an increase in f_{O_2} favors the reaction from left to right, which stabilises iron in its higher oxidation state (wüstite), whereas low f_{O_2} stabilises iron in its metallic, lower oxidation state.

Geochemical Implications, Speciation, and Outgassed Composition Like minerals, gas species can exist in various oxidation/valence states depending on the oxygen fugacity. The redox state of gases in equilibrium with rocks is often described by the mineral buffers that govern the capacity of the rock to consume or release oxygen (e.g., Zahnle et al. 2020). As mentioned above, oxidation–reduction processes affect the geochemical behavior of elements of several stable oxidation states, and consequently, that of the other elements interacting and having some chemical affinities with them (e.g., siderophile elements for iron). Overall, the redox state of the mantle (and its oxygen fugacity) controls the molecular speciation of C–H–O–N–S-bearing fluids and melts (French 1966; Frost 1979; Holloway 1981; Wood et al. 1990; Holloway and Blank 1994; Hirschmann et al. 2012; Hirschmann 2012; Grewal et al. 2020). It influences the solid–melt–gas partitioning of volatile species (Holloway and Blank 1994; Libourel et al. 2003; Miyazaki et al. 2004; Hirschmann 2012; Armstrong et al. 2015; Boulliung et al. 2020; Gaillard et al. 2021) and trace elements in the silicate magma – and thus, the composition of the atmosphere –, their partitioning among silicate melt and molten or solid metallic iron (Drake et al. 1989; Hillgren 1991; Holzheid et al. 1994; Righter et al. 1997; Gaillard et al. 2022b), as well as the mineral saturation and bulk mineralogy (e.g., Feig et al. 2010, and references therein). Indeed, given an elemental inventory of C–H–O–N–S, the abundance of oxygen, f_{O_2}, critically affects the identity of molecular species outgassed and controls the relative abundances of the oxidized and reduced form of major gases (e.g., H_2/H_2O, CO/CO_2).

The question of atmospheric oxidation state (hence, of its composition) is thus inextricably interlinked to the mantle redox evolution (e.g., Kasting et al. 1993a; Lécuyer and Ricard 1999). Essentially, an oxidized magma, i.e., of high oxygen fugacity (for instance at the QFM buffer, consistently with present-day upper-mantle conditions), induces outgassing of oxidized volatile species, such as H_2O, CO_2, SO_2, and N_2. Conversely, a magma of reduced composition (of low oxygen fugacity) releases reduced volatile species, such as CO, H_2, CH_4, NH_3, and H_2S (e.g., Holland 1962; Frost 1979; Wood et al. 1990; Kasting 1993; Hirschmann 2012). This speciation process can be explained by the fact that an environment of high oxygen fugacity/abundance makes it readily available to bond with C–H–O–N–S fluids and produce oxygen-bearing compounds. Note however that redox changes during magma ascent (Sato 1978; Burgisser and Scaillet 2007), mixing (Ueki et al. 2020), and degassing (Mathez 1984; Humphreys et al. 2015) may occur, making the link between the redox state of magmas and their outgassed products less straightforward than commonly assumed.

Present-Day Redox State The Earth's present-day atmosphere is highly oxidized as its second most abundant constituent is O_2, which is a powerful electron acceptor. However, early magma ocean and subsequent long-term volcanic degassing only cannot explain this current characteristic feature, which certainly results from the complex interplay between geochemical and biotic processes (e.g., Holland 2006; Kasting 2013; Catling 2014; Catling and Zahnle

2020). Yet, at present-day, H_2O and CO_2 are the two most abundant gases released by volcanic degassing, which indicates that the Earth's present-day upper mantle is in an oxidized state (e.g., Frost and McCammon 2008). With CO_2 its most abundant constituent, Venus' atmosphere is currently relatively oxidized, despite being considered possibly weakly reducing in its lower part (e.g., Catling 2015). Surface–atmosphere interactions likely result in an oxidizing surface with a high oxygen fugacity at about the Magnetite-Hematite (MH) redox buffer (e.g., Fegley et al. 1997; Zolotov 2018). The mean FeO/MnO ratio measured at Venus' surface by Venera 13, 14, and Vega 2 is slightly less than that of the bulk silicate Earth (∼52 for Venus' surface, Surkov et al. 1984, 1986; Volkov et al. 1986; and ∼60 for the BSE). Used as a proxy of the planet's oxidation state (Wänke et al. 1973), it also suggests a rather oxidized surface and interior. If the present-day Venusian SO_2 atmospheric inventory originates from volcanic outgassing, it could indicate that at least some parts of the Venusian mantle are highly oxidized, at about the QFM buffer.

Early Oxidation State While present-day volcanic outgassing can be related to the current magma sources redox state, the earliest oxidation state of planetary mantles is much more speculative and little is known about the magma ocean initial and evolving redox conditions. The oldest clues available on Earth come from measurements on Hadean zircons, recording oxygen fugacity of Hadean magmatic melts identical to those in the present-day mantle, thus indicative of an oxidized upper mantle (at about QFM buffer) as early as 4.35 Gyr ago (Trail et al. 2011). Earth's oldest igneous rocks also suggest that the mantle redox state was only weakly reduced and has not varied significantly over at least the past 3.9 Gyr of Earth's history (Canil 1997; Delano 2001; Canil 2002; Lee et al. 2003; Li and Lee 2004; Rollinson et al. 2017; Nicklas et al. 2018). As today, the redox state was then likely set by the QFM buffer, so that the resulting volcanically-outgassed atmosphere would have been mostly made of H_2O, CO_2, and N_2, with small amounts of CO and H_2 (Holland 1962; Abelson 1966). There is no such records available for Venus and whether these conditions are systematic outcomes of planetary early evolution and can be generalized to early Venus or are Earth-specific is unclear.

Constraints from Prebiotic Chemistry Prebiotic chemistry can provide independent but indirect constraints on the environment at the surface of early Earth. Yet, the prevalence of an early oxidized environment suggested by geochemical evidence is hard to reconcile with the reduced conditions requirements inferred from chemical studies on the origin of life. Indeed, prebiotic chemistry experiments, starting from the famous Miller–Urey experiments in the early 1950s (Miller 1953, 1955; Miller and Urey 1959), have shown that amino acids and a wide number of other building blocks of living organisms can be synthesized from electrical discharges in highly reduced conditions with the presence of methane and ammonia and where free oxygen is absent (see Oro et al. 1990; McCollom 2013; Benner et al. 2020, for reviews). The fact that such conditions result in efficient abiotic synthesis of biologically important organic compounds suggested that the origin of life required a very reducing environment. Hence hinting that this was the case for the earliest terrestrial atmosphere overlying a solidified surface.

It should be noted that bridging the gap between the non-agnostic conditions under which prebiotic chemistry experiments are successful in producing life-essential compounds and actual early Earth's conditions where life emerged remains challenging and is still an extensive area of study (e.g., McCollom 2013). For instance, Cleaves et al. (2008) have suggested that yields of amino acids observed in more neutral (N_2/CO_2-dominated) or oxidized environment experiments may have been biased low/underestimated owing to oxidation of the

acids during sample processing. Then, using oxidation inhibitors during sample processing or adding $CaCO_3$ to buffer the pH of the aqueous phase would significantly increase the yields.

Energy sources other than electrical discharges/lightnings have also been invoked to synthesized complex biological molecules without necessarily requiring highly reducing environments (e.g., Chyba and Sagan 1992; Kurosawa et al. 2013). In particular, coronal mass ejection events from the active young Sun could trigger nitrogen fixation and ignite reactive chemistry yielding complex molecules in less reducing environments (Airapetian et al. 2016, 2020).

Based on the abundance of organic molecules in the Solar System, alternative scenarios have invoked exogenic sources of organics for the origin of life rather than an in-situ production (e.g., Anders 1989; Chyba et al. 1990; Chyba and Sagan 1992; Whittet 1997; Matthews and Minard 2006). This abundance of organic molecules may imply that they are not that hard to make (see Zahnle et al. 2010 and references therein for a thorough discussion). Yet, the extraterrestrial delivery of complex and organic materials by comets, asteroids, and interplanetary dust particles and their implications for the emergence of life is challenged by their survival upon impact (e.g., Whittet 1997; Pierazzo and Chyba 1999; Pasek and Lauretta 2008).

The apparent contradiction between the reducing conditions required by prebiotic chemistry and the likelihood of an oxidized early atmosphere (and mantle) might also be resolved by alternative scenarios involving an oxidizing surface environment. Such an environment may result from magma ocean degassing. But the oxidizing environment might experience a perturbation making it temporarily and/or locally reducing (Airapetian et al. 2016; Itcovitz et al. 2022). In fact, such transient conditions may actually be the most favorable for prebiotic chemistry (Benner et al. 2020).

Impact-Induced Degassing and Transient Reducing Environments To produce such a perturbation and reconcile geological evidence of an oxidizing past with the requirements for life's emergence, impact-induced degassing has been proposed. Gases are then directly released into the atmosphere on impact (Benlow and Meadows 1977; Jakosky and Ahrens 1979; Lange and Ahrens 1982; Matsui and Abe 1984, 1986b). It is an efficient mechanism to release strongly reduced species into the early atmosphere, and thus to provide favorable conditions for the origin of life despite a rather oxidized, volcanically-produced, environment (e.g., Zahnle et al. 2010, 2020). It is thought to proceed as follows: due to the energetics of impact, all of the volatiles carried by the impactors are expected to be vaporized, to equilibrate chemically with the other materials of the impactor, and to directly enter the atmosphere. Atmospheres resulting from impact degassing would then tend to have a composition reflective of the impacting bodies (rather than the proto-planet mantle). These are mostly volatile-rich and much more reduced than the mantle (e.g., Zahnle et al. 2010). Note that additional and more complex reactions between the impactor components and the impacted body's atmosphere or crust can increase the production rates of reduced species (e.g., Kasting 1990).

Models of impact-generated atmospheres generally suggest that the outgassing of reducing species dominates for a variety of meteoritic materials (e.g., carbonaceous, ordinary, and enstatite chondrites; Kasting 1990; Schaefer and Fegley 2007; Hashimoto et al. 2007; Sugita and Schultz 2009; Schaefer and Fegley 2010). If the gases of Earth's earliest atmosphere had equilibrated with material like that of primitive meteorites, the resulting atmosphere would be much more reduced than present-day volcanic gases (e.g., Zahnle et al. 2010). This is due to the reducing power of the substantial amounts of metallic iron and iron sulfides contained

in many meteorites, including ordinary and enstatite chondrites. Even for CI carbonaceous chondrites the resulting gases are rather strongly reducing owing to the reducing power of the abundant carbon contained in CI chondrites and present in reduced form (Hashimoto et al. 2007; Zahnle et al. 2010). These are the most highly oxidized meteorites (e.g., Urey and Craig 1953, Rubin et al. 1988, Krot et al. 2014; and Fig. 5.2 in Trieloff et al. 2006) and thus expected to generate the most highly oxidized gases among the different meteoritic sources. Note however that Schaefer and Fegley (2010) found that carbonaceous chondritic material such as CI, CM, and CV chondritic materials would rather produce oxidized atmospheres.

Yet, mixtures of solid meteoritic material (from highly oxidized carbonaceous chondritic material to highly reduced enstatite chondritic or eucritic materials) may also produce more oxidizing compositions (Schaefer and Fegley 2017). They are relevant to the mixing of materials from different locations in the solar nebula and thus representative of the primitive solar nebular materials. Indeed, because of variations in the abundance of buffering phases (such as metallic iron) and volatiles within the solid materials, gases produced out of their mixtures are not a straightforward linear mixture of the gases produced by individual materials. As a result, adding only a few percent of carbonaceous material to a differentiated body may be sufficient to raise the f_{O_2} of the mixture by several log units. Given the stochastic nature of accretion (Sossi et al. 2022) and since the oxygen fugacities differ between individual materials and their mixtures, the behavior in mixtures remains uncertain (Schaefer and Fegley 2017). Schaefer and Fegley (2017) also emphasized that other processes affecting the redox state of the atmosphere, such as hydrogen escape, photochemistry, or surface-atmosphere interactions, would certainly induce additional complexities and should be further investigated. For instance, they have found that oxidized materials become more oxidized by hydrogen loss whereas reduced materials do not. While NH_3- and methane-rich atmospheres are prone to efficient photochemical dissociation by solar ultraviolet radiation (e.g., Leighton and Steiner 1936; Lasaga et al. 1971; Kuhn and Atreya 1979; Kasting et al. 1983) and thus unlikely stable as steady states, impact-induced outgassing of infalling meteoritic material could repeatedly create transients and life emergence-favorable conditions many times.

Initial Redox State of the Magma Ocean and Its Evolution Based on the aforementioned direct and indirect constraints and processes, a consensual view may emerge. It suggests that the mantle oxidation state was relatively oxidized and close to its current state early in history, once the surface was solidified (i.e., post-magma ocean). The overlying atmosphere was also likely oxidized and composed dominantly of H_2O and CO_2. In such an oxidizing environment, impact-induced degassing transiently produced reduced conditions favorable for the development of life on Earth. Before the surface was solid, prior to the available geological records and to the setting of life-sustainable conditions on a solidified planet, the oxidation state of the earlier evolution stages, such as the magma ocean phase itself and its evolution upon cooling, is highly unconstrained. In particular, whether oxidized conditions are a direct/intrinsic consequence of the magma ocean evolution or inherited from other mechanisms related to planetary formation remains unclear. To address this issue, we discuss below the processes thought to affect the redox state of the earliest stages of planetary evolution, with particular emphasis on the magma ocean stage, and how they may be reconciled with the available constraints of the subsequent stages.

Hydrogen-Rich and Reducing Early Atmospheres A primordial H_2–He atmosphere captured from the solar nebula (see Sect. 2.1) would induce a reduced start. Before being lost after the

dissipation of the solar nebula (e.g., Zahnle et al. 2007), its reducing power could have affected both the surface and the mantle of the proto-planet. Similarly the H_2–He solar nebula could have reduced the planetesimals that subsequently encountered the planet, thus being a source of reduced materials (Zahnle et al. 2010). Tian et al. (2005) have suggested that in a hydrogen-rich early atmosphere, the escape rate of hydrogen would be energy-limited due to lower exospheric temperatures rather than diffusion-limited and thus operating much slower. In such a case, a primordial hydrogen-rich atmosphere and its reducing power would have been sustained longer and maintained after dissipation of the solar nebula. Without necessarily involving the solar nebula, on longer timescales, the balance between slow hydrogen escape and hydrogen outgassing (requiring a reducing upper mantle) could have preserved/induced an atmospheric hydrogen mixing ratio of up to 30% (Tian et al. 2005; Liggins et al. 2020) and sustained a reducing environment. Note however that Tian et al. (2005) hydrogen escape rate estimates may be biased low and are controversial (Catling 2006; Tian et al. 2006; Kuramoto et al. 2013; Tian 2015).

Link with Core Formation and Evidence for a Reduced Start The depth, timing, and timescale of metal–silicate equilibration, separation, and resulting core formation, play a critical role in determining the oxidation state of the magma ocean and crystallizing mantle. These processes are likely occurring throughout the accretion sequence and possibly extend through the different magma ocean stages. Because of the reducing power of metallic iron, metal–silicate equilibration necessarily implies a reducing environment (of low oxygen fugacity, near the IW buffer) imposed by the coexistence of metallic iron in equilibrium with silicate (Reaction (R2)), thought to significantly reduce the silicate melt (O'Neill 1991; Wade and Wood 2005; Frost and McCammon 2008; Rubie et al. 2011). One may then expect that the magma ocean was initially in such a reduced state, prior to the complete metal segregation to the core. Importantly, the redox state of the upper part of the mantle, where the gases originate, would mainly matter for the oxidation state of contemporary outgassed species.

The segregation of metallic iron through the mantle, as well as the pressure–temperature dependence of metal–silicate partition coefficients (e.g., Wade and Wood 2005) could induce a vertical zonation/gradient of the redox state. However, vigorous convection and mixing of the molten mantle could also buffer metallic iron sinking through Rayleigh-Taylor instabilities and could repeatedly bring reducing iron to shallow depths. In addition, effective convective re-entrainment could slow down iron accumulation at the base of the molten layer (alike crystals re-entrainment; e.g., Solomatov 2015). It could also buffer the formation of metal diapirs large enough to sink to the core, therefore delaying metal–silicate separation. Thus, the upper mantle may have remained in such a reduced state prior to at least advanced planetary differentiation and core formation (e.g., Catling and Claire 2005). Here the metallic iron would have sunk deep enough to no longer affect the upper mantle redox state, and every time the metallic iron of accreting planetesimals would merge into the mantle of the growing proto-planet. Yet, the latter effect strongly relies on the details of metallic iron distribution upon impact, itself influenced by impact parameters and mantle mixing (Deguen et al. 2014; Landeau et al. 2016, 2021; Maas et al. 2021; Itcovitz et al. 2022).

Keppler and Golabek (2019) suggested that, in the case of a highly reduced mantle resulting from metal–silicate equilibration, most of the carbon could be reduced to graphite, which is less dense than a peridotite melt. In such a case, regardless of metal–silicate equilibration depth, as long as such highly reduced conditions prevail somewhere within the magma ocean, graphite flotation and accumulation on top of the magma ocean may have imposed low f_{O_2} conditions in its shallow parts given the CCO buffer ($C + O_2 = CO_2$).

These mechanisms favor a reduced start, but predicting the early oxidation state of the shallow part of the magma ocean and the resulting atmospheric composition remains challenging. In part because linking core formation to the mantle oxidation state is not straightforward. Yet also because core formation itself is complex, and likely results from the interplay of different processes with lots of remaining uncertainties (e.g., Rubie et al. 2015b).

Changes of partition coefficients, phase separation and phase changes (and resulting density contrasts; e.g., Boukaré and Ricard 2017) under extreme and varying $P/T/f_{O_2}$ conditions relevant to magma ocean cooling could induce unknown yet possibly significant feedback that need more investigations. Furthermore, additional complexities regarding the fate of iron in the post-impact mantle and the details of metal–silicate equilibration in a turbulent molten mantle, as well as their influence on the mantle redox state have been poorly studied. Deguen et al. (2014) have shown that the turbulent mixing of a vigorously convecting magma ocean enhances equilibration. By considering the effect of rotation in the convective magma ocean in spherical geometry, Maas et al. (2021) emphasized that metal dispersion and settling also depend on the impactor's target latitude. Citron and Stewart (2022) and Itcovitz et al. (2022) recently showed that the impact parameters strongly influence the distribution, mixing, and availability of the reduced phases of the impactor (e.g., metallic iron) to potentially reduce the atmosphere. They also investigated the interactions between the post-impact atmosphere and the impact-generated melt phase. Importantly, the manner in which iron is accreted by and mixed with the target, and the timing and depth at which metal–silicate equilibration occurs requires further investigation to constrain the oxidation state of the shallow magma ocean layers upon impacts. It would also determine the oxidation state of the outgassed species, and hence the composition of the resulting atmosphere. Because most of the projectile iron (more than 70%) is deposited in the crust and upper mantle, where it is not available to reduce surface water, reducing environments could be less likely to arise after large impacts than previously suggested.

In any case, the fact that the molten mantle must have been in equilibrium with the metallic iron now forming the core, and hence, characterized by low oxygen fugacity, is hard to reconcile with the prevailing early oxidized conditions of the solidified surface, by the time minerals and rocks were formed as described before. From a reduced start, some mantle oxidation mechanisms must then have been in place to resolve this paradox.

Oxidation Mechanisms from a Reduced Start To explain the formation of the core in agreement with the abundance of siderophile elements of the mantle and their experimentally-determined partition coefficients, several models have been suggested. These have implications for the oxidation state of the mantle (e.g., Li and Agee 1996; Wood et al. 2006; Fischer et al. 2015). From a reduced start, several oxidation mechanisms have been proposed to increase the oxygen fugacity of the mantle to the QFM buffer (e.g., McCammon 2005b; Wood et al. 2006; Frost et al. 2008; Frost and McCammon 2008; Wood et al. 2009; Schaefer and Elkins-Tanton 2018; Armstrong et al. 2019).

Photo-dissociation of H_2O followed by the escape of H_2 from the atmosphere (Hunten 1993) may have caused oxidation of both the atmosphere and mantle by the leftover oxygen (Kasting et al. 1993a; Sharp et al. 2013). This mechanism likely occurred to some extent. The composition of martian meteorites (Dreibus and Wänke 1987) and the elevated abundance of light elements in its core (Khan et al. 2022) suggest that Mars was possibly more volatile-rich than Earth. If hydrogen escape was the main oxidizing mechanism, it is unclear why Mars produced basalts more reduced than MORB and indicative of a relatively more reduced (Herd et al. 2002; Wadhwa 2008) and FeO-rich (Wänke et al. 1988) mantle (at about the IW buffer), despite efficient atmospheric water loss through hydrodynamic escape

(Pepin 1991; Jakosky and Phillips 2001). Furthermore, while Venus likely experienced massive loss of hydrogen, its silicate portion is not significantly more oxidized than the Earth (Schaefer and Fegley 2017).

An alternative solution involves the increase of oxidation state of accreting bodies during late accretion (Wänke et al. 1988; O'Neill 1991; Wood et al. 2009; Rubie et al. 2011, 2015; Fischer et al. 2015; Shi et al. 2022), also referred to as heterogeneous accretion. This allows trace element partitioning models to match the present-day mantle FeO abundance, but fails to predict the current redox state-governing $Fe^{3+}/\Sigma Fe$ (which is the proportion of the Fe that is ferric) and the final oxygen fugacities of these models is generally still too low (typically at IW-2, which is about 5 $\log f_{O_2}$ units below the Earth's present-day value; e.g., Schaefer and Fegley 2017; Schaefer and Elkins-Tanton 2018).

Another possibility is that the mantle self-oxidized as a result of perovskite crystallization (Mao and Bell 1977; Frost et al. 2004; Wade and Wood 2005; Galimov 2005; Frost et al. 2008; Frost and McCammon 2008; Hirschmann 2012; Armstrong et al. 2019; Hirschmann 2022). At depth, the growth of silicate perovskite (bridgmanite), the dominant lower-mantle mineral, forced the disproportionation[6] of ferrous iron (Fe^{2+}) into ferric iron (Fe^{3+}) (dissolved in perovskite; McCammon 1997) plus iron metal (segregated to the core; Frost et al. 2004): $3FeO \longrightarrow Fe^0 + Fe_2O_3$ (or $4FeO \longrightarrow Fe^0 + Fe_3O_4$). Repeated crystallisation and dissolution of Fe^{3+}-containing perovskite at the base of the magma ocean acted as an "oxygen pump" (Wade and Wood 2005). This raised the oxygen fugacity of the growing mantle by releasing ferric (Fe^{3+}) iron to the magma ocean, while the produced reduced metallic iron segregated to the core (e.g., Armstrong et al. 2019). Infalling metallic iron from subsequent impactors would have been oxidized by the ferric iron, therefore raising the FeO content of the silicate magma and the oxygen fugacity of core separation. Mantle convection and homogenization would further raise the oxygen fugacity of the upper mantle to its present-day value toward the end of core formation and by the time of Hadean zircon formation (e.g., McCammon 2005a; Frost and McCammon 2008). This self-oxidation process relies on the ability of Earth's mantle to stabilize substantial amounts of perovskite at depth. It is essentially planetary size-dependent and could have thus operated similarly on Venus (assuming it experienced a deep enough magma ocean) but not on Mars (e.g., Wood et al. 2006). Note that Schaefer and Elkins-Tanton (2018) proposed that the disproportionation of Fe^{2+} would occur directly in the silicate melt phase in the magma ocean during equilibration with the sinking core-forming metal delivered by impactors, rather than during crystallization (see also Hirschmann 2022). This alternative scenario allows immediate separation of the metallic liquid, leaving the oxidized mantle material behind without requiring additional mixing nor complex scenarios of repeated crystallisation and melting of bridgmanite.

Thus, despite a favored early reduced start for the magma ocean, these oxidation mechanisms may have brought the molten mantle to an oxidized state before its complete solidification. If the planet is still molten once core formation is complete and the planet has a differentiated Fe metal and FeS core, Lupu et al. (2014) showed that the equilibrium of a molten surface of either bulk silicate Earth or continental crust composition results in the formation of H_2O–CO_2-dominated (i.e., oxidized) atmospheres. This corresponds to a case where metal–silicate segregation occurs before the last magma ocean episode or rapidly compared to its solidification.

Finally, an increasing amount of evidence has suggested that magma ocean evolution itself might be the determining factor in the evolution of the oxidation state of the magma

[6] A disproportionation reaction is a redox reaction in which the initial material of intermediate oxidation state undergoes oxidation as well as reduction and converts simultaneously to two compounds, one more oxidized and one more reduced.

ocean–atmosphere system (Armstrong et al. 2019; Solomatova and Caracas 2021). It may also reconcile the two favored end-members: a reduced start, owing to metal–silicate equilibration, and an oxidized end, as demonstrated by geological records. For instance, Maurice et al. (2023) suggested that the crystallization sequence of the magma ocean itself could be an oxidizing process, because of the incompatibility of ferric iron. This would imply that the shift towards an oxidized atmosphere would be a systematic outcome of the magma ocean evolution.

Indirect Evidence of Magma Ocean Redox State Different attempts recently aimed at assessing the oxidation state of the molten mantle prior to the aforementioned available direct or indirect constraints (Pahlevan et al. 2019; Deng et al. 2020; Thompson et al. 2021; Solomatova and Caracas 2021). Thompson et al. (2021) recently conducted laboratory investigations of meteorite outgassing on CM-type carbonaceous chondrites (i.e., undifferentiated), as representative samples of the bulk composition of material in the solar nebula. This was in order to assess the composition of resulting atmospheres. However, one should note that their experimental setup and procedure is more representative of outgassing from the molten interior of a planet (of bulk chondritic composition) rather than impact-induced degassing as modeled in the aforementioned studies. Indeed, by simply heating chondrites and measuring the abundances of released volatiles, they reproduce the conditions expected for the outgassing from a molten planet and resulting secondary atmosphere formation. Here shock-induced devolatilization does not occur. Yet, devolatilization along with atmospheric entry and structural changes upon impact most likely altered the chondrite that was sampled and its overall representativeness. They found that water would makeup most of such an outgassed atmosphere (66%), followed by CO (18%) and CO_2 (16%), thus producing a rather oxidizing atmosphere (Thompson et al. 2021).

Pahlevan et al. (2019) used hydrogen isotopic records (the deuterium content) of Earth's hydrosphere to independently assess the oxygen fugacity of terrestrial magma ocean outgassing. They emphasized that the preservation of a carbonaceous chondritic (i.e., undifferentiated) D/H signature in the terrestrial oceans requires a hydrogen-poor (relative to water, i.e., $H_2/H_2O < 0.3$) Earth's outgassed envelope. This is indicative of oxidizing conditions ($\log f_{O_2} > \mathrm{IW} + 1$) for last atmospheric equilibration with the magma ocean. In agreement with the earliest geological record (Trail et al. 2011), they concluded that oxidation of the silicate Earth occurred during the crystallization of the (last) magma ocean, and may not require later geological processes such as subduction (and associated oxidation through slab dehydration for instance; e.g., Wood et al. 1990; Kasting et al. 1993a) to reach the oxidized present-day state.

Earth and chondrites similar volatile isotopic compositions suggest that the source of terrestrial volatiles is chiefly chondritic (Marty 2012). Yet, the elemental composition of the bulk silicate Earth is depleted in C, N, and H relative to chondritic material. Accretion of some non-chondritic materials has thus been proposed to account for this depletion (Hirschmann 2016). Sakuraba et al. (2021) modeled the evolution of volatile abundances during the accretion by considering elemental partitioning, including the effect of the magma ocean redox state on volatile solubility and metal–silicate partition coefficient, and impact erosion. They found that the BSE depletion pattern can be reproduced from continuous accretion of chondritic bodies only, without the need of non-chondritic materials, but requires a relatively oxidized magma ocean ($\log f_{O_2} \approx \mathrm{IW} + 1$). In good agreement with Pahlevan et al. (2019), their results indicate a relatively oxidizing magma ocean at the end of the accretion stage.

Based on first-principles molecular dynamics calculations, Solomatova and Caracas (2021) showed that during the first stages of magma ocean evolution, C is rapidly devolatilized (in the form of CO_2). Yet H remains dissolved in the magma for longer and is volatilized (as H_2O) during later magma ocean stages. This would have resulted in the outgassing of a CO_2-rich and H_2O-depleted atmosphere during the early stages of the magma ocean. H_2O would have been outgassed later on with solidification, thus supporting the classically modeled outgassing sequence of coupled magma ocean–multi-species atmosphere models (e.g., Elkins-Tanton 2008; Lebrun et al. 2013; Salvador et al. 2017; Nikolaou et al. 2019; Bower et al. 2019). They also suggested that, despite the uncertain oxidation state after a giant impact, the amount of oxygen available in the system influences the speciation of the vaporized carbon. Hence more oxidized systems favor the release of more oxidized vapor species, i.e., CO_2 outgassing rather than CO. The composition of the melt itself also affects the composition of the vapor phase. In addition to increasing with the oxidation state, they demonstrated that the relative proportion of CO_2 to CO increases with decreasing density and temperature, thus suggesting that the abundance of atmospheric CO_2 increased with time and magma ocean cooling.

Deng et al. (2020) combined first-principle molecular dynamics simulations with thermodynamic modeling at relevant P/T conditions. They studied the redox controlling reactions in magma oceans. In agreement with Armstrong et al. (2019) high pressure experiments, they found that compared to ferrous iron (Fe^{2+}), ferric iron (Fe^{3+}) becomes increasingly energetically favorable with pressure because of its small partial molar volume in silicate melts under large compression (Fe^{3+}-bearing melts are more compressible). In a convectively homogenized magma ocean, this would produce a vertical gradient in oxygen fugacity (as proposed by Hirschmann 2012). Here the upper part being relatively more oxidized than the deeper part where redox values were taken to be representative of local equilibrium with reduced molten iron ponds, i.e., assuming that core–mantle equilibration occurred at the bottom of a relatively deep magma ocean (consistent with metal–silicate partitioning experiments; e.g., Li and Agee 1996; Fischer et al. 2015). Yet, before gradually decreasing downwards throughout the rest of the mantle, the relative oxygen fugacity first increases slightly with pressure in the uppermost mantle. The increasing trend was also reported previously in experiments establishing the effect of pressure on the $Fe^{3+}/\Sigma Fe$ ratio of silicate melts (Zhang et al. 2017). Yet, as Zhang et al. (2017) experiments were restricted to relatively shallow depths (up to 7 GPa), they concluded that oxygen fugacities at the surface of shallow magma oceans are more reduced than at depth. They also found that when extrapolated to higher pressures relevant for magma oceans on Mars- or Earth-/Venus-sized planets, atmospheres overlying magma oceans should be highly reduced and rich in H_2 and CO. Importantly, Deng et al. (2020) showed that this trend actually reverses at larger depth and emphasized that an oxidized upper mantle is a natural consequence of a magma ocean due to the increasing stability of ferric (oxidized) iron with depth, even at relatively reduced conditions, which raises the $Fe^{3+}/\Sigma Fe$ ratio of silicate melts in equilibrium with metal alloy. By calculating the speciation of volatiles to determine the composition of an outgassed atmosphere at chemical equilibrium with the underlying magma ocean, they found that the resulting early atmosphere of Earth-/Venus-sized planets (i.e., with deep magma oceans) should be enriched in H_2O ($\sim$70 mol%) and CO_2 ($\sim$15 mol%), and therefore, be highly oxidized.

However, Righter and Ghiorso (2012) used a different approach to estimate f_{O_2} and despite agreeing with a similar vertical zonation in magma oceans (from shallow oxidized portions to deep reduced portions), they argued that metal–silicate experiments would bias f_{O_2} estimations such that none of the magma ocean part would be more oxidized than the

IW buffer. Conversely to what is assumed in accretion models described previously, increasing the FeO content of planetary mantles during accretion may not lead to oxidation. It would rather lead to significant reduction relative to the IW buffer, therefore decreasing f_{O_2} from high to low during accretion. This view indicates that further investigations are needed but remains challenged by the apparent prevalence of oxidized conditions indicated in rock records. It also contrasts with the studies mentioned above (Pahlevan et al. 2019; Deng et al. 2020; Thompson et al. 2021; Solomatova and Caracas 2021), all suggesting that the degassing of the upper magma ocean produced oxidized species and was thus already in a relatively oxidized state early on.

Influence of the Magma Ocean Redox State on the Thermo-Chemical Evolution Because of the uncertainties regarding the magma ocean redox state, it is important to assess its influence on the thermo-chemical evolution of the magma ocean–atmosphere system. This has been the focus of recent studies that simulated the solidification and/or outgassing of the magma ocean while considering f_{O_2} as a free parameter, thus considering both reduced and oxidized conditions (Katyal et al. 2020; Bower et al. 2022; Gaillard et al. 2022a; Maurice et al. 2023).

Katyal et al. (2020) investigated the effect of mantle oxidation state on volatile outgassing and chemical speciation at the surface at specific conditions relevant to different steps of magma ocean evolution for various redox states. They showed that the oxidation state of the magma ocean, through the composition of the outgassed atmosphere, affects the atmospheric thermal opacity, surface pressure, and scale height, and thus, ultimately, the cooling rate of the magma ocean. Because of its relatively low mean molecular weight, a H_2/CO-dominated reduced atmosphere outgassed from a reduced magma ocean has a larger scale height than a H_2O/CO_2-dominated oxidized atmosphere (outgassed from a oxidized mantle, which is consistent with experimental determinations; e.g., Grewal et al. 2020) containing heavier species. The higher thermal blanketing effect of the latter dense and small scale height atmosphere made of efficient greenhouse gases is expected to slow down the cooling of the magma ocean. Conversely, a reduced mantle surrounded by reduced outgassed species is expected to cool down faster. Yet, the greenhouse effect of reduced species is far from being negligible. In particular for dense atmospheres, the collision-induced absorption (CIA) of reduced species such as H_2 and CH_4 can extend the outer edge of the habitable zone (Pierrehumbert and Gaidos 2011; Ramirez and Kaltenegger 2017, 2018) and maintain ancient Mars temperate (Ramirez et al. 2014; Wordsworth et al. 2017; Turbet et al. 2019, 2020; Godin et al. 2020). Note that both the atmospheric thermal opacity and scale height affect the thermal emission and transmission spectra that could be used to infer the oxidation state of an extrasolar planetary interior and constrain its evolution with time.

Bower et al. (2022) reached similar conclusions while considering additional C/H ratios and hydrogen budgets. As shown in earlier coupled magma ocean–atmosphere studies for oxidized species (Salvador et al. 2017; Nikolaou et al. 2019; Bower et al. 2019), because of their larger solubility in silicate melts the H-bearing species are outgassed later than C-bearing ones. This also applies to reduced conditions. Because of the combined influence of volatile solubility and redox reactions, Bower et al. (2022) emphasized that an atmosphere may evolve from dominantly CO-rich and reducing to H_2O-rich and oxidizing with cooling. They further suggested that the mode of crystallization (i.e., equilibrium versus fractional) would induce additional complexity. For example, the formation of an early surface lid (at around 30% of remaining melt), as a result of faster magma ocean freezing under equilibrium crystallization, could delay or even prevent subsequent outgassing of highly soluble volatile species (such as water).

Maurice et al. (2023) also reported that the redox state of the crystallizing magma ocean evolves systematically towards oxidizing conditions. This owing to the incompatibility of Fe^{3+} in the minerals resulting in its enrichment in the melt and in the increase of the oxygen fugacity throughout magma ocean crystallization. They showed that the outgassed atmosphere at the final stages of crystallization is consistently oxidized and dominated by H_2O and CO_2. Yet, unlike other studies, they found that the cooling and solidification of initially reduced magma oceans is slower than that of initially oxidized magma oceans. Indeed, despite the stronger greenhouse effect of oxidized atmospheric species, they emphasized that initially reduced atmospheres are not able to radiate as efficiently as oxidized atmospheres owing to their steeper lapse rate, so that the molten phase is protracted.

The Gaillard et al. (2022a) magma ocean static outgassing model also supports an enhanced outgassing of C-bearing species compared to H-bearing ones in all oxidation states. They further included N- and S-bearing species and predicted that an oxidized magma ocean would mainly outgas C–N–S. They therefore form atmospheres made of CO_2–SO_2–N_2–H_2O with relative proportions varying according to the degree of oxidation, while a reduced magma ocean would mainly outgas CO–H_2 with some CH_4 for the most reduced cases and N_2 otherwise.

Besides affecting the chemical composition of the outgassed atmosphere, and thus indirectly its thermal evolution through atmospheric opacity, the redox state may affect intrinsic properties of the magma ocean itself. Using high-temperature experiments, Lin et al. (2021) showed that oxygen fugacity has a direct effect on rock melting properties by affecting the liquidus. In particular, they reported that a higher oxygen abundance lowers the liquidus temperature of iron-free basalt at 1 atm, thus facilitating melting. How these findings apply to larger pressures is not yet clear, but they could have significant implications for magma ocean evolution. Indeed, these results suggest that oxidized interiors would melt to a greater extent compared to reduced mantles, and would thus sustain magma ocean and associated outgassing for longer periods of time.

Summary Overall, a number of lines of evidence suggest that the magma ocean was initially in a reducing state, because of the coexistence of metal and silicate melt, before the former fully segregated to the core. From then on, whether as a result of self-oxidation, metal segregation to the core, hydrogen escape, or oxidized material endowment (or a combination of all), the crystallizing magma ocean likely became more oxidized with time. Crystallization of the magma ocean is also required to concentrate enough incompatible species in the melt to reach melt-saturation of highly soluble volatile species and their extensive outgassing. By this time, the oxidation state of the magma ocean may have been high enough to reach the present-day QFM buffer. It would have produced an oxidized atmosphere, predominantly composed of H_2O–CO_2–N_2. This is consistent with the earliest terrestrial rock records (see Fig. 1 in Scaillet and Gaillard 2011, for a schematic reconstruction of the mantle redox state evolution). Given their similar size, density, and their vicinity in the Solar System, such a scenario may apply for both early Earth and Venus. Yet, the absence of measurements for the latter makes any statement even more speculative than for Earth. In such an early oxidizing environment after the surface solidified, late impact-induced degassing may have created local and transient reducing conditions. These would be favorable for prebiotic chemistry and life emergence on Earth, while other surface conditions may have compromised its development or sustainability on Venus.

While this scenario might tentatively reconcile the different available pieces of evidence (see Table 2 for a summary of the different early outgassed atmospheres and underlying assumptions/constraints), one should keep in mind that early atmospheric formation was most

Table 2 Early outgassed atmospheres and underlying constraints or assumptions

Associated mechanism	Reference(s)
Oxidized atmospheres: dominated by H_2O–CO_2–SO_2–N_2	
Geologic constraints	
Crystallization of terrestrial Hadean zircons 4.35 Gyr ago under oxidizing conditions	Trail et al. (2011)
Oxidation state of terrestrial Archean (up to 3.9 Gyr old) igneous rocks at-or-near current oxidizing state	Canil (1997), Delano (2001), Canil (2002), Lee et al. (2003), Li and Lee (2004), Rollinson et al. (2017), Nicklas et al. (2018)
Prebiotic chemistry	
Production of reduced organics triggered by coronal mass ejection events from the young Sun or impact energy	Kurosawa et al. (2013), Airapetian et al. (2016)
Exogenous delivery of reduced organic materials	Anders (1989), Chyba et al. (1990), Chyba and Sagan (1992), Whittet (1997), Matthews and Minard (2006)
Production of amino acids and other organic compounds using oxidation inhibitors	Cleaves et al. (2008)
Accretion	
Accreting bodies of increasing oxidation state (heterogeneous accretion) inferred from trace element abundances	Wänke et al. (1988), O'Neill (1991), Wood et al. (2009), Rubie et al. (2011, 2015), Fischer et al. (2015), Shi et al. (2022)
Elemental partitioning and impact erosion during continuous accretion of chondritic bodies	Sakuraba et al. (2021)
Impact-generated atmosphere from carbonaceous (CI, CM, CV) chondritic material	Schaefer and Fegley (2010, 2017)
Heating and outgassing experiments of carbonaceous chondrites	Thompson et al. (2021)
Core formation	
Core formation (rapidly) completed with metallic iron fully segregated from the silicate	Holland (1962), Kleine et al. (2002), Frost and McCammon (2008)
Deep metal–silicate separation	Li and Agee (1996), Fischer et al. (2015)
Chemical equilibrium with molten surface of bulk silicate Earth or molten Earth's continental crust composition	Lupu et al. (2014)
Impactor's iron not available to reduce the upper molten layers of the target or the atmosphere	Itcovitz et al. (2022), Citron and Stewart (2022)
Magma ocean evolution	
Gradient of the magma ocean redox state with oxidized shallow parts	Hirschmann (2012), Deng et al. (2020)
Disproportionation of FeO at depth to Fe metal and Fe_2O_3 components (in post-spinel and perovskite form)	Mao and Bell (1977), Frost et al. (2004), Galimov (2005), Wade and Wood (2005), Wood and Halliday (2005), Frost et al. (2008), Schaefer and Elkins-Tanton (2018), Armstrong et al. (2019), Hirschmann (2022)

likely a continuous, dynamic, and evolving process. It would have overlapped with stochastic planetary accretion, core formation, and cooling of possibly several episodes of more or less deep magma oceans (e.g., Tucker and Mukhopadhyay 2014). The magma oceans would have been influenced by several mechanisms at play during these early stages, where out-

Table 2 (*Continued*)

Associated mechanism	Reference(s)
Increasing outgassed CO_2/CO ratio with magma ocean cooling from ab initio molecular dynamics simulations	Solomatova and Caracas (2021)
Self-oxidation of the magma ocean with crystallization owing to Fe^{3+} incompatibility	Maurice et al. (2023)
Atmospheric evolution	
Preservation of carbonaceous chondritic D/H signature in the terrestrial oceans	Pahlevan et al. (2019)
Photodissociation of H_2O and(/or) atmospheric escape of H_2	Hunten (1993), Kasting et al. (1993a), Sharp et al. (2013)
Reduced atmospheres: dominated by H_2–CO–CH_4–NH_3–H_2S	
Prebiotic chemistry	
Production of amino acids and other organic compounds from electrical discharges	Miller (1953, 1955), Miller and Urey (1959)
Accretion	
Impact-induced degassing	Kasting (1990), Hashimoto et al. (2007), Sugita and Schultz (2009), Zahnle et al. (2010, 2020)
Impact-generated atmosphere from ordinary (H, L, LL) and enstatite (EH, EL) chondritic material	Schaefer and Fegley (2007, 2010, 2017)
Reduction of the magma ocean during accretion	Righter and Ghiorso (2012)
Core formation	
Incomplete metallic iron–silicate separation in the shallow part of the magma ocean	Holland (1962), O'Neill (1991), Frost and McCammon (2008)
Impactor's iron available to reduce the upper molten layers of the target and the atmosphere	Itcovitz et al. (2022), Citron and Stewart (2022)
Magma ocean evolution	
Graphite precipitation (requires a highly reducing magma ocean) and flotation at the surface of the magma ocean	Keppler and Golabek (2019)
Atmospheric evolution	
Reducing power of the primordial H_2-dominated atmosphere acting on proto-planets and constituting planetesimals	Zahnle et al. (2010)
Outgassing and slow (energy limited) escape of hydrogen	Tian et al. (2005), Liggins et al. (2020)

gassing of the growing planets' interior, impact degassing of accreting planetesimals, impact erosion, and atmospheric self-escape all affected both its physical and chemical properties over different time scales. A comprehensive theory explaining such a complex process requires further investigation of each of these contributions and would remain elusive without considering further inputs from incoming Venus exploration and ongoing exoplanets characterization.

3.3 Magma Ocean–Atmosphere Interactions

In the absence of a thick, long-lasting, viscous boundary layer at the surface of the magma ocean, thermal and volatile exchanges proceed efficiently between the molten interior and

the overlying atmosphere. This is the case for most of the magma ocean evolution sequence. Note that a crust-like, thin, viscous boundary layer might form at the surface, either as observed on lava lakes or by flotation of crystals less dense than the surrounding melt, but would be quickly, i.e., relative to the magma ocean cooling rate, destabilized and broken apart by bursting bubbles and strong convective currents. After having described the partitioning of volatile species between the different reservoirs of the planet in the previous section, we discuss below the interaction between the solidifying magma ocean and the outgassed atmosphere and how they can affect the evolution of the coupled system. In particular, we focus on the heat transfer and exchanges from the magma ocean to space and how they control the cooling of the molten interior.

In its most simple form, the conservation of energy at the top of a planet's atmosphere can be described schematically as the equilibrium between all the incoming, $F_{\downarrow}$, and outgoing, $F_{\uparrow}$, fluxes:

$$F_{\uparrow} = F_{\downarrow} \quad , \tag{16}$$

where the total outgoing flux $F_{\uparrow} = F_{\rm IR} + \alpha F_{\odot}$ comprises the thermal, infrared flux, $F_{\rm IR}$, representing the heat loss at the top of the atmosphere, and the reflected fraction α (i.e., the Bond albedo) of the gross incident solar radiation $F_{\odot}$ that peaks at shorter wavelengths given the higher temperature of the star (the so-called Wien peak, that is inversely proportional to the temperature), in the visible spectral range, hence referred to as the Outgoing Shortwave Radiation (OSR). The total incoming flux is the sum of the heat sources:

$$F_{\downarrow} = F_{\rm abs} + F_{\rm conv} \quad , \tag{17}$$

and includes the contribution of the net (incident minus reflected) solar flux absorbed by the planet, $F_{\rm abs}$ (Eq. (1)), and the heat flux coming from the planetary interior and generated by the convection of the magma ocean, $F_{\rm conv}$ (or $F_{\rm MO}$). Regarding thermal exchanges more specifically, the magma ocean–atmosphere system has then two incoming heat sources: the absorbed solar flux and the convective flux from the magma ocean, that must balance the thermal radiation $F_{\rm IR}$ emitted to space at the top of the atmosphere (Fig. 5; e.g., Zahnle et al. 1988; Abe 1993a):

$$F_{\rm IR} = F_{\rm abs} + F_{\rm conv} \quad . \tag{18}$$

During the magma ocean stage, the temperature of the mantle is so hot that the heat flux coming from the boiling convective mantle far exceeds the incoming solar flux ($F_{\rm conv} \gg F_{\rm abs}$). This implies that the outgoing thermal flux is dominated by the heat flux from the magma ocean: $F_{\rm IR} \approx F_{\rm conv}$. Because the heat flux received from the star is substantially lower than the planetary interior heat flux, i.e., the equilibrium temperature is much lower than the molten surface temperature, the planet has an excess of heat. To evacuate the excess of internal heat and reach thermal and radiative equilibrium with the stellar environment, the magma ocean cools down through convection. The generated heat flux $F_{\rm conv}$ is initially high and decreases with time. As $F_{\rm IR} \approx F_{\rm conv}$, the outgoing thermal flux also decreases with time.

The outgoing heat flux depends on the surface temperature, and the surface temperature itself results from the heat flux balance (Eq. (18)). It can be written $F_{\rm IR} = \sigma T_{\rm eff}^4 = \varepsilon\sigma T_{\rm surf}^4$, where σ is the Stefan–Boltzmann constant, $T_{\rm eff}$ the effective temperature of the planet,[7] and

[7] The effective temperature of the planet, $T_{\rm eff}$, is the temperature a black body would have to emit the same total amount of radiation ($F_{\rm IR}$). It should not be confused with the equilibrium temperature, $T_{\rm eq}$, which is the

ε is the emissivity of the atmosphere, which measures its effectiveness in emitting energy as thermal radiation.

In the absence of an atmosphere, as usually initially assumed as a result of giant impact in magma ocean–atmosphere models, Eq. (18) is evaluated at the surface of the planet from which thermal radiation is directly emitted to space. In such a case, the planet efficiently radiates the energy from the magma ocean and emits all incoming absorbed radiation ($\varepsilon = 1$). It loses heat to space as a black-body with a temperature of the planet's surface (dashed purple line, Fig. 4): the surface temperature equals the effective temperature, $T_{\text{surf}} = T_{\text{eff}}$. F_{IR} then only depends on T_{surf}, which is directly set by the magma ocean, and F_{IR} and F_{conv} decrease rapidly. In the absence of an atmosphere, complete solidification of a fully molten mantle and global magma ocean would theoretically proceed in less than 5000 years (Lebrun et al. 2013; Nikolaou et al. 2019).

Once the volatile species are exsolved out of the melt and reach the surface of the magma ocean, they progressively build-up the overlying atmosphere alongside magma ocean cooling and solidification. When an atmosphere is present, thermal emission to space is buffered by the blanketing effect of the atmosphere heat-trapping greenhouse gases that absorb part of the incoming (net solar plus interior) radiation ($\varepsilon < 1$). The surface temperature is then larger than the effective temperature ($T_{\text{surf}} > T_{\text{eff}}$). ε is inversely correlated with the atmospheric greenhouse effect: the smaller ε, the less radiation is emitted at the top of the atmosphere (F_{IR}), i.e., the stronger the blanketing effect. By buffering the amount of heat that can be radiated/dissipated to space through the atmosphere (F_{IR}), its blanketing effect buffers the magma ocean cooling rate. The surface temperature is then set by the equilibrium between the heat flux transported by convection in the magma ocean to the surface, and the heat flux that can be radiated through the atmosphere, from the surface of the magma ocean to space (e.g., Solomatov 2015).

The thermal opacity of the atmosphere is due to the absorption of radiation by greenhouse gases and is thus primarily a function of the atmospheric mass and composition, which are direct outcomes of magma ocean outgassing (Sects. 3.2.4 and 3.2.5). For instance, H_2O and CO_2 are two powerful greenhouse gases that can delay the complete magma ocean solidification for a few millions to hundred millions of years, depending on their atmospheric concentration (e.g., Hamano et al. 2013; Lebrun et al. 2013; Salvador et al. 2017; Nikolaou et al. 2019). During this phase where the outgoing emissions at the top of the atmosphere are dominated by the convective flux from the molten mantle (i.e., $F_{\text{IR}} \approx F_{\text{conv}}$), the evolution of the magma ocean and of the atmosphere are thus inextricably coupled and cannot be addressed separately.

Based on the heat fluxes equilibrium, the thermal evolution can be divided in two main phases: the first one, where thermal emissions going out of the atmosphere are primarily controlled by the convective flux coming from the magma ocean (i.e., $F_{\text{IR}} \approx F_{\text{conv}}$), as described above, and a second phase starting when F_{conv} decreases below the absorbed solar radiation and becomes negligible in front of it, where F_{IR} is dominated by F_{abs} (i.e., $F_{\text{IR}} \approx F_{\text{abs}} \gg F_{\text{conv}}$). The transition between these two phases may be defined as the time where the convective heat flux from the mantle becomes an order of magnitude lower than the absorbed solar flux ($F_{\text{conv}} \leq 0.1 \times F_{\text{abs}}$) and be referred to as the end of the rapid cooling stage ("ERCS"; Salvador et al. 2017).

From this moment, the planet has lost its excess internal heat and has reached global radiative equilibrium with its stellar environment. The molten interior and associated heat

temperature the planet would be at if only heated by the host star, i.e., if the planet was at equilibrium with the absorbed radiation.

is no longer dominantly driving the thermal evolution. Both the surface temperature and the thermal emissions at the top of the atmosphere are then set by the radiative equilibrium between the net incoming absorbed solar radiation and the outgoing thermal radiation (e.g., Leconte et al. 2013), and are thus mainly controlled by atmospheric-related parameters: the absorbed solar flux and the atmospheric opacity. Note that the surface temperature reached at global radiative equilibrium may be above (e.g., if the planet absorbs a large amount of sunlight) or below the melting point of the surface. The complete solidification of the molten mantle, i.e., the end of the magma ocean phase, is independent of and should be distinguished from the ERCS/global radiative balance.

For a planet located at a given distance from its host star, because of the relatively slow variation of the total incoming solar flux with time (if stellar properties and orbital distance remain relatively stable), all F_{abs}-governing parameters are relatively constant and unrelated to the thermal evolution, besides the Bond albedo (Eq. (1)). Thus, the formation of a water ocean at the surface critically depends on two main atmospheric properties: its Bond albedo and greenhouse effect, both ultimately relying on the surface temperature and pressure prevailing at the ERCS, that are directly inherited from the magma ocean cooling and outgassing sequences.

In that respect, clouds play a vital role. Indeed, they both regulate the amount of solar energy reaching the surface through their albedo (Pluriel et al. 2019), and affect the amount of heat radiated back into space through their greenhouse effect. Because of their potential cooling or warming effect, their presence, properties, location, and distribution may drastically impact the surface conditions reached at the ERCS. However, they remain the major source of uncertainties in current climate models and in future Earth's climate predictions (e.g., Kasting and Catling 2003; Siebesma et al. 2020). In particular, accounting for their time-dependent, 3D spatial distribution, dynamics and microphysical properties to constrain their optical properties and global contribution is highly challenging. Modelling cloud formation and behavior throughout magma ocean cooling and assessing their significance for the early surface conditions suffers from additional complexities due to the prevailing extreme conditions. Different cloud configurations and their implications regarding the surface conditions of Venus at the ERCS and early water ocean formation are further discussed in the following section.

When discussing the outcomes of the magma ocean phase in the next Section, we focus on the aftermath of the evolutionary phase affected by the mechanisms described throughout Sect. 3. This involves the conditions reached at the ERCS (Fig. 12), regardless of whether the mantle has fully solidified or not at the time global radiative balance is reached. Indeed, the subsequent surface conditions and evolution of both the interior and of the atmosphere rely on other processes. Even if the mantle is still molten at the ERCS, its dynamics may significantly differ from that of the pre-ERCS magma ocean convection, since the excess internal energy would have then been lost and a thermal steady-state reached.

4 Outcomes of the Magma Ocean Phase and Implications for the Long-Term Evolution of Venus

4.1 Surface Conditions and Potential Early Habitability

At the end of the rapid cooling stage, the conditions may allow for liquid water to condense at the surface and enable ocean formation. Water ocean formation essentially requires both the atmospheric water vapor pressure and the temperature at the surface to lay between

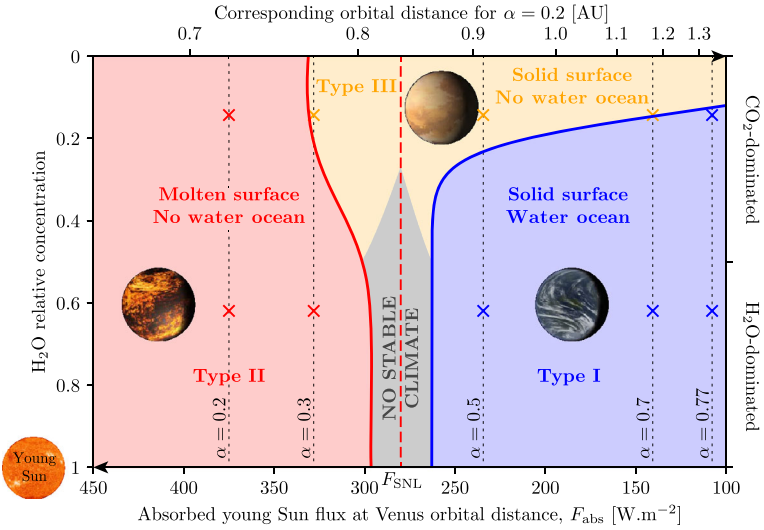

Fig. 12 Schematic summary of the various surface conditions reached at the End of the Rapid Cooling Stage (ERCS), i.e., when the heat flux coming from the interior becomes negligible compared to the net absorbed stellar flux. From then on, the latter balances the outgoing thermal radiation and this balance mainly controls the climate. The solid lines represent the transitions between the different types of surface conditions, but note that these are not hard limits. The crosses correspond to the ones shown in Figs. 4 and 13 for H_2O- and CO_2-dominated atmospheres, respectively. Note that alternative atmospheric compositions (e.g., reduced atmospheres or desert worlds) would alter the location and shape of the limits separating the different types of planets (see text). From any surface conditions reached at the ERCS and resulting from the magma ocean evolution, Venus may have transitioned to any other states before reaching its present-day conditions (see Fig. 14)

the triple and critical points of water. We describe below which magma ocean evolution scenarios would favor water ocean formation, both early on at the ERCS and later, and scenarios where water ocean formation is unlikely.

Insufficient Accreted or Outgassed Water Prior to magma ocean evolution, the amount of water delivered to the planet during the accretion phase may be the first limiting factor for ocean formation. If the planet accreted dry or did not get enough bulk water, water ocean formation at the end of the rapid cooling stage is compromised (uppermost part of Fig. 12). Unless a substantial amount of water is delivered later in history, through a "late veneer" for instance, and temperate conditions are met, water formation is unlikely over the entire planet lifetime (Fig. 14). Yet, as discussed in Sect. 2.2.1, this dry accretion scenario is currently not favored by planetary formation models for Venus. In addition, as discussed in Sect. 2, based on Venus proximity with Earth, their similar density, and its high atmospheric D/H ratio, a substantial, likely Earth-like, early water endowment is the prevailing scenario for Venus today.

As described in Sect. 3, the amount of atmospheric water vapor is a direct outcome of magma ocean cooling and outgassing. If the water vapor mixing ratio of the outgassed atmosphere is too low (i.e., the relative amount of outgassed water is low), insufficient vapor pressure would prevent water saturation pressure to be reached at the surface. This would happen if magma ocean outgassing is not efficient for water or produces a reduced atmosphere. Early ocean formation at the ERCS would then be impossible (uppermost part of Fig. 12). Later ocean formation could still be possible if enough mantellic remnant water is

volcanically outgassed during the long-term evolution of the planet, if atmospheric water is delivered by late impacts, and/or if the redox state of the mantle or atmosphere evolves and becomes more oxidized (Fig. 14). Such late oxidation could be the result of volatile cycling and geo-/photo-chemical evolution, involving atmospheric hydrogen escape and surface oxidation processes.

H_2O-Dominated Atmospheres Provided there is sufficient atmospheric water at the ERCS, the surface temperature determines whether water vapor saturation pressure can be reached and a water ocean forms. Recall that surface temperature at the ERCS results from the global radiative balance between the net incoming absorbed solar flux, F_{abs}, and the thermal outgoing flux the planet is able to radiate to space, F_{IR}. Both fluxes rely on atmospheric state and composition. These are direct outcomes of the magma ocean outgassing and evolution: atmospheric mass, composition, thermal profile, resulting clouds (and distribution), aerosols types and locations.

For steam, H_2O-dominated atmospheres, the existence of the outgoing radiation limit with respect to surface temperature, at about 280 $W.m^{-2}$ (dashed red line in Fig. 4), creates two drastically different types of surface conditions at the ERCS (Fig. 12; Hamano et al. 2013; Salvador et al. 2017). If the planet's outgoing thermal flux is lower than the radiation limit (i.e., $F_{IR} \approx F_{abs} < F_{SNL}$), the resulting climate should be temperate. Surface temperatures would be below the water critical temperature and allow water ocean formation (e.g., blue crosses in Figs. 4 and 12). Such planets are expected to have a solidified surface at the ERCS and are referred to as "Type I" planets following Hamano et al. (2013) classification (blue area in Fig. 12). For Venus, an early habitable state could be reconciled with the present-day conditions via water loss resulting from later on atmospheric escape (Fig. 14; see Sect. 4.2). Yet, ocean water would first have to be vaporized, reach the upper atmosphere, and photodissociate. The hydrogen would be lost to space, while most of the oxygen would remain. If temperate conditions and oceans are stable, water loss would be less efficient than if water were found mainly in the vapor phase.

Conversely, at the ERCS if the planet absorbs more solar energy than the Simpson–Nakajima radiation limit ($F_{IR} \approx F_{abs} > F_{SNL}$), climate stability can only be achieved at a surface temperature above $T_{surf} \approx 1500$ K (e.g., red crosses in Figs. 4 and 12; Abe and Matsui 1988; Zahnle et al. 1988; Kasting 1988; Hamano et al. 2013; Goldblatt et al. 2013; Marcq et al. 2017; Salvador et al. 2017). At this temperature, which is above the solidus temperature of silicates, the planet surface is expected to be molten and able to radiate in the visible and near-infrared (NIR). It would have an emission peak around 5 μm (Wien peak), thus allowing emission through the 4 μm water vapor absorption window to balance the absorbed solar flux and achieve radiative equilibrium. Such molten surface planets at the ERCS are referred to as "Type II" planets (red area in Fig. 12; Hamano et al. 2013). Because the planet is at global radiative balance, the surface of type II planets are expected to remain molten and the magma ocean phase is sustained until there is a decrease of the net absorbed solar flux or a decrease of the atmospheric water abundance (Fig. 14). Atmospheric water could be lost via escape processes. The absorbed flux could then decrease owing to the weakening greenhouse effect or via the formation of reflective clouds triggered by a change of rotation rate or water condensation in the upper atmosphere.

The critical distance separating Type I and Type II planets is actually equivalent to the inner edge of the circumstellar habitable zone (IHZ). The latter is defined in relation to the radiation limit of the runaway greenhouse state and is classically calculated using atmospheric models (e.g., Kasting et al. 1993b; Selsis et al. 2007; Kopparapu et al. 2013; Leconte et al. 2013; Ramirez 2018). Such models typically start with temperate Earth-like surface

conditions, with a surface water ocean and an H_2O-dominated atmosphere. From this baseline configuration, they vary the surface temperature (or the insolation; e.g., Leconte et al. 2013) to evaluate the atmospheric/climate response. They then calculate the corresponding solar flux needed to sustain the specified surface temperature. Note that this surface temperature variation could result from a change of insolation, absorbed stellar flux, or greenhouse gases concentration. They proceed until the ocean evaporates and a runaway greenhouse state is reached. The corresponding net absorbed and/or emitted critical flux is translated into a critical insolation threshold and orbital distance – this defines the inner edge of the habitable zone.

Compared to those studies, early evolution magma ocean models start with molten surfaces, where the water is outgassed from the interior and first found in the atmosphere in the vapor phase rather than being condensed into an ocean. As soon as enough water is outgassed, these atmospheres are in a runaway-greenhouse-like state. Coupled models then simulate the cooling and solidification of the magma ocean. As the interior flux decreases, their atmospheres evolve toward thermal equilibrium (reached at the ERCS, when the interior flux becomes negligible compared to the absorbed stellar flux), where their outgoing thermal emission balances the absorbed part of the incoming sunlight. The habitability of the planet is then assessed via the likelihood of water ocean formation given the surface conditions reached at the ERCS. Here, the location of the inner edge of the habitable zone is thus evaluated the other way round. They start from hot, uninhabitable conditions. They next evaluate the insolation threshold and corresponding orbital distance at which a stable climatic state (i.e., $F_{\mathrm{IR}} \approx F_{\mathrm{abs}}$) is able to produce a water ocean at the surface of the solidified planet.

It is important to emphasize that while the habitable zone boundaries are generally expressed in terms of insolation thresholds and orbital distances from the star, these two parameters only consider the incoming stellar flux $F_{\downarrow}$. Yet, the parameter that determines the climate state and associated surface conditions is the net absorbed stellar flux F_{abs}, where the albedo is critical. Accordingly, a planet of high Bond albedo (e.g., due to a highly reflective cloud cover) may sustain temperate surface conditions and have an early water ocean (type I planet). This is despite being closer to the star than a type II planet of lower albedo and with an incident flux larger than the predicted insolation threshold. Any parameter affecting the planetary albedo may thus dramatically alter the fate of the planet especially if it is located near the edge of the habitable zone, as is the case for Venus (e.g., Hamano et al. 2013). Provided that Venus' orbital parameters have remained stable and accounting for the lower luminosity of the young Sun (e.g., Gough 1981; Bahcall et al. 2001), the amount of absorbed stellar radiation F_{abs} and associated surface conditions depend upon the Bond albedo (Fig. 12).

CO_2-Dominated Atmospheres Similar to IHZ studies, Hamano et al. (2013) type I and II planet classification is based on steam, water-dominated atmospheres. Indeed, the runaway greenhouse occurs in such atmospheres because their main component is both a condensable and thermal absorber species. For atmospheres that are more diluted with respect to their water vapor concentrations (i.e., those whose composition is not water-dominated but non-condensable[8] species-dominated), the strong runaway greenhouse effect of H_2O-dominated atmospheres is buffered. For instance, as the longwave radiative forcing, or thermal absorption, of CO_2 is lower than that of H_2O (e.g., Kiehl and Trenberth 1997), CO_2-dominated atmospheres are more transparent/less opaque to thermal radiation as a result of atmospheric

[8] At least for conditions where water would be able to condense.

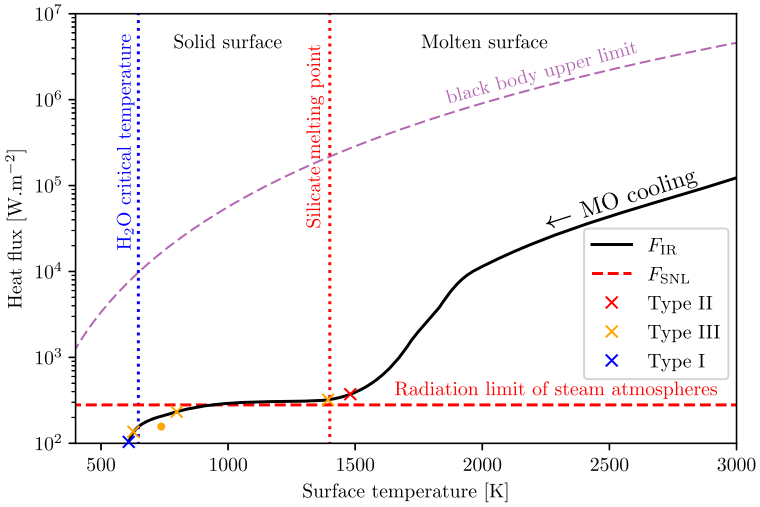

Fig. 13 Outgoing thermal flux emitted at the top of the atmosphere (F_{IR}, black line) as a function of surface temperature for a CO_2-dominated atmosphere. Compared to H_2O-dominated atmospheres (Fig. 4), global radiative equilibrium and stable climatic states can be reached at intermediate surface conditions between temperate Type I (e.g., blue cross, where $\alpha = 0.77$) and molten surface Type II (e.g., red cross, where $\alpha = 0.2$) planets. These Type III planets (e.g., orange crosses, where $\alpha = [0.3, 0.5, 0.7]$ from right to left) have solidified at the ERCS ($T_{\mathrm{surf}} < T_{\mathrm{solidus}}$) but water does not condense at the surface. This either because the atmosphere is too dry and the saturation vapor pressure of water is not reached or because the temperature is too high and above the critical temperature of water ($T_{\mathrm{surf}} > 647$ K). The crosses correspond to the ones shown in the upper part of Fig. 12. The orange dot denotes present-day Venus

water vapor dilution and associated lower specific humidity (Salvador et al. 2017). Owing to their increased thermal transparency, CO_2-dominated atmospheres are able to radiate thermally (F_{IR}) even above the Simpson–Nakajima limit in response to an increase of temperature or net absorbed solar flux. These CO_2-dominated atmospheres thus maintain radiative balance at intermediate surface temperatures in contrast to H_2O-dominated atmospheres which are thermally opaque. In order to reach radiative balance, H_2O-dominated atmospheres have to reach higher temperatures to radiate again and stabilize their climate. Here the radiation limit of steam H_2O-dominated atmospheres is no longer relevant. The sharp climatic transition and surface temperature jump between type I and type II planets are soften and additional intermediate stable climate states can be achieved (Fig. 13). These climate states can have intermediate surface temperatures, including temperatures greater than that of the critical point of water, where water ocean formation is not possible (orange crosses in Figs. 13 and 12). In addition to a decrease in atmospheric opacity, the decrease of water vapor partial pressure implied by the atmospheric water vapor dilution effect can prevent water ocean formation even below the critical temperature of water. This is the case if the water vapor saturation pressure is not reached at the surface (e.g., lowermost orange cross in Fig. 13). Thus, for CO_2-dominated atmospheres, water ocean formation becomes highly sensitive to the atmospheric volatile concentration. The water vapor mixing ratio can prevent water ocean formation at any orbital distance if it is too low (Fig. 12). At the ERCS, intermediate and stable surface conditions between that of type I and II planets can be achieved where the surface has completely solidified thanks to surface temperatures below the solidus temperature but where no water ocean is formed (Figs. 12, 13 and 14). Planets reaching this state are referred to as "Type III" planets (orange area in Fig. 12; Salvador et al. 2017).

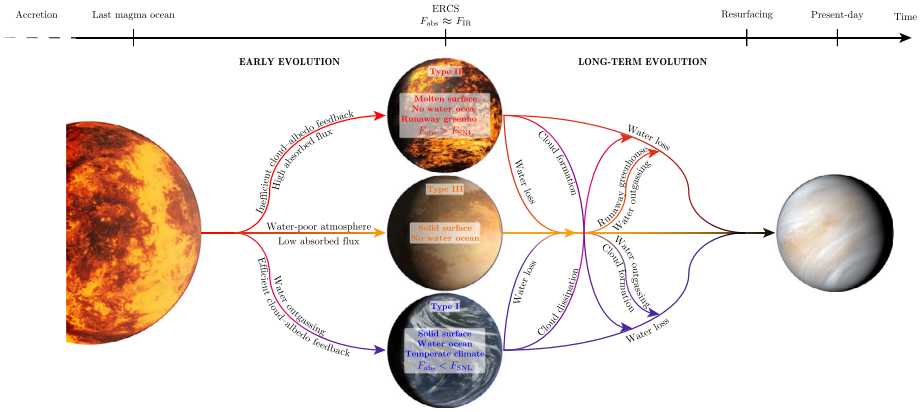

Fig. 14 Possible evolution pathways taken by Venus from the last major magma ocean episode to the present day (not to scale). The End of the Rapid Cooling Stage (ERCS) separates the early and long-term evolution and is reached when the heat flux coming from the interior becomes negligible compared to the net absorbed stellar flux (F_{abs}; Eq. (1)). From then on, the latter balances the outgoing thermal radiation (F_{IR}) and this balance mainly controls the climate. F_{SNL} is the radiation limit of steam atmospheres. Early evolution: Relatively dry accretion or inefficient magma ocean outgassing of water owing to its retention in the interior or a reduced upper mantle would induce low concentrations of water vapor in the atmosphere. This would prevent the formation of water oceans even if the surface has solidified at the ERCS owing to relatively low absorbed fluxes (MO to Type III; orange area of Fig. 12). Water outgassing from the magma ocean would result in temperate conditions at the ERCS if an efficient cloud–albedo feedback operates (MO to Type I; blue area of Fig. 12). If not, regardless of the water content, high absorbed fluxes would induce a molten surface at the ERCS (MO to Type II; red area of Fig. 12). Long-term evolution: Changes of the amount of water vapor in the atmosphere and of the absorbed stellar flux may trigger transitions from one type to another. Atmospheric water loss could be due to atmospheric escape (Sect. 4.2) or to its incorporation into the interior. It could induce the evaporation of the ocean (Type I to III) or the solidification of the surface by weakening the greenhouse effect (Type II to III). Although less likely, volcanic outgassing of CO_2 would have the same effect. Conversely, an increase of the amount of water vapor in the atmosphere through volcanic outgassing or late accretion of water-rich bodies could trigger a late runaway greenhouse (Type III to II) or the formation of water ocean (Type III to I) depending on the absorbed stellar flux. A temperate climate would thus be favored by synchronous formation of reflective clouds on the dayside of the planet, possibly helped by rotation rate changes, but threatened by the brightening Sun. If the atmosphere is already water-dominated, cloud formation would also initiate a temperate climate era (Type II to I) but their dissipation would end it (Type I to II). Note that these are just examples of the possible mechanisms and that the location of the transitions between the different branches are not indicative of their timing

Type III planets may experience post-ERCS habitable periods if the atmospheric water vapor mixing ratio increases enough, through long-term volcanic outgassing for instance, and provided that the absorbed flux remains/decreases below the runaway greenhouse threshold (Fig. 14). If not, a runaway greenhouse would prevent the formation of water oceans and the planet would be desiccated via atmospheric escape.

Desert Worlds Abe et al. (2011) modeled the climate of desert worlds with globally limited but locally abundant surface water, also referred to as "land planets", to assess their habitability. This is an intermediate case between H_2O- and CO_2-dominated atmospheres. Because the tropics of such land planets have very low relative humidities, the air is unsaturated in those regions where longwave radiation can be efficiently emitted above the traditional runaway greenhouse limit. Compared to planets with globally abundant liquid water, land planets thus have a wider habitable zone. They can sustain moderate climates where liquid water remains stable at the poles despite being closer to their host stars. Abe

et al. (2011) suggested that if Venus were such a land planet with a 1 bar N_2-dominated atmosphere with 345 ppm CO_2, it could have remained habitable until as recently as 1 billion years ago.

Zsom et al. (2013) studied a more extreme case of hot desert/dry worlds representative of greenhouse gas-poor atmospheres. Here the atmospheric composition was dominated by a non-greenhouse gas (e.g., N_2) with low relative humidity (∼1%), and low CO_2 mixing ratio (10^{-4}). They showed that the reduced greenhouse effect may bring the inner edge of the habitable zone as close as 0.38 AU from a Sun-like star, for a surface albedo of 0.8. For a more moderate surface albedo of 0.2, it would be 0.59 AU. Note that for such arid planets where the water budget is limited (e.g., Abe et al. 2011), their definition of habitability is not restricted to the formation of a global water ocean. Despite having a water reservoir limited to cold areas such as the poles or the night side (Abe et al. 2011; Menou 2013; Leconte et al. 2013) they also consider a planet habitable when: (i) water is able to precipitate mostly in the form of rain on a large fraction of the planet's surface, and (ii) where the water reservoir is stable on a multi-billion-year timescale. This way, most of the surface water is in liquid form, a large fraction of the planet remains habitable, and the water cycle is not broken (Zsom et al. 2013). While both early and present-day Venus could be located within this extended habitable zone, this particular atmospheric configuration is hard to relate to any early Venusian evolution scenario. While a low relative humidity could be explained by low water delivery, an inefficient or highly reduced magma ocean outgassing, a low CO_2 mixing ratio is hard to reconcile with the present-day atmospheric CO_2 inventory. Indeed, CO_2 is poorly soluble in the magma ocean and likely outgassed early. Otherwise, if C is not outgassed as CO_2, the outgassing of other carbon-bearing reduced species would challenge the restricted atmospheric composition and the absence of other greenhouse gases required in the Zsom et al. (2013) and Abe et al. (2011) calculations.

Critical Albedo Value The key to form early oceans under temperate climates at the ERCS is an optimal magma ocean cooling and outgassing sequence, producing enough water vapor in an atmosphere absorbing the right range of solar flux (e.g., Fig. 12). Abe and Matsui (1988) and Kasting (1988) used 1D radiative-convective, cloud-free atmospheric models to simulate the climates and surface conditions associated with hot H_2O–CO_2 atmospheres. They found that if Venus initially accreted a similar amount of water to Earth, a proto-ocean could form on early Venus. With Pollack (1971), they suggested that clouds could play a crucial role in producing early oceans on Venus by increasing the albedo and deflecting part of the incoming sunlight to space.

Salvador et al. (2017) estimated that less than 0.1 Earth water ocean initially dissolved within the early Venusian magma ocean and efficiently outgassed into the atmosphere would be sufficient to form a water ocean at the ERCS. They used the insolation of the young Sun (∼70% of its current value; e.g., Gough 1981; Bahcall et al. 2001) while using Venus' present-day geometric albedo (∼0.7) and atmospheric CO_2 content (∼90 bar). They also found that using an albedo of 0.45 would reflect enough sunlight to form a water ocean at the ERCS if only 0.3 Earth's ocean of water were initially dissolved within the magma ocean and efficiently outgassed (Fig. 12). This is in good agreement with Abe (1993a), who showed that for an albedo of 0.35, early Venus would lie at the critical flux between a habitable and a runaway greenhouse state, indicating that a water ocean would be stable at Venus' surface for a larger albedo (their Fig. 3). More recent modeling by Krissansen-Totton et al. (2021) showed that all transient habitable solutions for early Venus have a Bond albedo larger than 0.4.

The Importance of Clouds As noted above clouds might be the critical factor in producing an albedo suitable for temperate surface conditions, by reducing the amount of absorbed sunlight at Venus' distance. Venus' present-day thick sulfuric acid (H_2SO_4) cloud cover is responsible for its high albedo, reflecting more than 75% of incoming stellar flux back to space (Moroz et al. 1985; see Titov et al. 2013, for a review). Despite being 30% closer from the Sun, Venus presently absorbs less solar energy than the Earth does: $F_{\text{abs}}^{\female} \approx 157\ \text{W} \cdot \text{m}^{-2}$ (Moroz et al. 1985) versus $F_{\text{abs}}^{\oplus} \approx 240\ \text{W.m}^{-2}$ on average. The corresponding equilibrium temperatures are ~231 K for Venus and 255 K for the Earth (assuming an albedo of 0.75 and 0.29, respectively). Note that the thick cloud layer also constitutes a second infrared opacity source in the Venusian atmosphere (the first being the 92 bars of CO_2), and contributes about 140 K to the greenhouse effect (Titov et al. 2013).

Given the flux received from the young Sun at Venus' orbital distance, if early Venus had enough atmospheric water at the ERCS and a high albedo, water ocean formation would have been likely (Fig. 12; Salvador et al. 2017). Several physical mechanisms and associated cloud effects could produce a high enough albedo to allow water oceans to form on early Venus. While maximizing the cooling effect of clouds by neglecting their warming effect, i.e., by assuming that clouds are transparent to IR outgoing radiation, Selsis et al. (2007) estimated that covering 100% and 50% of a planet's dayside with highly reflecting clouds can produce albedos as high as 0.8 and 0.6. This would shift the runaway greenhouse limit and associated inner edge of the habitable zone to an orbital distance of 0.46 AU and 0.68 AU for the current Sun. Such a highly optimistic habitable zone would encompass both present-day and early Venus.

Using a 3D general circulation model with a modern cloud scheme and Earth-like atmospheric compositions, Yang et al. (2014) showed that Venus' slow planetary rotation rate (of about 243 Earth days; e.g., Carpenter 1970; Campbell et al. 2019; Margot et al. 2021) would induce an albedo high enough to support temperate conditions. Indeed, by weakening the Coriolis force and extending daytime illumination compared to faster rotating planets, slow rotation rates promote strong convergence and convection in the substellar region. This produces a large area of optically thick clouds in the most illuminated part of the atmosphere, which greatly increases the albedo and decreases surface temperatures (as first evidenced for tidally locked planets; see Yang et al. 2013). Even at Venus' present-day orbital distance and insolation, this mechanism would sustain low enough surface temperatures to support surface liquid water.

Way et al. (2016) used early Venus' insolation and an Earth-like atmospheric composition to model the climatic history of Venus via 3D GCM simulations. They included a slow rotation rate like Yang et al. (2014), its present-day orbital parameters, modern topography from the Magellan mission, and an ocean volume consistent with the Pioneer Venus measured D/H ratio (Donahue et al. 1982). By modeling the climate dynamics and resulting surface conditions for several hypothetical scenarios, Way et al. (2016) showed that early Venus could have sustained stable water oceans and a temperate climate until as recently as 0.715 Ga ago. The 0.715 Ga was chosen as the approximate time of Venus' global resurfacing event (e.g., McKinnon et al. 1997). Following Yang et al. (2014) and Abe et al. (2011) they demonstrated that the rotation rate, through the cloud–albedo feedback, and the availability/distribution of surface water play a key role in climate circulation and heat redistribution resulting in the possible habitability of ancient Venus (Fig. 14). Extending their previous analysis to a significantly larger parameter space, Way and Del Genio (2020) showed that a shallow water ocean and habitable conditions could have persisted nearly 3 billion years. They speculated that this clement period ended via large igneous provinces formation (LIPs) before the global resurfacing period (lowermost branch of Fig. 14). However, if liquid water

is not initially present at the surface, subsequent habitability is rather unlikely. Hence the importance of the early history of Venus and its magma ocean evolution cannot be understated.

Another important finding regarding the early history and relevant to magma ocean outcomes is that, while early water oceans and temperate climates would be confidently sustained for a few billion years, if liquid water is not initially present at the surface, subsequent habitability and formation of water ocean is likely compromised. It would require to both replenish the atmosphere with water through volcanic outgassing or late accretion and form reflective clouds on the planet's dayside (from type III to type I branch in Fig. 14) while reconciling such scenarios with existing constraints (e.g., Way and Del Genio 2020; Krissansen-Totton et al. 2021). An early enough slow rotation rate and associated highly reflective clouds feedback might then be critical.

At present we have no constraints on early Venus' rotation rate. Its current slow retrograde rotation rate could be a result of a number of processes working together or separately over Venus' lifetime (e.g., Cottereau et al. 2011; Hoolst 2015):

- core–mantle friction (e.g., Goldreich and Peale 1970; Lago and Cazenave 1979; Dobrovolskis 1980);
- solid-body tides (e.g., Correia and Laskar 2003; Hoolst 2015; Way and Del Genio 2020);
- spin–orbit resonance with the Earth (e.g., Goldreich and Peale 1967; Gold and Soter 1969; Bills 2005);
- thermal atmospheric tides (e.g., Gold and Soter 1969; Ingersoll and Dobrovolskis 1978; Dobrovolskis and Ingersoll 1980; Leconte et al. 2015) specific to its dense atmosphere (e.g., Correia and Laskar 2001);
- an impactor (e.g., McCord 1968; Alemi and Stevenson 2006).

In particular, most of these mechanisms depend on the atmospheric thickness, interior structure, or insolation. While insolation was negligible compared to the magma ocean convective flux, the atmosphere was building up and the interior structure was evolving throughout the magma ocean rapid cooling stage. This makes any estimation of the rotation rate at that time and post-ERCS highly challenging.

The cloud–albedo feedback for slowly rotating planets appears to extend the habitable zone to Venus' orbital distance (Yang et al. 2014; Way et al. 2016). Yet such temperate conditions are only possible with a pre-existing water ocean condensed at the surface and an Earth-like, water-poor atmosphere. However, it may not apply to planets with hot and steamy atmospheres. Here water does not condense into water oceans at the surface and is found entirely in the atmosphere, as expected for an efficiently outgassing magma ocean. Under such conditions, 3D GCM simulations by Turbet et al. (2021) demonstrated that water clouds form preferentially on the nightside, while being absent on the dayside. Their result is independent of the planetary rotation speed or day length. Such a day–night cloud asymmetry appears to prevent the efficient cloud–albedo effect at the sub-stellar point found by Yang et al. (2014). The Turbet et al. (2021) result induces strong solar absorption by atmospheric water vapor on the dayside and strong greenhouse effect by clouds (i.e., a net warming effect of clouds) on the nightside. Without the cloud–albedo effect at the substellar point, Turbet et al. (2021) suggested that if water is not first condensed into oceans (as discussed above) Venus would inevitably maintain a runaway greenhouse state from early on (uppermost branch of Fig. 14). High surface temperatures would prevent water oceans from forming at the surface, which would be in agreement with Hamano et al. (2013) cloud-free predictions identifying Venus as a type II planet.

Limitations and Perspectives The modeling of Turbet et al. (2021) is more realistic than previous 1D studies in assessing early water ocean formation on Venus under magma ocean-related, hot and steamy conditions. Extensive work yet remains to provide a conclusive statement. Firstly, cloud and atmospheric circulation feedback can vary non-linearly and non-monotonically with the rotation period (Jansen et al. 2019). Turbet et al. (2021) state that the applicability of their results to a wide range of rotation periods and to a slowly rotating Venus should be quantitatively confirmed by a comprehensive sensitivity study. This would also allow for a full characterization of day–night heat transport patterns on hot planets where water is found in the vapor phase in the atmosphere. It would also quantify the atmospheric circulation, climate dynamics, and resulting cloud effects (Noda et al. 2017).

As discussed in Sect. 3, the hot surface temperatures found in the early evolution stages are not ad-hoc conditions: the atmosphere is not an isolated system but instead, its bulk properties result from and are embedded in the coupled magma ocean–atmosphere evolution. Depending on the processes considered, water outgassing efficiency may vary significantly, and the differential outgassing of CO_2 and H_2O may induce additional complexities. To model a realistic early evolution and predict accurate associated surface conditions, such sophisticated 3D GCMs need to be coupled to molten interior models to consider self-consistent outgassing and cooling sequences. Such coupled models could thus account for evolving atmospheric properties, such as composition, surface pressure, and thermal surface boundary conditions, while considering interior–atmosphere feedback and possible non-linearities such as climatic hysteresis and multi-stability (e.g., Abe et al. 2011; Goldblatt 2015; Ishiwatari et al. 2021).

However, if the magma ocean covers the entire surface of the planet its heat flux is likely to be isotropic for most of the rapid cooling stage and would not depend on local time or latitude. The atmosphere would be uniformly and dominantly heated from below, such that atmospheric circulation and associated heat redistribution may not be affected by day–night or latitude-dependent insolation gradients. How the interior flux-controlled climate dynamics would look like in an outgassing atmosphere and how it would transition to a more classic (solar flux-dominated) climate circulation at the ERCS is unknown. In the latter the sunlight becomes the dominant energy source, and the implications for atmospheric circulation patterns and planet surface conditions again remain unknown. These questions will certainly benefit from the ongoing efforts and future improvements of both interior, atmosphere, and coupled numerical models (Sect. 5).

Krissansen-Totton et al. (2021) have developed a sophisticated coupled interior–atmosphere framework accounting for an extensive number of processes. These include geochemical cycling, atmospheric escape, and consistent atmospheric redox evolution, to self-consistently model the thermo-chemical evolution of Venus from the magma ocean stage to present-day. In light of all presently available atmospheric and surface constraints, they show that both habitable and never-habitable histories are possible, and that none can be conclusively ruled out. Indeed, both cases can successfully produce the current dense CO_2-dominated atmosphere with low water and oxygen content. They get consistent ^{40}Ar and ^{4}He outgassed abundances, and inferred surface heat flow. Importantly, they emphasize that Venus' habitability relies critically on the value of the Bond albedo, which appears to be the main controlling factor. Hence they demonstrate yet again the importance of the cloud–albedo feedback described above.

As it is generally the case for many processes affecting Venus history and evolution, there is a pressing need to update the precision of available constraints to disentangle Venus past. Upcoming missions may provide key in-situ measurements that may significantly help in constraining the likelihood of the different scenarios discussed herein (see Widemann et al. 2023, for an extensive discussion).

4.2 Atmospheric Escape and the Fate of Water

A high water vapor content in the early atmosphere of Venus has to be reconciled with its present-day low concentrations of water and oxygen (e.g., Johnson and de Oliveira 2019). It has long been hypothesized that Venus underwent large scale atmospheric escape during its evolution, providing a way to lose its water (e.g., Ingersoll 1969; Rasool and de Bergh 1970; Pollack 1971; Kasting and Pollack 1983). Several mechanisms can be responsible for atmospheric escape and may have operated to various extent throughout Venus evolution (Fig. 14). They include thermal hydrodynamic escape, non-thermal (suprathermal) escape, and mechanical impact erosion that are all discussed below. Note that high energies and temperatures resulting from extreme post-impact conditions may also be responsible for early intense atmospheric escape (Modirrousta-Galian and Korenaga 2023).

4.2.1 Hydrodynamic Escape

Part of the water loss could have occurred early during the evolution of the planet (Lammer et al. 2018). At that time, the EUV flux from the Sun was at its highest (Tu et al. 2015), powering hydrodynamic escape of water and possibly heavier species like noble gases and CO_2. Strong EUV heated the upper atmosphere, exciting and photo-dissociating the gas molecules (Lammer 2013). Water being easily dissociated implies that the upper atmosphere was likely dominated by hydrogen (in terms of number of atoms) and oxygen (in terms of mass) (Kasting and Pollack 1983). This upper atmosphere expanded hydrodynamically and "flowed" outward to escape into space. H loss is very efficient (O loss potentially less so; e.g., Chassefière 1996) and can also drag off heavier species (Watson et al. 1981; Erkaev et al. 2014). Hydrodynamic losses are usually estimated by using a simple energy-limited approximation (Watson et al. 1981; Odert et al. 2018).

Mass fractionation can occur as a result of hydrodynamic escape (Hunten 1973; Hunten et al. 1987). Numerous studies have tried to explain the isotopic profile of noble gases through hydrodynamic escape (Sekiya et al. 1980; Hunten et al. 1987; Sasaki and Nakazawa 1988; Zahnle et al. 1990; Pepin 1991; Gillmann et al. 2009; Odert et al. 2018). Simulations have identified scenarios that could reproduce fractionation consistent with current observations. However, the scarcity of data regarding the structure, temperature, and composition of the atmosphere, the energy deposition, the solar wind, and the solar nebula dissipation time implies that the problem is under-constrained, with multiple solutions explaining the available data. In addition, large error bars on the measurements allow for a wide range of acceptable evolutionary scenarios. Finally, the building blocks of the primitive atmosphere themselves may have already been subject to outgassing (Lichtenberg et al. 2019) and escape (Odert et al. 2018) before accretion and thus already fractionated.

The rotation rate of the star is one of the main factors governing EUV emissions (Johnstone et al. 2021). The EUV flux decreases with time as rotation rates decrease (Güdel et al. 1997). During the first 200 Myr, a fast rotating Sun could emit about 500 times higher EUV fluxes than at present-day. A slowly rotating Sun could reach around 30 times present-day EUV fluxes. Most G-stars EUV fluxes converge to a common evolutionary path after 1.5 Gyr. Whether the Sun was a slow, moderate or fast rotator 4+ billion years ago is uncertain. While some clues such as the overall escape intensity or lunar regolith Na and K depletion suggest a slow to moderate rotation rate, the question remains unsolved (Odert et al. 2018; Saxena et al. 2019; Johnstone et al. 2021). Since atmospheric thermal escape depends on the EUV flux heating the upper atmosphere of a planet, uncertainties on EUV fluxes translate into uncertainties in loss rates, with fast stellar rotators leading to more efficient loss.

Loss of water from hydrodynamic escape can be massive but is strongly parameter dependent. The energy available for escape and photodissociation is defined by the EUV flux and therefore, cumulative losses would vary by more than an order of magnitude whether the Sun was a slow or fast rotator. For example, over the first 500 Myr evolution, one Earth ocean equivalent could escape an Earth-like planet orbiting a slow-rotating Sun-like star, compared to 45 Earth oceans for a fast-rotating star (Johnstone 2020). Estimations for Venus are similar, with a total loss ranging from a few (Gillmann et al. 2009) to 15–20 Earth oceans equivalent (Odert et al. 2018). CO_2 can also be lost this way, on the order of 10 bar, for moderate stellar rotators, and up to 100 s of bars for fast rotating stars (Odert et al. 2018), in which case CO_2 is probably photodissociated too. Finally, oxygen escapes together with hydrogen. In the case of fast-rotating stars, the loss of O is efficient and can be so high that most of the initial constituents of water could be lost to space (requiring the loss of tens of Earth oceans; Odert et al. 2018). However, for lower EUV fluxes oxygen loss is less efficient than H escape, which means that oxygen would accumulate in the atmosphere (Gillmann et al. 2009; Wordsworth and Pierrehumbert 2013; Luger and Barnes 2015; Johnstone 2020). The overall escape for planets orbiting slow stellar rotators is weaker but mass fractionation between H and O is more efficient. Considering both aspects, the final remaining oxygen after a hydrodynamic escape phase is of similar order regardless of the rotation rate: around 300–400 bar (Johnstone 2020).

Oxygen accumulation is an interesting problem on Venus, as free oxygen is practically absent from the present-day atmosphere (Johnson and de Oliveira 2019). During the magma ocean phase and the possible extended runaway greenhouse phase, it could have been efficiently trapped and re-injected into the mantle through interaction with the hot surface (Hamano et al. 2013; Wordsworth 2016; Wordsworth et al. 2018), thus oxidizing the interior. If it became the main species in the upper atmosphere, it could also have escaped (Tian 2015). However, those sinks stop with the solidification of the magma ocean and the rise of a volcanically-produced, CO_2-dominated atmosphere (Gillmann et al. 2020).

Later in the evolution, enhanced magmatic production causing extensive resurfacing combined with crustal oxidation could also provide a substantial oxygen sink (Way and Del Genio 2020; Krissansen-Totton et al. 2021), but other later sinks such as non-thermal escape and solid surface oxidation are likely inefficient. It is therefore likely that most of any build-up of oxygen caused by hydrodynamic escape would have been removed by the end of the magma ocean phase, by the time the molten surface completely solidified (Gillmann et al. 2020) or shortly after that (Warren and Kite 2023). While several sink mechanisms can be effective in depleting atmospheric oxygen throughout Venus' early and long-term evolution to match the present-day atmospheric composition, removing water from the atmosphere appears to be more difficult than removing oxygen (Krissansen-Totton et al. 2021). This may confine the end of the habitable period to 1–3 Gyr ago or limit the amount of surface liquid water during that period.

In summary, hydrodynamic escape acts as a potential massive sink of volatiles that could desiccate a planet's atmosphere; but the magnitude of early escape and its consequences for planetary evolution are not governed solely by that sink. Instead they depend on the availability and state of water in the system, which ultimately rely on the interactions with the solidifying magma ocean.

4.2.2 Non-thermal Escape

Along with further possible episodes of hydrodynamic escape in a H-rich atmosphere, even after magma ocean solidification, long-term, non-thermal escape will lead to the loss of

water over the last 4 billion years. Over this timescale spanning the entire planet lifetime, it is unlikely that the existence of water oceans limits volatile and water loss, given the relatively fast exchanges between the ocean and the atmosphere. However, the structure of the atmosphere can have large consequences on loss mechanisms. For example, without a functioning cold trap an atmosphere risks a wet stratosphere and is thus prone to efficient water photodissociation and H escape. Kasting et al. (1993b) demonstrated that once an Earth-like planet enters a moist greenhouse state where the stratospheric water vapor mixing ratio is at least 3×10^{-3} v/v one may lose an entire Earth's ocean worth of H over ~4.5 Gyr via photodissociation of H_2O and hydrogen diffusion-limited escape.

The efficiency of the escape is governed by the atmospheric composition, itself inherited from atmosphere–interior interaction during the magma ocean phase. As an example, a thick CO_2 atmosphere outgassed from the magma ocean can reduce the exosphere temperature, and thus lead to slower escape (e.g., Way et al. 2023). This could have buffered the escape of N_2 in the CO_2-rich atmosphere of Venus and has been suggested to explain the larger amount of N_2 in Venus' atmosphere compared to Earth (Lammer et al. 2018).

Interaction between surface minerals and the atmosphere can further affect atmospheric composition both during the magma ocean phase and afterward (see Gillmann et al. 2022, for more details). Fresh surface basalt can trap oxygen by oxidizing iron (e.g., Gillmann et al. 2009, 2020). It has also been suggested that N_2 could have been trapped by the magma ocean before being released later on by volcanism (Wordsworth et al. 2018). The specific effects of this process depends on the composition and structure of the atmosphere, as determined by its primordial evolution.

4.2.3 Impact Erosion

On growing planets, impact erosion is another possible – yet hard to estimate – atmospheric loss process (e.g., Cameron 1983; Melosh and Vickery 1989; Griffith and Zahnle 1995). In this case, atmospheric escape results from the kinetic energy imparted to the atmosphere by the impact of large objects. When large asteroids or comets collide onto protoplanets with atmospheres, hot vapor plumes and high-speed ejecta resulting from the impact may also provide sufficient energy for part of the atmosphere to escape and be lost to space (e.g., Melosh and Vickery 1989; Zahnle 1990; Ahrens 1993). For giant impacts atmospheric escape can also be caused by subsequent global ground motion (e.g., Genda and Abe 2003, 2005; Schlichting et al. 2015).

Quantitative estimates for impact-induced atmospheric escape have been proposed by Vickery and Melosh (1990), Newman et al. (1999), Shuvalov and Artemieva (2002). Further realistic numerical simulations have been developed by Svetsov (2007) and Shuvalov (2009), who considered the cratering flow induced by impacts on Earth and Mars. Escaping efficiency generally depend on properties such as impactor sizes, impact velocities and angles of impact. These rely on planetary accretion scenarios. The size of impactors typically increases with time as planetesimals grow and would favor impact-induced atmospheric erosion. Yet the frequency of impact decreases with time, which buffers net escaping efficiency.

Atmospheric properties, and in particular density, also affect impact-induced erosion efficiency. For a given impact low density tenuous atmospheres are prone to efficient impact-induced erosion. However, when impactors enter dense atmospheres, such as the ones typically expected for type II planets, aerial burst and projectile fragmentation upon entry may enhance atmospheric erosion (Shuvalov et al. 2014).

Overall, impact-induced atmospheric erosion efficiency and consequences on atmospheric evolution result from a subtle balance between erosion and atmospheric replenishment through impact-induced degassing. It strongly depends on the timing and timescale of

giant impacts relative to that of magma ocean solidification and outgassing. Any conclusive estimation assessing its importance is challenged by the large uncertainties regarding how multiple magma ocean events may be embedded into a bombardment history.

While EUV-driven hydrodynamic escape on early Venus would have (weakly; Kasting and Pollack 1983; Johnstone 2020) contributed to the D/H fractionation, impact erosion does not cause isotopic fractionation because the atmosphere escapes *en masse* in this mechanism. Compared to other flux-triggered escape mechanisms, impact erosion is not sensitive to the presence of a magnetic field. Erosion processes could have been important to set absolute atmospheric abundances (Sakuraba et al. 2019; Gillmann et al. 2020). However, in the presence of condensed reservoirs like liquid water, impact erosion during the late accretion could have affected the atmospheric elemental composition by favoring the escape of inert gases from the atmosphere (Sakuraba et al. 2019). Thus the effect of impact erosion on isotopic composition and elemental abundance is tightly linked to both the accretional history and thermal evolution, and therefore remains hard to assess.

4.3 Initial Conditions for the Long-Term Evolution of the Interior

4.3.1 Water, Mantle Properties and Evolution

Magma ocean outgassing efficiency and oxidation state are responsible for the water inventory left inside the planet. Atmospheric radiative balance and resulting circulation, escape processes, atmosphere–surface interactions, and volcanic outgassing govern the surface water inventory once the surface has solidified (see Gillmann et al. 2022, for an extensive discussion). The different magma ocean evolution pathways and outcomes discussed above are associated with a broad diversity of scenarios regarding water distribution between the planetary interior, the atmosphere, and the amount lost to space (Fig. 14). Whether Venus' mantle is completely water-depleted at the ERCS and left dry for its long-term evolution, partially depleted, or water-rich remains unclear. Yet, the amount of mantellic water inherited from magma ocean evolution and its distribution would strongly influence the long-term evolution and surface conditions of the planet, by affecting both the atmosphere and the mantle.

For instance, water in the mantle lowers the melting temperature (e.g., Hirschmann 2006; Ni et al. 2016), thus possibly favoring mantle melting and triggering volcanism and volcanic outgassing. If a substantial amount of water is supplied to the atmosphere through post-ERCS volcanic outgassing while the planet is habitable at ERCS, it may trigger a runaway greenhouse. This could lead to complete vaporization of the ocean followed by water photodissociation and hydrogen loss in the upper atmosphere, thus sterilizing the planet and making it uninhabitable. If the magma ocean outgassing efficiency of water were low (e.g., Hier-Majumder and Hirschmann 2017; Miyazaki and Korenaga 2021; Salvador and Samuel 2023), there may not have been enough water to form an ocean at the ERCS. Yet post-ERCS volcanic outgassing may supply enough water for clouds to form in the upper atmosphere, increase the albedo, and possibly create transient temperate conditions suitable for water ocean formation (from type III to type I branch in Fig. 14). If Venus were a faster rotator early on, the decrease of its planetary rotation rate could have helped in the formation of reflective clouds. On the other hand, a decrease in water outgassing rate associated with a steady loss of atmospheric water would slow down atmospheric replenishment and could result in thinner and dissipating clouds (Bullock and Grinspoon 2001). Cloud dissipation would induce a decrease in the Bond albedo and an increase in the absorbed solar flux and surface temperature. This could trigger a runaway greenhouse and vaporize any existing water ocean, making Venus exit a temperate climate (from type I to type II branch in Fig. 14).

Water also decreases mantle viscosity (e.g., Lange 1994) which in turn controls the rheology and convective dynamics of the interior (e.g., Karato 2015). Seismic wave propagation and mantle electrical conductivity are also affected by the mantellic water content (see Karato 2015, for a review). The spatial distribution of mantellic water and potential vertical and horizontal variations could then induce local changes of mantle properties and possibly lead to very different rheological behaviour and tectonic regimes (e.g., Korenaga 2011). The low viscosity layer under the stiff lithosphere, i.e., the asthenosphere, is thought to result from the presence of localized volatiles in Earth's mantle. This could be sustained by long-term volatile recycling (Richards and Lenardic 2018) and may promote plate tectonics on Earth (Bunge et al. 1996; Richards et al. 2001). Its absence on modern Venus (inferred from gravity/topography; e.g., Kiefer et al. 1986) together with the dry conditions at the surface have been historically invoked to explain the lack of modern Earth-style plate tectonics (Bercovici et al. 2000).

Indeed, the state of water at the planetary surface has crucial implications for the mantle convective regime. The presence or absence of liquid water at the planetary surface affects the rheological behavior of the lithosphere, lithosphere–mantle lubrication, upper mantle hydration, and plate bending (Grevemeyer et al. 2018). These may all influence subduction initiation, sustainability, and the prevailing tectonic regime (Regenauer-Lieb et al. 2001; Gerya et al. 2008; Bercovici and Ricard 2014; Korenaga et al. 2017; Stern 2018; Westall et al. 2023). In turn, those differences that are inextricably inherited from the magma ocean evolution affect magmatic and tectonic processes throughout the entire thermochemical evolution of the planet (e.g., Smrekar et al. 2007; Stamenković and Breuer 2014). This has implications for the mantle convection regime (e.g., Weller and Kiefer 2020), thermal history, volatile redistribution (e.g., Korenaga 2017) and outgassing (e.g., Driscoll and Bercovici 2013), that must all ultimately match present-day conditions (see Rolf et al. 2022; Gillmann et al. 2022, for reviews).

4.3.2 Late Impacts

After the end of the hypothetical last global magma ocean phase caused by the final giant impact (or Moon-forming impact in the case of Earth), a number of subsequent and additional large impacts may have occurred (Rubie et al. 2015), during the so-called "late accretion". The highly siderophile elements in Earth's mantle could be explained by such collisions (Chyba 1991). If they occurred, they also certainly affected water distribution (Sakuraba et al. 2019, 2021). As discussed previously, large impacts could have opposite effects on the planet's atmosphere depending on the balance between atmospheric erosion and replenishment (e.g., Pham et al. 2011). Large collisions could also cause widespread melting of the mantle of the target body and deplete its shallow layers through subsequent degassing of the molten parts (see Gillmann et al. 2022).

In cases where the impactor is not fully vaporized upon impact, the collision could also inject water-bearing material from the impactor into the impacted mantle. The nature of the material, as well as the portion of the total water inventory delivered to Venus during this late accretion era are still debated. It has been suggested that significant amounts of water could be delivered to a planet's surface and/or mantle through these late impacts (Albarede 2009). On the other hand, recent studies and Earth-based isotopic data imply that most of a terrestrial planet's water inventory is already accreted by the end of its main accretion phase (e.g., Gillmann et al. 2020), and that late accretion is mostly composed of volatile-poor material (e.g., Fischer-Gödde and Kleine 2017; Dauphas 2017). Depending on the composition of the impactors and on how they merge with the target (e.g., Itcovitz et al.

2022; Citron and Stewart 2022), the oxidation state of both the atmosphere and mantle could be significantly affected, with implications for prebiotic chemistry (Sect. 3.2.5 and Table 2). Late collisions could also have affected the mantellic convection style of the planet, since impacts could favor lithospheric damage and mobility, and thus trigger subduction (Gillmann et al. 2016; O'Neill et al. 2017; Borgeat and Tackley 2022).

4.3.3 Interior–Atmosphere Volatile Exchanges: The Carbonate–Silicate Cycle

After the magma ocean has fully solidified, solid-state convection takes over in mixing the entire mantle. It is most likely already in place in the solid-state part of the mantle while the upper molten mantle continues to cool down (e.g., Maurice et al. 2017; Ballmer et al. 2017). It produces partial melting, and ultimately volcanism and outgassing, thereby bringing water and other volatiles to the surface while locally depleting the mantle. The convection regime of the mantle thus determines the specifics of the volatile exchanges (see Rolf et al. 2022; Gillmann et al. 2022) and is therefore thought to play a major role in how young planets could branch in or out of a habitable state (Fig. 14). Long-term climate stability is required to maintain habitability throughout eons and is believed to rely on specific interior–atmosphere volatile cycling such as the critical carbon cycle and associated CO_2-climate feedback (e.g., Walker et al. 1981; Kasting et al. 1993b; Kasting and Catling 2003; Ramirez 2018).

On Earth, to compensate for the increase in surface temperature due to the brightening Sun, long-term habitability may have required quick removal of most of the early atmospheric CO_2 outgassed during the magma ocean phase (or delivered to the atmosphere by other means), thus reducing the greenhouse effect. Interaction with the surface and interior of the planet (and convection regime) would be involved in the process. The mechanism is not yet understood, given the significant differences between the conditions at that time and at present-day. Notably, the higher temperatures of a thicker atmosphere or the lack of modern-day plate tectonics. The latter plays a major role in the present-day carbon cycle and volatile return flux from the atmosphere into the Earth's interior.

The carbon cycle regulates the atmospheric concentration of CO_2 and has several different parts. The most important one in terms of long-term climate ($t > 10^6$ years) is the inorganic carbonate–silicate cycle. It results from slow interactions of atmospheric CO_2 with the crustal rock reservoir (e.g., Holland 1978; Walker et al. 1981; Kasting et al. 1993b; Kasting and Catling 2003). Dissolution of atmospheric CO_2 into liquid water drives the cycle. CO_2 is first dissolved into rainwater to form carbonic acid that dissolves continental silicate rocks over time. The products of such silicate weathering, including calcium (Ca^{2+}), magnesium (Mg^{2+}), and bicarbonate (HCO_3^-) ions, flow within streams and rivers into the ocean. There they react with more ocean-dissolved atmospheric CO_2 to precipitate as carbonate minerals. Those carbonates deposit and accumulate on the seafloor where they are buried in sediments. Their subduction, with that of continental carbonates and carbonatized oceanic basalt, injects carbon into the mantle (e.g., Sleep and Zahnle 2001). At depth, high temperatures and pressures force carbonate minerals to recombine with SiO_2 to reform silicate minerals while releasing CO_2. Following this so-called carbonate metamorphism, the released CO_2 is eventually volcanically outgassed and thus re-enters the atmosphere, therefore closing the cycle.

Because evaporation (and hence, precipitation) and chemical reaction rates rise with surface temperature, silicate weathering rates increase with increasing surface temperatures. This consumes more atmospheric CO_2, and buffers the rise of surface temperature. Conversely, atmospheric CO_2 consumption by silicate weathering decreases when surface temperatures fall, while volcanically-outgassed atmospheric CO_2 concentrations increase and

counteract falling temperatures. This carbonate–silicate cycle thus contains a negative feedback regulating surface temperatures and atmospheric CO_2 concentrations. It is responsible for long-term climate stability (e.g., Walker et al. 1981; Sleep and Zahnle 2001; Kasting 2019).

If ancient Venus had liquid water, emerged lands (to allow silicate weathering), and an initially CO_2-dominated atmosphere, the carbonate–silicate cycle may have been in place, therefore stabilizing a long-term temperate climate (Way and Del Genio 2020). Via this cycle, Venus' atmosphere could have evolved toward a more Earth-like atmospheric composition (i.e., CO_2-poor) and maintained a stable temperate climate against the brightening Sun. In addition, temporarily sequestering CO_2 in carbonates through an effective carbonate–silicate cycle permits elevated H_2O loss before CO_2 is volcanically outgassed and returned to the atmosphere, which is key to recover the modern Venusian atmospheric composition from habitable scenarios (Krissansen-Totton et al. 2021).

Yet, the existence and efficiency of an early carbonate–silicate cycle on Venus strongly relies on its mantle dynamic regime and associated convection/tectonic style. Subduction from an active/mobile-lid regime (possibly plate tectonics) would allow for the complete cycle to operate. Other non-classical tectonic signatures of convective regimes, such as a post-magma ocean, non-plate tectonic, sluggish subduction may be alternative ways of injecting CO_2 into the mantle and removing it from the atmosphere (Foley et al. 2014). On the other hand, a stagnant lid regime, possibly operating today on Venus (e.g., Smrekar et al. 2007), limits the magnitude of any recycling of atmosphere/surface species into the mantle. However, even in this regime, progressive burial of material by successive lava flows could ultimately allow temporary storage of volatiles, or even a limited return flux of material into the mantle, provided the water-bearing minerals are not destabilized by the increasing pressure and temperature conditions before delamination (Höning et al. 2021).

Thus, the present-day stagnant lid regime likely prevents significant incorporation of CO_2 into the mantle and could even be responsible for its accumulation into the atmosphere through long-term volcanism (e.g., Way and Del Genio 2020; Krissansen-Totton et al. 2021; Gillmann et al. 2022). However, it is clear that terrestrial planets, including Earth itself, experience different tectonic styles through the eons (e.g., Stern 2018; Spencer et al. 2021), indicating that other mantle convective regimes certainly prevailed in Venus' past. This could allow for a transient effective carbonate–silicate cycle under a habitable climate. Yet, for both planets, the various convective regimes that have been in place, their relative timing and transition time scales and the magnitude of associated volatile exchanges remain unclear (e.g., Stern 2018).

5 Perspectives and Future Research Directions

Many parameters and processes with direct or indirect implications for the magma ocean phase and evolution remain highly unconstrained. The influence of some of them has not even been assessed yet. They concern both the molten interior and the outgassed atmosphere themselves, but also include external and indirect factors such as the planet's early environment and history.

Accretion Sequence and Stellar Environment The magma ocean phase is not an isolated process: it is inextricably embedded into the accretion sequence and related to the evolution of the stellar environment. To provide a more accurate understanding of the early evolution

of rocky planets and implications for their habitability and long-term evolution, magma ocean models should be coupled to stellar evolution and planetary formation models.

In particular, planetary formation models would provide self-consistent constraints regarding volatile delivery timing, type, and budget (e.g., Morbidelli et al. 2012; Li et al. 2016; Burger et al. 2020; Venturini et al. 2020). They would also provide the frequency and energetics of impacts, and avoid making implicit assumptions regarding number occurrence of magma oceans, timing, initial depth, thermal state (e.g., Nakajima et al. 2021), and evolving chemical constituents abundance and distribution (e.g., Maas et al. 2021; Itcovitz et al. 2022; Citron and Stewart 2022). In particular, the effect of late giant impacts, that may affect volatile species and melt redistribution, atmospheric and mantle oxidation states, atmospheric erosion or replenishment (e.g., Pham et al. 2011; Modirrousta-Galian and Korenaga 2023), would be worth systematically assessing.

Stellar evolution models would allow for a more realistic treatment of upper atmospheric properties, including photochemistry and escape (e.g., Airapetian et al. 2020). This may in turn affect the heat flux balance and resulting climate stability, dynamics, and circulation, as well as atmospheric volatile abundance and oxidation state.

Molten Interior Regarding the mechanisms at play within the molten interior, many fluid dynamics aspects of terrestrial magma oceans emphasized in Solomatov (2000) remain poorly understood. They include the mode of crystallization (fractional vs equilibrium) resulting from the competition between crystals settling and re-entrainment, the convective regime or the effect of rotation (Maas and Hansen 2015, 2019). Additional complexities may arise from the convection in a multi-phase system (Boukaré and Ricard 2017), or spatial and time variations of melt and crystal properties such as density, viscosity, crystals size and shape, or chemical affinity. In that respect, magma ocean numerical models could significantly benefit from advances in characterization of material properties and behaviors at magma ocean extreme conditions performed by laboratory experiments.

The oxidation state of the molten mantle is also highly unconstrained. It is influenced by the timing, location, extent, and fashion of metal–silicate separation and how it may evolves in space and time. Yet it is highly influential regarding the partitioning behavior of chemical elements and the identity of outgassed volatile species.

Some possibly critical physical aspects of magma ocean outgassing have been poorly studied. For example, the processes of bubble formation, nucleation, and ascent; and the crystal–melt–gas partitioning and chemical affinity of many volatile species at magma ocean relevant conditions remain uncertain. Ingassing processes are generally not considered in magma ocean studies. Yet, how, when, which, and how much volatile species could be reincorporated into the melt and then into the mantle may alter many aspects of the early and long-term evolution.

The thermo-chemical conditions at the base of the molten mantle, the interaction with the underlying metallic core (Foley and Driscoll 2016), and the potential existence of a basal magma ocean (Labrosse et al. 2007; O'Rourke 2020) have also received little attention in the framework of magma ocean–atmosphere evolution modeling. Yet, all of these processes may significantly affect the convective dynamics, outgassing, heat transfer, dynamo generation, and chemical differentiation of the solidifying mantle, and their relative influence remains to be quantified.

Long-Term Evolution of the Interior Addressing the subsequent long-term evolution of the planet requires considering the outcomes of the early molten evolution as potential initial states. Indeed, considering the surface conditions, the heat budget, and the distribution of

volatiles resulting from the magma ocean evolution would help constrain the solid-state mantle convective regime, and the sustainability of possible habitable climates. Furthermore, the transition from the magma ocean to the solidified mantle may significantly affect the post-magma ocean mantellic convective regime and the long-term evolution of the planet (Maurice et al. 2017; Ballmer et al. 2017; Agrusta et al. 2019; Bolrão et al. 2021). In particular the transition to a global solid-state convecting mantle can be affected by the coexistence of convective layers of different rheological behavior, i.e., one melt-dominated and another crystal-dominated, and how they interact. Coupling the highly influential magma ocean evolution with subsequent solid-state mantle convection models would thus help reconcile the modelled evolution paths with the present-day observed constraints, allowing one to assess the likelihood of different evolutionary pathways (e.g., Gillmann et al. 2022).

Atmospheric State and Properties Planets are complex systems and their evolution results from the strong interaction between the different planetary reservoirs. Understanding their evolving surface conditions and determining their potential past habitability demand to account for both atmospheric and interior processes.

As discussed earlier, the evolving Bond albedo of Venus and resulting absorbed sunlight is one of the most important parameters to solve its potential habitability. Yet, the contribution of clouds remains poorly constrained and assessing the effect of realistic clouds remains a key challenge for atmospheric modeling. In particular, microphysical and optical properties of aerosols, including photochemical hazes and others cloud condensation nuclei, as well as their time-dependent 3D spatial distribution are poorly constrained, and even more uncertain under extreme magma ocean conditions.

The occurrence of silicate vapor atmospheres after giant impacts is expected but their behavior and how they affect the thermo-chemical state of the planet is unknown. The resulting cloud behaviour, heat redistribution, climate circulation and escape post-impacts, changes in atmospheric composition, oxidation state throughout the magma ocean cooling, as well as the climatic transition from an interior- to a sunlit-heated atmosphere are all poorly understood. Further coupling between sophisticated interior outgassing and thermal evolution models with 3D climate models are required to provide a self-consistent scenario. Yet the development of such coupled models is hobbled by our understanding of these processes and by current computational capabilities. For now, a feasible and promising avenue would be to use available parameterized models to conduct sensitivity studies and assess the relative influence of each of these processes.

Observational Constraints and Future Missions In addition to these modeling shortcomings, our understanding of Venus history and present state is challenged by the lack of in-situ measurements as well as by important uncertainties in existing observations. Along with the aforementioned future research directions, forthcoming planned Venus missions are expected to significantly improve our comprehension of Venus' past evolution and present state. How these missions are expected to address key science questions regarding Venus evolution is discussed in Widemann et al. (2023, this issue).

Crucial measurements include elemental abundances and isotopic composition of noble gases (He, Ne, Ar, Kr, Xe), and stable isotopes (C, H, O, N, S) in the atmosphere. These are well suited to track outgassing throughout the coupled interior–atmosphere evolution (see Table 1 in Baines et al. 2013). For a thorough discussion see Avice et al. (2022, this collection). As an example, hydrogen isotopic measurements may provide valuable insight into the primordial atmospheric composition and associated early mantle oxidation state (Pahlevan et al. 2019).

Regarding planetary formation, tungsten isotopic composition can be used to constrain the timing of core formation and planetary growth rate (e.g., Zahnle et al. 2007). In particular, because W is moderately siderophile and Hf is lithophile, Hf/W ratios are strongly fractionated by core formation. The ^{182}Hf–^{182}W chronometer can then be used to assess planetary formation time-scales that ultimately relate to the energetic of accretion and thus have direct implications regarding the timing of the magma ocean phase, its initial depth and spatial extent. Constraints on core formation timing can be used to infer the depth and timing of metal–silicate separation. They would also infer the resulting molten mantle oxidation state and hence, that of the outgassed volatile species.

As discussed throughout the chapter, water (and its distribution) is a key element for early planetary evolution, but it is also highly influential over the entire planet's lifetime. A present-day signature of the evolution path taken could be the amount of remaining water in the mantle. The water content of the mantle affects its properties, the resulting mantle dynamics, rheology, tectonic style, melting behavior, and outgassing. It also affects the surface composition and mineralogy. Any constraint on these parameters could be in-turn used to inform the amount of mantellic water associated with the interior state, thus providing indirect hints of the past and of the evolutionary pathway. Surface mineralogy measurements could similarly indicate what conditions prevailed by the time ancient rocks or mineral inclusions have been put in place.

Finally, together with future missions dedicated to Venus (e.g., Widemann et al. 2023, this collection), the expanding field of rocky exoplanets detection and characterization is key to improve our general understanding of planetary formation, evolution, and habitability, that will in turn inform Venus' evolutionary history and help us unveil the potential habitable past of our closest planetary neighbor (see Way et al. 2023, this collection).

6 Conclusion

Given the strong coupling between all planetary reservoirs, the magma ocean stage has critical implications for terrestrial planet evolution and habitability. Importantly, it determines the initial chemical and thermal state that will dictate the pathways taken by the planet during its entire history. In addition to being a required ingredient for the emergence and development of life, water abundance and distribution between the planetary layers influences many of the processes at play. Its partitioning is the result of magma ocean crystallization and is of primary importance. The present-day dichotomy between Earth and Venus surface conditions and habitable state might be directly inherited from the cooling and solidification of the coupled magma ocean–atmosphere system. If not, the latter remains the determining factor by setting the initial conditions for the long-term evolution of the planet.

Many uncertainties, unconstrained processes and associated parameters still exist and need further investigation in the coming years to build a consistent picture of the earliest stages of planetary evolution. Combined with interdisciplinary modeling efforts, future measurements of Earth's twin planet may provide significant clues to the early mechanisms at play. They could also shed light not only on Venus' and Earth's distant pasts, but also improve our understanding of what makes a planet habitable and how to search for life elsewhere in the Universe.

Acknowledgements The authors thank the anonymous reviewer for their comments who helped us to greatly improve the manuscript. The authors also thank Tilman Spohn and team members of the International Space Science Institute in Bern for hosting the "Venus: Evolution through Time" workshop. AS also warmly thanks them for inviting him as a visiting scientist. AS gratefully acknowledges support from NASA's Habitable

Worlds Program (No. 80NSSC20K0226). MJW acknowledges support from the GSFC Sellers Exoplanet Environments Collaboration (SEEC) and ROCKE-3D: The evolution of solar system worlds through time, funded by the NASA Planetary and Earth Science Divisions Internal Scientist Funding Model. Work by C.G. was carried out within the framework of the NCCR PlanetS.

Funding Open Access funding enabled and organized by Projekt DEAL.

Declarations

Competing Interests The authors have no conflict of interest to declare that are relevant to the content of this article.

References

Abe Y (1993a) Physical state of the very early Earth. Lithos 30(3–4):223–235. https://doi.org/10.1016/0024-4937(93)90037-D

Abe Y (1993b) Thermal evolution and chemical differentiation of the terrestrial magma ocean. In: Takahashi E, Jeanloz R, Rubie D (eds) Evolution of the Earth and planets. AGU, Washington DC, pp 41–54. https://doi.org/10.1029/GM074p0041

Abe Y (1997) Thermal and chemical evolution of the terrestrial magma ocean. Phys Earth Planet Inter 100(1–4):27–39. https://doi.org/10.1016/S0031-9201(96)03229-3.

Abe Y, Matsui T (1985) The formation of an impact-generated H_2O atmosphere and its implications for the early thermal history of the Earth. J Geophys Res, Solid Earth 90(S02):545–559. https://doi.org/10.1029/JB090iS02p0C545

Abe Y, Matsui T (1988) Evolution of an impact-generated H_2O–CO_2 atmosphere and formation of a hot proto-ocean on Earth. J Atmos Sci 45(21):3081–3101. https://doi.org/10.1175/1520-0469(1988)045<3081:EOAIGH>2.0.CO;2

Abe Y, Ohtani E, Okuchi T, Righter K, Drake M (2000) Water in the early Earth. In: Canup R, Righter K et al (eds) Origin of the Earth and Moon. University of Arizona Press, Tucson, pp 413–433

Abe Y, Abe-Ouchi A, Sleep NH, Zahnle KJ (2011) Habitable zone limits for dry planets. Astrobiology 11(5):443–460. https://doi.org/10.1089/ast.2010.0545

Abelson PH (1966) Chemical events on the primitive Earth. Proc Natl Acad Sci 55(6):1365–1372. https://doi.org/10.1073/pnas.55.6.1365

Agrusta R, Morison A, Labrosse S, Deguen R, Alboussiére T, Tackley PJ, Dubuffet F (2019) Mantle convection interacting with magma oceans. Geophys J Int 220(3):1878–1892. https://doi.org/10.1093/gji/ggz549

Ahrens TJ (1993) Impact erosion of terrestrial planetary atmospheres. Annu Rev Earth Planet Sci 21(1):525–555

Airapetian VS, Glocer A, Gronoff G, Hébrard E, Danchi W (2016) Prebiotic chemistry and atmospheric warming of early Earth by an active young Sun. Nat Geosci 9(6):452–455. https://doi.org/10.1038/ngeo2719

Airapetian VS, Barnes R, Cohen O, Collinson GA, Danchi WC, Dong CF, Del Genio AD, France K, Garcia-Sage K, Glocer A, Gopalswamy N, Grenfell JL, Gronoff G, Güdel M, Herbst K, Henning WG, Jackman CH, Jin M, Johnstone CP, Kaltenegger L, Kay CD, Kobayashi K, Kuang W, Li G, Lynch BJ, Lüftinger T, Luhmann JG, Maehara H, Mlynczak MG, Notsu Y, Osten RA, Ramirez RM, Rugheimer S, Scheucher M, Schlieder JE, Shibata K, Sousa-Silva C, Stamenković V, Strangeway RJ, Usmanov AV, Vergados P, Verkhoglyadova OP, Vidotto AA, Voytek M, Way MJ, Zank GP, Yamashiki Y (2020) Impact of space weather on climate and habitability of terrestrial-type exoplanets. Int J Astrobiol 19(2):136–194. https://doi.org/10.1017/S1473550419000132

Albarede F (2009) Volatile accretion history of the terrestrial planets and dynamic implications. Nature 461(7268):1227–1233

Alemi A, Stevenson D (2006) Why Venus has no Moon. In: AAS/division for planetary sciences meeting abstracts #38, AAS/division for planetary sciences meeting abstracts. p 07.03

Altwegg K, Balsiger H, Bar-Nun A, Berthelier JJ, Bieler A, Bochsler P, Briois C, Calmonte U, Combi M, De Keyser J, Eberhardt P, Fiethe B, Fuselier S, Gasc S, Gombosi TI, Hansen KC, Hässig M, Jackel A, Kopp E, Korth A, LeRoy L, Mall U, Marty B, Mousis O, Neefs E, Owen T, Reme H, Rubin M, Semon T, Tzou CY, Waite H, Wurz P (2015) 67P/Churyumov-Gerasimenko, a Jupiter family comet with a high D/H ratio. Science 347(6220):3. https://doi.org/10.1126/science.1261952

Amelin Y, Lee DC, Halliday AN, Pidgeon RT (1999) Nature of the Earth's earliest crust from hafnium isotopes in single detrital zircons. Nature 399:252 EP. https://doi.org/10.1038/20426

Anders E (1989) Pre-biotic organic matter from comets and asteroids. Nature 342(6247):255–257. https://doi.org/10.1038/342255a0

Andrault D (2019) Thermodynamical constraints on the crystallization of a deep magma-ocean on Earth. C R Géosci. https://doi.org/10.1016/j.crte.2018.06.003

Andrault D, Bolfan-Casanova N, Nigro GL, Bouhifd MA, Garbarino G, Mezouar M (2011) Solidus and liquidus profiles of chondritic mantle: implication for melting of the Earth across its history. Earth Planet Sci Lett 304(1–2):251–259. https://doi.org/10.1016/j.epsl.2011.02.006

Andrault D, Petitgirard S, Lo Nigro G, Devidal JL, Veronesi G, Garbarino G, Mezouar M (2012) Solid-liquid iron partitioning in Earth's deep mantle. Nature 487(7407):354–357. https://doi.org/10.1038/nature11294

Andrault D, Monteux J, Bars ML, Samuel H (2016) The deep Earth may not be cooling down. Earth Planet Sci Lett 443:195–203. https://doi.org/10.1016/j.epsl.2016.03.020

Andrault D, Bolfan-Casanova N, Bouhifd MA, Boujibar A, Garbarino G, Manthilake G, Mezouar M, Monteux J, Parisiades P, Pesce G (2017) Toward a coherent model for the melting behavior of the deep Earth's mantle. Phys Earth Planet Inter 265:67–81. https://doi.org/10.1016/j.pepi.2017.02.009

Andrews SM, Huang J, Pérez LM, Isella A, Dullemond CP, Kurtovic NT, Guzmán VV, Carpenter JM, Wilner DJ, Zhang S, Zhu Z, Birnstiel T, Bai XN, Benisty M, Hughes AM, Öberg KI, Ricci L (2018) The disk substructures at high angular resolution project (DSHARP). I. Motivation, sample, calibration, and overview. Astrophys J Lett 869(2):L41. https://doi.org/10.3847/2041-8213/aaf741

Armitage PJ, Eisner JA, Simon JB (2016) Prompt planetesimal formation beyond the snow line. Astrophys J Lett 828(1):L2. https://doi.org/10.3847/2041-8205/828/1/L2

Armstrong LS, Hirschmann MM, Stanley BD, Falksen EG, Jacobsen SD (2015) Speciation and solubility of reduced C–O–H–N volatiles in mafic melt: Implications for volcanism, atmospheric evolution, and deep volatile cycles in the terrestrial planets. Geochim Cosmochim Acta 171:283–302. https://doi.org/10.1016/j.gca.2015.07.007

Armstrong K, Frost DJ, McCammon CA, Rubie DC, Ballaran TB (2019) Deep magma ocean formation set the oxidation state of Earth's mantle. Science 365(6456):903–906. https://doi.org/10.1126/science.aax8376

Asimow PD (2018) Chap. 15 - Melts under extreme conditions from shock experiments. In: Kono Y, Sanloup C (eds) Magmas under pressure, vol 15. Elsevier, Amsterdam, pp 387–418. https://doi.org/10.1016/B978-0-12-811301-1.00015-0

Asimow PD, Langmuir CH (2003) The importance of water to oceanic mantle melting regimes. Nature 421(6925):815–820. https://doi.org/10.1038/nature01429

Asphaug E (2014) Impact origin of the moon? Annu Rev Earth Planet Sci 42(1):551–578. https://doi.org/10.1146/annurev-earth-050212-124057

Asphaug E, Agnor CB, Williams Q (2006) Hit-and-run planetary collisions. Nature 439(7073):155–160. https://doi.org/10.1038/nature04311

Avice G, Marty B (2020) Perspectives on atmospheric evolution from noble gas and nitrogen isotopes on Earth, Mars & Venus. Space Sci Rev 216(3):36. https://doi.org/10.1007/s11214-020-00655-0

Avice G, Marty B, Burgess R (2017) The origin and degassing history of the Earth's atmosphere revealed by Archean xenon. Nat Commun 8:15455. https://doi.org/10.1038/ncomms15455

Avice G, Parai R, Jacobson S, Labidi J, Trainer MG, Petkov MP (2022) Noble gases and stable isotopes track the origin and early evolution of the Venus atmosphere. Space Sci Rev 218(8):60. https://doi.org/10.1007/s11214-022-00929-9

Badro J, Brodholt JP, Piet H, Siebert J, Ryerson FJ (2015) Core formation and core composition from coupled geochemical and geophysical constraints. Proc Natl Acad Sci 112(40):12310–12314. https://doi.org/10.1073/pnas.1505672112

Bahcall JN, Pinsonneault MH, Basu S (2001) Solar models: current epoch and time dependences, neutrinos, and helioseismological properties. Astrophys J 555(2):990. https://doi.org/10.1086/321493

Baines KH, Atreya SK, Bullock MA, Grinspoon DH, Mahaffy P, Russell CT, Schubert G, Zahnle K (2013) The atmospheres of the terrestrial planets: clues to the origins and early evolution of Venus, Earth, and Mars. In: Mackwell SJ, Simon-Miller AA, Harder JW, Bullock MA (eds) Comparative climatology of terrestrial planets. University of Arizona Press, Tucson, pp 137–160. https://doi.org/10.2458/azu_uapress_9780816530595-ch006

Baker DR, Alletti M (2012) Fluid saturation and volatile partitioning between melts and hydrous fluids in crustal magmatic systems: the contribution of experimental measurements and solubility models. Earth-Sci Rev 114:298–324. https://doi.org/10.1016/j.earscirev.2012.06.005

Ballmer MD, Lourenço DL, Hirose K, Caracas R, Nomura R (2017) Reconciling magma-ocean crystallization models with the present-day structure of the Earth's mantle. Geochem Geophys Geosyst 18(7):2785–2806. https://doi.org/10.1002/2017GC006917

Banzhaf W (2003) Self-organizing systems. In: Meyers RA (ed) Encyclopedia of physical science and technology, 3rd edn. Academic Press, New York, pp 589–598. https://doi.org/10.1016/B0-12-227410-5/00681-5

Barth P, Carone L, Barnes R, Noack L, Mollière P, Henning T (2021) Magma ocean evolution of the TRAPPIST-1 planets. Astrobiology 21(11):1325–1349. https://doi.org/10.1089/ast.2020.2277

Bekaert DV, Broadley MW, Marty B (2020) The origin and fate of volatile elements on Earth revisited in light of noble gas data obtained from comet 67P/Churyumov-Gerasimenko. Sci Rep 10(1):5796. https://doi.org/10.1038/s41598-020-62650-3

Benlow A, Meadows AJ (1977) The formation of the atmospheres of the terrestrial planets by impact. Astrophys Space Sci 46(2):293–300. https://doi.org/10.1007/BF00644376

Benner SA, Bell EA, Biondi E, Brasser R, Carell T, Kim HJ, Mojzsis SJ, Omran A, Pasek MA, Trail D (2020) When did life likely emerge on Earth in an RNA-first process? ChemSystemsChem 2(2):e1900035. https://doi.org/10.1002/syst.201900035

Bennett VC, Nutman AP, McCulloch MT (1993) Nd isotopic evidence for transient, highly depleted mantle reservoirs in the early history of the Earth. Earth Planet Sci Lett 119(3):299–317. https://doi.org/10.1016/0012-821X(93)90140-5

Benz W, Slattery WL, Cameron AGW (1986) The origin of the moon and the single-impact hypothesis I. Icarus 66(3):515–535. https://doi.org/10.1016/0019-1035(86)90088-6

Bercovici D, Ricard Y (2014) Plate tectonics, damage and inheritance. Nature 508:513 EP. https://doi.org/10.1038/nature13072

Bercovici D, Ricard Y, Richards MA (2000) The relation between mantle dynamics and plate tectonics: a primer. In: Richards MA, Gordon RG, Van Der Hilst RD (eds) The history and dynamics of global plate motions. AGU, Washington DC, pp 5–46. https://doi.org/10.1029/GM121p0005

Berg MTL, Bromiley GD, Le Godec Y, Philippe J, Mezouar M, Perrillat JP, Potts NJ (2018) Rapid Core Formation in Terrestrial Planets by Percolative Flow: in-Situ Imaging of Metallic Melt Migration Under High Pressure/Temperature Conditions. Front Earth Sci 6(77). https://doi.org/10.3389/feart.2018.00077

Berlo K, Gardner JE, Blundy JD (2011) Timescales of magma degassing. In: Timescales of magmatic processes: from core to atmosphere, vol 11. Wiley, New York. https://doi.org/10.1002/9781444328509.ch11

Bhatia GK (2021) Early thermal evolution of the embryos of Earth: role of ^{26}Al and impact-generated steam atmosphere. Planet Space Sci 207:105335. https://doi.org/10.1016/j.pss.2021.105335

Bills BG (2005) Variations in the rotation rate of Venus due to orbital eccentricity modulation of solar tidal torques. J Geophys Res, Planets 110(E11). https://doi.org/10.1029/2003JE002190

Binder AB (1986) The initial thermal state of the Moon. In: Hartmann W, Phillips R, Taylor G (eds) Origin of the Moon. Lunar and Planetary Institute, p 425. https://ui.adsabs.harvard.edu/abs/1986ormo.conf..425B/abstract

Birch F (1952) Elasticity and constitution of the Earth's interior. J Geophys Res 57(2):227–286

Birnstiel T, Klahr H, Ercolano B (2012) A simple model for the evolution of the dust population in protoplanetary disks. Astron Astrophys 539:A148. https://doi.org/10.1051/0004-6361/201118136

Bitsch B, Johansen A, Lambrechts M, Morbidelli A (2015) The structure of protoplanetary discs around evolving young stars. Astron Astrophys 575:A28. https://doi.org/10.1051/0004-6361/201424964

Bizzarro M, Baker JA, Haack H, Ulfbeck D, Rosing M (2003) Early history of Earth's crust–mantle system inferred from hafnium isotopes in chondrites. Nature 421(6926):931–933. https://doi.org/10.1038/nature01421

Blum J, Wurm G (2008) The growth mechanisms of macroscopic bodies in protoplanetary disks. Annu Rev Astron Astrophys 46(1):21–56. https://doi.org/10.1146/annurev.astro.46.060407.145152

Bodenheimer P, Lin DNC (2002) Implications of extrasolar planets for understanding planet formation. Annu Rev Earth Planet Sci 30(1):113–148. https://doi.org/10.1146/annurev.earth.30.091201.140357

Bolfan-Casanova N, Keppler H, Rubie DC (2003) Water partitioning at 660 km depth and evidence for very low water solubility in magnesium silicate perovskite. Geophys Res Lett 30(17). https://doi.org/10.1029/2003GL017182

Bollard J, Connelly JN, Whitehouse MJ, Pringle EA, Bonal L, Jørgensen JK, Nordlund Å, Moynier F, Bizzarro M (2017) Early formation of planetary building blocks inferred from Pb isotopic ages of chondrules. Sci Adv 3(8):e1700407. https://doi.org/10.1126/sciadv.1700407

Bolrão DP, Ballmer MD, Morison A, Rozel AB, Sanan P, Labrosse S, Tackley PJ (2021) Timescales of chemical equilibrium between the convecting solid mantle and over- and underlying magma oceans. Solid Earth 12(2):421–437. https://doi.org/10.5194/se-12-421-2021

Borgeat X, Tackley PJ (2022) Hadean/Eoarchean tectonics and mantle mixing induced by impacts: a three-dimensional study. Prog Earth Planet Sci 9(1):38. https://doi.org/10.1186/s40645-022-00497-0

Boslough M, Weldon R, Ahrens T (1980) Impact-induced water loss from serpentine, nontronite and kernite. In: Lunar and planetary science conference proceedings, vol 3, pp 2145–2158. https://ui.adsabs.harvard.edu/abs/1980LPSC...11.2145B/abstract

Boss AP (1986) The origin of the moon. Science 231(4736):341–345. https://doi.org/10.1126/science.231.4736.341

Boukaré CE, Ricard Y (2017) Modeling phase separation and phase change for magma ocean solidification dynamics. Geochem Geophys Geosyst. https://doi.org/10.1002/2017GC006902

Boukaré CE, Ricard Y, Fiquet G (2015) Thermodynamics of the MgO-FeO-SiO_2 system up to 140 GPa: application to the crystallization of Earth's magma ocean. J Geophys Res, Solid Earth 120(9):6085–6101. https://doi.org/10.1002/2015JB011929

Boulliung J, Füri E, Dalou C, Tissandier L, Zimmermann L, Marrocchi Y (2020) Oxygen fugacity and melt composition controls on nitrogen solubility in silicate melts. Geochim Cosmochim Acta 284:120–133. https://doi.org/10.1016/j.gca.2020.06.020

Bouvier A, Blichert-Toft J, Moynier F, Vervoort JD, Albarède F (2007) Pb–Pb dating constraints on the accretion and cooling history of chondrites. Geochim Cosmochim Acta 71(6):1583–1604. https://doi.org/10.1016/j.gca.2006.12.005

Bower DJ, Kitzmann D, Wolf AS, Sanan P, Dorn C, Oza AV (2019) Linking the evolution of terrestrial interiors and an early outgassed atmosphere to astrophysical observations. Astron Astrophys 631:A103. https://doi.org/10.1051/0004-6361/201935710

Bower DJ, Hakim K, Sossi PA, Sanan P (2022) Retention of water in terrestrial magma oceans and carbon-rich early atmospheres. Planet Sci. J. 3(4):93. https://doi.org/10.3847/psj/ac5fb1

Boyet M, Carlson RW (2005) ^{142}Nd evidence for early (>4.53 Ga) global differentiation of the silicate Earth. Science 309(5734):576–581. https://doi.org/10.1126/science.1113634

Boyet M, Blichert-Toft J, Rosing M, Storey M, Télouk P, Albarède F (2003) ^{142}Nd evidence for early Earth differentiation. Earth Planet Sci Lett 214(3):427–442. https://doi.org/10.1016/S0012-821X(03)00423-0

Brasser R, Mojzsis SJ (2020) The partitioning of the inner and outer Solar System by a structured protoplanetary disk. Nat Astron 4(5):492–499. https://doi.org/10.1038/s41550-019-0978-6

Brasser R, Matsumura S, Ida S, Mojzsis SJ, Werner SC (2016) Analysis of terrestrial planet formation by the grand tack model: system architecture and tack location. Astrophys J 821(2):75. https://doi.org/10.3847/0004-637X/821/2/75

Briceño C, Vivas AK, Calvet N, Hartmann L, Pacheco R, Herrera D, Romero L, Berlind P, Sánchez G, Snyder JA, Andrews P (2001) The CIDA-QUEST large-scale survey of orion OB1: evidence for rapid disk dissipation in a dispersed stellar population. Science 291(5501):93–96. https://doi.org/10.1126/science.291.5501.93

ALMA Partnership, Brogan CL, Pérez LM, Hunter TR, Dent WRF, Hales AS, Hills RE, Corder S, Fomalont EB, Vlahakis C, Asaki Y, Barkats D, Hirota A, Hodge JA, Impellizzeri CMV, Kneissl R, Liuzzo E, Lucas R, Marcelino N, Matsushita S, Nakanishi K, Phillips N, Richards AMS, Toledo I, Aladro R, Broguiere D, Cortes JR, Cortes PC, Espada D, Galarza F, Appadoo DG, Ramirez LG, Humphreys EM, Jung T, Kameno S, Laing RA, Leon S, Marconi G, Mignano A, Nikolic B, Nyman LA, Radiszcz M, Remijan A, Rodón JA, Sawada T, Takahashi S, Tilanus RPJ, Vilaro BV, Watson LC, Wiklind T, Akiyama E, Chapillon E, de Gregorio-Monsalvo I, Francesco JD, Gueth F, Kawamura A, Lee CF, Luong QN, Mangum J, Pietu V, Sanhueza P, Saigo K, Takakuwa S, Ubach C, van Kempen T, Wootten A, Carrizo AC, Francke H, Gallardo J, Garcia J, Gonzalez S, Hill T, Kaminski T, Kurono Y, Liu HY, Lopez C, Morales F, Plarre K, Schieven G, Testi L, Videla L, Villard E, Andreani P, Hibbard JE, Tatematsu K (2015) The 2014 ALMA long baseline campaign: first results from high angular resolution observations toward the HL tau region. Astrophys J Lett 808(1):L3. https://doi.org/10.1088/2041-8205/808/1/L3

Brož M, Chrenko O, Nesvorný D, Dauphas N (2021) Early terrestrial planet formation by torque-driven convergent migration of planetary embryos. Nat Astron 5(9):898–902. https://doi.org/10.1038/s41550-021-01383-3

Budde G, Burkhardt C, Brennecka GA, Fischer-Gödde M, Kruijer TS, Kleine T (2016) Molybdenum isotopic evidence for the origin of chondrules and a distinct genetic heritage of carbonaceous and non-carbonaceous meteorites. Earth Planet Sci Lett 454:293–303. https://doi.org/10.1016/j.epsl.2016.09.020

Bullock MA, Grinspoon DH (2001) The recent evolution of climate on Venus. Icarus 150(1):19–37. https://doi.org/10.1006/icar.2000.6570

Bunge HP, Richards MA, Baumgardner JR (1996) Effect of depth-dependent viscosity on the planform of mantle convection. Nature 379(6564):436–438. https://doi.org/10.1038/379436a0

Burger C, Bazsó Á, Schäfer CM (2020) Realistic collisional water transport during terrestrial planet formation - self-consistent modeling by an N-body-SPH hybrid code. Astron Astrophys 634:A76. https://doi.org/10.1051/0004-6361/201936366

Burgisser A, Scaillet B (2007) Redox evolution of a degassing magma rising to the surface. Nature 445(7124):194–197. https://doi.org/10.1038/nature05509

Burkhardt C, Kleine T, Bourdon B, Palme H, Zipfel J, Friedrich JM, Ebel DS (2008) Hf–W mineral isochron for Ca, Al-rich inclusions: age of the solar system and the timing of core formation in planetesimals. Geochim Cosmochim Acta 72(24):6177–6197. https://doi.org/10.1016/j.gca.2008.10.023

Burkhardt C, Spitzer F, Morbidelli A, Budde G, Render JH, Kruijer TS, Kleine T (2021) Terrestrial planet formation from lost inner solar system material. Sci Adv 7(52):eabj7601. https://doi.org/10.1126/sciadv.abj7601

Cameron AG (1983) Origin of the atmospheres of the terrestrial planets. Icarus 56(2):195–201

Cameron A (1986) The impact theory for origin of the moon. In: Hartmann W, Phillips R, Taylor G (eds) Origin of the Moon, Lunar and Planetary Institute, p 609. https://ui.adsabs.harvard.edu/abs/1986ormo.conf..609C/abstract

Cameron AGW, Ward WR (1976) The origin of the moon. In: Lunar and planetary science conference, vol 7, pp 120–122. https://ui.adsabs.harvard.edu/abs/1976LPI.....7..120C/abstract

Campbell BA, Campbell DB, Carter LM, Chandler JF, Giorgini JD, Margot JL, Morgan GA, Nolan MC, Perillat PJ, Whitten JL (2019) The mean rotation rate of Venus from 29 years of Earth-based radar observations. Icarus 332:19–23. https://doi.org/10.1016/j.icarus.2019.06.019

Canil D (1997) Vanadium partitioning and the oxidation state of Archaean komatiite magmas. Nature 389(6653):842–845. https://doi.org/10.1038/39860

Canil D (2002) Vanadium in peridotites, mantle redox and tectonic environments: Archean to present. Earth Planet Sci Lett 195(1):75–90. https://doi.org/10.1016/S0012-821X(01)00582-9

Canup RM (2004) Simulations of a late lunar-forming impact. Icarus 168(2):433–456. https://doi.org/10.1016/j.icarus.2003.09.028

Canup RM (2008) Accretion of the Earth. Philos Trans R Soc, Math Phys Eng Sci 366(1883):4061–4075. https://doi.org/10.1098/rsta.2008.0101

Canup RM (2012) Forming a moon with an Earth-like composition via a giant impact. Science 338(6110):1052–1055. https://doi.org/10.1126/science.1226073

Canup RM, Asphaug E (2001) Origin of the moon in a giant impact near the end of the Earth's formation. Nature 412:708 EP. https://doi.org/10.1038/35089010

Caracas R, Hirose K, Nomura R, Ballmer MD (2019) Melt–crystal density crossover in a deep magma ocean. Earth Planet Sci Lett 516:202–211. https://doi.org/10.1016/J.EPSL.2019.03.031

Caro G (2011) Early silicate Earth differentiation. Annu Rev Earth Planet Sci 39(1):31–58. https://doi.org/10.1146/annurev-earth-040610-133400

Caro G, Bourdon B, Birck JL, Moorbath S (2003) ^{146}Sm–^{142}Nd evidence from Isua metamorphosed sediments for early differentiation of the Earth's mantle. Nature 423(6938):428–432. https://doi.org/10.1038/nature01668

Carpenter R (1970) A radar determination of the rotation of Venus. Astron J 75:61. https://doi.org/10.1086/110941

Carroll MR, Holloway JR (eds) (1994) Volatiles in magmas, vol 30. Mineralogical Society of America, Washington

Castaing B, Gunaratne G, Heslot F, Kadanoff L, Libchaber A, Thomae S, Wu XZ, Zaleski S, Zanetti G (1989) Scaling of hard thermal turbulence in Rayleigh-Bénard convection. J Fluid Mech 204:1–30. https://doi.org/10.1017/S0022112089001643

Cataldi G, Brandeker A, Olofsson G, Larsson B, Liseau R, Blommaert J, Fridlund M, Ivison R, Pantin E, Sibthorpe B, Vandenbussche B, Wu Y (2014) Herschel/HIFI observations of ionised carbon in the Pictoris debris disk. Astron Astrophys 563:A66. https://doi.org/10.1051/0004-6361/201323126

Catling DC (2006) Comment on "A hydrogen-rich early Earth atmosphere". Science 311(5757):38. https://doi.org/10.1126/science.1117827

Catling DC (2014) 6.7 - The great oxidation event transition. In: Holland HD, Turekian KK (eds) Treatise on geochemistry, 2nd edn. Elsevier, Oxford, pp 177–195. https://doi.org/10.1016/B978-0-08-095975-7.01307-3

Catling DC (2015) 10.13 - Planetary atmospheres. In: Schubert G (ed) Treatise on geophysics, 2nd edn. Elsevier, Oxford, pp 429–472. https://doi.org/10.1016/B978-0-444-53802-4.00185-8

Catling DC, Claire MW (2005) How Earth's atmosphere evolved to an oxic state: a status report. Earth Planet Sci Lett 237(1):1–20. https://doi.org/10.1016/j.epsl.2005.06.013
Catling DC, Zahnle KJ (2020) The Archean atmosphere. Sci Adv 6(9). https://doi.org/10.1126/sciadv.aax1420
Chambers JE (2001) Making more terrestrial planets. Icarus 152(2):205–224. https://doi.org/10.1006/icar.2001.6639
Chambers JE (2010) Terrestrial planet formation. In: Seager S (ed) Exoplanets. University of Arizona Press, Tucson, pp 297–317
Chambers JE (2016) Pebble accretion and the diversity of planetary systems. Astrophys J 825(1):63. https://doi.org/10.3847/0004-637X/825/1/63
Chassefière E (1996) Hydrodynamic escape of oxygen from primitive atmospheres: applications to the cases of Venus and Mars. Icarus 124(2):537–552. https://doi.org/10.1006/icar.1996.0229
Chaussidon M, Gounelle M (2007) Short-lived radioactive nuclides in meteorites and early solar system processes. C R Géosci 339(14):872–884. https://doi.org/10.1016/j.crte.2007.09.005
Chillà F, Schumacher J (2012) New perspectives in turbulent Rayleigh-Bénard convection. Eur Phys J E 35(7):58. https://doi.org/10.1140/epje/i2012-12058-1
Chyba CF (1991) Terrestrial mantle siderophiles and the lunar impact record. Icarus 92(2):217–233
Chyba C, Sagan C (1992) Endogenous production, exogenous delivery and impact-shock synthesis of organic molecules: an inventory for the origins of life. Nature 355(6356):125–132. https://doi.org/10.1038/355125a0
Chyba CF, Thomas PJ, Brookshaw L, Sagan C (1990) Cometary delivery of organic molecules to the early Earth. Science 249(4967):366–373. https://doi.org/10.1126/science.11538074
Citron RI, Stewart ST (2022) Large impacts onto the early Earth: planetary sterilization and iron delivery. Planet Sci. J. 3(5):116. https://doi.org/10.3847/psj/ac66e8
Cleaves HJ, Chalmers JH, Lazcano A, Miller SL, Bada JL (2008) A reassessment of prebiotic organic synthesis in neutral planetary atmospheres. Orig Life Evol Biosph 38(2):105–115. https://doi.org/10.1007/s11084-007-9120-3
Clement MS, Kaib NA, Raymond SN, Walsh KJ (2018) Mars' growth stunted by an early giant planet instability. Icarus 311:340–356. https://doi.org/10.1016/j.icarus.2018.04.008
Clement MS, Kaib NA, Raymond SN, Chambers JE, Walsh KJ (2019) The early instability scenario: terrestrial planet formation during the giant planet instability, and the effect of collisional fragmentation. Icarus 321(7):78–790. https://doi.org/10.1016/j.icarus.2018.12.033
Clement MS, Raymond SN, Kaib NA (2019b) Excitation and depletion of the asteroid belt in the early instability scenario. Astron J 157(1):38. https://doi.org/10.3847/1538-3881/aaf21e
Clement MS, Kaib NA, Raymond SN, Chambers JE (2021) The early instability scenario: Mars' mass explained by Jupiter's orbit. Icarus 367:114585. https://doi.org/10.1016/j.icarus.2021.114585
Clesi V, Bouhifd MA, Bolfan-Casanova N, Manthilake G, Schiavi F, Raepsaet C, Bureau H, Khodja H, Andrault D (2018) Low hydrogen contents in the cores of terrestrial planets. Sci Adv 4(3). https://doi.org/10.1126/sciadv.1701876
Clesi V, Monteux J, Qaddah B, Le Bars M, Wacheul JB, Bouhifd MA (2020) Dynamics of core-mantle separation: influence of viscosity contrast and metal/silicate partition coefficients on the chemical equilibrium. Phys Earth Planet Inter 306:106547. https://doi.org/10.1016/j.pepi.2020.106547
Correia ACM, Laskar J (2001) The four final rotation states of Venus. Nature 411:767 EP. https://doi.org/10.1038/35081000
Correia ACM, Laskar J (2003) Different tidal torques on a planet with a dense atmosphere and consequences to the spin dynamics. J Geophys Res, Planets 108(E11). https://doi.org/10.1029/2003JE002059
Cottereau L, Rambaux N, Lebonnois S, Souchay J (2011) The various contributions in Venus rotation rate and LOD. Astron Astrophys 531:A45. https://doi.org/10.1051/0004-6361/201116606
Ćuk M, Stewart ST (2012) Making the moon from a fast-spinning Earth: a giant impact followed by resonant despinning. Science 338(6110):1047–1052. https://doi.org/10.1126/science.1225542
Dasgupta R, Grewal DS (2019) Origin and early differentiation of carbon and associated life-essential volatile elements on Earth. In: Deep carbon. Cambridge University Press, Cambridge, pp 4–39
Dauphas N (2017) The isotopic nature of the Earth's accreting material through time. Nature 541(7638):521–524
Dauphas N, Morbidelli A (2014) 6.1 - Geochemical and planetary dynamical views on the origin of Earth's atmosphere and oceans. In: Holland HD, Turekian KK (eds) Treatise on geochemistry, 2nd edn. Elsevier, Oxford, pp 1–35. https://doi.org/10.1016/B978-0-08-095975-7.01301-2
Deguen R, Landeau M, Olson P (2014) Turbulent metal–silicate mixing, fragmentation, and equilibration in magma oceans. Earth Planet Sci Lett 391:274–287. https://doi.org/10.1016/j.epsl.2014.02.007
Dehant V, Debaille V, Dobos V, Gaillard F, Gillmann C, Goderis S, Grenfell JL, Höning D, Javaux EJ, Karatekin Ö, Morbidelli A, Noack L, Rauer H, Scherf M, Spohn T, Tackley P, Van Hoolst T, Wünnemann

K (2019) Geoscience for understanding habitability in the solar system and beyond. Space Sci Rev. https://doi.org/10.1007/s11214-019-0608-8
Delano JW (2001) Redox history of the Earth's interior since ~3900 Ma: implications for prebiotic molecules. Orig Life Evol Biosph 31(4):311–341. https://doi.org/10.1023/A:1011895600380
DeMeo FE Carry B (2014) Solar system evolution from compositional mapping of the asteroid belt. Nature 505(7485):629–634. https://doi.org/10.1038/nature12908
Demouchy S, Bolfan-Casanova N (2016) Distribution and transport of hydrogen in the lithospheric mantle: a review. Lithos 240–243:402–425. https://doi.org/10.1016/j.lithos.2015.11.012
Deng J, Du Z, Karki BB, Ghosh DB, Lee KKM (2020) A magma ocean origin to divergent redox evolutions of rocky planetary bodies and early atmospheres. Nat Commun 11(1):2007. https://doi.org/10.1038/s41467-020-15757-0
Dent WRF, Wyatt MC, Roberge A, Augereau JC, Casassus S, Corder S, Greaves JS, de Gregorio-Monsalvo I, Hales A, Jackson AP, Hughes AM, Lagrange AM, Matthews B, Wilner D (2014) Molecular gas clumps from the destruction of icy bodies in the β pictoris debris disk. Science 343(6178):1490–1492. https://doi.org/10.1126/science.1248726
Dobrovolskis AR (1980) Atmospheric tides and the rotation of Venus II. Spin evolution. Icarus 41(1):18–35. https://doi.org/10.1016/0019-1035(80)90157-8
Dobrovolskis AR, Ingersoll AP (1980) Atmospheric tides and the rotation of Venus I. Tidal theory and the balance of torques. Icarus 41(1):1–17. https://doi.org/10.1016/0019-1035(80)90156-6
Donahue TM (1999) New analysis of hydrogen and deuterium escape from Venus. Icarus 141(2):226–235. https://doi.org/10.1006/icar.1999.6186
Donahue TM, Hoffman JH, Hodges RR, Watson AJ (1982) Venus was wet: a measurement of the ratio of deuterium to hydrogen. Science 216(4546):630–633. https://doi.org/10.1126/science.216.4546.630
Drake MJ (2000) Accretion and primary differentiation of the Earth: a personal journey. Geochim Cosmochim Acta 64(14):2363–2369. https://doi.org/10.1016/S0016-7037(00)00372-0
Drake MJ, Newsom HE, Capobianco CJ (1989) V, Cr, and Mn in the Earth, Moon, EPB, and SPB and the origin of the Moon: experimental studies. Geochim Cosmochim Acta 53(8):2101–2111. https://doi.org/10.1016/0016-7037(89)90328-1
Drążkowska J, Alibert Y (2017) Planetesimal formation starts at the snow line. Astron Astrophys 608:A92. https://doi.org/10.1051/0004-6361/201731491
Drążkowska J, Dullemond CP (2018) Planetesimal formation during protoplanetary disk buildup. Astron Astrophys 614:A62. https://doi.org/10.1051/0004-6361/201732221
Drążkowska J, Alibert Y, Moore B (2016) Close-in planetesimal formation by pile-up of drifting pebbles. Astron Astrophys 594:A105. https://doi.org/10.1051/0004-6361/201628983
Dreibus G, Wänke H (1987) Volatiles on Earth and Mars: a comparison. Icarus 71(2):225–240. https://doi.org/10.1016/0019-1035(87)90148-5
Driscoll P, Bercovici D (2013) Divergent evolution of Earth and Venus: influence of degassing, tectonics, and magnetic fields. Icarus 226(2):1447–1464. https://doi.org/10.1016/j.icarus.2013.07.025
Edmonds M, Woods AW (2018) Exsolved volatiles in magma reservoirs. J Volcanol Geotherm Res 368:13–30. https://doi.org/10.1016/j.jvolgeores.2018.10.018
Elkins-Tanton LT (2008) Linked magma ocean solidification and atmospheric growth for Earth and Mars. Earth Planet Sci Lett 271(1–4):181–191. https://doi.org/10.1016/j.epsl.2008.03.062
Elkins-Tanton LT (2011) Formation of early water oceans on rocky planets. Astrophys Space Sci 332(2):359–364. https://doi.org/10.1007/s10509-010-0535-3
Elkins-Tanton LT (2012) Magma oceans in the inner solar system. Annu Rev Earth Planet Sci 40:113–139. https://doi.org/10.1146/annurev-earth-042711-105503
Elkins-Tanton LT, Grove TL (2011) Water (hydrogen) in the lunar mantle: results from petrology and magma ocean modeling. Earth Planet Sci Lett 307(1–2):173–179. https://doi.org/10.1016/j.epsl.2011.04.027
Elkins-Tanton LT, Parmentier EM, Hess PC (2003) Magma ocean fractional crystallization and cumulate overturn in terrestrial planets: implications for Mars. Meteorit Planet Sci 38(12):1753–1771. https://doi.org/10.1111/j.1945-5100.2003.tb00013.x
Elkins-Tanton LT, Weiss BP, Zuber MT (2011) Chondrites as samples of differentiated planetesimals. Earth Planet Sci Lett 305(1):1–10. https://doi.org/10.1016/j.epsl.2011.03.010
Emsenhuber A, Asphaug E, Cambioni S, Gabriel TSJ, Schwartz SR (2021) Collision chains among the terrestrial planets. II. An asymmetry between Earth and Venus. Planet Sci. J. 2(5):199. https://doi.org/10.3847/psj/ac19b1
Erkaev NV, Lammer H, Elkins-Tanton LT, Stökl A, Odert P, Marcq E, Dorfi EA, Kislyakova KG, Kulikov Y, Leitzinger M, Güdel M (2014) Escape of the Martian protoatmosphere and initial water inventory. Planet Space Sci 98:106–119. https://doi.org/10.1016/j.pss.2013.09.008
Faul UH, Jackson I (2007) Diffusion creep of dry, melt-free olivine. J Geophys Res, Solid Earth 112(B4). https://doi.org/10.1029/2006JB004586

Fegley B, Zolotov MY, Lodders K (1997) The oxidation state of the lower atmosphere and surface of Venus. Icarus 125(2):416–439. https://doi.org/10.1006/icar.1996.5628
Feig ST, Koepke J, Snow JE (2010) Effect of oxygen fugacity and water on phase equilibria of a hydrous tholeiitic basalt. Contrib Mineral Petrol 160(4):551–568. https://doi.org/10.1007/s00410-010-0493-3
Fiquet G (2018) Chap. 4 - Melting in the Earth's deep interior. In: Kono Y, Sanloup C (eds) Magmas under pressure. Elsevier, Amsterdam, pp 115–134. https://doi.org/10.1016/B978-0-12-811301-1.00004-6
Fiquet G, Auzende AL, Siebert J, Corgne A, Bureau H, Ozawa H, Garbarino G (2010) Melting of peridotite to 140 gigapascals. Science 329(5998):1516–1518. https://doi.org/10.1126/science.1192448
Fischer RA, Nakajima Y, Campbell AJ, Frost DJ, Harries D, Langenhorst F, Miyajima N, Pollok K, Rubie DC (2015) High pressure metal–silicate partitioning of Ni, Co, V, Cr, Si, and O. Geochim Cosmochim Acta 167:177–194. https://doi.org/10.1016/j.gca.2015.06.026
Fischer-Gödde M, Kleine T (2017) Ruthenium isotopic evidence for an inner solar system origin of the late veneer. Nature 541(7638):525–527
Fish RA, Goles GG, Anders E (1960) The record in the meteorites. III. On the development of meteorites in asteroidal bodies. Astrophys J 132:243. https://doi.org/10.1086/146918
Flasar FM, Birch F (1973) Energetics of core formation: a correction. J Geophys Res 78(26):6101–6103. https://doi.org/10.1029/JB078i026p06101
Foley BJ, Driscoll PE (2016) Whole planet coupling between climate, mantle, and core: implications for rocky planet evolution. Geochem Geophys Geosyst 17(5):1885–1914. https://doi.org/10.1002/2015GC006210
Foley BJ, Bercovici D, Elkins-Tanton LT (2014) Initiation of plate tectonics from post-magma ocean thermochemical convection. J Geophys Res, Solid Earth 119(11):8538–8561. https://doi.org/10.1002/2014JB011121
French BM (1966) Some geological implications of equilibrium between graphite and a C-H-O gas phase at high temperatures and pressures. Rev Geophys 4(2):223–253. https://doi.org/10.1029/RG004i002p00223
Frost BR (1979) Mineral equilibria involving mixed-volatiles in a C-O-H fluid phase; the stabilities of graphite and siderite. Am J Sci 279(9):1033–1059. https://doi.org/10.2475/ajs.279.9.1033
Frost BR (1991) Chap. 1. Introduction to oxygen fugacity and its petrologic importance. Rev Mineral Geochem 25(1):1–9. https://doi.org/10.1515/9781501508684-004
Frost DJ, McCammon CA (2008) The redox state of Earth's mantle. Annu Rev Earth Planet Sci 36(1):389–420. https://doi.org/10.1146/annurev.earth.36.031207.124322
Frost DJ, Liebske C, Langenhorst F, McCammon CA, Trønnes RG, Rubie DC (2004) Experimental evidence for the existence of iron-rich metal in the Earth's lower mantle. Nature 428(6981):409–412. https://doi.org/10.1038/nature02413
Frost DJ, Mann U, Asahara Y, Rubie DC (2008) The redox state of the mantle during and just after core formation. Philos Trans R Soc, Math Phys Eng Sci 366(1883):4315–4337. http://www.jstor.org/stable/25197401
Fu RR, Young ED, Greenwood RC, Elkins-Tanton LT (2017) Silicate melting and volatile loss during differentiation in planetesimals. In: Planetesimals: early differentiation and consequences for planets. Cambridge University Press, Cambridge. https://doi.org/10.1017/9781316339794.006
Gabriel TSJ, Cambioni S (2023) The role of giant impacts in planet formation. Annu Rev Earth Planet Sci 51(1):671–695. https://doi.org/10.1146/annurev-earth-031621-055545
Gaillard F, Bouhifd MA, Füri E, Malavergne V, Marrocchi Y, Noack L, Ortenzi G, Roskosz M, Vulpius S (2021) The diverse planetary ingassing/outgassing paths produced over billions of years of magmatic activity. Space Sci Rev 217(1):22. https://doi.org/10.1007/s11214-021-00802-1
Gaillard F, Bernadou F, Roskosz M, Bouhifd MA, Marrocchi Y, Iacono-Marziano G, Moreira M, Scaillet B, Rogerie G (2022a) Redox controls during magma ocean degassing. Earth Planet Sci Lett 577:117255. https://doi.org/10.1016/j.epsl.2021.117255
Gaillard F, Malavergne V, Bouhifd MA, Rogerie G (2022b) A speciation model linking the fate of carbon and hydrogen during core – magma ocean equilibration. Earth Planet Sci Lett 577:117266. https://doi.org/10.1016/j.epsl.2021.117266
Galimov EM (2005) Redox evolution of the Earth caused by a multi-stage formation of its core. Earth Planet Sci Lett 233(3):263–276. https://doi.org/10.1016/j.epsl.2005.01.026
Gallet F, Charbonnel C, Amard L, Brun S, Palacios A, Mathis S (2017) Impacts of stellar evolution and dynamics on the habitable zone: the role of rotation and magnetic activity. Astron Astrophys 597:A14. https://doi.org/10.1051/0004-6361/201629034
Garvin J, Getty S, Arney G, Johnson N, Malespin C, Webster C, Ravine M, Lorenz R, Kiefer W, Atreya S et al (2020) Deep atmosphere of Venus investigation of noble gases, chemistry, and imaging plus (DAVINCI+): discovering a new Venus via a flyby, probe, orbiter mission. In: AGU fall meeting abstracts, vol 2020, p P026–0001

Garvin JB, Getty SA, Arney GN, Johnson NM, Kohler E, Schwer KO, Sekerak M, Bartels A, Saylor RS, Elliott VE, Goodloe CS, Garrison MB, Cottini V, Izenberg N, Lorenz R, Malespin CA, Ravine M, Webster CR, Atkinson DH, Aslam S, Atreya S, Bos BJ, Brinckerhoff WB, Campbell B, Crisp D, Filiberto JR, Forget F, Gilmore M, Gorius N, Grinspoon D, Hofmann AE, Kane SR, Kiefer W, Lebonnois S, Mahaffy PR, Pavlov A, Trainer M, Zahnle KJ, Zolotov M (2022) Revealing the mysteries of Venus: the DAVINCI mission. Planet Sci. J. 3(5):117. https://doi.org/10.3847/PSJ/ac63c2

Geiss J, Gloeckler G (1998) Abundances of deuterium and helium-3 in the protosolar cloud. Space Sci Rev 84(1):239–250. https://doi.org/10.1023/A:1005039822524

Genda H (2016) Origin of Earth's oceans: an assessment of the total amount, history and supply of water. Geochem J 50(1):27–42. https://doi.org/10.2343/geochemj.2.0398

Genda H, Abe Y (2003) Survival of a proto-atmosphere through the stage of giant impacts: the mechanical aspects. Icarus 164(1):149–162. https://doi.org/10.1016/S0019-1035(03)00101-5

Genda H, Abe Y (2005) Enhanced atmospheric loss on protoplanets at the giant impact phase in the presence of oceans. Nature 433(7028):842–844

Gerya TV, Connolly JAD, Yuen DA (2008) Why is terrestrial subduction one-sided? Geology 36(1):43–46. https://doi.org/10.1130/G24060A.1

Ghanbarzadeh S, Hesse MA, Prodanović M (2017) Percolative core formation in planetesimals enabled by hysteresis in metal connectivity. Proc Natl Acad Sci 114(51):13406–13411. https://doi.org/10.1073/pnas.1707580114

Gillmann C, Chassefière E, Lognonné P (2009) A consistent picture of early hydrodynamic escape of Venus atmosphere explaining present Ne and Ar isotopic ratios and low oxygen atmospheric content. Earth Planet Sci Lett 286(3–4):503–513. https://doi.org/10.1016/j.epsl.2009.07.016

Gillmann C, Golabek GJ, Tackley PJ (2016) Effect of a single large impact on the coupled atmosphere-interior evolution of Venus. Icarus 268:295–312. https://doi.org/10.1016/j.icarus.2015.12.024

Gillmann C, Golabek G, Raymond S, Schönbächler M, Tackley P, Dehant V, Vinciane D (2020) Dry late accretion inferred from Venus's coupled atmosphere and internal evolution. Nat Geosci 13:1–5. https://doi.org/10.1038/s41561-020-0561-x

Gillmann C, Way MJ, Avice G, Breuer D, Golabek GJ, Höning D, Krissansen-Totton J, Lammer H, O'Rourke JG, Persson M, Plesa AC, Salvador A, Scherf M, Zolotov MY (2022) The long-term evolution of the atmosphere of Venus: processes and feedback mechanisms. Space Sci Rev 218(7):56. https://doi.org/10.1007/s11214-022-00924-0

Godin PJ, Ramirez RM, Campbell CL, Wizenberg T, Nguyen TG, Strong K, Moores JE (2020) Collision-induced absorption of CH_4-CO_2 and H_2-CO_2 complexes and their effect on the ancient Martian atmosphere. J Geophys Res, Planets 125(12):e2019JE006357. https://doi.org/10.1016/10.1029/2019JE006357

Gold T, Soter S (1969) Atmospheric tides and the resonant rotation of Venus. Icarus 11(3):356–366. https://doi.org/10.1016/0019-1035(69)90068-2

Goldblatt C (2015) Habitability of waterworlds: runaway greenhouses, atmospheric expansion, and multiple climate states of pure water atmospheres. Astrobiology 15. https://doi.org/10.1089/ast.2014.1268

Goldblatt C, Watson AJ (2012) The runaway greenhouse: implications for future climate change, geoengineering and planetary atmospheres. Philos Trans R Soc Lond Ser A 370(1974):4197–4216. https://doi.org/10.1098/rsta.2012.0004. arXiv:1201.1593

Goldblatt C, Robinson TD, Zahnle KJ, Crisp D (2013) Low simulated radiation limit for runaway greenhouse climates. Nat Geosci 6(8):661–667. https://doi.org/10.1038/ngeo1892

Goldreich P, Peale S (1967) Spin-orbit coupling in the solar system. II. The resonant rotation of Venus. Astron J 72:662–666. https://doi.org/10.1086/110289

Goldreich P, Peale S (1970) The obliquity of Venus. Astron J 75:273. https://doi.org/10.1086/110975

Gomes R, Levison HF, Tsiganis K, Morbidelli A (2005) Origin of the cataclysmic late heavy bombardment period of the terrestrial planets. Nature 435:466–469. https://doi.org/10.1038/nature03676

Gonnermann HM (2015) Magma fragmentation. Annu Rev Earth Planet Sci 43(1):431–458. https://doi.org/10.1146/annurev-earth-060614-105206

Gough DO (1981) Solar interior structure and luminosity variations. Sol Phys 74(1):21–34. https://doi.org/10.1007/BF00151270

Gounelle M (2011) The asteroid–comet continuum: in search of lost primitivity. Elements 7(1):29–34. https://doi.org/10.2113/gselements.7.1.29

Greenberg R, Wacker JF, Hartmann WK, Chapman CR (1978) Planetesimals to planets: numerical simulation of collisional evolution. Icarus 35(1):1–26. https://doi.org/10.1016/0019-1035(78)90057-X

Grevemeyer I, Ranero CR, Ivandic M (2018) Structure of oceanic crust and serpentinization at subduction trenches. Geosphere 14(2):395–418. https://doi.org/10.1130/GES01537.1

Grewal DS, Dasgupta R, Farnell A (2020) The speciation of carbon, nitrogen, and water in magma oceans and its effect on volatile partitioning between major reservoirs of the Solar System rocky bodies. Geochim Cosmochim Acta 280:281–301. https://doi.org/10.1016/j.gca.2020.04.023

Griffith CA, Zahnle K (1995) Influx of cometary volatiles to planetary moons: the atmospheres of 1000 possible titans. J Geophys Res, Planets 100(E8):16907–16922
Grossmann S, Lohse D (2000) Scaling in thermal convection: a unifying theory. J Fluid Mech 407:27–56. https://doi.org/10.1017/S0022112099007545
Güdel M, Guinan EF, Skinner SL (1997) The X-ray sun in time: a study of the long-term evolution of coronae of solar-type stars. Astrophys J 483(2):947–960. https://doi.org/10.1086/304264
Haghighipour N, Boss AP (2003) On pressure gradients and rapid migration of solids in a nonuniform solar nebula. Astrophys J 583(2):996. https://doi.org/10.1086/345472
Halliday AN (2004) Mixing, volatile loss and compositional change during impact-driven accretion of the Earth. Nature 427(6974):505–509. https://doi.org/10.1038/nature02275
Halliday AN (2013) The origins of volatiles in the terrestrial planets. Geochim Cosmochim Acta 105:146–171. https://doi.org/10.1016/j.gca.2012.11.015
Hallis LJ, Huss GR, Nagashima K, Taylor GJ, Halldórsson SA, Hilton DR, Mottl MJ, Meech KJ (2015) Evidence for primordial water in Earth's deep mantle. Science 350(6262):795–797. https://doi.org/10.1126/science.aac4834
Hamano K, Abe Y, Genda H (2013) Emergence of two types of terrestrial planet on solidification of magma ocean. Nature 497(7451):607–610. https://doi.org/10.1038/nature12163
Hamano K, Kawahara H, Abe Y, Onishi M, Hashimoto GL (2015) Lifetime and spectral evolution of a magma ocean with a steam atmosphere: its detectability by future direct imaging. Astrophys J 806(2):216. https://doi.org/10.1088/0004-637X/806/2/216
Hanel RA, Conrath BJ, Jennings DE, Samuelson RE (2003) Retrieval of physical parameters from measurements. In: Exploration of the solar system by infrared remote sensing, 2nd edn. Cambridge University Press, Cambridge, pp 352–404. https://doi.org/10.1017/CBO9780511536106.010
Hansen BMS (2009) Formation of the terrestrial planets from a narrow annulus. Astrophys J 703(1):1131–1140. https://doi.org/10.1088/0004-637X/703/1/1131
Harper CL, Jacobsen SB (1996) Evidence for 182Hf in the early Solar System and constraints on the timescale of terrestrial accretion and core formation. Geochim Cosmochim Acta 60(7):1131–1153. https://doi.org/10.1016/0016-7037(96)00027-0
Harrison TM (2009) The hadean crust: evidence from >4 Ga zircons. Annu Rev Earth Planet Sci 37(1):479–505. https://doi.org/10.1146/annurev.earth.031208.100151
Harrison TM, Blichert-Toft J, Müller W, Albarede F, Holden P, Mojzsis SJ (2005) Heterogeneous hadean hafnium: evidence of continental crust at 4.4 to 4.5 Ga. Science 310(5756):1947–1950. https://doi.org/10.1126/science.1117926
Hartmann WK (1986) Moon origin: the impact-trigger hypothesis. In: Hartmann W, Phillips R, Taylor G (eds) Origin of the Moon, Lunar and Planetary Institute, pp 579–608. https://ui.adsabs.harvard.edu/abs/1986ormo.conf..579H/abstract
Hartmann WK, Davis DR (1975) Satellite-sized planetesimals and lunar origin. Icarus 24(4):504–515. https://doi.org/10.1016/0019-1035(75)90070-6
Hashimoto GL, Abe Y, Sugita S (2007) The chemical composition of the early terrestrial atmosphere: Formation of a reducing atmosphere from CI-like material. J Geophys Res, Planets 112(E5). https://doi.org/10.1029/2006JE002844
Hayashi C, Nakazawa K, Mizuno H (1979) Earth's melting due to the blanketing effect of the primordial dense atmosphere. Earth Planet Sci Lett 43(1):22–28. https://doi.org/10.1016/0012-821X(79)90152-3
Helffrich G, Kaneshima S (2004) Seismological constraints on core composition from Fe-O-S liquid immiscibility. Science 306(5705):2239–2242. https://doi.org/10.1126/science.1101109
Herbert F, Sonett CP, Wiskerchen MJ (1977) Model 'zero-age' lunar thermal profiles resulting from electrical induction. J Geophys Res 82(14):2054–2060. https://doi.org/10.1029/JB082i014p02054
Herd CDK, Borg LE, Jones JH, Papike JJ (2002) Oxygen fugacity and geochemical variations in the Martian basalts: implications for Martian basalt petrogenesis and the oxidation state of the upper mantle of Mars. Geochim Cosmochim Acta 66(11):2025–2036. https://doi.org/10.1016/S0016-7037(02)00828-1
Hier-Majumder S, Hirschmann MM (2017) The origin of volatiles in the Earth's mantle. Geochem Geophys Geosyst 18(8). https://doi.org/10.1002/2017GC006937. arXiv:1011.1669v3
Hillgren VJ (1991) Partitioning behavior of NI, CO, MO, and W between basaltic liquid and Ni-rich metal: implications for the origin of the moon and lunar core formation. Geophys Res Lett 18(11):2077–2080. https://doi.org/10.1029/91GL02534
Hirose K, Labrosse S, Hernlund J (2013) Composition and state of the core. Annu Rev Earth Planet Sci 41(1):657–691. https://doi.org/10.1146/annurev-earth-050212-124007
Hirose K, Wood B, Vočadlo L (2021) Light elements in the Earth's core. Nat. Rev. Earth Environ. 2(9):645–658. https://doi.org/10.1038/s43017-021-00203-6
Hirschmann MM (2006) Water, melting, and the deep Earth H_2O cycle. Annu Rev Earth Planet Sci 34(1):629–653. https://doi.org/10.1146/annurev.earth.34.031405.125211

Hirschmann MM (2012) Magma ocean influence on early atmosphere mass and composition. Earth Planet Sci Lett 341–344:48–57. https://doi.org/10.1016/j.epsl.2012.06.015
Hirschmann MM (2016) Constraints on the early delivery and fractionation of Earth's major volatiles from C/H, C/N, and C/S ratios. Am Mineral 101(3):540–553. https://doi.org/10.2138/am-2016-5452
Hirschmann MM (2021) Iron-wüstite revisited: a revised calibration accounting for variable stoichiometry and the effects of pressure. Geochim Cosmochim Acta 313:74–84. https://doi.org/10.1016/j.gca.2021.08.039
Hirschmann MM (2022) Magma oceans, iron and chromium redox, and the origin of comparatively oxidized planetary mantles. Geochim Cosmochim Acta 328:221–241. https://doi.org/10.1016/j.gca.2022.04.005
Hirschmann MM, Aubaud C, Withers AC (2005) Storage capacity of H_2O in nominally anhydrous minerals in the upper mantle. Earth Planet Sci Lett 236(1):167–181. https://doi.org/10.1016/j.epsl.2005.04.022
Hirschmann MM, Withers AC, Ardia P, Foley NT (2012) Solubility of molecular hydrogen in silicate melts and consequences for volatile evolution of terrestrial planets. Earth Planet Sci Lett 345–348:38–48. https://doi.org/10.1016/j.epsl.2012.06.031
Hirth G, Kohlstedt DL (1995) Experimental constraints on the dynamics of the partially Molten upper mantle: 2. Deformation in the dislocation creep regime. J Geophys Res, Solid Earth 100(B8):15441–15449. https://doi.org/10.1029/95JB01292
Hirth G, Kohlstedt DL (1996) Water in the oceanic upper mantle: implications for rheology, melt extraction and the evolution of the lithosphere. Earth Planet Sci Lett 144(1):93–108. https://doi.org/10.1016/0012-821X(96)00154-9
Hirth G, Kohlstedt DL (2004) Rheology of the upper mantle and the mantle wedge: a view from the experimentalists. In: Eiler J (ed) Inside the subduction factory. AGU, Washington DC, pp 83–105. https://doi.org/10.1029/138GM06
Hoehler TM, Som SM, Kiang NY (2018) Life's requirements. In: Deeg HJ, Belmonte JA (eds) Handbook of exoplanets. Springer, Berlin, pp 2795–2816. https://doi.org/10.1007/978-3-319-55333-7_74
Holland HD (1962) Model for the evolution of the Earth's atmosphere. In: Engel AEJ, James HL, Leonard BF (eds) Petrologic studies: a volume in honor of A. F. Buddington. The Geological Society of America, New York, pp 447–477. https://doi.org/10.1130/Petrologic.1962.447
Holland HD (1978) The chemistry of the atmosphere and oceans. Wiley, New York
Holland HD (2006) The oxygenation of the atmosphere and oceans. Philos Trans R Soc B, Biol Sci 361(1470):903–915. https://doi.org/10.1098/rstb.2006.1838
Holloway JR (1981) Volatile interactions in magmas. In: Thermodynamics of minerals and melts. Springer, New York, pp 273–293. https://doi.org/10.1007/978-1-4612-5871-1_13
Holloway JR, Blank JG (1994) Application of experimental results to C-O-H species in natural melts. In: Carroll MR, Holloway JR (eds) Volatiles in magmas, vol 6. Mineralogical Society of America, Washington. https://doi.org/10.1515/9781501509674-012
Holzheid A, Borisov A, Palme H (1994) The effect of oxygen fugacity and temperature on solubilities of nickel, cobalt, and molybdenum in silicate melts. Geochim Cosmochim Acta 58(8):1975–1981. https://doi.org/10.1016/0016-7037(94)90429-4
Höning D, Baumeister P, Grenfell JL, Tosi N, Way MJ (2021) Early habitability and crustal decarbonation of a stagnant-lid Venus. J Geophys Res, Planets 126(10):e2021JE006895
Hoolst TV (2015) 10.04 - Rotation of the terrestrial planets. In: Schubert G (ed) Treatise on geophysics, 2nd edn. Elsevier, Oxford, pp 121–151. https://doi.org/10.1016/B978-0-444-53802-4.00168-8
Hopp T, Dauphas N, Abe Y, Aléon J, Alexander CMO, Amari S, Amelin Y, Bajo K, Bizzarro M, Bouvier A, Carlson RW, Chaussidon M, Choi BG, Davis AM, Rocco TD, Fujiya W, Fukai R, Gautam I, Haba MK, Hibiya Y, Hidaka H, Homma H, Hoppe P, Huss GR, Ichida K, Iizuka T, Ireland TR, Ishikawa A, Ito M, Itoh S, Kawasaki N, Kita NT, Kitajima K, Kleine T, Komatani S, Krot AN, Liu MC, Masuda Y, McKeegan KD, Morita M, Motomura K, Moynier F, Nakai I, Nagashima K, Nesvorný D, Nguyen A, Nittler L, Onose M, Pack A, Park C, Piani L, Qin L, Russell SS, Sakamoto N, Schönbächler M, Tafla L, Tang H, Terada K, Terada Y, Usui T, Wada S, Wadhwa M, Walker RJ, Yamashita K, Yin QZ, Yokoyama T, Yoneda S, Young ED, Yui H, Zhang AC, Nakamura T, Naraoka H, Noguchi T, Okazaki R, Sakamoto K, Yabuta H, Abe M, Miyazaki A, Nakato A, Nishimura M, Okada T, Yada T, Yogata K, Nakazawa S, Saiki T, Tanaka S, Terui F, Tsuda Y, Watanabe S, Yoshikawa M, Tachibana S, Yurimoto H (2022) Ryugu's nucleosynthetic heritage from the outskirts of the Solar System. Sci Adv 8(46):eadd8141. https://doi.org/10.1126/sciadv.add8141
Horan MF, Smoliar MI, Walker RJ (1998) 182W and 187Re-187Os systematics of iron meteorites: chronology for melting, differentiation, and crystallization in asteroids. Geochim Cosmochim Acta 62(3):545–554. https://doi.org/10.1016/S0016-7037(97)00368-2
Hostetler C, Drake M (1980) On the early global melting of the terrestrial planets. In: Lunar and planetary science conference proceedings, vol 11, pp 1915–1929

Hughes AM, Duchêne G, Matthews BC (2018) Debris disks: structure, composition, and variability. Annu Rev Astron Astrophys 56(1):541–591. https://doi.org/10.1146/annurev-astro-081817-052035
Humphreys MCS, Brooker RA, Fraser DG, Burgisser A, Mangan MT, McCammon C (2015) Coupled interactions between volatile activity and Fe oxidation state during Arc crustal processes. J Petrol 56(4):795–814. https://doi.org/10.1093/petrology/egv017
Hunten DM (1973) The escape of light gases from planetary atmospheres. J Atmos Sci 30(8):1481–1494. https://doi.org/10.1175/1520-0469(1973)030<1481:TEOLGF>2.0.CO;2
Hunten DM (1993) Atmospheric evolution of the terrestrial planets. Science 259(5097):915–920. https://doi.org/10.1126/science.259.5097.915
Hunten DM, Pepin RO, Walker JCG (1987) Mass fractionation in hydrodynamic escape. Icarus 69(3):532–549. https://doi.org/10.1016/0019-1035(87)90022-4
Ida S, Yamamura T, Okuzumi S (2019) Water delivery by pebble accretion to rocky planets in habitable zones in evolving disks. Astron Astrophys 624:A28. https://doi.org/10.1051/0004-6361/201834556
Iizuka-Oku R, Yagi T, Gotou H, Okuchi T, Hattori T, Sano-Furukawa A (2017) Hydrogenation of iron in the early stage of Earth's evolution. Nat Commun 8(1):14096. https://doi.org/10.1038/ncomms14096
Ikoma M, Genda H (2006) Constraints on the mass of a habitable planet with water of nebular origin. Astrophys J 648(1):696–706. https://doi.org/10.1086/505780
Ikoma M, Elkins-Tanton L, Hamano K, Suckale J (2018) Water partitioning in planetary embryos and protoplanets with magma oceans. Space Sci Rev 214(4):76. https://doi.org/10.1007/s11214-018-0508-3. arXiv:1804.09294
Ingersoll AP (1969) The runaway greenhouse: a history of water on Venus. J Atmos Sci 26(6):1191–1198. https://doi.org/10.1175/1520-0469(1969)026<1191:TRGAHO>2.0.CO;2
Ingersoll AP, Dobrovolskis AR (1978) Venus' rotation and atmospheric tides. Nature 275(5675):37–38. https://doi.org/10.1038/275037a0
Ishiwatari M, Takehiro S, Nakajima K, Hayashi YY (2002) A numerical study on appearance of the runaway greenhouse state of a three-dimensional gray atmosphere. J Atmos Sci 59(22):3223–3238. https://doi.org/10.1175/1520-0469(2002)059<3223:ANSOAO>2.0.CO;2
Ishiwatari M, Nakajima K, Takehiro S, Hayashi YY, Kawai Y, Takahashi YO (2021) Revision of "Dependence of climate states of gray atmosphere on solar constant: from the runaway greenhouse to the snowball states" by Ishiwatari et al. (2007). J Geophys Res, Atmos 126(11):e2019JD031761. https://doi.org/10.1029/2019JD031761
Itcovitz JP, Rae ASP, Citron RI, Stewart ST, Sinclair CA, Rimmer PB, Shorttle O (2022) Reduced atmospheres of post-impact worlds: the early Earth. Planet Sci. J. 3(5):115. https://doi.org/10.3847/psj/ac67a9
Izidoro A, Bitsch B, Dasgupta R (2021a) The effect of a strong pressure bump in the Sun's natal disk: terrestrial planet formation via planetesimal accretion rather than pebble accretion. Astrophys J 915(1):62. https://doi.org/10.3847/1538-4357/abfe0b
Izidoro A, Bitsch B, Raymond SN, Johansen A, Morbidelli A, Lambrechts M, Jacobson SA (2021b) Formation of planetary systems by pebble accretion and migration - Hot super-Earth systems from breaking compact resonant chains. Astron Astrophys 650:A152. https://doi.org/10.1051/0004-6361/201935336
Izidoro A, Dasgupta R, Raymond SN, Deienno R, Bitsch B, Isella A (2022) Planetesimal rings as the cause of the Solar System's planetary architecture. Nat Astron 6(3):357–366. https://doi.org/10.1038/s41550-021-01557-z
Jacobsen SB (2005) The Hf-W isotopic system and the origin of the Earth and Moon. Annu Rev Earth Planet Sci 33(1):531–570. https://doi.org/10.1146/annurev.earth.33.092203.122614
Jacobson SA, Morbidelli A (2014) Lunar and terrestrial planet formation in the Grand Tack scenario. Philos Trans R Soc A, Math Phys Eng Sci 372(2024):20130174. https://doi.org/10.1098/rsta.2013.0174
Jacobson SA, Walsh KJ (2015) Earth and terrestrial planet formation. In: The early Earth. Am. Geophys. Union, Washington, pp 49–70. https://doi.org/10.1002/9781118860359.ch3
Jakosky BM, Ahrens T (1979) The history of an atmosphere of impact origin. In: Lunar and planetary science conference proceedings, vol 3, pp 2727–2739. https://ui.adsabs.harvard.edu/abs/1979LPSC...10.2727J
Jakosky BM, Phillips RJ (2001) Mars' volatile and climate history. Nature 412(6843):237–244. https://doi.org/10.1038/35084184
Jansen T, Scharf C, Way M, Genio AD (2019) Climates of warm Earth-like planets. II. Rotational "Goldilocks" zones for fractional habitability and silicate weathering. Astrophys J 875(2):79. https://doi.org/10.3847/1538-4357/ab113d
Jaupart C, Labrosse S, Lucazeau F, Mareschal JC (2015) 7.06 - Temperatures, heat, and energy in the mantle of the Earth. In: Schubert G (ed) Treatise on geophysics, 2nd edn. Elsevier, Oxford, pp 223–270. https://doi.org/10.1016/B978-0-444-53802-4.00126-3
Ji J, Guo D, Liu J, Chen S, Ling Z, Ding X, Han K, Chen J, Cheng W, Zhu K, Liu J, Wang J, Chen J, Ouyang Z (2022) The 1:2,500,000-scale geologic map of the global Moon. Sci Bull. https://doi.org/10.1016/j.scib.2022.05.021

Johansen A, Lambrechts M (2017) Forming planets via pebble accretion. Annu Rev Earth Planet Sci 45(1):359–387. https://doi.org/10.1146/annurev-earth-063016-020226
Johansen A, Youdin A, Low MMM (2009) Particle clumping and planetesimal formation depend strongly on metallicity. Astrophys J 704(2):L75–L79. https://doi.org/10.1088/0004-637X/704/2/L75
Johansen A, Blum J, Tanaka H, Ormel C, Bizzarro M, Rickman H (2014) The multifaceted planetesimal formation process. In: Beuther H et al (eds) Protostars and planets VI. University of Arizona Press, Tucson, p 547. https://doi.org/10.2458/azu_uapress_9780816531240-ch024
Johansen A, Ronnet T, Bizzarro M, Schiller M, Lambrechts M, Nordlund Å, Lammer H (2021) A pebble accretion model for the formation of the terrestrial planets in the Solar System. Sci Adv 7(8):eabc0444. https://doi.org/10.1126/sciadv.abc0444.
Johnson NM de Oliveira MRR (2019) Venus atmospheric composition in situ data: a compilation. Earth Space Sci 6(7):1299–1318. https://doi.org/10.1029/2018EA000536
Johnson KTM, Dick HJB (1992) Open system melting and temporal and spatial variation of peridotite and basalt at the Atlantis II Fracture Zone. J Geophys Res, Solid Earth 97(B6):9219–9241. https://doi.org/10.1029/92JB00701
Johnstone CP (2020) Hydrodynamic escape of water vapor atmospheres near very active stars. Astrophys J 890(1):79. https://doi.org/10.3847/1538-4357/ab6224
Johnstone CP, Bartel M, Güdel M (2021) The active lives of stars: a complete description of the rotation and XUV evolution of F, G, K, and M dwarfs. Astron Astrophys 649:A96. https://doi.org/10.1051/0004-6361/202038407. arXiv:2009.07695
Karato S (2015) 9.05 - Water in the evolution of the Earth and other terrestrial planets. In: Schubert G (ed) Treatise on geophysics, 2nd edn. Elsevier, Oxford, pp 105–144. https://doi.org/10.1016/B978-0-444-53802-4.00156-1
Kasting JF (1988) Runaway and moist greenhouse atmospheres and the evolution of Earth and Venus. Icarus 74(3):472–494. https://doi.org/10.1016/0019-1035(88)90116-9
Kasting JF (1990) Bolide impacts and the oxidation state of carbon in the Earth's early atmosphere. Orig Life Evol Biosph 20(3):199–231. https://doi.org/10.1007/BF01808105
Kasting JF (1993) Earth's early atmosphere. Science 259(5097):920–926. https://doi.org/10.1126/science.11536547
Kasting JF (2013) What caused the rise of atmospheric O_2? Chem Geol 362:13–25. https://doi.org/10.1016/j.chemgeo.2013.05.039
Kasting JF (2014) 6.6 - Modeling the archean atmosphere and climate. In: Holland HD, Turekian KK (eds) Treatise on geochemistry, 2nd edn. Elsevier, Oxford, pp 157–175. https://doi.org/10.1016/B978-0-08-095975-7.01306-1
Kasting JF (2019) The Goldilocks planet? How silicate weathering maintains Earth "just right". Elements 15(4):235–240. https://doi.org/10.2138/gselements.15.4.235
Kasting JF, Catling D (2003) Evolution of a habitable planet. Annu Rev Astron Astrophys 41(1):429–463. https://doi.org/10.1146/annurev.astro.41.071601.170049
Kasting JF, Pollack JB (1983) Loss of water from Venus. I. Hydrodynamic escape of hydrogen. Icarus 53(3):479–508. https://doi.org/10.1016/0019-1035(83)90212-9
Kasting JF, Zahnle KJ, Walker JCG (1983) Photochemistry of methane in the Earth's early atmosphere. Precambrian Res 20(2):121–148. https://doi.org/10.1016/0301-9268(83)90069-4
Kasting JF, Eggler DH, Raeburn SP (1993a) Mantle redox evolution and the oxidation state of the archean atmosphere. J Geol 101(2):245–257. https://doi.org/10.1086/648219
Kasting JF, Whitmire DP, Reynolds RT (1993b) Habitable zones around main sequence stars. Icarus 101(1):108–128. https://doi.org/10.1006/icar.1993.1010
Katyal N, Ortenzi G, Lee Grenfell J, Noack L, Sohl F, Godolt M, García Muñoz A, Schreier F, Wunderlich F, Rauer H (2020) Effect of mantle oxidation state and escape upon the evolution of Earth's magma ocean atmosphere. Astron Astrophys 643:A81. https://doi.org/10.1051/0004-6361/202038779
Kaula WM (1979) Thermal evolution of Earth and Moon growing by planetesimal impacts. J Geophys Res, Solid Earth 84:999–1008. https://doi.org/10.1029/JB084iB03p00999
Ke Y, Solomatov VS (2006) Early transient superplumes and the origin of the Martian crustal dichotomy. J Geophys Res, Planets 111(E10). https://doi.org/10.1029/2005JE002631
Ke Y, Solomatov VS (2009) Coupled core-mantle thermal evolution of early Mars. J Geophys Res, Planets 114(E7). https://doi.org/10.1029/2008JE003291
Kennedy GM, Kenyon SJ (2008) Planet formation around stars of various masses: the snow line and the frequency of giant planets. Astrophys J 673(1):502. https://doi.org/10.1086/524130
Keppler H, Bolfan-Casanova N (2006) Thermodynamics of water solubility and partitioning. Rev Mineral Geochem 62(1):193–230. https://doi.org/10.2138/rmg.2006.62.9
Keppler H, Golabek G (2019) Graphite floatation on a magma ocean and the fate of carbon during core formation. Geochem Perspect Lett 11:12–17. https://doi.org/10.7185/geochemlet.1918

Khan A, Sossi PA, Liebske C, Rivoldini A, Giardini D (2022) Geophysical and cosmochemical evidence for a volatile-rich Mars. Earth Planet Sci Lett 578:117330. https://doi.org/10.1016/j.epsl.2021.117330
Kiefer WS, Richards MA, Hager BH, Bills BG (1986) A dynamic model of Venus's gravity field. Geophys Res Lett 13(1):14–17. https://doi.org/10.1029/GL013i001p00014
Kiehl JT, Trenberth KE (1997) Earth's annual global mean energy budget. Bull Am Meteorol Soc 78(2):197–208. https://doi.org/10.1175/1520-0477(1997)078<0197:EAGMEB>2.0.CO;2
Kislyakova K, Noack L (2020) Electromagnetic induction heating as a driver of volcanic activity on massive rocky planets. Astron Astrophys 636:L10. https://doi.org/10.1051/0004-6361/202037924
Kislyakova KG, Noack L, Johnstone CP, Zaitsev VV, Fossati L, Lammer H, Khodachenko ML, Odert P, Güdel M (2017) Magma oceans and enhanced volcanism on TRAPPIST-1 planets due to induction heating. Nat Astron 1(12):878–885. https://doi.org/10.1038/s41550-017-0284-0
Kleine T, Walker RJ (2017) Tungsten isotopes in planets. Annu Rev Earth Planet Sci 45(1):389–417. https://doi.org/10.1146/annurev-earth-063016-020037
Kleine T, Münker C, Mezger K, Palme H (2002) Rapid accretion and early core formation on asteroids and the terrestrial planets from Hf–W chronometry. Nature 418(6901):952–955. https://doi.org/10.1038/nature00982
Kleine T, Touboul M, Bourdon B, Nimmo F, Mezger K, Palme H, Jacobsen SB, Yin QZ, Halliday AN (2009) Hf–W chronology of the accretion and early evolution of asteroids and terrestrial planets. Geochim Cosmochim Acta 73(17):5150–5188. https://doi.org/10.1016/j.gca.2008.11.047
Kokubo E, Ida S (1996) On runaway growth of planetesimals. Icarus 123(1):180–191. https://doi.org/10.1006/icar.1996.0148
Kokubo E, Ida S (1998) Oligarchic growth of protoplanets. Icarus 131(1):171–178. https://doi.org/10.1006/icar.1997.5840
Kokubo E, Ida S (2000) Formation of protoplanets from planetesimals in the solar nebula. Icarus 143(1):15–27. https://doi.org/10.1006/icar.1999.6237
Kono Y (2018) Chap. 10 - Viscosity measurement. In: Kono Y, Sanloup C (eds) Magmas under pressure. Elsevier, Amsterdam, pp 261–280. https://doi.org/10.1016/B978-0-12-811301-1.00010-1
Kopp G, Lean JL (2011) A new, lower value of total solar irradiance: Evidence and climate significance. Geophys Res Lett 38(1). https://doi.org/10.1029/2010GL045777
Kopparapu RK, Ramirez R, Kasting JF, Eymet V, Robinson TD, Mahadevan S, Terrien RC, Domagal-Goldman S, Meadows V, Deshpande R (2013) Habitable zones around main-sequence stars: new estimates. Astrophys J 770(1). https://doi.org/10.1088/0004-637X/770/1/82
Korenaga J (2011) Thermal evolution with a hydrating mantle and the initiation of plate tectonics in the early Earth. J Geophys Res, Solid Earth 116(12):1–20. https://doi.org/10.1029/2011JB008410
Korenaga J (2017) On the extent of mantle hydration caused by plate bending. Earth Planet Sci Lett 457:1–9. https://doi.org/10.1016/j.epsl.2016.10.011
Korenaga J, Planavsky NJ, Evans DA (2017) Global water cycle and the coevolution of the Earth's interior and surface environment. Philos Trans R Soc A, Math Phys Eng Sci 375(2094). https://doi.org/10.1098/rsta.2015.0393
Kortenkamp SJ, Wetherill GW, Inaba S (2001) Runaway growth of planetary embryos facilitated by massive bodies in a protoplanetary disk. Science 293(5532):1127–1129. https://doi.org/10.1126/science.1062391
Kral Q, Matrà L, Wyatt MC, Kennedy GM (2017) Predictions for the secondary CO, C and O gas content of debris discs from the destruction of volatile-rich planetesimals. Mon Not R Astron Soc 469(1):521–550. https://doi.org/10.1093/mnras/stx730
Kral Q, Davoult J, Charnay B (2020) Formation of secondary atmospheres on terrestrial planets by late disk accretion. Nat Astron 4(8):769–775. https://doi.org/10.1038/s41550-020-1050-2
Krishnamurti R, Howard LN (1981) Large-scale flow generation in turbulent convection. Proc Natl Acad Sci. https://doi.org/10.1073/pnas.78.4.1981
Krissansen-Totton J, Fortney JJ, Nimmo F (2021) Was Venus ever habitable? Constraints from a coupled interior–atmosphere–redox evolution model. Planet Sci. J. 2(5):216. https://doi.org/10.3847/psj/ac2580
Krot AN, Keil K, Scott ERD, Goodrich CA, Weisberg MK (2014) 1.1 - Classification of meteorites and their genetic relationships. In: Holland HD, Turekian KK (eds) Treatise on geochemistry, 2nd edn. Elsevier, Oxford, pp 1–63. https://doi.org/10.1016/B978-0-08-095975-7.00102-9
Kruijer TS, Burkhardt C, Budde G, Kleine T (2017) Age of Jupiter inferred from the distinct genetics and formation times of meteorites. Proc Natl Acad Sci 114(26):6712–6716. https://doi.org/10.1073/pnas.1704461114
Kruijer TS, Kleine T, Borg LE (2020) The great isotopic dichotomy of the early Solar System. Nat Astron 4(1):32–40. https://doi.org/10.1038/s41550-019-0959-9
Kuhn WR, Atreya SK (1979) Ammonia photolysis and the greenhouse effect in the primordial atmosphere of the Earth. Icarus 37(1):207–213. https://doi.org/10.1016/0019-1035(79)90126-X

Kuramoto K, Matsui T (1996) Partitioning of H and C between the mantle and core during the core formation in the Earth: its implications for the atmospheric evolution and redox state of early mantle. J Geophys Res, Planets 101(E6):14909–14932. https://doi.org/10.1029/96JE00940

Kuramoto K, Umemoto T, Ishiwatari M (2013) Effective hydrodynamic hydrogen escape from an early Earth atmosphere inferred from high-accuracy numerical simulation. Earth Planet Sci Lett 375:312–318. https://doi.org/10.1016/j.epsl.2013.05.050

Kurosawa K, Sugita S, Ishibashi K, Hasegawa S, Sekine Y, Ogawa NO, Kadono T, Ohno S, Ohkouchi N, Nagaoka Y Matsui T (2013) Hydrogen cyanide production due to mid-size impacts in a redox-neutral N2-rich atmosphere. Orig Life Evol Biosph 43(3):221–245. https://doi.org/10.1007/s11084-013-9339-0

Labrosse S, Hernlund JW, Coltice N (2007) A crystallizing dense magma ocean at the base of the Earth's mantle. Nature 450(7171):866–869. https://doi.org/10.1038/nature06355

Lago B, Cazenave A (1979) Possible dynamical evolution of the rotation of Venus since formation. Moon Planets 21(2):127–154. https://doi.org/10.1007/BF00897084

Lambrechts M, Johansen A (2014) Forming the cores of giant planets from the radial pebble flux in protoplanetary discs. Astron Astrophys 572:A107. https://doi.org/10.1051/0004-6361/201424343

Lammer H (2013) Origin and evolution of planetary atmospheres. Springer, Berlin. https://doi.org/10.1007/978-3-642-32087-3

Lammer H, Zerkle AL, Gebauer S, Tosi N, Noack L, Scherf M, Pilat-Lohinger E, Güdel M, Grenfell JL, Godolt M, Nikolaou A (2018) Origin and evolution of the atmospheres of early Venus, Earth and Mars. Astron. Astrophys. Rev. 26:2. https://doi.org/10.1007/s00159-018-0108-y

Lammer H, Brasser R, Johansen A, Scherf M, Leitzinger M (2020a) Formation of Venus, Earth and Mars: constrained by isotopes. Space Sci Rev 217(1):7. https://doi.org/10.1007/s11214-020-00778-4

Lammer H, Leitzinger M, Scherf M, Odert P, Burger C, Kubyshkina D, Johnstone C, Maindl T, Schäfer CM, Güdel M, Tosi N, Nikolaou A, Marcq E, Erkaev NV, Noack L, Kislyakova KG, Fossati L, Pilat-Lohinger E, Ragossnig F, Dorfi EA (2020b) Constraining the early evolution of Venus and Earth through atmospheric Ar, Ne isotope and bulk K/U ratios. Icarus 339:113551. https://doi.org/10.1016/j.icarus.2019.113551

Landeau M, Olson P, Deguen R, Hirsh BH (2016) Core merging and stratification following giant impact. Nat Geosci 9(1). https://doi.org/10.1038/ngeo2808

Landeau M, Deguen R, Phillips D, Neufeld JA, Lherm V, Dalziel SB (2021) Metal-silicate mixing by large Earth-forming impacts. Earth Planet Sci Lett 564:116888. https://doi.org/10.1016/j.epsl.2021.116888

Lange RA (1994) Chap. 9. The effect of H_20, CO_2 and F on the density and viscosity of silicate melts. In: Carroll MR, Holloway JR (eds) Volatiles in magmas, vol 9. Mineralogical Society of America, Washington, pp 331–370. https://doi.org/10.1515/9781501509674-015

Lange MA, Ahrens TJ (1982) The evolution of an impact-generated atmosphere. Icarus 51(1):96–120. https://doi.org/10.1016/0019-1035(82)90031-8

Lasaga AC, Holland HD, Dwyer MJ (1971) Primordial oil slick. Science 174(4004):53–55. https://doi.org/10.1126/science.174.4004.53

Lebrun T, Massol H, ChassefièRe E, Davaille A, Marcq E, Sarda P, Leblanc F, Brandeis G (2013) Thermal evolution of an early magma ocean in interaction with the atmosphere. J Geophys Res, Planets 118(6):1155–1176. https://doi.org/10.1002/jgre.20068

Lecar M, Podolak M, Sasselov D, Chiang E (2006) On the location of the snow line in a protoplanetary disk. Astrophys J 640(2):1115–1118. https://doi.org/10.1086/500287

Leconte J, Forget F, Charnay B, Wordsworth R, Pottier A (2013) Increased insolation threshold for runaway greenhouse processes on Earth-like planets. Nature 504(7479):268. https://doi.org/10.1038/nature12827

Leconte J, Forget F, Charnay B, Wordsworth R, Selsis F, Millour E, Spiga A (2013) 3D climate modeling of close-in land planets: circulation patterns, climate moist bistability, and habitability. Astron Astrophys 554:A69. https://doi.org/10.1051/0004-6361/201321042

Leconte J, Wu H, Menou K, Murray N (2015) Asynchronous rotation of Earth-mass planets in the habitable zone of lower-mass stars. Science 347(6222):632–635. https://doi.org/10.1126/science.1258686

Lécuyer C, Ricard Y (1999) Long-term fluxes and budget of ferric iron: implication for the redox states of the Earth's mantle and atmosphere. Earth Planet Sci Lett 165(2):197–211. https://doi.org/10.1016/S0012-821X(98)00267-2

Lee DC, Halliday AN (1995) Hafnium–tungsten chronometry and the timing of terrestrial core formation. Nature 378(6559):771–774. https://doi.org/10.1038/378771a0

Lee DC, Halliday AN (1997) Core formation on Mars and differentiated asteroids. Nature 388(6645):854–857. https://doi.org/10.1038/42206

Lee T, Papanastassiou DA, Wasserburg GJ (1976) Demonstration of ^{26}Mg excess in Allende and evidence for ^{26}Al. Geophys Res Lett 3(1):41–44. https://doi.org/10.1029/GL003i001p00041

Lee CTA, Brandon AD, Norman M (2003) Vanadium in peridotites as a proxy for paleo-fO_2 during partial melting: prospects, limitations, and implications. Geochim Cosmochim Acta 67(16):3045–3064. https://doi.org/10.1016/S0016-7037(03)00268-0

Leighton PA, Steiner AB (1936) The photochemical decomposition of methane. J Am Chem Soc 58(9):1823. https://doi.org/10.1021/ja01300a512

Lejeune AM, Richet P (1995) Rheology of crystal-bearing silicate melts: an experimental study at high viscosities. J Geophys Res, Solid Earth 100(B3):4215–4229. https://doi.org/10.1029/94JB02985

Lesher CE, Spera FJ (2015) Chap. 5 - Thermodynamic and transport properties of silicate melts and magma. In: Sigurdsson H (ed) The encyclopedia of volcanoes, 2nd edn. Academic Press, Amsterdam, pp 113–141. https://doi.org/10.1016/B978-0-12-385938-9.00005-5

Levison HF, Kretke KA, Duncan MJ (2015) Growing the gas-giant planets by the gradual accumulation of pebbles. Nature 524(7565):322–324. https://doi.org/10.1038/nature14675

Li J, Agee CB (1996) Geochemistry of mantle-core differentiation at high pressure. Nature 381(6584):686–689. https://doi.org/10.1038/381686a0

Li ZXA, Lee CTA (2004) The constancy of upper mantle fO_2 through time inferred from V/Sc ratios in basalts. Earth Planet Sci Lett 228(3):483–493. https://doi.org/10.1016/j.epsl.2004.10.006

Li Y, Dasgupta R, Tsuno K, Monteleone B, Shimizu N (2016) Carbon and sulfur budget of the silicate Earth explained by accretion of differentiated planetary embryos. Nat Geosci. https://doi.org/10.1038/ngeo2801

Li Y, Vočadlo L, Sun T, Brodholt JP (2020) The Earth's core as a reservoir of water. Nat Geosci 13(6):453–458. https://doi.org/10.1038/s41561-020-0578-1

Libourel G, Marty B, Humbert F (2003) Nitrogen solubility in basaltic melt. Part I. Effect of oxygen fugacity. Geochim Cosmochim Acta 67(21):4123–4135. https://doi.org/10.1016/S0016-7037(03)00259-X

Lichtenberg T, Golabek G, Burn R, Meyer M, Alibert Y, Gerya T, Mordasini C (2019) A water budget dichotomy of rocky protoplanets from 26al-heating. Nat Astron 307. https://doi.org/10.1038/s41550-018-0688-5

Lichtenberg T, Bower DJ, Hammond M, Boukrouche R, Sanan P, Tsai SM, Pierrehumbert RT (2021) Vertically resolved magma ocean–protoatmosphere evolution: H_2, H_2O, CO_2, CH_4, CO, O_2, and N_2 as primary absorbers. J Geophys Res, Planets 126(2):e2020JE006711. https://doi.org/10.1029/2020JE006711

Lichtenberg T, Drążkowska J, Schönbächler M, Golabek GJ, Hands TO (2021b) Bifurcation of planetary building blocks during Solar System formation. Science 371(6527):365–370. https://doi.org/10.1126/science.abb3091

Liggins P, Shorttle O, Rimmer PB (2020) Can volcanism build hydrogen-rich early atmospheres? Earth Planet Sci Lett 550:116546. https://doi.org/10.1016/j.epsl.2020.116546

Lin Y, van Westrenen W, Mao HK (2021) Oxygen controls on magmatism in rocky exoplanets. Proc Natl Acad Sci 118(45). https://doi.org/10.1073/pnas.2110427118. https://www.pnas.org/content/118/45/e2110427118

Litasov KD, Ohtani E (2007) Effect of water on the phase relations in Earth's mantle and deep water cycle. In: Ohtani E (ed) Special paper of the geological society of America, vol 421. Geol. Soc. Am., Boulder, pp 115–156. https://doi.org/10.1130/2007.2421(08)

Liu B, Johansen A, Lambrechts M, Bizzarro M, Haugbølle T (2022) Natural separation of two primordial planetary reservoirs in an expanding solar protoplanetary disk. Sci Adv 8(16):eabm3045. https://doi.org/10.1126/sciadv.abm3045

Liu B, Raymond SN, Jacobson SA (2022b) Early solar system instability triggered by dispersal of the gaseous disk. Nature 604(7907):643–646. https://doi.org/10.1038/s41586-022-04535-1

Lugaro M, Ott U, Kereszturi Á (2018) Radioactive nuclei from cosmochronology to habitability. Prog Part Nucl Phys 102:1–47. https://doi.org/10.1016/j.ppnp.2018.05.002

Luger R, Barnes R (2015) Extreme water loss and abiotic O_2 buildup on planets throughout the habitable zones of M dwarfs. Astrobiology 15(2):119–143. https://doi.org/10.1089/ast.2014.1231

Lugmair GW, Shukolyukov A (1998) Early solar system timescales according to 53Mn-53Cr systematics. Geochim Cosmochim Acta 62(16):2863–2886. https://doi.org/10.1016/S0016-7037(98)00189-6

Lupu RE, Zahnle K, Marley MS, Schaefer L, Fegley B, Morley C, Cahoy K, Freedman R, Fortney JJ (2014) The atmospheres of earthlike planets after giant impact events. Astrophys J 784(1):27. https://doi.org/10.1088/0004-637X/784/1/27

Maas C, Hansen U (2015) Effects of Earth's rotation on the early differentiation of a terrestrial magma ocean. J Geophys Res, Solid Earth 120(11):7508–7525. https://doi.org/10.1002/2015JB012053

Maas C, Hansen U (2019) Dynamics of a terrestrial magma ocean under planetary rotation: a study in spherical geometry. Earth Planet Sci Lett 513:81–94. https://doi.org/10.1016/j.epsl.2019.02.016

Maas C, Manske L, Wünnemann K, Hansen U (2021) On the fate of impact-delivered metal in a terrestrial magma ocean. Earth Planet Sci Lett 554:116680. https://doi.org/10.1016/j.epsl.2020.116680

Mackwell SJ, Zimmerman ME, Kohlstedt DL (1998) High-temperature deformation of dry diabase with application to tectonics on Venus. J Geophys Res, Solid Earth 103(B1):975–984. https://doi.org/10.1029/97JB02671

Malavergne V, Bureau H, Raepsaet C, Gaillard F, Poncet M, Surblé S, Sifré D, Shcheka S, Fourdrin C, Deldicque D, Khodja H (2019) Experimental constraints on the fate of H and C during planetary core-mantle differentiation. Implications for the Earth. Icarus 321:473–485. https://doi.org/10.1016/j.icarus.2018.11.027

Malkus WVR (1954) Discrete transitions in turbulent convection. Proc R Soc Lond, Ser A, Math Phys Eng Sci 225(1161):185–195. https://doi.org/10.1098/rspa.1954.0196

Mallmann G, O'Neill HSC (2009) The crystal/melt partitioning of V during mantle melting as a function of oxygen fugacity compared with some other elements (Al, P, Ca, Sc, Ti, Cr, Fe, Ga, Y, Zr and Nb). J Petrol 50(9):1765–1794. https://doi.org/10.1093/petrology/egp053

Mao HK, Bell PM (1977) Disproportionation equilibrium in iron-bearing systems at pressures above 100 Kbar with applications to chemistry of the Earth's mantle. In: Saxena SK, Bhattacharji S, Annersten H, Stephansson O (eds) Energetics of geological processes. Springer, Berlin, pp 236–249. https://doi.org/10.1007/978-3-642-86574-9_12

Marcq E, Salvador A, Massol H, Davaille A (2017) Thermal radiation of magma ocean planets using a 1-D radiative-convective model of H_2O-CO_2 atmospheres. J Geophys Res, Planets 122(7):1539–1553. https://doi.org/10.1002/2016JE005224

Margot JL, Campbell DB, Giorgini JD, Jao JS, Snedeker LG, Ghigo FD, Bonsall A (2021) Spin state and moment of inertia of Venus. Nat Astron 5(7):676–683. https://doi.org/10.1038/s41550-021-01339-7

Marsh BD (1981) On the crystallinity, probability of occurrence, and rheology of lava and magma. Contrib Mineral Petrol 78(1):85–98. https://doi.org/10.1007/BF00371146

Martin RG, Livio M (2012) On the evolution of the snow line in protoplanetary discs. Mon Not R Astron Soc Lett 425(1):L6–L9. https://doi.org/10.1111/j.1745-3933.2012.01290.x

Marty B (2012) The origins and concentrations of water, carbon, nitrogen and noble gases on Earth. Earth Planet Sci Lett 313–314:56–66. https://doi.org/10.1016/j.epsl.2011.10.040

Marty B, Yokochi R (2006) Water in the early Earth. Rev Mineral Geochem 62(1):421–450. https://doi.org/10.2138/rmg.2006.62.18

Marty B, Avice G, Sano Y, Altwegg K, Balsiger H, Hässig M, Morbidelli A, Mousis O, Rubin M (2016) Origins of volatile elements (H, C, N, noble gases) on Earth and Mars in light of recent results from the Rosetta cometary mission. Earth Planet Sci Lett 441:91–102. https://doi.org/10.1016/j.epsl.2016.02.031

Marty B, Altwegg K, Balsiger H, Bar-Nun A, Bekaert DV, Berthelier JJ, Bieler A, Briois C, Calmonte U, Combi M, De Keyser J, Fiethe B, Fuselier SA, Gasc S, Gombosi TI, Hansen KC, Hässig M, Jäckel A, Kopp E, Korth A, Le Roy L, Mall U, Mousis O, Rème H, Owen T, Rubin M, Sémon T, Tzou CY, Waite JH, Wurz P (2017) Xenon isotopes in 67P/Churyumov-Gerasimenko show that comets contributed to Earth's atmosphere. Science 356(6342):1069–1072. https://doi.org/10.1126/science.aal3496

Massol H, Hamano K, Tian F, Ikoma M, Abe Y, Chassefière E, Davaille A, Genda H, Güdel M, Hori Y, Leblanc F, Marcq E, Sarda P, Shematovich VI, Stökl A, Lammer H (2016) Formation and evolution of protoatmospheres. Space Sci Rev 205:153–211. https://doi.org/10.1007/s11214-016-0280-1

Mathez EA (1984) Influence of degassing on oxidation states of basaltic magmas. Nature 310(5976):371–375. https://doi.org/10.1038/310371a0

Matrà L, MacGregor MA, Kalas P, Wyatt MC, Kennedy GM, Wilner DJ, Duchene G, Hughes AM, Pan M, Shannon A, Clampin M, Fitzgerald MP, Graham JR, Holland WS, Panić O, Su KYL (2017) Detection of exocometary CO within the 440 Myr old fomalhaut belt: a similar CO + CO_2 ice abundance in exocomets and solar system comets. Astrophys J 842(1):9. https://doi.org/10.3847/1538-4357/aa71b4

Matrà L, Öberg KI, Wilner DJ, Olofsson J, Bayo A (2019) On the ubiquity and stellar luminosity dependence of exocometary CO gas: detection around M dwarf TWA 7. Astron J 157(3):117. https://doi.org/10.3847/1538-3881/aaff5b

Matsui T, Abe Y (1984) The formation of an impact-generated H_2O atmosphere and its implications for the early thermal history of the Earth. In: Lunar and planetary science XV, pp 517–518. https://ui.adsabs.harvard.edu/abs/1984LPI....15..517M

Matsui T, Abe Y (1986a) Formation of a 'magma ocean' on the terrestrial planets due to the blanketing effect of an impact-induced atmosphere. Earth Moon Planets 34(3):223–230. https://doi.org/10.1007/BF00145081

Matsui T, Abe Y (1986b) Impact-induced atmospheres and oceans on Earth and Venus. Nature 322(6079):526–528. https://doi.org/10.1038/322526a0

Matsui T, Abe Y (1986c) Origin of the Moon and its early thermal evolution. In: Hartmann W, Phillips R, Taylor G (eds) Origin of the Moon, Lunar and Planetary Institute, pp 453–468. https://ui.adsabs.harvard.edu/abs/1986ormo.conf..453M/abstract

Matthews CN, Minard RD (2006) Hydrogen cyanide polymers, comets and the origin of life. Faraday Discuss 133:393–401. https://doi.org/10.1039/B516791D
Maurice M, Tosi N, Samuel H, Plesa AC, Hüttig C, Breuer D (2017) Onset of solid-state mantle convection and mixing during magma ocean solidification. J Geophys Res, Planets 122(3):577–598. https://doi.org/10.1002/2016JE005250
Maurice M, Dasgupta R, Hassanzadeh P (2023) Redox evolution of the crystallizing terrestrial magma ocean and its influence on the outgassed atmosphere. Planet Sci. J. 4(2):31. https://doi.org/10.3847/PSJ/acb2ca
McCammon C (1997) Perovskite as a possible sink for ferric iron in the lower mantle. Nature 387(6634):694–696. https://doi.org/10.1038/42685
McCammon C (2005a) The paradox of mantle redox. Science 308(5723):807–808. https://doi.org/10.1126/science.1110532
McCammon CA (2005b) Mantle oxidation state and oxygen fugacity: constraints on mantle chemistry, structure, and dynamics. In: Earth's deep mantle: structure, composition, and evolution. Am. Geophys. Union, Washington, pp 219–240. https://doi.org/10.1029/160GM14
McCollom TM (2013) Miller-urey and beyond: what have we learned about prebiotic organic synthesis reactions in the past 60 years? Annu Rev Earth Planet Sci 41(1):207–229. https://doi.org/10.1146/annurev-earth-040610-133457
McCord TB (1968) The loss of retrograde satellites in the solar system. J Geophys Res 73(4):1497–1500. https://doi.org/10.1029/JB073i004p01497
McKenzie D (2011) Compaction and crystallization in magma chambers: towards a model of the skaergaard intrusion. J Petrol 52(5):905–930. https://doi.org/10.1093/petrology/egr009
McKinnon WB, Zahnle KJ, Ivanov BA, Melosh HJ (1997) Cratering on Venus: models and observations. In: Bougher SW, Hunten DM, Phillips RJ (eds) Venus II: geology, geophysics, atmosphere, and solar wind environment, p 969
Meech K, Raymond S (2020) Origin of Earth's water: sources and constraints. In: Meadows VS, Arney GN, Schmidt BE, Des Marais DJ (eds) Planetary astrobiology. University of Arizona Press, Tucson, p 325. https://doi.org/10.2458/azu_uapress_9780816540068
Mei S, Kohlstedt DL (2000) Influence of water on plastic deformation of olivine aggregates: 2. Dislocation creep regime. J Geophys Res, Solid Earth 105(B9):21471–21481. https://doi.org/10.1029/2000JB900180
Melosh HJ (1990) Giant impacts and the thermal state of the early Earth. In: Newsom HE, Jones JH (eds) Origin of the Earth, Lunar and Planetary Institute, pp 69–83
Melosh H, Vickery A (1989) Impact erosion of the primordial atmosphere of Mars. Nature 338(6215):487–489
Menou K (2013) Water-trapped worlds. Astrophys J 774(1):51. https://doi.org/10.1088/0004-637X/774/1/51
Merk R, Breuer D, Spohn T (2002) Numerical modeling of $^{2}6$Al-induced radioactive melting of asteroids considering accretion. Icarus https://doi.org/10.1006/icar.2002.6872
Miller SL (1953) A production of amino acids under possible primitive Earth conditions. Science 117(3046):528–529. https://doi.org/10.1126/science.117.3046.528
Miller SL (1955) Production of some organic compounds under possible primitive Earth Conditions1. J Am Chem Soc 77(9):2351–2361. https://doi.org/10.1021/ja01614a001
Miller SL, Urey HC (1959) Organic compound synthesis on the primitive Earth. Science 130(3370):245–251. https://doi.org/10.1126/science.130.3370.245
Miyazaki Y, Korenaga J (2021) Inefficient Water Degassing Inhibits Ocean Formation on Rocky Planets: an Insight from Self-Consistent Mantle Degassing Models. Astrobiology. https://doi.org/10.1089/ast.2021.0126
Miyazaki Y, Korenaga J (2022) A wet heterogeneous mantle creates a habitable world in the Hadean. Nature 603(7899):86–90. https://doi.org/10.1038/s41586-021-04371-9
Miyazaki A, Hiyagon H, Sugiura N, Hirose K, Takahashi E (2004) Solubilities of nitrogen and noble gases in silicate melts under various oxygen fugacities: implications for the origin and degassing history of nitrogen and noble gases in the Earth. Geochim Cosmochim Acta 68(2):387–401. https://doi.org/10.1016/S0016-7037(03)00484-8
Modirrousta-Galian D, Korenaga J (2023) The three regimes of atmospheric evaporation for super-earths and sub-neptunes. Astrophys J 943(1):11. https://doi.org/10.3847/1538-4357/ac9d34
Mojzsis SJ, Brasser R, Kelly NM, Abramov O, Werner SC (2019) Onset of giant planet migration before 4480 million years ago. Astrophys J 881(1):44. https://doi.org/10.3847/1538-4357/ab2c03
Monteux J, Ricard Y, Coltice N, Dubuffet F, Ulvrova M (2009) A model of metal-silicate separation on growing planets. Earth Planet Sci Lett 287(3–4):353–362. https://doi.org/10.1016/j.epsl.2009.08.020
Moore G (2008) Interpreting H_2O and CO_2 contents in melt inclusions: constraints from solubility experiments and modeling. Rev Mineral Geochem 69:333–361. https://doi.org/10.2138/rmg.2008.69.9

Morbidelli A, Chambers J, Lunine JI, Petit JM, Robert F, Valsecchi GB, Cyr KE (2000) Source regions and timescales for the delivery of water to the Earth. Meteorit Planet Sci 35(6):1309–1320. https://doi.org/10.1111/j.1945-5100.2000.tb01518.x

Morbidelli A, Lunine JI, O'Brien DP, Raymond SN, Walsh KJ (2012) Building terrestrial planets. Annu Rev Earth Planet Sci 40:251–275. https://doi.org/10.1146/annurev-earth-042711-105319

Morbidelli A, Nesvorny D, Laurenz V, Marchi S, Rubie DC, Elkins-Tanton L, Wieczorek M, Jacobson S (2018) The timeline of the lunar bombardment: revisited. Icarus 305:262–276. https://doi.org/10.1016/j.icarus.2017.12.046

Morbidelli A, Baillié K, Batygin K, Charnoz S, Guillot T, Rubie DC, Kleine T (2022) Contemporary formation of early Solar System planetesimals at two distinct radial locations. Nat Astron 6(1):72–79. https://doi.org/10.1038/s41550-021-01517-7

Moroz VI, Ekonomov AP, Moshkin BE, Revercomb HE, Sromovsky LA, Schofield JT, Spänkuch D, Taylor FW, Tomasko MG (1985) Solar and thermal radiation in the Venus atmosphere. Adv Space Res 5(11):197–232. https://doi.org/10.1016/0273-1177(85)90202-9

Mosenfelder JL, Asimow PD, Ahrens TJ (2007) Thermodynamic properties of Mg_2SiO_4 liquid at ultra-high pressures from shock measurements to 200 GPa on forsterite and wadsleyite. J Geophys Res, Solid Earth 112(B6). https://doi.org/10.1029/2006JB004364

Nakajima M, Stevenson DJ (2015) Melting and mixing states of the Earth's mantle after the Moon-forming impact. Earth Planet Sci Lett 427:286–295. https://doi.org/10.1016/j.epsl.2015.06.023

Nakajima S, Hayashi YY, Abe Y (1992) A study on the "runaway greenhouse effect" with a one-dimensional radiative–convective equilibrium model. J Atmos Sci 49(23):2256–2266. https://doi.org/10.1175/1520-0469(1992)049<2256:ASOTGE>2.0.CO;2

Nakajima M, Golabek GJ, Wünnemann K, Rubie DC, Burger C, Melosh HJ, Jacobson SA, Manske L, Hull SD (2021) Scaling laws for the geometry of an impact-induced magma ocean. Earth Planet Sci Lett 568:116983. https://doi.org/10.1016/j.epsl.2021.116983

Nesvorný D (2018) Dynamical evolution of the early solar system. Annu Rev Astron Astrophys 56(1):137–174. https://doi.org/10.1146/annurev-astro-081817-052028

Nesvorný D, Vokrouhlický D, Bottke WF, Levison HF (2018) Evidence for very early migration of the Solar System planets from the Patroclus–Menoetius binary Jupiter Trojan. Nat Astron 2(11):878–882. https://doi.org/10.1038/s41550-018-0564-3

Newman WI, Symbalisty EM, Ahrens TJ, Jones EM (1999) Impact erosion of planetary atmospheres: some surprising results. Icarus 138(2):224–240

Newsom HE, Ross Taylor S (1989) Geochemical implications of the formation of the moon by a single giant impact. Nature 338(6210):29–34. https://doi.org/10.1038/338029a0

Ni H, Zhang L, Guo X (2016) Water and partial melting of Earth's mantle. Sci China Earth Sci 59(4):720–730. https://doi.org/10.1007/s11430-015-5254-8

Nicklas RW, Puchtel IS, Ash RD (2018) Redox state of the Archean mantle: evidence from V partitioning in 3.5–2.4 Ga komatiites. Geochim Cosmochim Acta 222:447–466. https://doi.org/10.1016/j.gca.2017.11.002

Nikolaou A, Katyal N, Tosi N, Godolt M, Lee Grenfell J, Rauer H (2019) What factors affect the duration and outgassing of the terrestrial magma ocean? Astrophys J 875:11. https://doi.org/10.3847/1538-4357/ab08ed

Nimmo F, Kleine T (2015) Early differentiation and core formation. In: Badro J, Walter M (eds) The early Earth: accretion and differentiation. AGU, Washington DC, pp 83–102. https://doi.org/10.1002/9781118860359.ch5

Noack L, Godolt M, Von Paris P, Plesa AC, Stracke B, Breuer D, Rauer H (2014) Can the interior structure influence the habitability of a rocky planet? Planet Space Sci 98:14–29. https://doi.org/10.1016/j.pss.2014.01.003

Noack L, Kislyakova KG, Johnstone CP, Güdel M, Fossati L (2021) Interior heating and outgassing of proxima centauri b: identifying critical parameters. Astron Astrophys 651:1–17. https://doi.org/10.1051/0004-6361/202040176

Noda S, Ishiwatari M, Nakajima K, Takahashi YO, Takehiro S, Onishi M, Hashimoto GL, Kuramoto K, Hayashi YY (2017) The circulation pattern and day-night heat transport in the atmosphere of a synchronously rotating aquaplanet: dependence on planetary rotation rate. Icarus 282:1–18. https://doi.org/10.1016/j.icarus.2016.09.004

Nomura R, Ozawa H, Tateno S, Hirose K, Hernlund J, Muto S, Ishii H, Hiraoka N (2011) Spin crossover and iron-rich silicate melt in the Earth/'s deep mantle. Nature 473(7346):199–202. https://doi.org/10.1038/nature09940

Nomura R, Hirose K, Uesugi K, Ohishi Y, Tsuchiyama A, Miyake A, Ueno Y (2014) Low core-mantle boundary temperature inferred from the solidus of pyrolite. Science 343(6170):522–525. https://doi.org/10.1126/science.1248186

Nyquist LE, Reese YD, Wiesmann H, Shih CY, Takeda H (2001) Live ^{53}Mn and ^{26}Al in an unique cumulate eucrite with very calcic feldspar (An∼ 98). Meteorit. Planet. Sci. Suppl. 36:A151–A152
Nyquist LE, Kleine T, Shih CY, Reese YD (2009) The distribution of short-lived radioisotopes in the early solar system and the chronology of asteroid accretion, differentiation, and secondary mineralization. Geochim Cosmochim Acta 73(17):5115–5136. https://doi.org/10.1016/j.gca.2008.12.031
O'Brien DP, Walsh KJ, Morbidelli A, Raymond SN, Mandell AM (2014) Water delivery and giant impacts in the 'Grand Tack' scenario. Icarus 239:74–84. https://doi.org/10.1016/j.icarus.2014.05.009
O'Brien DP, Izidoro A, Jacobson SA, Raymond SN, Rubie DC (2018) The delivery of water during terrestrial planet formation. Space Sci Rev 214(1):47. https://doi.org/10.1007/s11214-018-0475-8
Odert P, Lammer H, Erkaev N, Nikolaou A, Lichtenegger H, Johnstone C, Kislyakova K, Leitzinger M, Tosi N (2018) Escape and fractionation of volatiles and noble gases from Mars-sized planetary embryos and growing protoplanets. Icarus 307:327–346. https://doi.org/10.1016/j.icarus.2017.10.031
Ohtani E (2020) The role of water in Earth's mantle. Nat Sci Rev 7(1):224–232. https://doi.org/10.1093/nsr/nwz071
Okuchi T (1997) Hydrogen partitioning into Molten iron at high pressure: implications for Earth's core. Science 278(5344):1781–1784
Olson P, Sharp ZD (2018) Hydrogen and helium ingassing during terrestrial planet accretion. Earth Planet Sci Lett 498:418–426. https://doi.org/10.1016/j.epsl.2018.07.006
Olson PL, Sharp ZD (2019) Nebular atmosphere to magma ocean: a model for volatile capture during Earth accretion. Phys Earth Planet Inter 294. https://doi.org/10.1016/j.pepi.2019.106294
O'Neill H (1991) The origin of the moon and the early history of the Earth—a chemical model. Part 2: the Earth. Geochim Cosmochim Acta 55(4):1159–1172. https://doi.org/10.1016/0016-7037(91)90169-6
O'Neill C, Marchi S, Zhang S, Bottke W (2017) Impact-driven subduction on the Hadean Earth. Nat Geosci 10(10):793–797. https://doi.org/10.1038/ngeo3029
Ormel CW (2017) The emerging paradigm of pebble accretion. In: Pessah M, Gressel O (eds) Formation, evolution, and dynamics of young solar systems. Springer, Cham, pp 197–228. https://doi.org/10.1007/978-3-319-60609-5_7
Oro J, Miller SL, Lazcano A (1990) The origin and early evolution of life on Earth. Annu Rev Earth Planet Sci 18(1):317–356. https://doi.org/10.1146/annurev.ea.18.050190.001533
O'Rourke JG (2020) Venus: a thick basal magma ocean may exist today. Geophys Res Lett 47(4):e86126. https://doi.org/10.1029/2019GL086126
Ottonello G, Richet P, Papale P (2018) Bulk solubility and speciation of H_2O in silicate melts. Chem Geol 479:176–187. https://doi.org/10.1016/J.CHEMGEO.2018.01.008
Pahlevan K, Schaefer L, Hirschmann MM (2019) Hydrogen isotopic evidence for early oxidation of silicate Earth. Earth Planet Sci Lett 526:115770. https://doi.org/10.1016/j.epsl.2019.115770
Pan V, Holloway JR, Hervig RL (1991) The pressure and temperature dependence of carbon dioxide solubility in tholeiitic basalt melts. Geochim Cosmochim Acta 55(6):1587–1595. https://doi.org/10.1016/0016-7037(91)90130-W
Papale P (1997) Modeling of the solubility of a one-component H_2O or CO_2 fluid in silicate liquids. Contrib Mineral Petrol 126(3):237–251. https://doi.org/10.1007/s004100050247
Papale P (1999) Modeling of the solubility of a two-component $H_2O + CO_2$ fluid in silicate liquids. Am Mineral 84(4):477–492. https://doi.org/10.1007/s004100050247
Papale P, Moretti R, Barbato D (2006) The compositional dependence of the saturation surface of $H_2O + CO_2$ fluids in silicate melts. Chem Geol https://doi.org/10.1016/j.chemgeo.2006.01.013
Parfitt EA, Wilson L (2008) Fundamentals of physical volcanology. Blackwell, Malden. https://www.wiley.com/en-us/Fundamentals+of+Physical+Volcanology-p-9780632054435
Pasek M, Lauretta D (2008) Extraterrestrial flux of potentially prebiotic C, N, and P to the early Earth. Orig Life Evol Biosph 38(1):5–21. https://doi.org/10.1007/s11084-007-9110-5
Patočka V, Calzavarini E, Tosi N (2020) Settling of inertial particles in turbulent Rayleigh-Bénard convection. Phys Rev Fluids 5(11):114304. https://doi.org/10.1103/PhysRevFluids.5.114304
Patočka V, Tosi N, Calzavarini E (2022) Residence time of inertial particles in 3D thermal convection: implications for magma reservoirs. Earth Planet Sci Lett 591:117622. https://doi.org/10.1016/j.epsl.2022.117622
Pepin RO (1991) On the origin and early evolution of terrestrial planet atmospheres and meteoritic volatiles. Icarus 92(1):2–79. https://doi.org/10.1016/0019-1035(91)90036-S
Peslier AH, Schönbächler M, Busemann H, Karato SI (2017) Water in the Earth's interior: distribution and origin. Space Sci Rev 212(1–2):743–810. https://doi.org/10.1007/s11214-017-0387-z
Pham LBS, Karatekin Ö Dehant V (2011) Effects of impacts on the atmospheric evolution: comparison between Mars, Earth, and Venus. Planet Space Sci 59(10):1087–1092. https://doi.org/10.1016/j.pss.2010.11.010

Piani L, Marrocchi Y, Rigaudier T, Vacher LG, Thomassin D, Marty B (2020) Earth's water may have been inherited from material similar to enstatite chondrite meteorites. Science 369(6507):1110–1113. https://doi.org/10.1126/science.aba1948

Pierazzo E, Chyba CF (1999) Amino acid survival in large cometary impacts. Meteorit Planet Sci 34(6):909–918. https://doi.org/10.1111/j.1945-5100.1999.tb01409.x

Pierrehumbert RT (2010) Principles of planetary climate. Cambridge University Press, Cambridge. https://doi.org/10.1017/CBO9780511780783

Pierrehumbert R, Gaidos E (2011) Hydrogen greenhouse planets beyond the habitable zone. Astrophys J Lett 734(1):L13. https://doi.org/10.1088/2041-8205/734/1/L13

Pluriel W, Marcq E, Turbet M (2019) Modeling the albedo of Earth-like magma ocean planets with H_2O-CO_2 atmospheres. Icarus 317:583–590. https://doi.org/10.1016/j.icarus.2018.08.023. arXiv:1809.02036

Poirier JP (1994) Light elements in the Earth's outer core: a critical review. Phys Earth Planet Inter 85(3):319–337. https://doi.org/10.1016/0031-9201(94)90120-1

Pollack JB (1971) A nongrey calculation of the runaway greenhouse: implications for Venus' past and present. Icarus 14(3):295–306. https://doi.org/10.1016/0019-1035(71)90001-7

Prša A, Harmanec P, Torres G, Mamajek E, Asplund M, Capitaine N, Christensen-Dalsgaard J, Depagne É, Haberreiter M, Hekker S, Hilton J, Kopp G, Kostov V, Kurtz DW, Laskar J, Mason BD, Milone EF, Montgomery M, Richards M, Schmutz W, Schou J, Stewart SG (2016) Nominal values for selected solar and planetary quantities: IAU 2015 resolution B3. Astron J 152(2):41. https://doi.org/10.3847/0004-6256/152/2/41

Quintana EV, Barclay T, Borucki WJ, Rowe JF, Chambers JE (2016) The frequency of giant impacts on Earth-like worlds. Astrophys J 821(2):126. https://doi.org/10.3847/0004-637X/821/2/126

Quitté G, Birck JL, Allègre CJ (2000) 182Hf–182W systematics in eucrites: the puzzle of iron segregation in the early solar system. Earth Planet Sci Lett 184(1):83–94. https://doi.org/10.1016/S0012-821X(00)00303-4

Ramirez RM (2018) A more comprehensive habitable zone for finding life on other planets. Geosciences 8(280). https://doi.org/10.3390/geosciences8080280. https://www.mdpi.com/2076-3263/8/8/280

Ramirez RM, Kaltenegger L (2017) A volcanic hydrogen habitable zone. Astrophys J Lett 837(1):L4. https://doi.org/10.3847/2041-8213/aa60c8

Ramirez RM, Kaltenegger L (2018) A methane extension to the classical habitable zone. Astrophys J 858(2):72. https://doi.org/10.3847/1538-4357/aab8fa

Ramirez RM, Kopparapu R, Zugger ME, Robinson TD, Freedman R, Kasting JF (2014) Warming early Mars with CO_2 and H_2. Nat Geosci 7(1):59–63. https://doi.org/10.1038/ngeo2000

Ramirez RM, Abbot DS, Airapetian V, Fujii Y, Hamano K, Levi A, Robinson TD, Schaefer L, Wolf ET, Wordsworth RD (2018) The continued importance of habitability studies. In: National academies of sciences engineering and medicine. Exoplanet science strategy - white papers. National Academies Press. https://doi.org/10.48550/arXiv.1803.00215

Rasool SI de Bergh C (1970) The runaway greenhouse and the accumulation of CO_2 in the Venus atmosphere. Nature 226(5250):1037–1039. https://doi.org/10.1038/2261037a0

Raymond SN, Izidoro A (2017) Origin of water in the inner solar system: planetesimals scattered inward during Jupiter and Saturn's rapid gas accretion. Icarus 297:134–148. https://doi.org/10.1016/j.icarus.2017.06.030

Raymond SN, Izidoro A (2017b) The empty primordial asteroid belt. Sci Adv 3(9):e1701138. https://doi.org/10.1126/sciadv.1701138

Raymond SN, Morbidelli A (2014) The grand tack model: a critical review. In: Complex planetary systems. Proceedings of the international astronomical union, vol 310, pp 194–203. https://doi.org/10.1017/S1743921314008254. arXiv:1409.6340

Raymond SN, Morbidelli A (2022) Planet formation: key mechanisms and global models. In: Astrophysics and space science library, vol 466. Springer, Cham, pp 3–82. https://doi.org/10.1007/978-3-030-88124-5_1

Raymond SN, Nesvorný D (2022) Origin and dynamical evolution of the asteroid belt. In: Marchi S, Raymond CA, Russell CT (eds) Vesta and Ceres: insights from the Dawn Mission for the origin of the solar system. Cambridge planetary science. Cambridge University Press, Cambridge, pp 227–249. https://doi.org/10.1017/9781108856324.019

Raymond SN, Quinn T, Lunine JI (2004) Making other earths: dynamical simulations of terrestrial planet formation and water delivery. Icarus 168(1):1–17. https://doi.org/10.1016/j.icarus.2003.11.019

Raymond SN, Quinn T, Lunine JI (2006) High-resolution simulations of the final assembly of Earth-like planets I. Terrestrial accretion and dynamics. Icarus 183(2):265–282. https://doi.org/10.1016/j.icarus.2006.03.011

Raymond SN, O'Brien DP, Morbidelli A, Kaib NA (2009) Building the terrestrial planets: constrained accretion in the inner solar system. Icarus 203(2):644–662. https://doi.org/10.1016/j.icarus.2009.05.016

Raymond SN, Kokubo E, Morbidelli A, Morishima R, Walsh KJ (2014) Terrestrial planet formation at home and abroad. In: Protostars and planets VI. University of Arizona Press, Tucson, pp 595–618. https://doi.org/10.2458/azu_uapress_9780816531240-ch026

Raymond SN, Izidoro A, Morbidelli A (2020) Solar system formation in the context of extrasolar planets. In: Meadows VS, Arney GN, Schmidt BE, Des Marais DJ (eds) Planetary astrobiology. University of Arizona Press, Tucson, p 287. https://doi.org/10.2458/azu_uapress_9780816540068

Regenauer-Lieb K, Yuen DA, Branlund J (2001) The initiation of subduction: criticality by addition of water? Science 294(5542):578–580. https://doi.org/10.1126/science.1063891

Reufer A, Meier MMM, Benz W, Wieler R (2012) A hit-and-run giant impact scenario. Icarus 221(1):296–299. https://doi.org/10.1016/j.icarus.2012.07.021

Ribas I, Guinan EF, Güdel M, Audard M (2005) Evolution of the solar activity over time and effects on planetary atmospheres. I. High-energy irradiances (1–1700 Å). Astrophys J 622(1):680–694. https://doi.org/10.1086/427977

Ricard Y (2015) 7.02 - Physics of mantle convection. In: Schubert G (ed) Treatise on geophysics, 2nd edn. Elsevier, Oxford, pp 23–71. https://doi.org/10.1016/B978-0-444-53802-4.00127-5

Ricard Y, Šrámek O, Dubuffet F (2009) A multi-phase model of runaway core–mantle segregation in planetary embryos. Earth Planet Sci Lett 284(1):144–150. https://doi.org/10.1016/j.epsl.2009.04.021

Richards MA, Lenardic A (2018) The cathles parameter (Ct): a geodynamic definition of the asthenosphere and implications for the nature of plate tectonics. Geochem Geophys Geosyst 19(12):4858–4875. https://doi.org/10.1029/2018GC007664

Richards MA, Yang WS, Baumgardner JR, Bunge HP (2001) Role of a low-viscosity zone in stabilizing plate tectonics: Implications for comparative terrestrial planetology. Geochem Geophys Geosyst 2(8). https://doi.org/10.1029/2000GC000115

Righter K, Drake MJ (1997) Metal-silicate equilibrium in a homogeneously accreting Earth: new results for Re. Earth Planet Sci Lett 146(3):541–553. https://doi.org/10.1016/S0012-821X(96)00243-9

Righter K, Drake MJ (1999) Effect of water on metal–silicate partitioning of siderophile elements: a high pressure and temperature terrestrial magma ocean and core formation. Earth Planet Sci Lett 171(3):383–399. https://doi.org/10.1016/S0012-821X(99)00156-9

Righter K, Ghiorso MS (2012) Redox systematics of a magma ocean with variable pressure-temperature gradients and composition. Proc Natl Acad Sci 109(30):11955–11960. https://doi.org/10.1073/pnas.1202754109

Righter K, Drake MJ, Yaxley G (1997) Prediction of siderophile element metal-silicate partition coefficients to 20 GPa and 2800 °C: the effects of pressure, temperature, oxygen fugacity, and silicate and metallic melt compositions. Phys Earth Planet Inter 100(1):115–134. https://doi.org/10.1016/S0031-9201(96)03235-9

Robert F, Gautier D, Dubrulle B (2000) The solar system D/H ratio: observations and theories. Space Sci Rev 92(1):201–224. https://doi.org/10.1023/A:1005291127595

Robie RA, Hemingway BS, Fisher JR (1978) Thermodynamic properties of minerals and related substances at 298.15 K and 1 bar (10^5 pascals) pressure and at higher temperatures. https://doi.org/10.3133/b1452. Tech. Rep. http://pubs.er.usgs.gov/publication/b1452

Rolf T, Weller M, Gülcher A, Byrne P, O'Rourke JG, Herrick R, Bjonnes E, Davaille A, Ghail R, Gillmann C, Plesa AC, Smrekar S (2022) Dynamics and evolution of Venus' mantle through time. Space Sci Rev 218(8):70. https://doi.org/10.1007/s11214-022-00937-9

Rollinson H, Adetunji J, Lenaz D, Szilas K (2017) Archaean chromitites show constant Fe3+/ΣFe in Earth's asthenospheric mantle since 3.8 Ga. Lithos 282–283:316–325. https://doi.org/10.1016/j.lithos.2017.03.020

Rubie DC, Melosh HJ, Reid JE, Liebske C, Righter K (2003) Mechanisms of metal–silicate equilibration in the terrestrial magma ocean. Earth Planet Sci Lett 205(3):239–255. https://doi.org/10.1016/S0012-821X(02)01044-0

Rubie DC, Frost DJ, Mann U, Asahara Y, Nimmo F, Tsuno K, Kegler P, Holzheid A, Palme H (2011) Heterogeneous accretion, composition and core–mantle differentiation of the Earth. Earth Planet Sci Lett 301(1):31–42. https://doi.org/10.1016/j.epsl.2010.11.030

Rubie DC, Jacobson SA, Morbidelli A, O'Brien DP, Young ED, de Vries J, Nimmo F, Palme H, Frost DJ (2015) Accretion and differentiation of the terrestrial planets with implications for the compositions of early-formed Solar System bodies and accretion of water. Icarus 248:89–108. https://doi.org/10.1016/j.icarus.2014.10.015

Rubie DC, Nimmo F, Melosh HJ (2015b) 9.03 - Formation of the Earth's core. In: Schubert G (ed) Treatise on geophysics, 2nd edn. Elsevier, Oxford, pp 43–79. https://doi.org/10.1016/B978-0-444-53802-4.00154-8

Rubin AE, Fegley B, Brett R (1988) Oxidation state in chondrites. In: Kerridge JF, Matthews MS (eds) Meteorites and the early solar system. University of Arizona Press, Tucson, pp 488–511. https://ui.adsabs.harvard.edu/abs/1988mess.book..488R

Rufu R, Aharonson O, Perets HB (2017) A multiple-impact origin for the Moon. Nat Geosci 10. https://doi.org/10.1038/ngeo2866
Safronov VS (1972) Evolution of the protoplanetary cloud and formation of the Earth and planets. Keter Publishing House. https://www.semanticscholar.org/paper/Evolution-of-the-protoplanetary-cloud-and-formation-Safronov/97c82912840accc7096404cbea0b59d5f02d8c21
Safronov VS (1978) The heating of the Earth during its formation. Icarus 33(1):3–12. https://doi.org/10.1016/0019-1035(78)90019-2
Saito H, Kuramoto K (2017) Formation of a hybrid-type proto-atmosphere on Mars accreting in the solar nebula. Mon Not R Astron Soc 475(1):1274–1287. https://doi.org/10.1093/mnras/stx3176
Sakuraba H, Kurokawa H, Genda H (2019) Impact degassing and atmospheric erosion on Venus, Earth, and Mars during the late accretion. Icarus 317:48–58. https://doi.org/10.1016/J.ICARUS.2018.05.035
Sakuraba H, Kurokawa H, Genda H, Ohta K (2021) Numerous chondritic impactors and oxidized magma ocean set Earth's volatile depletion. Sci Rep 11(1):20894. https://doi.org/10.1038/s41598-021-99240-w
Salvador A, Samuel H (2023) Convective outgassing efficiency in planetary magma oceans: insights from computational fluid dynamics. Icarus 390:115265. https://doi.org/10.1016/j.icarus.2022.115265
Salvador A, Massol H, Davaille A, Marcq E, Sarda P, Chassefière E (2017) The relative influence of H_2O and CO_2 on the primitive surface conditions and evolution of rocky planets. J Geophys Res, Planets 122(7):1458–1486. https://doi.org/10.1002/2017JE005286
Samuel H, Tackley PJ, Evonuk M (2010) Heat partitioning in terrestrial planets during core formation by negative diapirism. Earth Planet Sci Lett 290(1):13–19. https://doi.org/10.1016/j.epsl.2009.11.050
Sasaki S, Nakazawa K (1986) Metal-silicate fractionation in the growing Earth: energy source for the terrestrial magma ocean. J Geophys Res, Solid Earth 91(B9):9231–9238. https://doi.org/10.1029/JB091iB09p09231
Sasaki S, Nakazawa K (1988) Origin of isotopic fractionation of terrestrial Xe: hydrodynamic fractionation during escape of the primordial H_2-He atmosphere. Earth Planet Sci Lett 89(3):323–334. https://doi.org/10.1016/0012-821X(88)90120-3
Sato M (1978) Oxygen fugacity of basaltic magmas and the role of gas-forming elements. Geophys Res Lett 5(6):447–449. https://doi.org/10.1029/GL005i006p00447
Sato T, Okuzumi S, Ida S (2016) On the water delivery to terrestrial embryos by ice pebble accretion. Astron Astrophys 589:A15. https://doi.org/10.1051/0004-6361/201527069
Savage PS, Moynier F, Boyet M (2022) Zinc isotope anomalies in primitive meteorites identify the outer solar system as an important source of Earth's volatile inventory. Icarus 386:115172. https://doi.org/10.1016/j.icarus.2022.115172
Saxena P, Killen RM, Airapetian V, Petro NE, Curran NM, Mandell AM (2019) Was the sun a slow rotator? Sodium and potassium constraints from the lunar regolith. Astrophys J Lett 876(1):L16. https://doi.org/10.3847/2041-8213/ab18fb
Scaillet B, Gaillard F (2011) Redox state of early magmas. Nature 480(7375):48–49. https://doi.org/10.1038/480048a
Schaefer L, Elkins-Tanton LT (2018) Magma oceans as a critical stage in the tectonic development of rocky planets. Philos Trans R Soc A, Math Phys Eng Sci 376(2132). https://doi.org/10.1098/rsta.2018.0109
Schaefer L, Fegley B (2007) Outgassing of ordinary chondritic material and some of its implications for the chemistry of asteroids, planets, and satellites. Icarus 186(2):462–483. https://doi.org/10.1016/j.icarus.2006.09.002
Schaefer L, Fegley BJ (2010) Chemistry of atmospheres formed during accretion of the Earth and other terrestrial planets. Icarus 208(1):438–448. https://doi.org/10.1016/j.icarus.2010.01.026
Schaefer L, Fegley B (2017) Redox states of initial atmospheres outgassed on rocky planets and planetesimals. Astrophys J 843:120. https://doi.org/10.3847/1538-4357/aa784f
Schaefer L, Wordsworth RD, Berta-Thompson Z, Sasselov D (2016) Predictions of the atmospheric composition of GJ 1132b. Astrophys J 829(2):63. https://doi.org/10.3847/0004-637X/829/2/63
Schlichting HE, Sari R, Yalinewich A (2015) Atmospheric mass loss during planet formation: the importance of planetesimal impacts. Icarus 247:81–94. https://doi.org/10.1016/j.icarus.2014.09.053
Schnetzler C, Philpotts J (1971) Alkali, alkaline Earth and rare-Earth element concentrations in some Apollo 12 soils, rocks, and separated phases. In: Lunar and planetary science conference proceedings, vol 2, p 1101. https://ui.adsabs.harvard.edu/abs/1971LPSC....2.1101S/abstract
Schubert G, Turcotte DL, Olson P (2001) Mantle convection in the Earth and planets. Cambridge University Press, Cambridge. https://doi.org/10.1017/CBO9780511612879
Sekiya M, Nakazawa K, Hayashi C (1980) Dissipation of the rare gases contained in the primordial Earth's atmosphere. Earth Planet Sci Lett 50(1):197–201. https://doi.org/10.1016/0012-821X(80)90130-2
Selsis F, Kating JF, Levrard B, Paillet J, Ribas I, Delfosse X (2007) Habitable planets around the star Gliese 581? Astron Astrophys 476(3):1373–1387. https://doi.org/10.1051/0004-6361:20078091

Shahar A, Schauble EA, Caracas R, Gleason AE, Reagan MM, Xiao Y, Shu J, Mao W (2016) Pressure-dependent isotopic composition of iron alloys. Science 352(6285):580–582. https://doi.org/10.1126/science.aad9945
Sharp ZD (2017) Nebular ingassing as a source of volatiles to the Terrestrial planets. Chem Geol 448:137–150. https://doi.org/10.1016/j.chemgeo.2016.11.018
Sharp ZD, McCubbin FM, Shearer CK (2013) A hydrogen-based oxidation mechanism relevant to planetary formation. Earth Planet Sci Lett 380:88–97. https://doi.org/10.1016/j.epsl.2013.08.015
Shcheka SS, Wiedenbeck M, Frost DJ, Keppler H (2006) Carbon solubility in mantle minerals. Earth Planet Sci Lett 245(3):730–742. https://doi.org/10.1016/j.epsl.2006.03.036
Shi L, Lu W, Kagoshima T, Sano Y, Gao Z, Du Z, Liu Y, Fei Y, Li Y (2022) Nitrogen isotope evidence for Earth's heterogeneous accretion of volatiles. Nat Commun 13(1):4769. https://doi.org/10.1038/s41467-022-32516-5
Shibazaki Y, Ohtani E, Terasaki H, Suzuki A, Ki F (2009) Hydrogen partitioning between iron and ringwoodite: implications for water transport into the Martian core. Earth Planet Sci Lett 287(3):463–470. https://doi.org/10.1016/j.epsl.2009.08.034
Shuvalov V (2009) Atmospheric erosion induced by oblique impacts. Meteorit Planet Sci 44(8):1095–1105. https://doi.org/10.1111/j.1945-5100.2009.tb01209.x
Shuvalov VV, Artemieva NA (2002) Atmospheric erosion and radiation impulse induced by impacts. In: Catastrophic events and mass extinctions: impacts and beyond. Geological society of America. https://doi.org/10.1130/0-8137-2356-6.695
Shuvalov V, Kührt E, de Niem D, Wünnemann K (2014) Impact induced erosion of hot and dense atmospheres. Planet Space Sci 98:120–127
Siebesma A, Bony S, Jakob C, Stevens B (eds) (2020) Clouds and climate: climate science's greatest challenge Cambridge University Press, Cambridge. https://doi.org/10.1017/9781107447738
Siggia E (1994) High Rayleigh number convection. Annu Rev Fluid Mech 26(1):137–168. https://doi.org/10.1146/annurev.fluid.26.1.137
Simpson GC (1927) Some studies in terrestrial radiation. Memoirs of the Royal Meteorological Society 11(16):69–95
Skemer P, Warren JM, Hansen LN, Hirth G, Kelemen PB (2013) The influence of water and LPO on the initiation and evolution of mantle shear zones. Earth Planet Sci Lett 375:222–233. https://doi.org/10.1016/j.epsl.2013.05.034
Sleep NH, Zahnle KJ (2001) Carbon dioxide cycling and implications for climate on ancient Earth. J Geophys Res, Planets 106(E1):1373–1399. https://doi.org/10.1029/2000JE001247
Smith J, Anderson A, Newton R, Olsen E, Crewe A, Isaacson M, Johnson D, Wyllie P (1970) Petrologic history of the moon inferred from petrography, mineralogy and petrogenesis of Apollo 11 rocks. Geochim Cosmochim Acta, Suppl 11:897–925. Proceedings of the Apollo 11 Lunar Science Conference, https://ui.adsabs.harvard.edu/abs/1970GeCAS...1..897S
Smrekar SE, Elkins-Tanton L, Leitner JJ, Lenardic A, Mackwell S, Moresi L, Sotin C, Stofan ER (2007) Tectonic and thermal evolution of Venus and the role of volatiles: implications for understanding the terrestrial planets. In: Exploring Venus as a terrestrial planet. Am. Geophys. Union, Washington, pp 45–71. https://doi.org/10.1029/176GM05
Smrekar SE, Davaille A, Sotin C (2018) Venus interior structure and dynamics. Space Sci Rev 214(5):88. https://doi.org/10.1007/s11214-018-0518-1
Smrekar S, Hensley S, Nybakken R, Wallace MS, Perkovic-Martin D, You TH, Nunes D, Brophy J, Ely T, Burt E, Dyar MD, Helbert J, Miller B, Hartley J, Kallemeyn P, Whitten J, Iess L, Mastrogiuseppe M, Younis M, Prats P, Rodriguez M, Mazarico E (2022) VERITAS (Venus emissivity, radio science, InSAR, topography, and spectroscopy): a discovery mission. In: 2022 IEEE aerospace conference (AERO), pp 1–20. https://doi.org/10.1109/AERO53065.2022.9843269
Solomatov V (2000) Fluid dynamics of a terrestrial magma ocean. In: Origin of the Earth and Moon, pp 323–338
Solomatov V (2007) 9.04 - Magma oceans and primordial mantle differentiation. In: Schubert G (ed) Treatise on geophysics. Elsevier, Amsterdam, pp 91–119. https://doi.org/10.1016/B978-044452748-6.00141-3
Solomatov V (2015) 9.04 - Magma oceans and primordial mantle differentiation. In: Schubert G (ed) Treatise on geophysics, 2nd edn. Elsevier, Oxford, pp 81–104. https://doi.org/10.1016/B978-0-444-53802-4.00155-X
Solomatov VS, Stevenson DJ (1993) Nonfractional crystallization of a terrestrial magma ocean. J Geophys Res, Planets 98(E3):5391–5406. https://doi.org/10.1029/92JE02579
Solomatova NV, Caracas R (2021) Genesis of a CO_2-rich and H_2O-depleted atmosphere from Earth's early global magma ocean. Sci Adv 7(41):eabj0406. https://doi.org/10.1126/sciadv.abj0406
Solomon SC (1979) Formation, history and energetics of cores in the terrestrial planets. Phys Earth Planet Inter 19(2):168–182. https://doi.org/10.1016/0031-9201(79)90081-5

Sonett CP, Colburn DS, Schwartz K (1968) Electrical heating of meteorite parent bodies and planets by dynamo induction from a pre-main sequence T tauri "solar wind". Nature 219(5157):924–926. https://doi.org/10.1038/219924a0

Sossi PA, Stotz IL, Jacobson SA, Morbidelli A, O'Neill HSC (2022) Stochastic accretion of the Earth. Nat Astron 6(8):951–960. https://doi.org/10.1038/s41550-022-01702-2

Sparks RSJ (1978) The dynamics of bubble formation and growth in magmas: a review and analysis. J Volcanol Geotherm Res 3(1):1–37. https://doi.org/10.1016/0377-0273(78)90002-1

Sparks RSJ, Barclay J, Jaupart C, Mader HM, Phillips JC (1994) Chapter 11a. Physical aspects of magma degassing I. Experimental and theoretical constraints on vesiculation. In: Carroll MR, Holloway JR (eds) Volatiles in magmas. Mineralogical Society of America, Washington, pp 413–446. https://doi.org/10.1515/9781501509674-017

Spencer CJ, Mitchell RN, Brown M (2021) Enigmatic mid-proterozoic orogens: hot, thin, and low. Geophys Res Lett 48(16):e2021GL093312. https://doi.org/10.1029/2021GL093312.

Šrámek O, Ricard Y, Dubuffet F (2010) A multiphase model of core formation. Geophys J Int 181(1):198–220. https://doi.org/10.1111/j.1365-246X.2010.04528.x

Šrámek O, Milelli L, Ricard Y, Labrosse S (2012) Thermal evolution and differentiation of planetesimals and planetary embryos. Icarus 217(1):339–354. https://doi.org/10.1016/j.icarus.2011.11.021

Srinivasan G, Papanastassiou DA, Wasserburg GJ, Bhandari N, Goswami JN (2000) Re-examination of ^{26}Al-^{26}Mg systematics in the Piplia Kalan eucrite. Lunar and Planetary Science XXXI, 1795

Stamenković V, Breuer D (2014) The tectonic mode of rocky planets: part 1 – driving factors, models & parameters. Icarus 234:174–193. https://doi.org/10.1016/j.icarus.2014.01.042

Steller T, Burkhardt C, Yang C, Kleine T (2022) Nucleosynthetic zinc isotope anomalies reveal a dual origin of terrestrial volatiles. Icarus 386:115171. https://doi.org/10.1016/j.icarus.2022.115171

Stephant A, Remusat L Robert F (2016) Water in type I chondrules of Paris CM chondrite. Geochim Cosmochim Acta 199:75–90. https://doi.org/10.1016/j.gca.2016.11.031

Stephant A, Garvie LAJ, Mane P, Hervig R, Wadhwa M (2018) Terrestrial exposure of a fresh Martian meteorite causes rapid changes in hydrogen isotopes and water concentrations. Sci Rep 8(1):12385. https://doi.org/10.1038/s41598-018-30807-w

Stephant A, Anand M, Tartèse R, Zhao X, Degli-Alessandrini G, Franchi IA (2020) The hydrogen isotopic composition of lunar melt inclusions: an interplay of complex magmatic and secondary processes. Geochim Cosmochim Acta 284:196–221. https://doi.org/10.1016/j.gca.2020.06.017

Stern RJ (2018) The evolution of plate tectonics. Philos Trans R Soc A, Math Phys Eng Sci 376(2132):20170406. https://doi.org/10.1098/rsta.2017.0406

Stevens RJAM, van der Poel EP, Grossmann S, Lohse D (2013) The unifying theory of scaling in thermal convection: the updated prefactors. J Fluid Mech 730:295–308. https://doi.org/10.1017/jfm.2013.298

Stevens RJAM, Blass A, Zhu X, Verzicco R, Lohse D (2018) Turbulent thermal superstructures in Rayleigh-Bénard convection. Phys Rev Fluids 3(4):041501. https://doi.org/10.1103/PhysRevFluids.3.041501

Stevenson D (1990) Fluid dynamics of core formation. In: Newsom H, Jones J (eds) Origin of the Earth. Oxford University Press, London, pp 231–249

Stevenson DJ (2001) Mars' core and magnetism. Nature 412(6843):214–219. https://doi.org/10.1038/35084155

Stökl A, Dorfi EA, Johnstone CP, Lammer H (2016) Dynamical accretion of primordial atmospheres around planets with masses between 0.1 and 5 $M_{\oplus}$ in the habitable zone. Astrophys J 825(2):86. https://doi.org/10.3847/0004-637X/825/2/86

Sugita S, Schultz PH (2009) Efficient cyanide formation due to impacts of carbonaceous bodies on a planet with a nitrogen-rich atmosphere. Geophys Res Lett 36(20). https://doi.org/10.1029/2009GL040252

Surkov YA, Barsukov VL, Moskalyeva LP, Kharyukova VP, Kemurdzhian AL (1984) New data on the composition, structure, and properties of Venus rock obtained by Venera 13 and Venera 14. J Geophys Res, Solid Earth 89(S02):B393–B402. https://doi.org/10.1029/JB089iS02p0B393

Surkov YA, Moskalyova LP, Kharyukova VP, Dudin AD, Smirnov GG, Zaitseva SY (1986) Venus rock composition at the Vega 2 landing site. J Geophys Res, Solid Earth 91(B13):E215–E218. https://doi.org/10.1029/JB091iB13p0E215

Svetsov V (2007) Atmospheric erosion and replenishment induced by impacts of cosmic bodies upon the Earth and Mars. Sol Syst Res 41(1):28–41

Tagawa S, Sakamoto N, Hirose K, Yokoo S, Hernlund J, Ohishi Y, Yurimoto H (2021) Experimental evidence for hydrogen incorporation into Earth's core. Nat Commun 12(1):2588. https://doi.org/10.1038/s41467-021-22035-0

Takei Y, Holtzman BK (2009a) Viscous constitutive relations of solid-liquid composites in terms of grain boundary contiguity: 1. Grain boundary diffusion control model. J Geophys Res, Solid Earth 114(B6). https://doi.org/10.1029/2008JB005850

Takei Y, Holtzman BK (2009b) Viscous constitutive relations of solid-liquid composites in terms of grain boundary contiguity: 2. Compositional model for small melt fractions. J Geophys Res, Solid Earth 114(B6). https://doi.org/10.1029/2008JB005851

Tateno S, Hirose K, Ohishi Y (2014) Melting experiments on peridotite to lowermost mantle conditions. J Geophys Res, Solid Earth 119(6):4684–4694. https://doi.org/10.1002/2013JB010616

Taylor SR (1986) The origin of the Moon: geochemical considerations. In: Hartmann W, Phillips R, Taylor G (eds) Origin of the Moon, Lunar and Planetary Institute, pp 125–143. https://ui.adsabs.harvard.edu/abs/1986ormo.conf..125T/abstract

Taylor G, Norman M (1992) Evidence for magma oceans on asteroids, the Moon, and Earth. Houston: Lunar Planet Inst pp 58–75. https://adsabs.harvard.edu/full/1992pcmo.work...58T

Thomas CW, Liu Q, Agee CB, Asimow PD, Lange RA (2012) Multi-technique equation of state for Fe_2SiO_4 melt and the density of Fe-bearing silicate melts from 0 to 161 GPa. J Geophys Res, Solid Earth 117(10):1–18. https://doi.org/10.1029/2012JB009403

Thompson MA, Telus M, Schaefer L, Fortney JJ, Joshi T, Lederman D (2021) Composition of terrestrial exoplanet atmospheres from meteorite outgassing experiments. Nat Astron 5(6):575–585. https://doi.org/10.1038/s41550-021-01338-8

Tian F (2015) Atmospheric escape from solar system terrestrial planets and exoplanets. Annu Rev Earth Planet Sci 43(1):459–476. https://doi.org/10.1146/annurev-earth-060313-054834

Tian F, Toon OB, Pavlov AA, De Sterck H (2005) A hydrogen-rich early Earth atmosphere. Science 308(5724):1014–1017. https://doi.org/10.1126/science.1106983

Tian F, Toon OB, Pavlov AA (2006) Response to comment on "A hydrogen-rich early Earth atmosphere". Science 311(5757):38. https://doi.org/10.1126/science.1118412

Tikoo SM, Elkins-Tanton LT (2017) The fate of water within Earth and super-earths and implications for plate tectonics. Philos Trans R Soc A, Math Phys Eng Sci 375(2094):20150394. https://doi.org/10.1098/rsta.2015.0394

Titov DV, Piccioni G, Drossart P, Markiewicz WJ (2013) Radiative energy balance in the Venus atmosphere. In: Bengtsson L, Bonnet R-M, Grinspoon D, Koumoutsaris S, Lebonnois S, Titov D (eds) Towards understanding the climate of Venus: applications of terrestrial models to our sister planet. Springer, New York, pp 23–53. https://doi.org/10.1007/978-1-4614-5064-1_4

Tonks WB, Melosh HJ (1992) Core formation by giant impacts. Icarus 100(2):326–346. https://doi.org/10.1016/0019-1035(92)90104-F

Tonks WB, Melosh HJ (1993) Magma ocean formation due to giant impacts. J Geophys Res, Planets 98(E3):5319–5333. https://doi.org/10.1029/92JE02726

Tozer DC (1965) Thermal history of the Earth: I. The formation of the core. Geophys J Int 9(2–3):95–112. https://doi.org/10.1111/j.1365-246X.1965.tb02064.x

Trail D, Watson EB, Tailby ND (2011) The oxidation state of Hadean magmas and implications for early Earth's atmosphere. Nature 480(7375):79–82. https://doi.org/10.1038/nature10655

Trieloff M, Palme H, Brandner W (2006) The origin of solids in the early Solar System. In: Klahr H, Brandner W (eds) Planet formation: theory, observations, and experiments. Cambridge astrobiology. Cambridge University Press, Cambridge, pp 64–89. https://doi.org/10.1017/CBO9780511536571.006

Tu L, Johnstone CP, Güdel M, Lammer H (2015) The extreme ultraviolet and X-ray sun in time: high-energy evolutionary tracks of a solar-like star. Astron Astrophys 577:L3. https://doi.org/10.1051/0004-6361/201526146

Tucker JM, Mukhopadhyay S (2014) Evidence for multiple magma ocean outgassing and atmospheric loss episodes from mantle noble gases. Earth Planet Sci Lett 393:254–265. https://doi.org/10.1016/j.epsl.2014.02.050

Turbet M, Tran H, Pirali O, Forget F, Boulet C, Hartmann JM (2019) Far infrared measurements of absorptions by $CH_4 + CO_2$ and $H_2 + CO_2$ mixtures and implications for greenhouse warming on early Mars. Icarus 321:189–199. https://doi.org/10.1016/j.icarus.2018.11.021

Turbet M, Boulet C, Karman T (2020) Measurements and semi-empirical calculations of $CO_2 + CH_4$ and $CO_2 + H_2$ collision-induced absorption across a wide range of wavelengths and temperatures. Application for the prediction of early Mars surface temperature. Icarus 346:113762. https://doi.org/10.1016/j.icarus.2020.113762

Turbet M, Bolmont E, Chaverot G, Ehrenreich D, Leconte J, Marcq E (2021) Day–night cloud asymmetry prevents early oceans on Venus but not on Earth. Nature 598(7880):276–280. https://doi.org/10.1038/s41586-021-03873-w

Ueki K, Inui M, Matsunaga K, Okamoto N, Oshio K (2020) Oxidation during magma mixing recorded by symplectites at Kusatsu–Shirane Volcano, Central Japan. Earth Planets Space 72(1):68. https://doi.org/10.1186/s40623-020-01192-4

Umemoto K, Hirose K (2015) Liquid iron-hydrogen alloys at outer core conditions by first-principles calculations. Geophys Res Lett 42(18):7513–7520. https://doi.org/10.1002/2015GL065899

Urbain G, Bottinga Y, Richet P (1982) Viscosity of liquid silica, silicates and alumino-silicates. Geochim Cosmochim Acta 46(6):1061–1072. https://doi.org/10.1016/0016-7037(82)90059-X
Urey HC (1955) The cosmic abundances of potassium, uranium, and thorium and the heat balances of the Earth, the Moon, and Mars. Proc Natl Acad Sci USA 41(3):127–144. https://doi.org/10.1073/pnas.41.3.127
Urey HC, Craig H (1953) The composition of the stone meteorites and the origin of the meteorites. Geochim Cosmochim Acta 4(1):36–82. https://doi.org/10.1016/0016-7037(53)90064-7
Venturini J, Ronco MP, Guilera OM (2020) Setting the stage: planet formation and volatile delivery. Space Sci Rev 216(5):86. https://doi.org/10.1007/s11214-020-00700-y
Vickery AM, Melosh HJ (1990) Atmospheric erosion and impactor retention in large impacts, with application to mass extinctions. Spec Pap, Geol Soc Am 247:289–300
Volkov VP, Zolotov MY, Khodakovsky IL (1986) Lithospheric-atmospheric interaction on Venus. In: Saxena SK (ed) Chemistry and physics of terrestrial planets. Springer, New York, pp 136–190. https://doi.org/10.1007/978-1-4612-4928-3_4
Von Zahn U, Kumar S, Niemann H, Prinn R (1983) Composition of the Venus atmosphere. In: Venus. The University of Arizona Press, Tucson
Wacheul JB Le Bars M (2018) Experiments on fragmentation and thermo-chemical exchanges during planetary core formation. Phys Earth Planet Inter 276:134–144. https://doi.org/10.1016/j.pepi.2017.05.018
Wade J, Wood BJ (2005) Core formation and the oxidation state of the Earth. Earth Planet Sci Lett 236(1):78–95. https://doi.org/10.1016/j.epsl.2005.05.017
Wadhwa M (2008) Redox conditions on small bodies, the Moon and Mars. Rev Mineral Geochem 68(1):493–510. https://doi.org/10.2138/rmg.2008.68.17
Wadhwa M, Srinivasan G, Carlson R (2006) Timescales of planetesimal differentiation in the early solar system. In: Lauretta DS, McSween HY (eds) Meteorites and the early solar system II. University of Arizona Press, Tucson, p 715
Walker JCG, Hays PB, Kasting JF (1981) A negative feedback mechanism for the long-term stabilization of Earth's surface temperature. J Geophys Res, Oceans 86(C10):9776–9782. https://doi.org/10.1029/JC086iC10p09776
Wallace PJ, Plank T, Edmonds M, Hauri EH (2015) Chap. 7 – Volatiles in magmas. In: Sigurdsson H (ed) The encyclopedia of volcanoes, 2nd edn. Academic Press, San Diego, pp 163–183. https://doi.org/10.1016/B978-0-12-385938-9.00007-9
Walsh KJ, Morbidelli A, Raymond SN, O'Brien DP, Mandell AM (2011) A low mass for Mars from Jupiter's early gas-driven migration. Nature 475(7355):206–209. https://doi.org/10.1038/nature10201
Wang H, Weiss BP, Bai XN, Downey BG, Wang J, Wang J, Suavet C, Fu RR, Zucolotto ME (2017) Lifetime of the solar nebula constrained by meteorite paleomagnetism. Science 355(6325):623–627. https://doi.org/10.1126/science.aaf5043
Wänke H, Baddenhausen H, Dreibus G, Jagoutz E, Kruse H, Palme H, Spettel B, Teschke F (1973) Multielement analyses of Apollo 15, 16, and 17 samples and the bulk composition of the moon. In: Lunar and planetary science conference proceedings, vol 4, p 1461. https://ui.adsabs.harvard.edu/abs/1973LPSC...4.1461W/abstract
Wänke H, Dreibus G, Runcorn SK, Turner G, Woolfson MM (1988) Chemical composition and accretion history of terrestrial planets. Philos Trans R Soc Lond A, Math Phys Eng Sci 325(1587):545–557. https://doi.org/10.1098/rsta.1988.0067
Warren PH (1985) The magma ocean concept and lunar evolution. Annu Rev Earth Planet Sci 13(1):201–240. https://doi.org/10.1146/annurev.ea.13.050185.001221
Warren PH (2011) Stable-isotopic anomalies and the accretionary assemblage of the Earth and Mars: a subordinate role for carbonaceous chondrites. Earth Planet Sci Lett 311(1):93–100. https://doi.org/10.1016/j.epsl.2011.08.047
Warren AO, Kite ES (2023) Narrow range of early habitable Venus scenarios permitted by modeling of oxygen loss and radiogenic argon degassing. Proc Natl Acad Sci 120(11):e2209751120. https://doi.org/10.1073/pnas.2209751120
Watson AJ, Donahue TM, Walker JCG (1981) The dynamics of a rapidly escaping atmosphere: applications to the evolution of Earth and Venus. Icarus 48(2):150–166. https://doi.org/10.1016/0019-1035(81)90101-9
Way M, Del Genio AD (2020) Venusian habitable climate scenarios: modeling venus through time and applications to slowly rotating Venus-like exoplanets. J Geophys Res, Planets 125(5). https://doi.org/10.1029/2019je006276
Way MJ, Del Genio AD, Kiang NY, Sohl LE, Grinspoon DH, Aleinov I, Kelley M, Clune T (2016) Was Venus the first habitable world of our solar system? Geophys Res Lett 43(16):8376–8383. https://doi.org/10.1002/2016GL069790
Way MJ, Ostberg C, Foley BJ, Gillmann C, Höning D, Lammer H, O'Rourke J, Persson M, Plesa AC, Salvador A, Scherf M, Weller M (2023) Synergies between Venus & exoplanetary observations. Space Sci Rev 219(13):64. https://doi.org/10.1007/s11214-023-00953-3

Weidenschilling SJ (1977) Aerodynamics of solid bodies in the solar nebula. Mon Not R Astron Soc 180(2):57–70. https://doi.org/10.1093/mnras/180.2.57
Weller MB, Kiefer WS (2020) The physics of changing tectonic regimes: implications for the temporal evolution of mantle convection and the thermal history of Venus. J Geophys Res, Planets 125(1):e2019JE005960. https://doi.org/10.1029/2019je005960
Westall F, Brack A (2018) The importance of water for life. Space Sci Rev 214(2):50. https://doi.org/10.1007/s11214-018-0476-7
Westall F, Höning D, Avice G, Gentry D, Gerya T, Gillmann C, Izenberg N, Way MJ, Wilson C (2023) The habitability of Venus and a comparison to early Earth. Space Sci Rev 219:17. https://doi.org/10.1007/s11214-023-00960-4
Wetherill GW (1976) The role of large bodies in the formation of the Earth and moon. In: Lunar and planetary science conference proceedings, vol 3, pp 3245–3257. https://ui.adsabs.harvard.edu/abs/1976LPSC....7.3245W/abstract
Wetherill GW (1978) Accumulation of the terrestrial planets. In: Gehrels T, Matthews MS (eds) IAU colloq. 52: protostars and planets, p p 565. https://ui.adsabs.harvard.edu/abs/1978prpl.conf..565W
Wetherill GW (1985) Occurrence of giant impacts during the growth of the terrestrial planets. Science 228(4701):877–879. https://doi.org/10.1126/science.228.4701.877
Wetherill GW (1990) Formation of the Earth. Annu Rev Earth Planet Sci 18(1):205–256. https://doi.org/10.1146/annurev.ea.18.050190.001225
Wetherill GW (1991) Why isn't Mars as big as Earth? In: Lunar and planetary science conference, vol 22, p 1495. https://ui.adsabs.harvard.edu/abs/1991LPI....22.1495W
White WM (2013) Geochemistry. Wiley, New York
Whittet DCB (1997) Is extraterrestrial organic matter relevant to the origin of life on Earth?. In: Whittet DCB (ed) Planetary and interstellar processes relevant to the origins of life Springer, Dordrecht, pp 249–262. https://doi.org/10.1007/978-94-015-8907-9_13
Widemann T, Smrekar SE, Garvin JB, Straume-Lindner AG, Ocampo AC, Voirin T, Hensley S, Dyar MD, Whitten JL, Nunes D, Getty S, Arney GN, Johnson NM, Kohler E, Spohn T, O'Rourke JR, Wilson C, Way MJ, Ostberg C, Westall F, Höning D, Jacobson S, Salvador A, Avice G, Breuer D, Carter L, Gilmore MS, Ghail R, Helbert J, Byrne P, Santos AR, Herrick RR, Izenberg N, Marcq E, Rolf T, Weller M, Gillmann C, Korablev O, Zelenyi LM, Zasova L, Gorinov D, Seth G, Rao CVN, Desai N (2023) Venus evolution through time: Key science questions, selected mission concepts and future investigations. Space Sci Rev 219. https://doi.org/10.1007/s11214-023-00992-w
Williams CD, Mukhopadhyay S (2019) Capture of nebular gases during Earth's accretion is preserved in deep-mantle neon. Nature 565(7737). https://doi.org/10.1038/s41586-018-0771-1
Winn JN, Fabrycky DC (2015) The occurrence and architecture of exoplanetary systems. Annu Rev Astron Astrophys 53(1):409–447. https://doi.org/10.1146/annurev-astro-082214-122246
Wood BJ (1995) The effect of H_2O on the 410-kilometer seismic discontinuity. Science 268(5207):74–76. https://doi.org/10.1126/science.268.5207.74
Wood BJ, Halliday AN (2005) Cooling of the Earth and core formation after the giant impact. Nature 437(7063):1345–1348. https://doi.org/10.1038/nature04129
Wood J, Dickey J Jr, Marvin U, Powell B (1970) Lunar anorthosites and a geophysical model of the moon. Geochim Cosmochim Acta, Suppl, 1:965–988. Proceeding of the Apollo 11 Lunar Science Conference
Wood BJ, Bryndzia LT, Johnson KE (1990) Mantle oxidation state and its relationship to tectonic environment and fluid speciation. Science 248(4953):337–345. https://doi.org/10.1126/science.248.4953.337
Wood BJ, Walter MJ, Wade J (2006) Accretion of the Earth and segregation of its core. Nature 441:825–833. https://doi.org/10.1038/nature04763
Wood BJ, Wade J, Kilburn MR (2009) Core formation and the oxidation state of the Earth: additional constraints from Nb, V and Cr partitioning. Geochim Cosmochim Acta 72(5):1415–1426. https://doi.org/10.1016/j.gca.2007.11.036
Wordsworth RD (2016) Atmospheric nitrogen evolution on Earth and Venus. Earth Planet Sci Lett 447:103–111. https://doi.org/10.1016/j.epsl.2016.04.002
Wordsworth RD, Pierrehumbert RT (2013) Water loss from terrestrial planets with CO_2-rich atmospheres. Astrophys J 778(2):154. https://doi.org/10.1088/0004-637X/778/2/154
Wordsworth R, Kalugina Y, Lokshtanov S, Vigasin A, Ehlmann B, Head J, Sanders C, Wang H (2017) Transient reducing greenhouse warming on early Mars. Geophys Res Lett 44(2):665–671. https://doi.org/10.1002/2016GL071766
Wordsworth RD, Schaefer LK, Fischer RA (2018) Redox evolution via gravitational differentiation on low-mass planets: implications for abiotic oxygen, water loss, and habitability. Astron J 155(5):195. https://doi.org/10.3847/1538-3881/aab608
Wu J, Desch SJ, Schaefer L, Elkins-Tanton LT, Pahlevan K, Buseck PR (2018) Origin of Earth's water: chondritic inheritance plus nebular ingassing and storage of hydrogen in the core. J Geophys Res, Planets 123(10):2691–2712. https://doi.org/10.1029/2018JE005698

Wyatt MC (2008) Evolution of debris disks. Annu Rev Astron Astrophys 46(1):339–383. https://doi.org/10.1146/annurev.astro.45.051806.110525
Yang J, Cowan NB, Abbot DS (2013) Stabilizing cloud feedback dramatically expands the habitable zone of tidally locked planets. Astrophys J Lett 771. https://doi.org/10.1088/2041-8205/771/2/L45
Yang J, Boué G, Fabrycky DC, Abbot DS (2014) Strong dependence of the inner edge of the habitable zone on planetary rotation rate. Astrophys J Lett. https://doi.org/10.1088/2041-8205/787/1/L2. arXiv:1404.4992
Yin Q, Jacobsen SB, Yamashita K, Blichert-Toft J, Télouk P, Albarède F (2002) A short timescale for terrestrial planet formation from Hf–W chronometry of meteorites. Nature 418(6901):949–952. https://doi.org/10.1038/nature00995
Yoshino T, Walter MJ, Katsura T (2003) Core formation in planetesimals triggered by permeable flow. Nature 422(6928):154–157. https://doi.org/10.1038/nature01459
Youdin AN, Goodman J (2005) Streaming instabilities in protoplanetary disks. Astrophys J 620(1):459–469. https://doi.org/10.1086/426895
Young ED, Shahar A, Schlichting HE (2023) Earth shaped by primordial H_2 atmospheres. Nature 616(7956):306–311. https://doi.org/10.1038/s41586-023-05823-0
Yuan L, Steinle-Neumann G (2020) Strong sequestration of hydrogen into the Earth's core during planetary differentiation. Geophys Res Lett 47(15):e2020GL088303. https://doi.org/10.1029/2020GL088303.
Zahnle KJ (1990) Atmospheric chemistry by large impacts. In: Global catastrophes in Earth history; an interdisciplinary conference on impacts, volcanism, and mass mortality. Geol. Soc. Am., Boulder, pp 271–288. https://doi.org/10.1130/SPE247-p271
Zahnle KJ, Kasting JF, Pollack JB (1988) Evolution of a steam atmosphere during Earth's accretion. Icarus 74(1):62–97
Zahnle K, Kasting JF, Pollack JB (1990) Mass fractionation of noble gases in diffusion-limited hydrodynamic hydrogen escape. Icarus 84(2):502–527. https://doi.org/10.1016/0019-1035(90)90050-J
Zahnle K, Arndt N, Cockell C, Halliday A, Nisbet E, Selsis F, Sleep NH (2007) Emergence of a habitable planet. Space Sci Rev 129:35–78. https://doi.org/10.1007/s11214-007-9225-z
Zahnle K, Schaefer L, Fegley B (2010) Earth's earliest atmospheres. Cold Spring Harb Perspect Biol 2(10):a004895–a004895. https://doi.org/10.1101/cshperspect.a004895
Zahnle KJ, Gacesa M, Catling DC (2019) Strange messenger: a new history of hydrogen on Earth, as told by Xenon. Geochim Cosmochim Acta 244:56–85. https://doi.org/10.1016/j.gca.2018.09.017
Zahnle KJ, Lupu R, Catling DC, Wogan N (2020) Creation and evolution of impact-generated reduced atmospheres of early Earth. Planet. Sci. J. 1(1):11. https://doi.org/10.3847/PSJ/ab7e2c
Zellner NEB (2017) Cataclysm no more: new views on the timing and delivery of lunar impactors. Orig Life Evol Biosph 47(3):261–280. https://doi.org/10.1007/s11084-017-9536-3
Zhang Y, Xu Z, Zhu M, Wang H (2007) Silicate melt properties and volcanic eruptions. Rev Geophys 45(4). https://doi.org/10.1029/2006RG000216
Zhang HL, Hirschmann MM, Cottrell E, Withers AC (2017) Effect of pressure on Fe3+/ΣFe ratio in a mafic magma and consequences for magma ocean redox gradients. Geochim Cosmochim Acta 204:83–103. https://doi.org/10.1016/j.gca.2017.01.023
Zolotov MY (2018) Gas-solid interactions on Venus and other solar system bodies. Rev Mineral Geochem 84:351–392. https://doi.org/10.2138/rmg.2018.84.10
Zsom A, Ormel CW, Güttler C, Blum J, Dullemond CP (2010) The outcome of protoplanetary dust growth: pebbles, boulders, or planetesimals? - II. Introducing the bouncing barrier. Astron Astrophys 513:A57. https://doi.org/10.1051/0004-6361/200912976
Zsom A, Seager S, de Wit J, Stamenković V (2013) Toward the minimum inner edge distance of the habitable zone. Astrophys J 778(2):109. https://doi.org/10.1088/0004-637X/778/2/109

Authors and Affiliations

Arnaud Salvador[1,2,3] · Guillaume Avice[4] · Doris Breuer[5] · Cédric Gillmann[6] · Helmut Lammer[7] · Emmanuel Marcq[8] · Sean N. Raymond[9] · Haruka Sakuraba[10] · Manuel Scherf[7,11,12] · M.J. Way[13,14]

✉ D. Breuer
doris.breuer@dlr.de

A. Salvador
arnaudsalvador@arizona.edu

G. Avice
avice@ipgp.fr

C. Gillmann
cgillmann@ethz.ch

H. Lammer
helmut.lammer@oeaw.ac.at

E. Marcq
emmanuel.marcq@latmos.ipsl.fr

S.N. Raymond
sean.raymond@u-bordeaux.fr

H. Sakuraba
sakuraba@eps.sci.titech.ac.jp

M. Scherf
manuel.scherf@oeaw.ac.at

M.J. Way
Michael.J.Way@nasa.gov

1 Department of Astronomy and Planetary Science, Northern Arizona University, Box 6010, Flagstaff, AZ 86011, USA

2 Habitability, Atmospheres, and Biosignatures Laboratory, University of Arizona, Tucson, AZ, USA

3 Present address: Lunar and Planetary Laboratory, University of Arizona, Tucson, AZ, USA

4 Université Paris Cité, Institut de physique du globe de Paris, CNRS, F-75005 Paris, France

5 DLR, Institute of Planetary Research, 12489 Berlin, Germany

6 Department of Earth Sciences, Institute of Geophysics, Geophysical Fluid Dynamics, ETH Zurich, Switzerland

7 Space Research Institute, Austrian Academy of Sciences, Graz, Austria

8 LATMOS/IPSL, UVSQ Université Paris-Saclay, Sorbonne Université, CNRS, Guyancourt, France

9 Laboratoire d'Astrophysique de Bordeaux, CNRS and Université de Bordeaux, Pessac, France

10 Department of Earth and Planetary Sciences, Tokyo Institute of Technology, Ookayama, Meguro-ku, Tokyo 152-8551, Japan

11 Institute of Physics, University of Graz, Graz, Austria

12 Institute for Geodesy, Technical University, Graz, Austria

13 NASA Goddard Institute for Space Studies, 2880 Broadway, New York, NY 10025, USA

14 Theoretical Astrophysics, Department of Physics and Astronomy, Uppsala University, Uppsala, Sweden